

# From field to globe:

*Upscaling of crop growth modelling*

Lenny G.J. van Bussel



**From field to globe:**  
Upscaling of crop growth modelling

Lenny Gertruda Johanna van Bussel

## **Thesis committee**

### **Thesis supervisors**

Prof. dr. ir. H. van Keulen  
Professor at the Plant Production Systems Group  
Wageningen University

Prof. dr. ir. M.K. van Ittersum  
Personal chair at the Plant Production Systems Group  
Wageningen University

### **Thesis co-supervisors**

Prof. dr. F.A. Ewert  
Professor of Crop Science  
Institute of Crop Science and Resource Conservation (INRES)  
University of Bonn

Dr. ir. P.A. Leffelaar  
Associate professor, Plant Production Systems Group  
Wageningen University

### **Other members**

Prof. dr. C. Kroeze, Wageningen University  
Prof. dr. A.J. Challinor, University of Leeds, UK  
Dr. J.B. Evers, Wageningen University  
Prof. dr. W. Cramer, Potsdam Institute for Climate Impact Research (PIK),  
Germany

This research was conducted under the auspices of the C.T. de Wit Graduate School for Production Ecology and resource Conservation (PE&RC).

**From field to globe:**  
Upscaling of crop growth modelling

Lenny Gertruda Johanna van Bussel

**Thesis**

submitted in fulfilment of the requirements  
for the degree of doctor  
at Wageningen University  
by the authority of the Rector Magnificus  
Prof. dr. M.J. Kropff,  
in the presence of the  
Thesis Committee appointed by the Academic Board  
to be defended in public  
on Wednesday 19 October 2011  
at 4 p.m. in the Aula.

Lenny Gertruda Johanna van Bussel  
From field to globe: Upscaling of crop growth modelling  
212 pages

Thesis, Wageningen University, Wageningen, The Netherlands (2011)  
With references, with summaries in English and Dutch

ISBN 978-94-6173-015-2

Aan Nellie en Frank,  
voor alle kansen en liefde die jullie mij gegeven hebben



# Abstract

Recently, the scale of interest for application of crop growth models has extended to the region or even globe with time frames of 50-100 years. The application at larger scales of a crop growth model originally developed for a small scale without any adaptation might lead to errors and inaccuracies. Moreover, application of crop growth models at large scales usually gives problems with respect to missing data.

Knowledge about the required level of modelling detail to accurately represent crop growth processes in crop growth models to be applied at large scales is scarce. In this thesis we analysed simulated potential yields, which resulted from models which apply different levels of detail to represent important crop growth processes. Our results indicated that, after location-specific calibration, models in which the same processes were represented with different levels of detail may perform similarly. Model performance was in general best for models which represented leaf area dynamics with the lowest level of detail. Additionally, the results indicated that the use of a different description of light interception significantly changes model outcomes. Especially the representation of leaf senescence was found to be critical for model performance.

Global crop growth models are often used with monthly weather data, while crop growth models were originally developed for daily weather data. We examined the effects of replacing daily weather data with monthly data. Results showed that using monthly weather data may result in higher simulated amounts of biomass. In addition, we found increasing detail in a modelling approach to give higher sensitivity to aggregation of input data.

Next, we investigated the impact of the use of spatially aggregated sowing dates and temperatures on the simulated phenology of winter wheat in Germany. We found simulated winter wheat phenology in Germany to be rather similar using either non-aggregated input data or aggregated input data with a 100 km × 100 km resolution.

Generation or simulation of input data for crop growth models is often necessary if the model is applied at large scales. We simulated sowing dates of several rainfed crops by assuming farmers to sow either when temperature exceeds a crop-specific threshold or at the onset of the wet season. For a large part of the globe our methodology is capable of simulating reasonable sowing dates. To simulate the end of the cropping period (i.e. harvesting dates) we developed



simple algorithms to generate unknown crop- and location-specific phenological parameters. In the main cropping regions of wheat the simulated lengths corresponded well with the observations; our methodology worked less well for maize (over- and underestimations of 0.5 to 1.5 month). Importantly, our evaluation of possible consequences for simulated yields related to uncertainties in simulated sowing and harvesting dates showed that simulated yields are rather similar using either simulated or observed sowing and harvesting dates (a maximum difference of 20%), indicating the applicability of our methodology in crop productivity assessments.

The thesis concludes with a discussion on a proposed structure of a global crop growth model which is expected to simulate reasonable potential yields at the global scale if only monthly aggregates of climate data at a  $0.5^\circ \times 0.5^\circ$  grid are available. The proposed model consists of a forcing function, defined in terms of sigmoidal and quadratic functions to represent light interception, combined with the radiation use efficiency approach, and phenology determining the allocation of biomass to the organs of the crop. Within the model sowing dates and phenological cultivar characteristics are simulated. Based on the proposed model the thesis finally derives directions for future research to further enhance global crop growth modelling.

# Table of contents

<b>Chapter 1</b>	General introduction	1
<b>Chapter 2</b>	Effects of modelling detail on simulated potential crop yields under a wide range of climatic conditions	15
<b>Chapter 3</b>	The effect of temporal aggregation of weather input data on crop growth models' results	45
<b>Chapter 4</b>	Effects of data aggregation on simulations of crop phenology	67
<b>Chapter 5</b>	Climate-driven simulation of global crop sowing dates	89
<b>Chapter 6</b>	Simulation of phenological development of wheat and maize at the global scale	111
<b>Chapter 7</b>	General discussion	139
<b>References</b>		155
<b>Appendices</b>	Appendix A	171
	Appendix B	179
<b>Summaries</b>	Summary	193
	Samenvatting (summary in Dutch)	197
<b>Dankwoord &amp; Acknowledgements</b>		201
<b>List of co-authors affiliations</b>		203
<b>About the author</b>	Curriculum Vitae	205
	List of peer-reviewed publications	207
	PE&RC Educational statement form	209
<b>Funding</b>		211





# Chapter 1

## **General introduction**

## 1. Global food production

The global demand for food has been projected to increase drastically (FAO, 2009; Government Office for Science, 2011). This increase is mainly the result of growth in population and a shift in consumption pattern, especially to animal products. In addition, increasing competition for land, water, and other resources between biomass production for food on the one side and biofuel on the other side, and the threat of global change will result in extra pressure on the global agricultural system (Koning and Van Ittersum, 2009; Godfray *et al.*, 2010).

An increase in global food production can be achieved by expansion of agricultural land (Keys and McConnell, 2005). However, the remaining potential for land conversion to agricultural use is small in large parts of the globe (e.g. in Japan, South Asia, and the Near East/North Africa). In other parts of the globe (e.g. in sub-Saharan Africa and Latin America) more land is available but it suffers from soil and terrain constraints, such as low fertility, steepness, or lack of infrastructure (FAO, 2003). Other options to increase global food production are improved varieties and intensification of agriculture on the current agricultural area, e.g. a higher or better balanced application of fertilizers and/or irrigation (Keys and McConnell, 2005), a better control of pests and diseases and in general an improved management, thus diminishing or even closing the gap between actual and potential yields.

Potential yield is defined in this thesis as the production determined by cultivar characteristics (related to physiology and phenology), weather conditions (especially temperature and solar radiation during the period of growth) and atmospheric CO<sub>2</sub> concentration, assuming ample water and nutrients available and full protection against weeds, pests, diseases, and abiotic stresses such as pollutants. If the supply of water or nutrients is suboptimal, potential yield levels are reduced and yields are defined as water-limited and nutrient-limited yields, respectively. Finally, actual yields are yield levels achieved by farmers with actual supplies of water and nutrients, and the effects of existing weeds, pests, diseases, and abiotic stresses on crop growth (based on Van Ittersum and Rabbinge, 1997).

Knowledge about the yield potential of the globe and other yield levels is important if one addresses questions such as “will the growing world population have enough to eat in the coming decades?”, “which regions will be most vulnerable to climate change?”, or “what will be possible increases in future irrigation water requirements?”. One possibility to obtain this knowledge is through a crop growth model that is able to simulate potential, water-limited, and nutrient-

limited production levels of important food crops at the global scale, i.e. under a wide range of climatic, soil, and socio-economic conditions.

Especially during the last decade several crop growth models have been applied at the global scale (hereafter also referred to as global crop growth models). Table 1.1 gives an overview and indicates some important characteristics for each model; statistical models are left out (e.g. Lobell *et al.*, 2011), because it is uncertain if present-day statistical relationships hold true under future climatic conditions (Challinor *et al.*, 2004; Challinor *et al.*, 2009). The availability of different global crop growth models provides the opportunity to compare their outcomes, a technique also applied with e.g. dynamic global vegetation models (Cramer *et al.*, 2001), regional climate models (Jacob *et al.*, 2007), and field scale crop growth models (Wolf *et al.*, 1996; Palosuo *et al.*, in press). If carried out in a well-designed experimental setup, the differences between model outcomes can be used to explore model uncertainties (Palosuo *et al.*, in press). It might then be clarified which parts of the models should be improved and which experimental work or data collection still needs to be done, with the consideration that a deviating model, as compared to other models that gave more similar results, is not necessarily wrong.

**Table 1.1**

Characteristics of several global crop growth models.

Model	Crop, location, spatial resolution	Objective	Cropping period	Weather data	Approach to simulate biomass production
GAEZ* (Fischer <i>et al.</i> , 2002)	Various crops, global, 0.5° x 0.5°	Computation of potential and water-limited crop yields and effects of specified levels of input and management conditions on production potentials	Selection of cropping period by optimization	Monthly means, quadratic spline functions give daily values	Potential crop yields are simulated based on an empirical approach which combines prevailing temperature and radiation regimes; water-limited crop yields are simulated based on potential and actual evapotranspiration combined with potential crop yields
SIMFOOD <sup>‡</sup> (Luyten, 1995; Penning de Vries <i>et al.</i> , 1997)	Various crops, global, region based	Quantification of future food security	Identification of potential cropping period based on minimum and maximum temperatures combined with minimum and maximum growing degree days	Monthly means, linear interpolation gives daily values	Potential productivity follows from intercepted radiation multiplied with a light use efficiency value; water-limited productivity follows from potential productivity multiplied with a water stress factor
GEPIC <sup>‡</sup> (Liu <i>et al.</i> , 2007)	Wheat, global, 0.5° x 0.5°	Simulation of crop yields and crop water productivity	Observed crop calendars are used	Daily data, observed and generated by a stochastic weather generator	Potential productivity is estimated based on the radiation use efficiency approach, combined with five stress factors (water, temperature, nitrogen, phosphorus and aeration)

Model	Crop, location, spatial resolution	Objective	Cropping period	Weather data	Approach to simulate biomass production
GLAM-MOSE2 <sup>‡</sup> (Challinor <i>et al.</i> , 2004; Osborne <i>et al.</i> , 2007) <sup>∞</sup>	Groundnut, global (mainly tropics), 2.5° latitude x 3.75° longitude	Estimation of crop productivity over a range of tropical environments, coupled with the climate system to investigate the two-way interactions between crops and climate	Sowing date is simulated within a prescribed sowing window, when surface soil moisture exceeds a threshold; end of cropping period when a specified amount of growing degree days has been accumulated	Crop growth model has been coupled with a climate model, with equations solved for every 30 minutes	Leaf area index increases with a prescribed maximum rate, which is reduced when the crop experiences water stress; daily biomass accumulation is simulated with help of a daily transpiration rate and a transpiration efficiency; a regional calibrated yield gap parameter is used to account for other stresses
LPJmL <sup>‡</sup> (Bondeau <i>et al.</i> , 2007)	Various crops, global, 0.5° x 0.5°	Quantification of multiple drivers (climate, CO <sub>2</sub> , land management, land use change) on the provision of future ecosystem services, investigation of the impact of agriculture on global carbon and water cycles	Deterministic simulation of sowing dates, based on temperature and precipitation thresholds; end of cropping period based on location specific growing degree days (as a function of sowing dates)	Monthly means, linear interpolation gives daily values	Development of leaf area index is forced with help of sigmoid and quadratic functions; growth is simulated using a combination of processes (photosynthesis, respiration, evapotranspiration); water stress reduces leaf area index growth and crop growth through a reduced photosynthetic rate



Model	Crop, location, spatial resolution	Objective	Cropping period	Weather data	Approach to simulate biomass production
DayCent <sup>‡</sup> (Stehfest <i>et al.</i> , 2007)	Various crops, global, 0.5° x 0.5°	Computation of global crop production, including the effects of irrigation and fertilizer application	Sowing months are simulated based on an optimization methodology; end of cropping period based on climate specific growing degree days	Monthly means, assuming identical values for all days within one month	Potential productivity is simulated based on solar insolation, biomass, temperature and a constant crop-specific energy-biomass conversion factor, which also includes management conditions and cultivar characteristics; limiting factors to account for water and nitrogen availability
PEGASUS <sup>‡</sup> (Deryng <i>et al.</i> , 2011)	Various crops, global, 10' x 10'	Explicit simulation of crop phenology and the influence of irrigation and fertilizer use on crop production	Sowing dates are simulated based on temperature thresholds and precipitation to potential evapotranspiration ratios, combined with location specific growing degree days; both derived from observations	Monthly means, linear interpolation gives daily values	Combination of light use efficiency approach with a surface energy and soil water budget model; dynamic allocation scheme of biomass to different organs, which determines leaf area index development; three limiting factors to account for temperature stress, and water and nutrient availability

\*Mainly empirical model

‡Mainly mechanistic model

∞Characteristics described mainly concern application of GLAM as described in Osborne *et al.* (2007)

## **2. Upscaling in crop growth modelling**

### **2.1 System analysis and crop growth modelling**

Crop growth modelling has its origin in systems thinking. A system is a limited part of reality that contains interrelated elements. Boundaries of this system should be chosen such that the desired part of reality can be explored, including all the interacting elements and that the effects of the environment on the system can be measured or sufficiently estimated, but the system itself should not influence the environment. A possible way to explore this system is to model it. A model is a simplified representation of a system (Penning de Vries, 1982). A simplification of a system is only possible by making assumptions, e.g. in the choice of processes included, the mathematical equations describing these processes and the interactions between elements and/or the environment (e.g. linear vs. non-linear), on the level of detail in these equations, on parameter values, and on initial conditions. It is important to link the extent of simplification to the objective of the model. Given the objective, the model should be kept as simple as possible, but enough detail should be incorporated to capture the effects of the major processes that determine the system's behaviour (De Wit, 1968).

Interactions between elements and/or the environment can be modelled mechanistically or empirically. A mechanistic approach (also called explanatory or process-based) considers causal relationships based on scientific understanding of the system to represent the mechanisms that characterise the system, translated in detailed mathematical equations. In contrast, an empirical approach contains no scientific understanding in terms of the causal relationships explaining the phenomena being modelled, thus reflecting little of the mechanisms that characterise the system (Thornley and France, 2007). The advantage of mechanistic approaches is their high explanatory power, but as a consequence, input data requirements (e.g. parameter values) are high as well. Input requirements of empirical approaches are often lower and the approaches are simpler to interpret by potential users (Whisler et al., 1986; Brooks and Tobias, 1996).

Crop growth models consist of a combination of empirical and mechanistic approaches (Whisler et al., 1986; Boote et al., 1996). During the last decades numerous crop growth models have been developed, mainly for the (homogeneous) plot and field scale (Van Ittersum et al., 2003; Hansen et al., 2006). The diversity in the modelling detail among those crop growth models is large, ranging from more empirical to more mechanistic models. Most crop growth models have in common the simulation of leaf area and some description

of photosynthesis (Ewert, 2004a). Both processes can be modelled with a varying degree of detail, normally dependent on the specific objective of the model. The level of detail of different processes should, however, be consistent within the model (Leffelaar, 1990). Concerning the relative importance of processes explaining yield variability, the accurate simulation of crop phenology has frequently been stressed as an essential requirement for satisfactory model performance (Jamieson et al., 2007; Craufurd and Wheeler, 2009).

The input data of crop growth models typically include daily weather, soil characteristics, and management (e.g. cultivar characteristics, sowing date, and irrigation/fertilizer management). Figure 1.1 gives a schematic overview of important processes per production level, as well as their possible interactions.

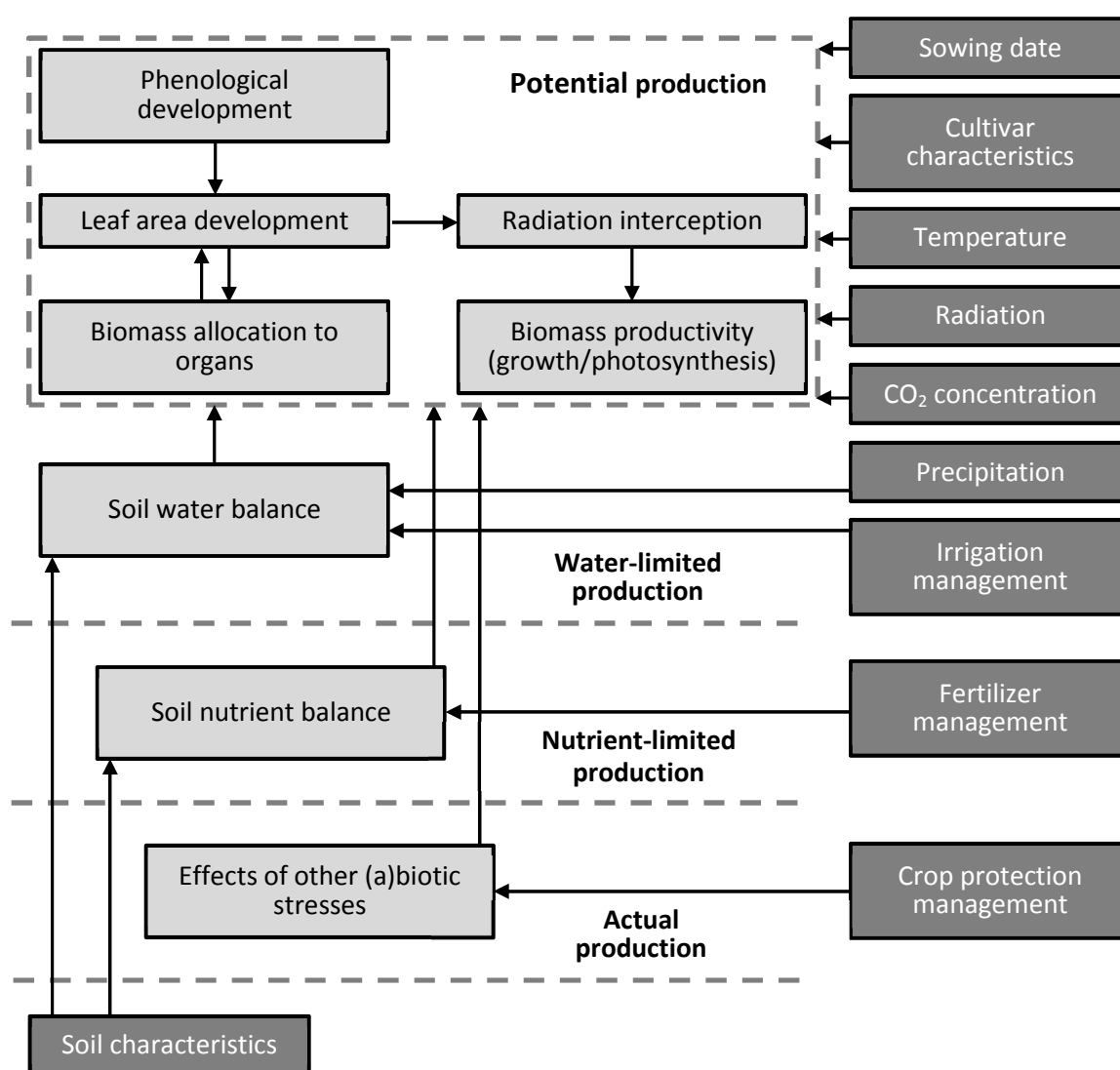


**Fig. 1.1** Schematic overview with possible important processes per production level; boxes in light grey indicate processes, boxes in dark grey indicate possible input data.

## 2.2 Upscaling issues

Recently the scale of interest for application of crop growth models has extended from the plot and field scale to the regional or even global scale. In addition, the time frame of the assessments has increased from a season or a year to much longer time frames, e.g. 50-100 years as considered in climate change impact studies (see e.g. Alcamo *et al.*, 2007; Franck *et al.*, 2011; Gerten *et al.*, 2011; Tao and Zhang, 2011). Crop growth models are also applied in large scale integrated assessment models such as IMAGE 2.4 (MNP, 2006) or SEAMLESS (Van Ittersum *et al.*, 2008). However, the application of a crop growth model originally developed for the plot or field scale at larger scales without any adaptation might lead to inaccuracies in model outcomes (Ewert *et al.*, 2005; Irmak *et al.*, 2005). These inaccuracies may result from a misinterpretation of the system at the larger scale or by feeding the model with incorrect input data (unsuitable spatial or temporal resolution, or inaccurate measurements), including parameter values (Scholten, 2008).

### 2.2.1 Systems analysis at larger scales

Misinterpretation of a system might arise because the importance of effects relevant at the original scale of a model might decrease at larger scales, while other factors, often not considered in the original model, may become more important at the large scale (Hansen and Jones, 2000; Ewert, 2004b). For example, at the European scale advances of technology over time, i.e. better management, better machinery, or improved varieties via progress in breeding, is expected to contribute more to changes in future crop productivity than changes in climate or CO<sub>2</sub> concentration (Ewert *et al.*, 2007). Nevertheless, technological development is often not accounted for in existing crop growth models (Ewert *et al.*, 2005). Values of model parameters related to cultivar characteristics can be used to represent effects of progress in breeding as an example of technological development. If a crop growth model is applied to simulate current crop productivity, parameter values to represent current cultivar characteristics are usually known and implemented in the model. If however, the model is used to simulate future crop productivity and if technology is expected to change in future, a methodology that adjusts parameter values should be included in the model. Including technological development in crop growth models implies therefore a change in boundaries of the system, i.e. in addition to biophysical processes and inputs, also processes and inputs translating technological development into parameter values should be incorporated in the crop growth model.

The shift in system boundaries when scaling up might change the required complexity of the model. One could argue that due to the additional processes that become important at the larger scale model complexity should increase (Hansen and Jones, 2000). Moreover, the variability in e.g. climatic conditions or socio-economic conditions typically increases with larger areas and time periods. To capture the effects of the different conditions and their interactions a mechanistic model will be helpful, particularly when estimations are made for future conditions. However, the high input data requirements that come with complex mechanistic models, can often not be fulfilled at larger scales. One could therefore also argue that simpler empirical models with lower input data requirements are more appropriate at larger scales (see e.g. Beven, 1989; De Vries *et al.*, 1998). Due to the lower data requirements, errors associated with uncertainties in input data are smaller. In addition, empirical models apply fewer non-linear relationships which is important to reduce uncertainties due to input data aggregation (Hansen and Jones, 2000). Nevertheless, application of an empirical model outside its original scope might lead to incorrect model outcomes (Challinor *et al.*, 2004; Challinor *et al.*, 2009). Finding the appropriate level of complexity is indeed considered as one of the most difficult steps in model development (Brooks and Tobias, 1996), also for large scale crop growth modelling.

### **2.2.2 Data availability and limitations**

The availability of input data at larger scales typically decreases compared with the plot or field scale. As a solution often aggregated data are used as input. Aggregation is usually an average or sum of the underlying detail. Both spatial and temporal aggregations are applied. The extent of aggregation will determine the degree to which local extreme values can still be distinguished in the aggregated data; this will have implications for model outcomes, especially in the case of complex models which apply non-linear relationships (Ewert, 2004b). Sensitivity analysis is a suitable methodology to identify which input variables result in the highest aggregation errors and could therefore be used to study if aggregation of specific input data is appropriate (Hansen and Jones, 2000). Finally, exploring the application of a crop growth model at larger scales can also indicate which required input data are missing and thus could give directions to future research. For example, the start and end of the cropping period and the corresponding phenological development are main determinants of crop yields and therefore necessary inputs to crop growth models. Only recently two global comprehensive data sets with global coverage of cropping calendars have been

developed (Portmann *et al.*, 2010; Sacks *et al.*, 2010). Thus, before the availability of these data sets global simulations of the start and end of the cropping period could only be evaluated to a limited extent.

### 3. Scope and Objectives

In order to adequately capture spatial and temporal heterogeneity in agricultural management and weather conditions by crop growth models at larger scales, a certain level of detail is required in the input data and in the model's complexity. Few studies have explored this required detail for weather and soil characteristics (see e.g. Easterling *et al.*, 1998; Olesen *et al.*, 2000). Knowledge with regard to the required spatial detail for other essential input data (e.g. sowing date and cultivar characteristics), the relation between temporal resolution of weather data and model complexity, and the appropriate level of model complexity at the global scale, is, however, scarce. As accurate simulation of phenology is important for crop growth models (Jamieson *et al.*, 2007; Craufurd and Wheeler, 2009), the correct consideration of the start and the physiological length of the cropping period is of particular importance. However, approaches to simulate the start of the cropping period and to consider differences in cropping period lengths between cultivars at the global scale are hardly available.

To support the upscaling of existing crop growth models for application at larger scales, this thesis aims therefore to give insight in four upscaling issues:

1. the possibilities to apply less complex modelling approaches, focussing on the processes of light interception and biomass productivity;
2. the effects of input data aggregation on model outcomes, in particular:
  - a. the effects of spatial aggregation of sowing dates and weather data on the simulation of phenology;
  - b. the effects of temporal aggregation of weather data on yield simulation, in relation with the level of detail applied in the model;
3. the possibility to generate missing input data, with a focus on the generation of sowing dates of various crops;
4. the possibility to generate parameter values, in particular parameters which represent phenological cultivar characteristics of wheat and maize, to adequately simulate the length of the cropping period, with special attention to the inter-annual variability in harvest dates.

The research was concentrated on the European and global scale and mainly concerned with potential production levels.

## 4. Outline

This thesis is composed of seven chapters, including the introduction. Chapters 2 to 6 present the main results of the study, with Chapter 2, 3 & 4 dealing with aggregation issues and Chapters 5 & 6 with the possibilities to generate required input data for application of crop growth models at the global scale. **Chapter 2** concentrates on the appropriate level of modelling detail for important processes to simulate potential yields at a large scale, i.e. under a wide range of climatic conditions. Several modelling approaches with varying degree of detail are compared. We concentrate on the light interception and biomass production processes and identify the importance of those two processes to adequately simulate potential yields. In addition, we show the importance of explaining underlying theoretical knowledge related to important parameter values. In **Chapter 3** we investigate the effects of temporal aggregation of weather input data on the outcomes of crop growth models. We study the relationship between the degree of complexity in a modelling approach and its sensitivity to temporal aggregation of input data. **Chapter 4** focuses on spatial aggregation of input data. First, we investigate the spatial heterogeneity in observed phenological data of winter wheat (emergence, ear-emergence, and harvesting dates). Next, we investigate whether aggregation of the spatial heterogeneity found leads to bias in model outcomes.

**Chapter 5** concentrates on the computation of sowing dates. We investigate if sowing dates under rainfed conditions can be satisfactorily generated from climatic conditions at the global scale. **Chapter 6** focuses on the simulation of the length on the cropping period. We describe methodologies to generate parameters to simulate phenological development of wheat and maize, which characterise the wide range of cultivars found across the globe.

Finally, **Chapter 7** discusses the main findings of this thesis. It explores methodological issues of large scale crop growth modelling. It concludes with directions for future research to improve global crop growth models.

## 5. Definitions used throughout this thesis

Definitions of terms such as scale, resolution, and detail are often not clear. To avoid confusion, I therefore first give a definition of each term, following Ewert (2004b) and Van Delden *et al.* (in press). *Scale* is defined as the characteristic dimension in time and space of a phenomenon or observation, and thus dimensions and units of measurement can be assigned. *Detail* relates to the spatial and temporal resolution and the complexity of the representation of processes. The *spatial resolution* is the grid size, the *temporal resolution* the

frequency of the observations or simulations. A higher resolution indicates more observations per time or spatial unit or a smaller grid size. *Complexity* is defined as the number of included relations and variables in a model. A *global crop growth model* is a crop growth model which is applied at the global scale.







## Chapter 2

# **Effects of modelling detail on simulated potential crop yields under a wide range of climatic conditions**

Based on:  
Adam, M., Van Bussel, L.G.J., Leffelaar, P.A., Van Keulen, H., Ewert, F.:  
Effects of modelling detail on simulated potential crop yields  
under a wide range of climatic conditions.  
Ecological Modelling, vol. 222 (2011), 131-143

## Abstract

Crop simulation models are widely applied at large scale for climate change impact assessment or integrated assessment studies. However, often a mismatch exists between data availability and the level of detail in the model used. Good modelling practice dictates to keep models as simple as possible, but enough detail should be incorporated to capture the major processes that determine the system's behaviour. The objective of this study was to investigate the effect of the level of detail incorporated in process-based crop growth models on simulated potential yields under a wide range of climatic conditions. We conducted a multi-site analysis and identified that by using a constant radiation use efficiency (*RUE*) value under a wide range of climatic conditions, the description of the process of biomass production may be over-simplified, as the effects of high temperatures and high radiation intensities on this parameter are ignored. Further, we found that particular attention should be given to the choice of the light interception approach in a crop model as determined by leaf area index (*LAI*) dynamics. The two *LAI* dynamics approaches considered in this study gave different simulated yields irrespective of the characteristics of the location and the light interception approaches better explained the differences in yield sensitivity to climatic variability than the biomass production approaches. Further analysis showed that differences between the two *LAI* dynamics approaches for simulated yields were mainly due to different representations of leaf senescence in both approaches. We concluded that a better understanding and modelling of leaf senescence, particularly its onset, is needed to reduce model uncertainty in yield simulations.

# 1. Introduction

A key rule in good modelling practice is that the choice of a model depends on the question asked (Van Waveren *et al.*, 1999). In crop modelling, a large variety of models has been developed since the 1960s, with each new model addressing a specific objective. Crop models have initially been developed for application at the field scale. Application of these models at larger scales such as for climate change impact assessments (Leemans, 1997, Ewert, 2004b, Challinor *et al.*, 2004 and Challinor *et al.*, 2009) or integrated assessment studies (Van Ittersum *et al.*, 2008) has become a common practice. However, for these applications, the required scale and objective of a crop growth model may go beyond the scope of the original model. Hence, the reuse of a model without any adaptation might lead to inaccuracies in model outputs, caused by (1) a misrepresentation of processes in the model, (2) incorrect input data (unsuitable temporal or spatial resolution, or inaccurate measurements), including parameter values (Scholten, 2008), or (3) a misinterpretation of the system, as the importance of effects relevant at lower levels may decrease at higher levels, while other factors, often not considered in the original crop model, may become more important (Ewert, 2004b).

Challinor *et al.* (2004) identified the need for process-based crop growth models to capture the impact of climatic variability on crop yields over large areas. One of the challenges to apply a model for simulating crop growth and development at higher aggregation levels (e.g. Europe, Therond *et al.*, in press) is to ensure that the model appropriately addresses the response of crops to the temperature and radiation gradients found in such a heterogeneous environment. The model must reproduce the behaviour of the system under a wide range of conditions, representing the spatial variability. Bondeau *et al.* (2007) also mention the use of process-based crop models at the global scale to improve the representation of feedbacks between crop physiology and climate. A process-based model integrates descriptions of the underlying processes of the cropping system to explain its behaviour at the higher system level (Hammer *et al.*, 2002), and usually includes at least two essential processes for crop growth, namely light interception by the leaf area and light utilization to produce biomass (Ewert, 2004a). In various crop growth models (Ritchie and Otter, 1985, Spitters and Schapendonk, 1990, Spitters, 1990, Jamieson *et al.*, 1998a, Stöckle *et al.*, 2003 and Bondeau *et al.*, 2007) we found that (1) leaf area index ( $LAI$ ,  $m^2$  leaf area  $m^{-2}$  ground area) dynamics and (2) biomass production are modelled with different mechanistic detail, usually depending on the main objective of the model. For the application of process-based crop growth models to larger scales, it is therefore

pertinent to consider which level of detail in these two processes is needed to adequately capture potential yield responses to different temperature and radiation regimes.

A distinction can be made between explanatory, i.e. detailed mechanistic approaches with a high level of modelling detail, and descriptive, i.e. summarized approaches with a lower level of modelling detail (Penning de Vries, 1982). Detailed models have a high explanatory power, containing most of the elements and interactions that characterize a system, but they are resource-intensive (e.g. in terms of input data and simulation time). Summarized (also called summary) models are easier to handle (e.g. less parameters are needed and the models are simpler to interpret), but are generally more descriptive, reflecting little of the mechanisms explaining the behaviour of the system, often containing simplified representations of complex processes. Selection of the appropriate level of detail for each process to include in a crop growth model is often seen as a critical step in model development (Brooks and Tobias, 1996). It is a common rule to keep the model as simple as possible given the objective, but enough detail should be incorporated to capture the major processes that determine the system's behaviour (De Wit, 1968). It is also acknowledged that an optimum situation exists in terms of explanatory capacity of a model and the number of processes considered (Leffelaar, 1990, Passioura, 1996 and Tittonell, 2008).

The objective of this study is to investigate the effect of the level of detail incorporated in a process-based crop growth model to simulate potential yields [i.e. growth is not limited by water- and nutrient shortages or the occurrence of pest and diseases (Goudriaan and Van Laar, 1994 and Van Ittersum and Rabbinge, 1997)] under a wide range of climatic conditions as typical for large scale applications. Particular focus is on the processes of light interception, determined by *LAI* dynamics, and light utilization for biomass production. We do not aim at developing the “best” large scale crop growth model, but the results of this study should improve the understanding of the relative importance of the different approaches to simulate potential crop yields at large scales, especially in response to spatial differences in radiation and temperature.

## 2. Materials and methods

We compared models with different modelling detail in the key growth processes light interception and light utilization, to simulate crop yields in response to temperature and radiation. The analysis follows two main steps:

1. Test of the models (i.e. the combinations of approaches) against measured data to ensure that all models are able to reproduce observed growth under field conditions for a range of climatic conditions. We selected experiments from different locations across the world that provided measurements of biomass and *LAI* and the associated weather data;
2. Systematic comparison of the behaviour of the models under a wide range of climatic conditions (following a climate gradient across Europe) to investigate the sensitivity of yield simulations to the use of the different approaches (i.e. different levels of detail) for the two growth processes examined.

### 2.1 Descriptions of the modelling approaches

We defined a detailed approach (also referred to as a more mechanistic approach) as one that describes a feature (e.g. crop growth) in terms of the processes at the underlying hierarchical level (Van Ittersum *et al.*, 2003). The description of the photosynthesis and respiration processes according to Farquhar *et al.* (1980) can be considered as a detailed approach for biomass production. In contrast, a summarized approach (also referred to as a descriptive approach) uses a simple relationship that describes the main responses of a feature (e.g. crop growth) to biotic and abiotic factors. Sinclair and Muchow (1999) identified the application of the radiation use efficiency concept to simulate biomass production from intercepted radiation as an example of such a summarized approach.

In this study, both light interception determined by the leaf area and light utilization to produce biomass were studied in a summarized and a detailed approach. Table 2.1 includes the key equations of the approaches studied. The associated parameter values can be found in Table 2.2.

**Table 2.1**

Key equations of the studied approaches applied for a) *LAI* dynamics and b) biomass production.

a)

Equations for the detailed <i>LAI</i> dynamics approach	Eq.
---	-----

*Juvenile phase ( $LAI < 0.75$  and development stage  $< 0.16$ ):*

$$\frac{dLAI_{growth}}{dt} = LAI \times R_g \times T_{eff} \quad (2.1)$$

with:  $T_{eff} = \max(0, [T_{average} - T_{base}])$

with:  $T_{eff}$  effective physiological temperature (°C),  $T_{average}$  average daily temperature (°C),

and  $T_{base}$  the base temperature (°C)

*Following the juvenile phase:*

$$\frac{dLAI_{growth}}{dt} = \frac{dW_{leaf}}{dt} \times S_{LA} \quad (2.2)$$

*After anthesis ( $fT_{sum\ sen}$ ) or in case of self-shading ( $LAI > LAI_{critical}$ ):*

$$\frac{dLAI_{sen}}{dt} = -R_d \times LAI \quad (2.3)$$

with:  $R_d = \max(R_{d-ag}, R_{d-sh})$

Equations for the summarized <i>LAI</i> dynamics approach	
---	--

*Before anthesis:*

$$fLAI_{max} = \frac{fT_{sum}}{fT_{sum} + e^{(l_1 - l_2 \times fT_{sum})}} \quad (2.4)$$

with:

$$fT_{sum} = \frac{T_{sum}}{fT_{sum\ totaal}}$$

with:  $T_{sum}$  temperature sum in °C days, representative of the development stage of the crop

$$l_1 = \ln\left(\frac{fT_{sum1}}{fLAI1} - fT_{sum1}\right) + l_2 \times fT_{sum1}$$

$$l_2 = \frac{\left(\ln\left[\frac{fT_{sum1}}{fLAI1} - fT_{sum1}\right] - \ln\left[\frac{fT_{sum2}}{fLAI2} - fT_{sum2}\right]\right)}{fT_{sum2} - fT_{sum1}}$$

*After anthesis:*

$$fLAI_{max} = \frac{(1 - fT_{sum})^2}{(1 - fT_{sum\ sen})^2}$$

*To guarantee sufficient biomass:*

$$LAI = \min(fLAI_{max} \times LAI_{max}, [B_{total} - B_{root}] \times S_{LA}) \quad (2.5)$$

with:  $B_{total}$  and  $B_{root}$  standing total and standing root biomass,

respectively (gC m<sup>-2</sup>)

b)

Equations for the detailed biomass production approach

$$A_{gd} = \left( \frac{J_e + J_c - \sqrt{(J_e + J_c)^2 - 4 \times \theta \times J_e \times J_c}}{2 \times \theta} \right) \times d_{\text{length}} \quad (2.6)$$

$$\text{with: } J_e = \frac{C_1 \times C_q \times R_{dr} \times 0.415 \times (1 - e^{-k \times LAI})}{d_{\text{length}}} \quad (2.7)$$

$$J_c = \frac{C_2 \times V_m}{24} \quad (2.8)$$

$$\text{with: } V_m = \left( \frac{1}{b} \right) \times \left( \frac{C_1}{C_2} \right) \times [(2 \times \theta - 1) \times s - (2 \times \theta \times s - C_2) \times \sigma] \times R_{dr} \times 0.415 \times (1 - e^{-k \times LAI}) \times C_q$$

with:  $R_{dr}$  daily incoming radiation ( $\text{MJ m}^{-2} \text{d}^{-1}$ ),  $d_{\text{length}}$  length of day ( $\text{h d}^{-1}$ ), $V_m$  Rubisco capacity ( $\text{gC d}^{-1} \text{m}^{-2}$ )

$$C_1 = \phi_{TC3} \times C_{\text{mass}} \times \alpha_{C3} \times \left( \frac{p_i - \Gamma_*}{(p_i + 2 \times \Gamma_*)} \right) \quad (2.9)$$

$$\text{with: } p_i = \lambda_{\text{max}} \times c_a \times P$$

$$C_2 = \frac{p_i - \Gamma_*}{p_i + K_C \times (1 + \frac{O_2}{K_O})} \quad (2.10a)$$

$$\text{with: } K_i = K_{25} \times Q_{10}^{(T-25)/10} \text{ with } i \text{ either C or O} \quad (2.10b)$$

$$\Gamma_* = \frac{[O_2]}{2 \times \tau} \quad (2.11)$$

with:  $\phi_{TC3}$  a temperature stress factor (–),  $C_{\text{mass}}$  atomic mass of carbon( $\text{g mol}^{-1}$ ),  $p_i$  internal partial pressure of  $\text{CO}_2$  (Pa),  $\Gamma_*$   $\text{CO}_2$  compensation point( $\mu\text{mol mol}^{-1}$ ), and  $[O_2]$  partial pressure of oxygen (Pa)

$$A_{nd} = A_{gd} - R_d \quad (2.12)$$

$$\text{with: } R_d = b \times V_m \quad (2.13)$$

$$\sigma = \left[ 1 - \frac{(C_2 - s)}{(C_2 - \theta \times s)} \right]^{1/2}$$

$$s = \frac{24}{d_{\text{length}}} \times b$$

$$NPP = A_{nd} - R_{\text{root}} - R_{\text{so}} - R_{\text{pool}} - R_g \quad (2.14)$$

with:  $R$  the maintenance respiration of roots, storage organs and a reserve pool,respectively ( $\text{gC d}^{-1} \text{m}^{-2}$ ), and  $R_g$  the growth respiration

$$\text{with: } R_g = \max[0, 0.25 \times (A_{nd} - R_{\text{root}} - R_{\text{so}} - R_{\text{pool}})] \quad (2.15)$$

Equations for the summarized biomass production approach

$$NPP = RUE \times PARINT \quad (2.16)$$

$$\text{with: } PARINT = R_{dr} \times 0.5 \times (1 - e^{-k \times LAI})$$



**Table 2.2**

Key parameters of the studied approaches applied and their default values. a) Common and *LAI* dynamics and b) biomass production.

a)

Symbol	Description	Default value and unit	Reference
Common parameters			
$C_f$	Conversion from carbon to dry matter	$0.46 \text{ gC (gDM)}^{-1}$	(a)
$k$	Light extinction factor	0.5 (–)	(b)
$S_{LA}$	Specific leaf area	$0.048 \text{ m}^2 \text{ (gC)}^{-1}$	(d)
$fT_{\text{sum sen}}$	Fraction of the total temperature sum when senescence starts (at anthesis)	0.60 (–)	(c)
$T_{\text{base}}$	Physiological base temperature	0 °C	(d)
<i>LAI</i> dynamics approaches			
Parameters for the detailed <i>LAI</i> dynamics approach			
$R_g$	Maximum relative growth rate of leaf area index during the juvenile stage	$0.009 \text{ (}^\circ\text{Cd)}^{-1}$	(d)
$LAI_{\text{initial}}$	Initial leaf area index	$0.012 \text{ m}^2 \text{ m}^{-2}$	(d)
$LAI_{\text{juvenile stage}}$	Threshold of leaf area index when juvenile stage ends	$0.75 \text{ m}^2 \text{ m}^{-2}$	(d)
$R_{\text{d-sh}}$	Relative death rate due to shading ( <i>LAI</i> dependent)	$0 - 0.03 \text{ d}^{-1}$	(d)
$R_{\text{d-ag}}$	Relative death rate due to ageing (temperature dependent)	$0.03 - 0.09 \text{ d}^{-1}$	(d)
$LAI_{\text{critical}}$	Critical leaf area index above which self-shading is considered	$4.0 \text{ m}^2 \text{ m}^{-2}$	(d)
Parameters for the summarized <i>LAI</i> dynamics approach			
$fLAI1$ and $fLAI2$	Fraction of leaf area index at specific points on the leaf area development curve corresponding to specific development stages	0.05 and 0.95 (–)	(c)
$fT_{\text{sum1}}$ and $fT_{\text{sum2}}$	Fraction of temperature sum at specific points on the leaf area development curve corresponding to specific development stages	0.15 and 0.50 (–)	(c)
$LAI_{\text{max}}$	Maximum leaf area index	$5.0 \text{ m}^2 \text{ m}^{-2}$	(c)

b)

---

Biomass production approaches

---

Parameters for Farquhar photosynthesis approach (C<sub>3</sub> plants)

---

$K_{25}$  and  $Q_{10}$  The value of the parameter at 25 °C and the relative change in the parameter for a 10 °C change in temperature, respectively

$K_C$	Michaelis constant for CO <sub>2</sub>	30 Pa ( $Q_{10}= 2.1$ )	(b)
$K_O$	Michaelis constant for O <sub>2</sub>	30 kPa ( $Q_{10}= 1.2$ )	(b)
$\tau$	CO <sub>2</sub> /O <sub>2</sub> specific ratio	2600 $\mu\text{mol } \mu\text{mol}^{-1}$ ( $Q_{10}= 0.57$ )	(b)
$\alpha_{C3}$	C3 quantum efficiency	0.08 $\mu\text{mol } \mu\text{mol}^{-1}$	(b)
$b$	$R_d/V_m$ ratio for C <sub>3</sub> plants	0.015	(b)
$C_q$	Conversion factor for solar radiation at 550 nm from MJ m <sup>-2</sup> d <sup>-1</sup> to mol m <sup>-2</sup> d <sup>-1</sup>	$4.6 \times 10^{-3}$	
$\theta$	Co-limitation parameter	0.7 (–)	(b)
$\lambda_{\text{max}}$	Optimal ratio of intercellular to ambient CO <sub>2</sub> concentration	0.8 (–)	(e)
$c_a^*$	Ambient CO <sub>2</sub> concentration for the year 1982	340 $\mu\text{mol mol}^{-1}$	(f)
$O_2^*$	Partial pressure of O <sub>2</sub>	20.9 kPa	(b)
$P^*$	Atmospheric pressure	100 kPa	(b)

---

Parameter for the radiation use efficiency approach

---

$RUE$  Radiation use efficiency based on  $PAR$  and total biomass 1.38 gC MJ<sup>-1</sup>

---

(a) Goudriaan and Van Laar (1994)

(b) Haxeltine and Prentice (1996a,b)

(c) derived from Neitsch et al. (2002)

(d) Van Keulen and Seligman (1987)

(e) Sitch et al. (2003)

(f) Carbon Cycle Model Linkage Project (McGuire et al., 2001)

\*These values represent assumptions about environmental conditions, not physiological parameters.

### 2.1.1 Leaf area index dynamics

The detailed  $LAI$  dynamics approach is based on temperature and leaf dry matter supply driven by the development stage of the crop (i.e. phenology). During the juvenile phase,  $LAI$  development is governed by temperature and its effect on cell division and extension, following an exponential growth pattern ( $R_g$ , Table 2.1, Eq. 2.1). After this exponential phase, leaf area expansion is governed by the supply of dry matter (Table 2.1, Eq. 2.2) and is calculated by multiplying the simulated rate of increase in leaf weight ( $dW_{\text{leaf}}/dt$ , gC m<sup>-2</sup> d<sup>-1</sup>), based on the total amount of biomass produced multiplied by a leaf biomass

allocation factor, with the specific leaf area ( $S_{LA}$ , Table 2.2). Finally, leaves senesce (Table 2.1, Eq. 2.3) due to (1) self-shading ( $r_{d-sh}$ , Table 2.2) when  $LAI$  reaches a critical value ( $LAI_{critical}$ , Table 2.2) and (2) ageing after anthesis (with time of anthesis defined by  $fT_{sum\ sen}$ , Table 2.2). The relative rate at which leaves age ( $r_{d-ag}$ , Table 2.2) depends on temperature:  $r_{d-ag}$  increases if temperature increases. This approach is used in the LINTUL model (Light, INTerception and Utilization, Spitters and Schapendonk, 1990; Spitters, 1990).

The summarized  $LAI$  dynamics approach is governed by the development stage of the crop. Leaf area development is calculated on the basis of a forcing function, comprising a sigmoid and a quadratic component (Table 2.1, Eq. 2.4).  $LAI$  at any point in time is calculated as a fraction of an exogenously defined  $LAI_{max}$  (Table 2.2) and two shape coefficients  $l_1$  and  $l_2$  (–) (Eq. 2.4). These coefficients are defined by the fractions  $fLAI1$  and  $fLAI2$  of the maximum  $LAI$  (Table 2.2), and the associated fractions of the temperature sum  $fT_{sum1}$  and  $fT_{sum2}$  (Table 2.2), representing points on the  $LAI$  versus development stage curve (Neitsch *et al.*, 2005) at specific development stages (e.g. end of juvenile stage, anthesis). The start of  $LAI$  senescence is defined by  $fT_{sum\ sen}$ , which is the fraction of the total growth cycle temperature sum at which senescence starts to exceed the formation of new leaf tissue. In agreement with what is applied in the more detailed approach, we set this starting point at anthesis. Finally, in this approach, potential  $LAI$  is reduced if the required biomass to support the calculated  $LAI$  is not available (Table 2.1, Eq. 2.5). This approach is applied in the LPJmL model (Lund–Potsdam–Jena managed Land, Bondeau *et al.*, 2007) and is derived from the SWAT model (Soil and Water Assessment Tool model, Neitsch *et al.*, 2005).

### 2.1.2 Biomass production

The detailed approach to describe the production of biomass is based on the description of the photosynthesis and respiration processes according to Farquhar *et al.* (1980) with simplifications introduced by Collatz *et al.* (1991) and Collatz *et al.*, (1992). The assimilatory process includes the conversion of  $CO_2$  into carbohydrates. Daily gross photosynthesis ( $A_{gd}$ ,  $gC\ m^{-2}\ d^{-1}$ ) is defined as a gradual transition between two limiting rates (Table 2.1, Eq. 2.6). Photosynthesis is determined either by the amount of intercepted light (depending on the light-limited  $CO_2$  assimilation rate,  $J_e$ ,  $gC\ m^{-2}\ h^{-1}$ , Table 2.1, Eq. 2.7) or by the available amount of the enzyme Rubisco (depending on the Rubisco-limited assimilation rate,  $J_c$ ,  $gC\ m^{-2}\ h^{-1}$ , Table 2.1, Eq. 2.8). Those rates are both influenced by ambient temperature (Table 2.1, Eqs 2.9, 2.10a, 2.10b and 2.11), via  $\tau$  (Table 2.2) and via  $K_C$  and  $K_O$ , the temperature-dependent Michaelis–

Menten constants for  $\text{CO}_2$  and  $\text{O}_2$  (Table 2.2), respectively. Daily *net* photosynthesis ( $A_{\text{nd}}$ ,  $\text{gC m}^{-2} \text{d}^{-1}$ , Table 2.1, Eq. 2.12) is calculated as daily gross photosynthesis minus “dark” respiration ( $R_{\text{d}}$ ,  $\text{gC m}^{-2} \text{d}^{-1}$ ).  $R_{\text{d}}$  is scaled to the maximum catalytic capacity of Rubisco per unit leaf area ( $V_{\text{m}}$ ,  $\text{gC m}^{-2} \text{d}^{-1}$ , Table 2.1, Eq. 2.13). To calculate net primary production ( $NPP$ ,  $\text{gC m}^{-2} \text{d}^{-1}$ , Table 2.1, Eq. 2.14), maintenance respiration for the various organs ( $R_{\text{i}}$ ,  $\text{gC m}^{-2} \text{d}^{-1}$ , for roots, storage organs, and carbohydrate pool, respectively) is subtracted from daily net photosynthesis and 25% of the remaining assimilates is assumed to be expended in growth respiration (Eq. 2.15). This approach is used in various models, but the present equations (Haxeltine and Prentice, 1996b) are implemented within the LPJmL model (Bondeau *et al.*, 2007).

Alternatively, the summarized approach is based on a linear relationship between accumulated intercepted radiation and accumulated biomass over the growing season. The slope of this linear relation is called radiation use efficiency ( $RUE$ , Table 2.2) (Monteith, 1977) and summarizes the combined effect of photosynthesis and respiration processes. The product of the daily intercepted amount of photosynthetically active radiation ( $PAR_{\text{INT}}$ ) and  $RUE$  gives the net increase in biomass over the day (Table 2.1, Eq. 2.16). This approach is used in models such as LINTUL (Spitters and Schapendonk, 1990), CropSyst (Stöckle *et al.*, 2003) and CERES (Ritchie and Otter, 1985).

These four approaches (two for  $LAI$  dynamics and two for biomass production) were combined resulting in four models (Table 2.3). Two of these models represent existing crop models, namely (1) LINTUL (Light, INTerception and UtiLiZation, Spitters and Schapendonk, 1990), resulting from the combination of  $RUE$  with the detailed  $LAI$  dynamics and (2) LPJmL (Lund–Potsdam–Jena managed Land, Bondeau *et al.*, 2007), resulting from the combination of the Farquhar photosynthesis approach with the summarized  $LAI$  dynamics. For the other two combinations we know of no crop models to which these refer to. However, some models have been developed combining the Farquhar photosynthesis model with a detailed  $LAI$  dynamics approach (e.g. Ewert *et al.*, 1999, Ewert and Porter, 2000 and Rodriguez *et al.*, 2001), but with different versions and implementations as the ones used here. We refer to the two latter combinations as the “detailed crop model” (Farquhar combined with the detailed  $LAI$  dynamics) and the “summarized crop model” ( $RUE$  combined with the summarized  $LAI$  dynamics).

**Table 2.3**

Overview of combination of processes and their derived models.

Light utilization approach (Biomass production)	Light interception approach ( <i>LAI</i> dynamics)	Model name
Farquhar photosynthesis combined with:	detailed	Detailed crop model*
	summarized	LPJmL (Lund-Potsdam-Jena managed Land, Bondeau et al., 2007)
<i>RUE</i> combined with:	detailed	LINTUL (Light, INTerception and Utilization, Spitters and Schapendonk, 1990)
	summarized	Summarized crop model*

\*Models resulting from the combinations of the different modelling approaches. We are not aware of crop models that use these particular combinations.

## 2.2 Model testing

To test the four models, measured *LAI* and biomass data for spring wheat, under optimal agronomic conditions for potential growth, from contrasting locations, were collected with their associated weather data: Australia (Meinke *et al.*, 1997), Europe (Van Oijen *et al.*, 1998, Bender *et al.*, 1999, Ewert and Pleijel, 1999 and Van Oijen and Ewert, 1999), and USA (Kimball *et al.*, 1995, Kimball *et al.*, 1999 and Ewert *et al.*, 2002) (Table 2.4). The locations vary in temperature conditions during the growing season: in the USA temperatures (i.e. number of days > 22.5 °C) are higher during the end of the growing season than in the Netherlands or Australia. Moreover, radiation levels during the growing season are higher in the USA than in the other locations.

The four models were calibrated with respect to phenology, *LAI* dynamics, and yield for these locations. The parameters  $fT_{\text{sum sen}}$ ,  $S_{\text{LA}}$ ,  $LAI_{\text{max}}$ , and total temperature sum ( $T_{\text{sum}}$ ) of the growth cycle were first estimated from the observed data, and subsequently calibrated according to model outputs (i.e. simulated *LAI* and yields). The calibration was done manually by trial-and-error, comparing the model outputs with the observations.

$R_g$  was calibrated on the basis of model outputs, guided by values found in the literature. For the biomass production approaches, *RUE* was directly estimated from the observed data: it was not calibrated, to avoid the compensation effect with the calibration on  $S_{\text{LA}}$ .

**Table 2.4**

Weather characteristics for the various locations of the experimental datasets.

Australia, Queensland	Europe, The Netherlands	USA, Arizona			
1993	1995	1996	1992 – 1993	1993 – 1994	1995 – 1996
Average temperature during the growing season (°C)					
15.5	14.8	13.4	15.2	14.7	15.5
Days < 7.5 °C					
2	7	12	1	9	7
Days > 22.5 °C					
4	9	3	10	10	16
Total radiation (MJ m <sup>-2</sup> growing season <sup>-1</sup> )					
2033	2042	1998	2579	2904	2649
Intercepted <i>PAR</i> (MJ m <sup>-2</sup> growing season <sup>-1</sup> )					
554	669	616	823	797	724

To evaluate the quality of the model outputs, we used the relative root mean square error (*r*RMSE) for yield and the relative mean absolute error (*r*MAE) for *LAI* dynamics (Wallach *et al.*, 2006):

$$rRMSE = \sqrt{\frac{\sum_{i=1}^n (S_i - O_i)^2}{n}} \times \frac{1}{\bar{O}} \quad (\text{Eq. 2.17})$$

$$rMAE = \left( \frac{1}{j} \sum_{i=1}^j \left( \frac{|S_i - O_i|}{O_i} \right) \right) \times \frac{1}{n} \quad (\text{Eq. 2.18})$$

where *n* is the number of locations, *j* the number of *LAI* observations over the growing season for each location, *S<sub>i</sub>* and *O<sub>i</sub>* simulated and observed values, respectively, and  $\bar{O}$  the average observed value.

### 2.3 Systematic comparison of model behaviour to climate variability

To investigate the relative importance of the two key growth processes on simulated crop yield and their ability to capture climatic variability, the models were run with weather data representing a wide range of climatic conditions in Europe (Fig. 2.1). Assessing model behaviour for a wide range of environmental conditions should demonstrate how robust the different approaches are under different conditions and therefore how suitable the different approaches are for applications at larger scales. Nine locations were selected across Europe: Denmark, the United Kingdom, the Netherlands, Germany, France (centre and South), Spain (centre and South), and Italy. They represent the European climatic gradient according to the classification from Metzger *et al.*, (2005). Daily data for minimum and maximum temperature and incoming short-wave radiation for the

year 1982 (for this specific year daily weather data were available for the nine locations) were extracted from a database described by Van Kraalingen (1990). In addition to location-specific weather data, the models were run with parameters for *LAI* dynamics and biomass production approaches as obtained from the calibration step for the Netherlands (assuming the values of the calibrated parameters  $fT_{\text{sum sen}}$ ,  $S_{\text{LA}}$ ,  $LAI_{\text{max}}$ , and the estimated value of *RUE* for the Netherlands to be representative for Europe). We adapted the phenology parameters for each location. As sowing and harvesting dates for spring wheat were not available for all locations, we used data for spring barley as a proxy (Table 2.5, Boons-Prins *et al.*, 1993).



**Fig. 2.1** Location of the nine weather stations, representing a climatic gradient (from Denmark to southern Spain). The 45°N line indicates the division of the climatic gradient in a northern and southern region.

**Table 2.5**

Location-specific phenological cultivar parameters used for the systematic comparison of models.

Countries	Latitude (°N)	Location*	Day of emergence (Day of year)	Temperature sum till maturity(i.e. harvesting date, (°Cd))
Denmark	57.1	North	90	1577
United Kingdom	52.35	North	51	1693
the Netherlands	52.1	North	85	1924
Germany	48.12	North	85	1383
France (centre)	47.97	North	64	1657
France (South)	43.62	South	36	2149
Italy	42.42	South	31	2044
Spain (centre)	40.45	South	31	2022
Spain (South)	37.42	South	31	2443

\*Regions at latitudes below 45°N are considered to be southern.

To evaluate the sensitivity of simulated yields to the modelling approaches, we performed an analysis of variance (ANOVA) to identify significant differences among simulated yields associated with the different approaches and locations (assumptions of ANOVA of normality of the data and homogeneity of variance were satisfied). With respect to location, we classified the nine locations into two categories (North versus South, using latitude as a criterion, Table 2.5) to be able to run the ANOVA and identified whether simulated yields significantly differed among the locations, but also between the different approaches (interaction effect) in the different locations.

The outcomes of this analysis indicate, as a first step, whether the simulated yields differ significantly among approaches and locations. But, they do not identify which process most strongly affects the simulated yield variability across locations. Therefore, we used the relative standard deviations ( $rSD$ ) (1) to determine if location-specific weather influenced the outcomes of a certain approach and thus if there is any effect of climatic variability on model outcomes and (2) understand the relative importance of the different light interception (i.e.  $LAI$  dynamics) and utilization (i.e. biomass production) approaches to capture this climatic variability:

$$rSD = \frac{\sigma_{yield}}{yield} \quad (\text{Eq. 2.19})$$

$rSD$  was calculated for (1)  $RUE$ , representing the light utilization approach, (2) intercepted photosynthetically active radiation ( $PAR$ ), representing the light interception approach, and (3) yield, which is the variable of interest and the integrated result of both processes.

Finally, a sensitivity analysis was carried out on parameters of the summarized and detailed approaches of  $LAI$  dynamics to evaluate the impact of a change in a given parameter on simulated yields. Parameter values given in Table 2.2 were used as default. We applied a range of variation in the parameters based on the variation found in the observed data and in the literature.  $LAI$  reached up to  $7 \text{ m}^2 \text{ m}^{-2}$  in the observed data (Meinke *et al.*, 1997). Furthermore, Hay and Porter (2006) indicated that 90% of the incoming radiation is usually intercepted at a  $LAI$  varying from 3 to  $5 \text{ m}^2 \text{ m}^{-2}$ . Therefore, we tested the sensitivity for this parameter from 3 to  $7 \text{ m}^2 \text{ m}^{-2}$ .  $S_{LA}$  varies from 0.036 to  $0.061 \text{ m}^2 (\text{gC})^{-1}$  in the observed data, in agreement with Stöckle *et al.* (2003). The first phase in  $LAI$  development, critical for  $LAI$  dynamics, is defined by the parameter  $R_g$  in the detailed approach. From calibration and values given in Van Delden *et al.* (2001) for spring wheat, we defined a range from 0.005 to  $0.013 (\text{°C d})^{-1}$  for  $R_g$ . Finally,



the timing of the onset of leaf senescence is defined by the parameter  $fT_{\text{sum sen}}$ , which varied from 0.5 to 0.7 in the observed data.

We varied each parameter within the defined range (Table 2.6) by small increments of  $\pm 1\text{--}4\%$ , depending on the parameter. We considered small increments to be able to identify the model sensitivity for the yield at harvest to each parameter. The sensitivity index ( $S_I$ ) is based on the local variation in the model output value with respect to the variation in the parameter:

$$S_I = \frac{\Delta_{\text{yield}}}{\Delta_{\text{parameter}}} \quad (\text{Eq. 2.20})$$

If  $S_I$  is small ( $S_I < 0.5$ ), it is assumed that the simulated yield is not highly sensitive to the parameter tested. This analysis gives some indication of the relative importance of the parameter for different locations and different approaches.

**Table 2.6**

Statistical setting used in the sensitivity analysis on the key parameter values of the light interception approaches.

Symbol	Description	Unit	Default	Standard deviation*	Increment	Source*
$S_{LA}$	Specific leaf area	$\text{m}^2 \text{gC}^{-1}$	0.048	0.0125	0.001	Own Dataset and Stöckle et al. (2003)
$R_g$	Relative growth rate of leaf area index during the juvenile phase	$^{\circ}\text{C}^{-1}\text{d}^{-1}$	0.009	0.004	0.0004	Van Delden et al. (2001)
$LAI_{\text{max}}$	Maximum leaf area index	$\text{m}^2 \text{m}^{-2}$	5	2	0.1	Own dataset and Hay and Porter (2006)
$fT_{\text{sum sen}}$	Fraction of the total temperature sum when senescence starts	unitless	0.6	0.1	0.01	Own dataset and Neitsch et al. (2002)

### 3. Results

#### 3.1 Test of the models with experimental data

After calibration, simulated yields reproduced the observed yield with a  $rRMSE$  ranging between 18% and 40% (Fig. 2.2), depending on the model. Agreement between simulated and observed yields was closest for models using the summarized  $LAI$  dynamics approach, especially when parameter values estimated from the observed data were used. The simulations of  $LAI$  dynamics support this observation. The models using the detailed  $LAI$  dynamics approach performed least satisfactorily with a  $rMAE$  of 0.50 versus a  $rMAE$  of 0.36 for the models using the summarized  $LAI$  dynamics approach. Although the  $rMAE$  and  $rRMSE$  values remain high, the results (Table 2.7) show that all approaches are able to reproduce variability in observed yield for a range of climatic conditions, especially the increasing yield for locations with higher amounts of radiation (USA 1992–93 and USA 1993–94) and the slight decrease for locations with recurrent high temperatures (USA 1995–96 and Europe 1995).

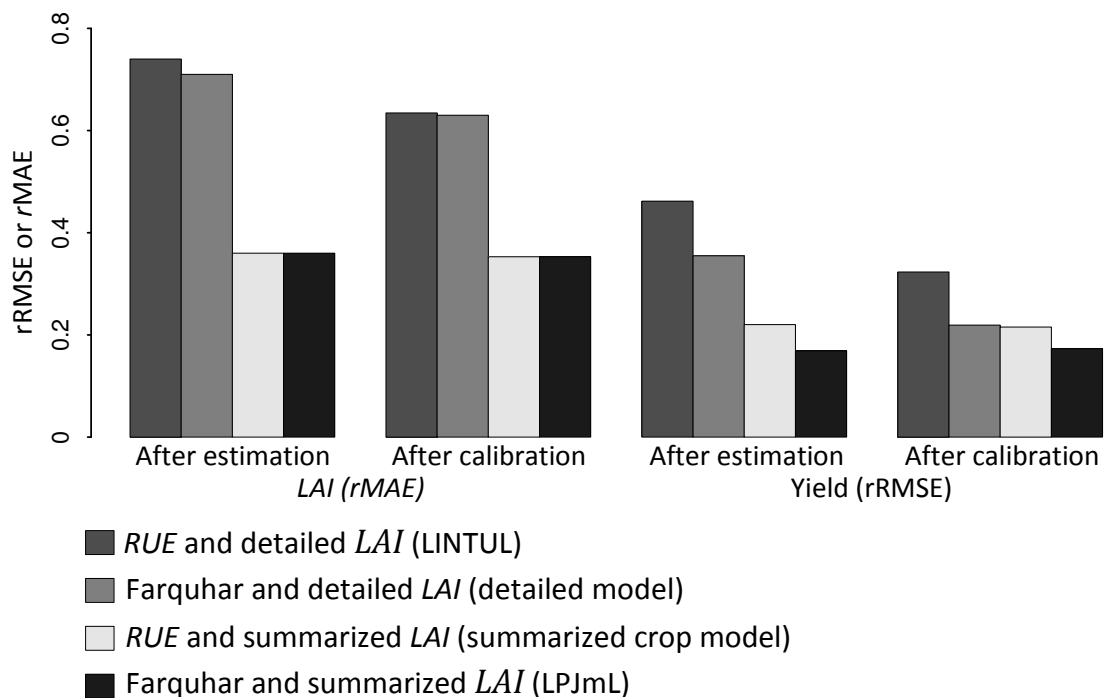


**Fig. 2.2** Averages, based on the six study sites, of the relative mean absolute error ( $rMAE$ ) to analyse the performance of the dynamics simulation and of the relative root mean square error ( $rRMSE$ ) to analyse the performance of simulated yield for the four studied models.

**Table 2.7**

Simulated and observed yields for the different locations after the calibration of the models.

	Australia, Queensland	Europe, The Netherlands	USA, Arizona		
	1993	1995	1996	1992-1993	1993-1994 1995-1996
Model name	Yield (t ha <sup>-1</sup> )				
LINTUL	9.8	5.4	5.0	6.1	6.6 5.2
Detailed crop model	7.6	5.6	5.9	9.0	8.8 8.2
Summarized crop model	7.8	6.0	6.0	6.6	6.6 6.5
LPJmL	6.7	6.3	6.5	8.5	8.4 8.3
Observations	7.2	7.6	9.1	8.0	8.2 6.8

If  $LAI_{max}$  is estimated from the observed data,  $LAI$  is simulated satisfactorily in the summarized  $LAI$  dynamics approach ( $rMAE = 0.36$ ), with no improvement through calibration (Fig. 2.2). Calibration is important in the detailed  $LAI$  dynamics approach, especially for  $R_g$ . The default value of  $R_g$  ( $0.009$  ( $^{\circ}Cd$ )<sup>-1</sup>) is based on Van Keulen and Seligman (1987) who included a wide range of data from different wheat cultivars (i.e. both spring and winter wheat) in their analysis. Spring wheat requires a higher value of  $R_g$ , corresponding to the range observed by Van Delden *et al.* (2001).

Finally, calibration of  $S_{LA}$  and  $fT_{sum\ sen}$  also improved the simulated yields, independent of the  $LAI$  dynamics approach (Eqs 2.2 & 2.5). With respect to the biomass production approaches, a lower value of  $RUE$  was estimated from the data for locations with higher temperatures and total accumulated radiation over the growing cycle (i.e. USA, Table 2.8). However, because of lack of data, it was not possible to define a clear relation between  $RUE$  on the one hand, and radiation and temperature on the other hand from our dataset. Table 2.8 gives the calibrated parameters for each location.

The models using the summarized  $LAI$  dynamics approach could simulate crop productivity reasonably well in locations with different radiation and temperature regimes (Fig. 2.2). However, this is achieved only when applying parameter values estimated from the dataset. When applying the models for a wider range of conditions, the issue of data availability needs to be considered.

**Table 2.8**

Parameter values after calibration, using experimental datasets.

Parameter	Unit	Australia, Queensland	Europe, The Netherlands	USA, Arizona
$fT_{\text{sum sen}}$	Unitless	0.61	0.54	0.55
$T_{\text{sum}}$	(°Cd)	1804	1609	2070
$R_g$	°C <sup>-1</sup> d <sup>-1</sup>	0.013	0.013	0.010
$S_{\text{LA}}$	m <sup>2</sup> gC <sup>-1</sup>	0.06	0.045	0.054
$LAI_{\text{max}}$	m <sup>2</sup> m <sup>-2</sup>	7	6.75	6.35
$RUE^*$	gC MJ <sup>-1</sup>	1.52	1.33	1.01

\*  $RUE$  was not calibrated (but estimated) to avoid a compensation error with the  $S_{\text{LA}}$  parameter.

**Table 2.9**Relative standard deviation ( $rSD$ ) to define the ability of each approach to capture climatic variability.

	Summarized $LAI$ dynamics approach		Detailed $LAI$ dynamics approach	
	LPJmL (Farquhar)	Summarized crop model ( $RUE$ )	Detailed crop model (Farquhar)	LINTUL ( $RUE$ )
$rSD$ yield	0.12	0.15	0.12	0.20
$rSD$ intercepted $PAR$	0.16	0.16	0.24	0.26
$rSD$ for $RUE$	0.04	0.00	0.04	0.00

**Table 2.10**

Analysis of variance to identify whether the different modelling approaches and locations (North versus South) result in significant differences in simulated yields.

Response: yield	Sum of squares	$df$	$F$ -value	$Pr(>F)$
Biomass production approach	0.30	1	0.56	0.46
$LAI$ dynamics approach	4.23	1	7.99	0.009**
Location (North versus South)	12.78	1	24.15	$3.50 \times 10^{-5}$ ***
Biomass production $\times$ $LAI$ dynamics approach	0.47	1	0.89	0.35
Biomass production approach $\times$ location	2.93	1	5.53	0.03*
$LAI$ dynamics approach $\times$ location	1.44	1	2.72	0.11
Biomass production approach $\times$ $LAI$ dynamics approach $\times$ location	0.91	1	1.73	0.20
Residuals	14.82	28		

$\times$  means that the different factors have been considered in the analysis.

\*\*\* 0.001

\*\* 0.01

\* 0.05

## 3.2 Model behaviour in response to climatic conditions

### 3.2.1 Sensitivity of simulated yield to the different modelling approaches

To investigate the behaviour of the models in capturing the effects of different climatic regimes as relevant for regional applications, we ran the four models with weather data from a climatic range across Europe. The parameter values (except for phenology) originated from the calibration for the Netherlands using our observation dataset and we considered them as representative for Europe. Simulated yields vary from a maximum of 8.38 Mg dry matter ha<sup>-1</sup> in southern Spain to a minimum of 4.44 Mg dry matter ha<sup>-1</sup> in Germany (Fig. 2.3). The minimum yield was simulated with the combination of the detailed *LAI* dynamics and the *RUE* approach (LINTUL), while the maximum was simulated with the combination of the summarized *LAI* dynamics and the *RUE* approach (summarized crop model). LINTUL shows the strongest response to climatic variability ( $\tau$ SD = 0.20, Table 2.9), while the two models using the Farquhar approach (LPJmL and detailed crop model) show the weakest response ( $\tau$ SD = 0.12, Table 2.9).

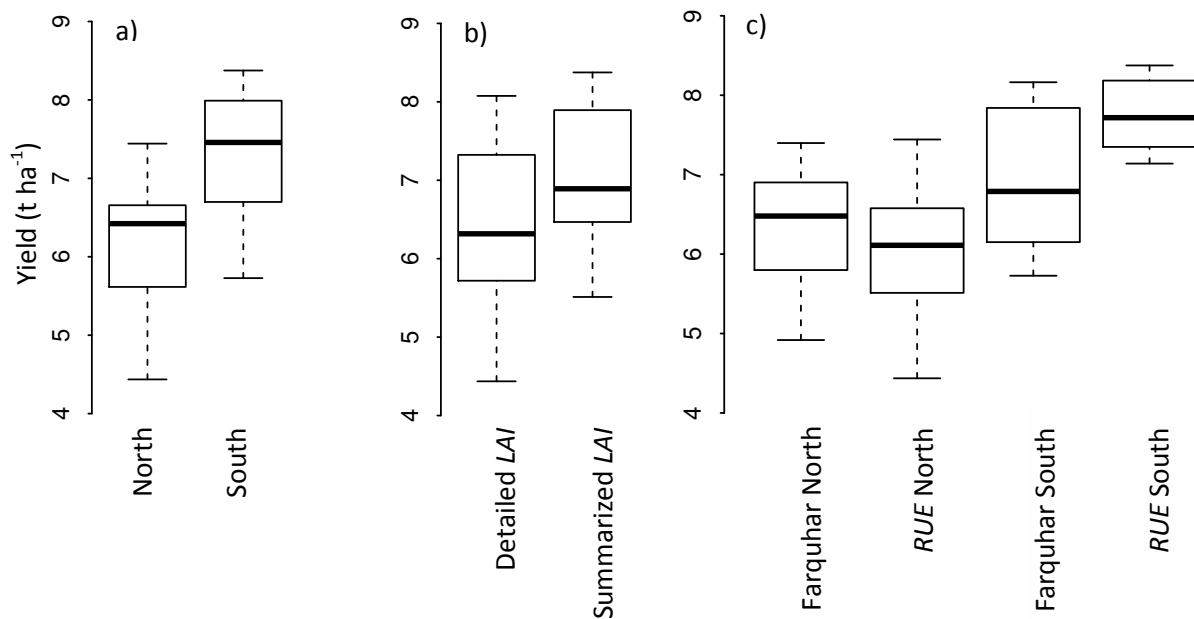


**Fig. 2.3** Ranges of simulated yields for a wide range of conditions in Europe according to: a) location (i.e. North versus South), b) *LAI* dynamics approaches per location (i.e. detailed *LAI* versus summarized *LAI*), and c) biomass production approaches depending on the locations (i.e. Farquhar North versus *RUE* North and Farquhar South versus *RUE* South).

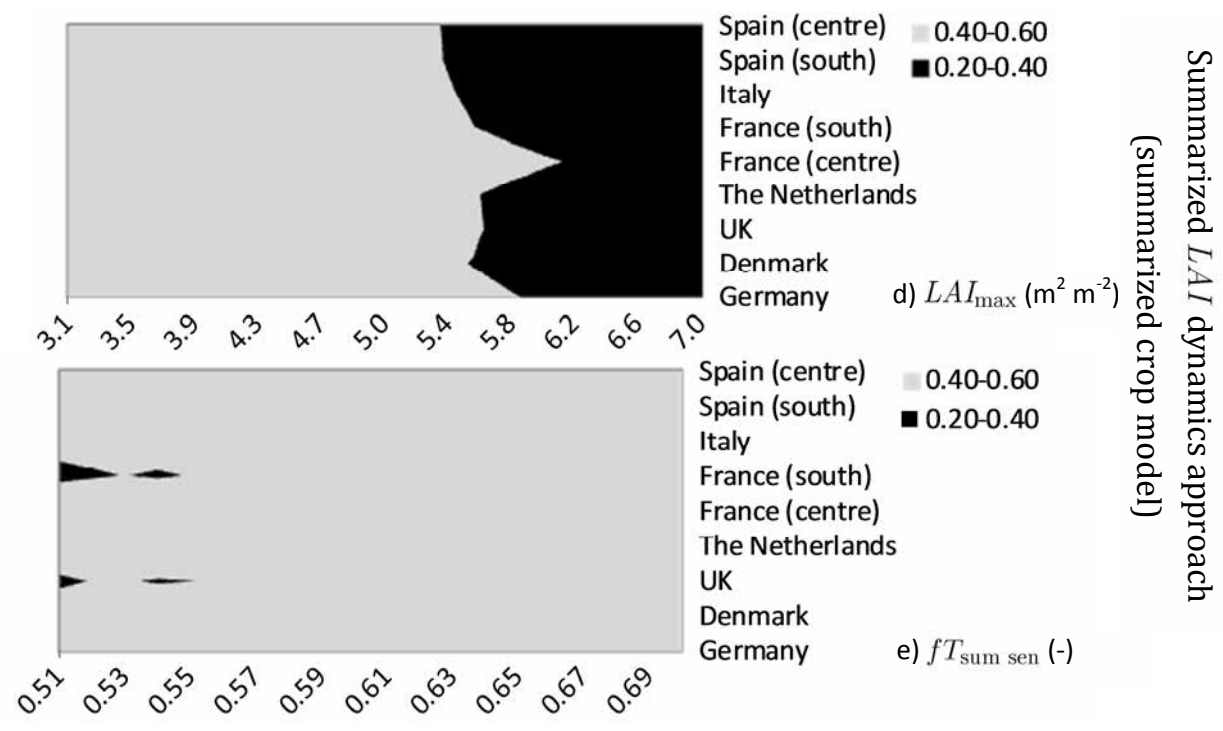
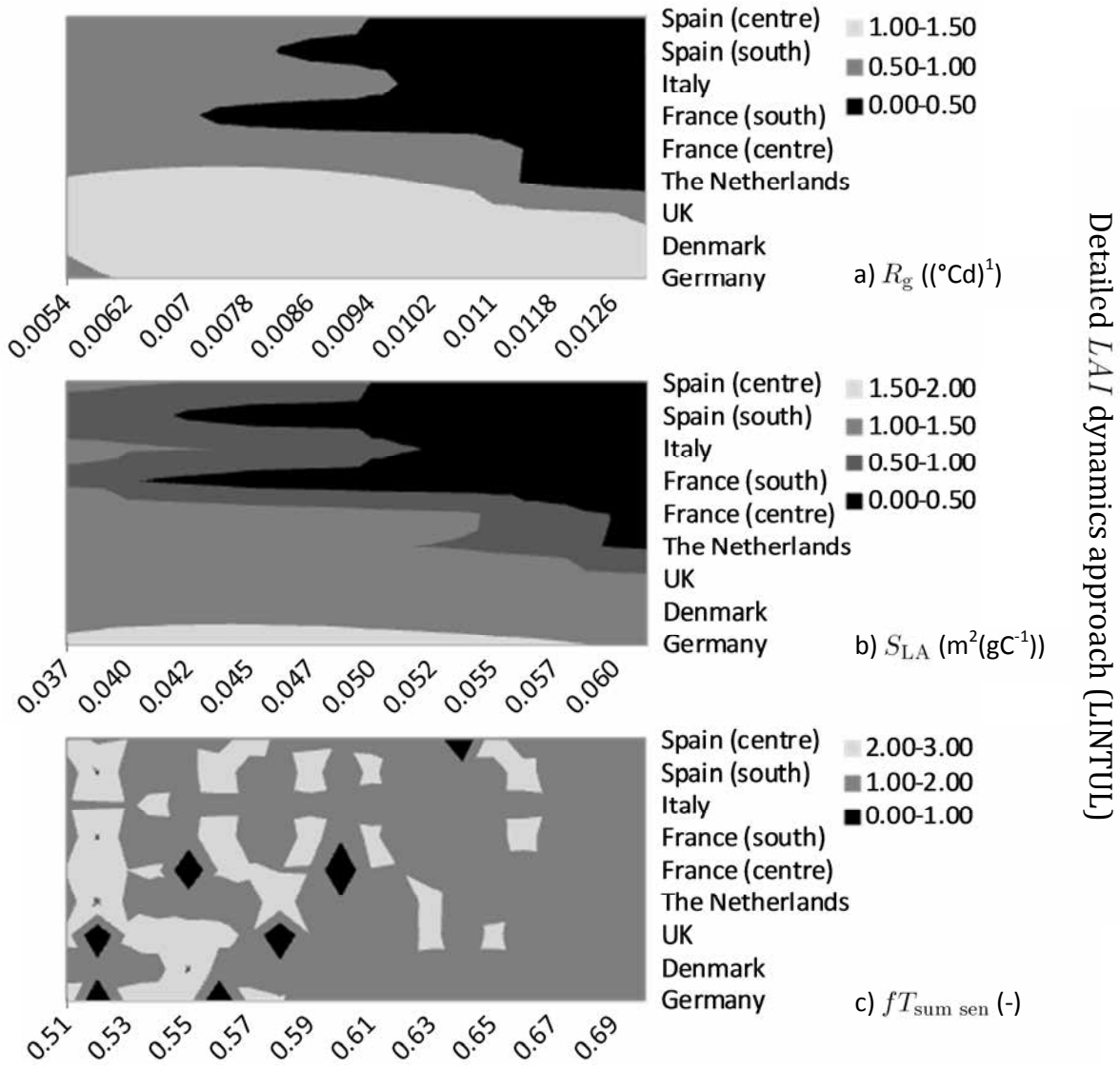
Further, to better understand which process is more sensitive to climatic variability, we used the relative standard deviations ( $rSD$ ) of  $RUE$  and intercepted  $PAR$  (Table 2.9). The calculated  $RUE$  value, based on outcomes from the Farquhar approach, is slightly influenced by climatic variability ( $rSD = 0.04$ ). Intercepted  $PAR$  shows the highest  $rSD$  values, especially when using the detailed  $LAI$  dynamics approach, demonstrating that this process is most sensitive to climatic variability ( $rSD = 0.24$ – $0.26$ ).

From the ANOVA (Table 2.10), we found that the location (i.e. northern versus southern regions) has a clear influence on simulated yields, independent of the approach chosen ( $p < 0.001$ ): simulated yields are higher in southern regions than in northern regions (Fig. 2.3a). Moreover, the choice of the  $LAI$  dynamics approach is important which is independent of the location ( $p < 0.01$ ): simulated yields are always higher with the summarized  $LAI$  dynamics approach (Fig. 2.3b).

Finally, the ANOVA demonstrates a significant difference in simulated yields for the two biomass production approaches, depending on location ( $p < 0.05$ ):  $RUE$  simulates higher yields in southern regions than the Farquhar approach, while the Farquhar approach simulates higher yields in northern regions (Fig. 2.3c). The latter results suggest that if the  $RUE$  approach is used it should be adjusted for the effects of temperature and radiation.

### 3.2.2 Sensitivity to parameter values for the $LAI$ dynamics approaches

The choice of the light interception approach has a significant influence on simulated yields (ANOVA results, Table 2.10) and this process most strongly reflects the effect of climatic variability on yields (indicated by a higher  $rSD$ , Table 2.9). Subsequently, we carried out a sensitivity analysis on key parameters of the light interception approaches to assess their relative importance for the simulated yields, when combined with the  $RUE$  approach. Fig. 2.4 shows the sensitivity index ( $S_I$ ) for the parameters tested in the two  $LAI$  dynamics approaches. The sensitivity of simulated yield is different for the different parameters considered (Fig. 2.4). The sensitivity of simulated yields is irregular in the detailed  $LAI$  dynamics approach, while it is smooth in the summarized  $LAI$  dynamics approach.



The relative growth rate of *LAI* in the exponential phase ( $R_g$ ), used in the detailed *LAI* dynamics approach, was varied from 0.005 to 0.013 ( $^{\circ}\text{Cd}$ )<sup>-1</sup>. The sensitivity of simulated yield to this parameter is variable, depending on location and the value of the parameter itself. On the one hand, simulated yields are highly sensitive to  $R_g$  in the northern locations (Germany, Denmark, the United Kingdom and partly the Netherlands) with a  $S_I$  between 1 and 1.5 (i.e. a change in  $R_g$  by 1% will result in a change in simulated yield of 1–1.5%). On the other hand, in the southern regions, a change in  $R_g$  has a relatively smaller impact on simulated yields, especially for values exceeding the default value of 0.009 ( $^{\circ}\text{Cd}$ )<sup>-1</sup> (Fig. 2.4a). From the calibration we obtained a value for  $R_g$  of 0.013 ( $^{\circ}\text{Cd}$ )<sup>-1</sup>, which implies that only simulated yields in Germany, Denmark and the United Kingdom will be highly sensitive to a variation in this value ( $S_I > 1$ ).

$S_{LA}$  (varying from 0.0036 to 0.06 m<sup>2</sup> (gC)<sup>-1</sup>) behaves similarly, with the exception of a higher sensitivity ( $S_I > 1$ ) in southern regions (i.e. Italy and Central Spain) with values of  $S_{LA} < 0.042$  m<sup>2</sup> (gC)<sup>-1</sup> (Fig. 2.4b). When using a value of 0.045 m<sup>2</sup> (gC)<sup>-1</sup> for  $S_{LA}$  (derived from the calibration for the Netherlands), the northern regions are highly sensitive ( $S_I > 1$ ) and most of the southern regions moderately sensitive ( $0.5 < S_I < 1$ ), except for southern France and southern Spain, where yield sensitivity is relatively small ( $S_I < 0.5$ ) to a variation in this parameter.

The sensitivity of simulated yield to  $fT_{\text{sum sen}}$  in the detailed *LAI* dynamics approach is high (Fig. 2.4c). For values of  $fT_{\text{sum sen}}$  exceeding 0.66, the sensitivity of simulated yield is uniform among locations ( $S_I > 1$ ). For values of  $fT_{\text{sum sen}}$  below 0.6, the yield is highly sensitive in many locations ( $S_I > 2$ ). However, interestingly, for a few locations and some specific values of  $fT_{\text{sum sen}}$ , the simulated yield is not sensitive to a change in its value (Fig. 2.4c, e.g. the United Kingdom for a value of 0.52).

**Fig. 2.4.** Sensitivity index ( $S_I$ ) of the yield for the main parameters according to the *LAI* dynamics approaches.  $S_I = 1$  means that the change of the parameter value will induce the same amount of change for the simulated yield. The symbol referring to the locations are the same as the one in Table 2.5. The parameters tested are: a)  $R_g$ : relative growth rate of leaf area index during the juvenile phase for the detailed *LAI* dynamics; b)  $S_{LA}$ : specific leaf area for the detailed *LAI* dynamics; c)  $fT_{\text{sum sen}}$ : fraction of the total temperature sum when senescence starts for the detailed *LAI* dynamics; d)  $LAI_{\text{max}}$ : maximum leaf area index for the summarized *LAI* dynamics; e)  $fT_{\text{sum sen}}$ : fraction of the total temperature sum when senescence starts for the summarized *LAI* dynamics.



For the model using the summarized  $LAI$  dynamics approach, the results of the sensitivity analysis are much more straightforward, with a moderate sensitivity ( $0.4 < S_I < 0.6$ ) of the simulated yield to both parameters  $LAI_{\max}$  (Fig. 2.4d) and  $fT_{\text{sum sen}}$  (Fig. 2.4e). For  $LAI_{\max}$  exceeding  $5.5 \text{ m}^2 \text{ m}^{-2}$ , the sensitivity of the simulated yield is even lower ( $0.2 < S_I < 0.4$ ), independent of the location.

## 4. Discussion

### 4.1 General behaviour of the models

All models simulated higher yields in southern regions than in northern regions (Fig. 2.3a), associated with longer growing seasons and higher radiation intensities during the growing season, due to earlier sowing dates and higher temperature sums till physiological maturity (Boons–Prins *et al.*, 1993, Table 2.5). The consequence is higher accumulated intercepted  $PAR$ , leading to higher biomass accumulation and therefore higher simulated yields. Such model outcomes are contrary to what is observed (yields are usually lower in southern regions than in northern regions in Europe, Van Oijen and Ewert, 1999). Indeed, the input data in terms of phenology were derived from spring barley, because of lack of available data for spring wheat (Boons–Prins *et al.*, 1993). This proxy may be questionable, as other studies report that spring wheat can be sown between November–December in Mediterranean regions (Russell and Wilson, 1994). The temperature sum till maturity for the Germany site is also questionable. Hence, this result underlines the importance of adequately including farmers' practices (e.g. sowing time and cultivar use) at different locations, as a response to the spatial variability in climate (Reidsma *et al.*, 2010). Further, it may not be sufficient to only adapt model parameters for phenology (e.g. Therond *et al.*, in press) for larger scale applications, but also to evaluate the use of approaches to simulate key growth processes in response to climatic variability.

### 4.2 Biomass production approaches

The two biomass production approaches result in significant differences in simulated yields, differentiated among locations. The  $RUE$  approach simulates higher yields in southern regions than the Farquhar approach, while the Farquhar approach simulates higher yields in northern regions (Fig. 2.3c). Using the  $RUE$  approach, with a constant  $RUE$  value for large scale applications (Tan and Shibasaki, 2003; Liu *et al.*, 2007), we might over-simplify, ignoring effects of high temperatures and high radiation intensities on net photosynthesis, which

are both considered in the Farquhar approach (Fig. 2.5) or on daily light use efficiency as reported in Choudhury (2000, 2001).

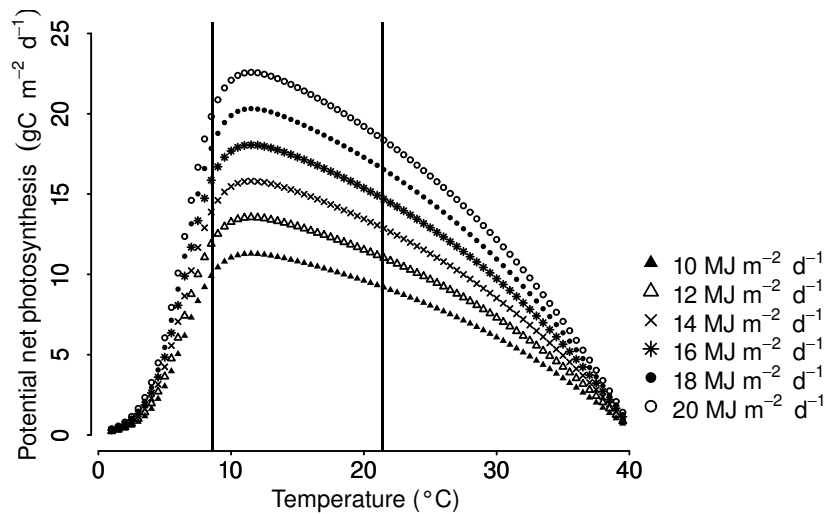


**Fig. 2.5** Potential net photosynthesis ( $A_{nd}$ ) as a function of temperature and a number of constant total radiation intensities at one  $\text{CO}_2$  concentration of 340 ppm, which represents the  $\text{CO}_2$  concentration in the year 1982. The two vertical lines indicate the temperature limits where  $A_{nd}$  is 75% of its maximum value (7.5 and 22.5 °C) for the Farquhar approach (detailed biomass production approach).

The use of a constant  $RUE$  (over the growing cycle as a whole) incorporates a lower conversion efficiency during the grain filling period due to, mostly, reallocation of assimilates to the grains (Van Keulen and Seligman, 1987). Moreover, when  $LAI$  reaches values of 3–4  $\text{m}^2 \text{m}^{-2}$ , the effect of radiation intensity on  $RUE$  reflects the light saturation effect. Higher radiation then leads to lower  $RUE$ , as the leaves at the top of the canopy are light saturated and thus, higher light absorption does not lead to higher assimilation (Hay and Porter, 2006). As a consequence, conversion efficiency calculated on the basis of total absorbed radiation is lower. Finally, this aggregated value of  $RUE$  also includes the temperature effect on respiration processes. So, to keep the model as simple as possible, i.e. to appropriately balance between data availability and model structure for large scale applications (Addiscott, 1998; Hansen and Jones, 2000; Jagtap and Jones, 2002), the  $RUE$  approach could be extended by incorporating the effects of temperature and radiation (Stöckle and Kemanian, 2009). Our observed data were too limited to define a significant relationship between  $RUE$  and radiation and temperature. We therefore propose to examine this relationship with more extensive datasets and consider adapting the seasonal

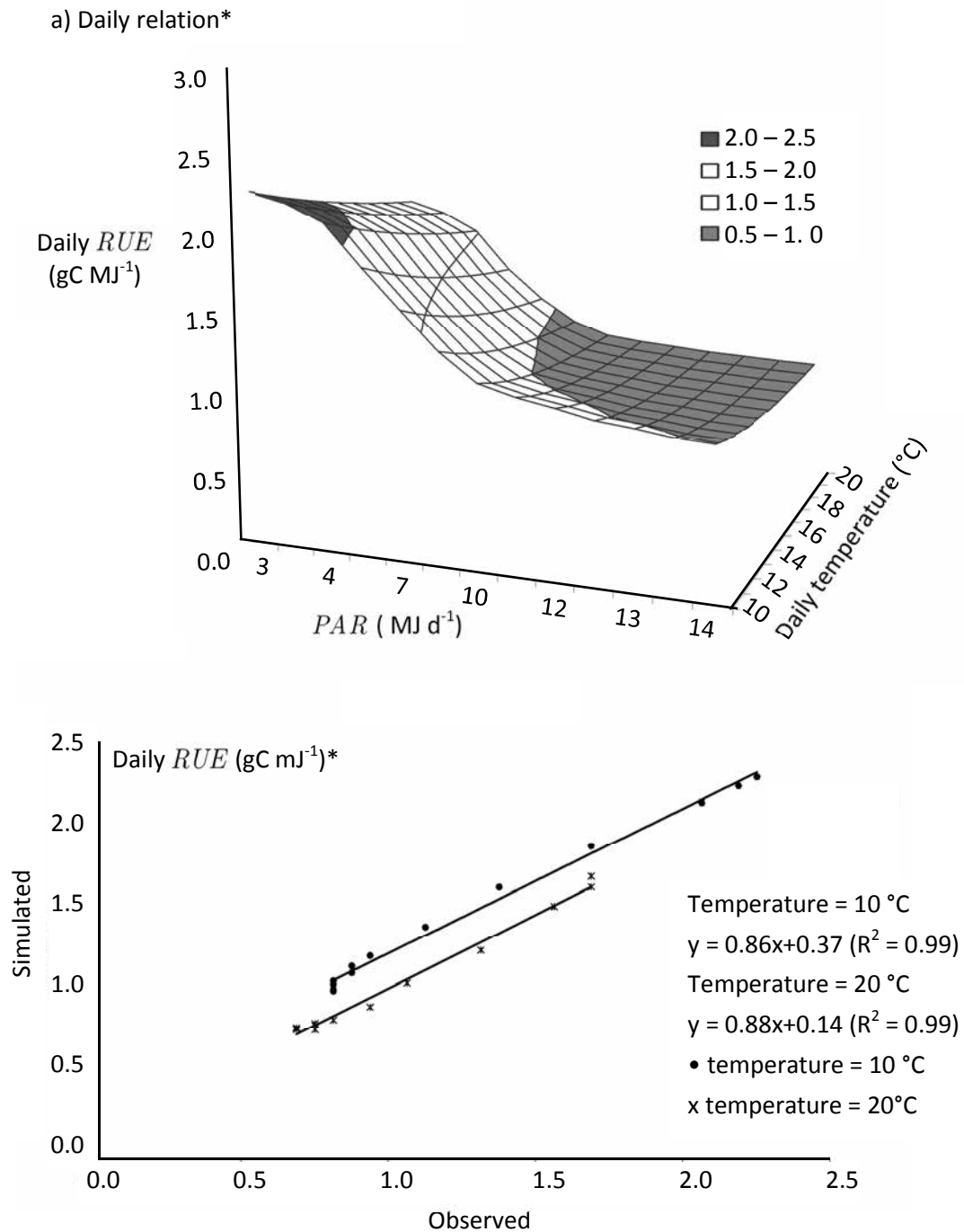


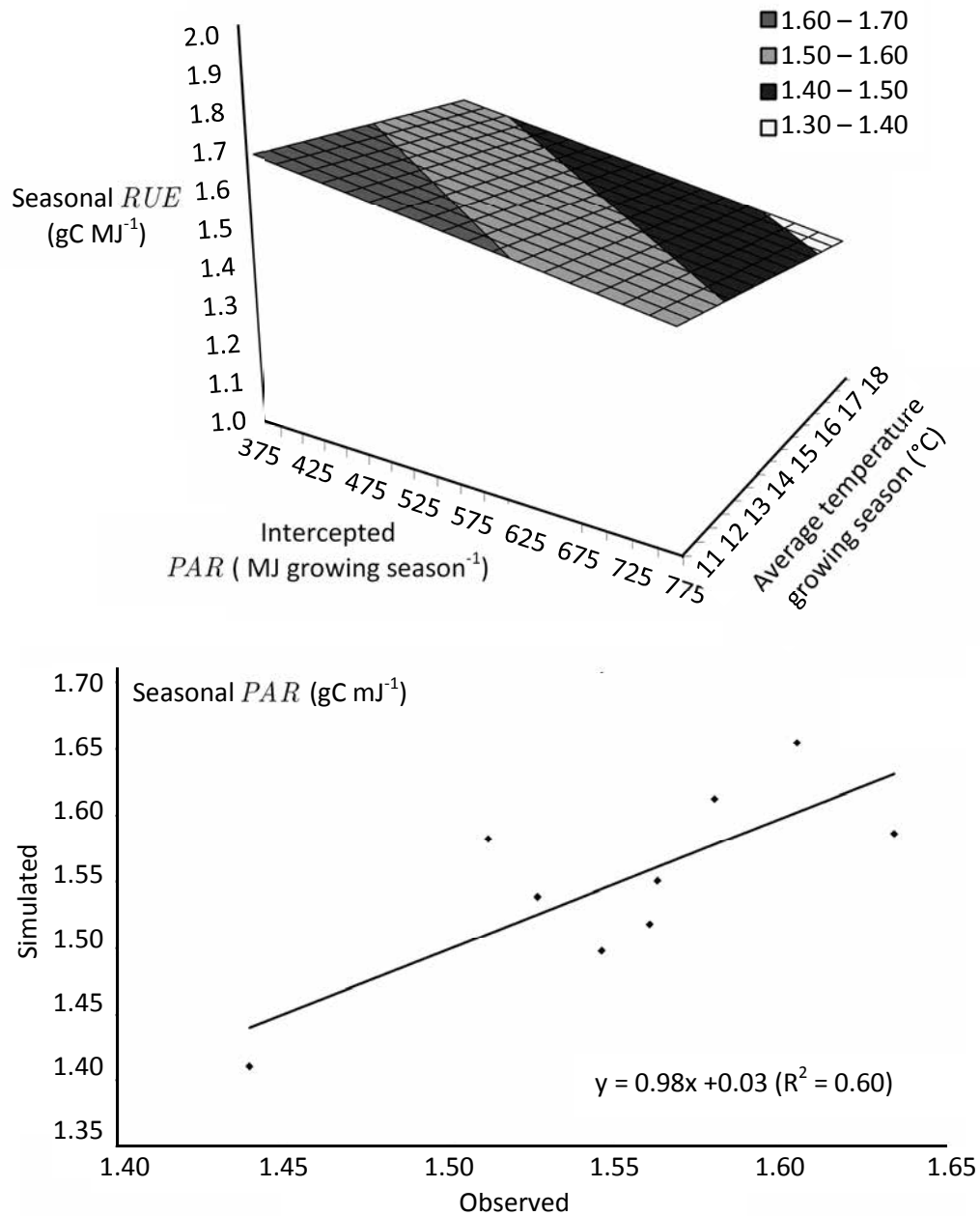
**Fig. 2.6** Scaling of *RUE* for large scale applications, from a) an exponential relation\* on a daily basis (from Choudhury, 2000) b) a linear relation\*\* on a seasonal basis: graphical representation of the relation and observed versus simulated *RUE* for both cases.

\*The daily *RUE* ranges 0.75 to 2.25 gC MJ<sup>-1</sup>, according to:

$$RUE = 0.75 + 2.5 \times \exp(-(0.016 \times \text{temp}) \times PAR) \text{ with } 10 \leq \text{temp} \leq 20 \text{ and } 3 \leq PAR \leq 14$$

temp = daily average temperature (°C) and *PAR* = daily photosynthetically active radiation (MJ m<sup>-2</sup> d<sup>-1</sup>).

## b) Seasonal relation\*\*



\*\*The seasonal RUE ranges 1.45 to 1.65 gC MJ<sup>-1</sup> according to:

$$RUE = 2.1 - 3.5 \times 10^{-4} \times PAR_{INT} + 2.5 \times 10^{-2} \times temp$$

with  $11 \leq temp \leq 18$  and  $375 \leq intercepted\ PAR \leq 800$

temp = average temperature during the growing season (°C) and intercepted PAR = intercepted photosynthetically active radiation (MJm<sup>-2</sup> growing season<sup>-1</sup>).

*RUE* value (Medlyn, 1998; Sinclair and Muchow, 1999) which can be supported by using results of the Farquhar photosynthesis algorithms (Mitchell *et al.*, 2000). Fig. 2.6 demonstrates how the effect of temperature and radiation on the value of *RUE* could be expressed on a daily basis (derived from Choudhury, 2001) and on a seasonal basis (derived from the present study), which is more appropriate for regional applications of crop growth models.

### 4.3 Leaf area index dynamics approaches

The two different light interception approaches result in significant differences in simulated yields, independent of the location considered, and most clearly capture climatic variability. These results confirm earlier work that identified light interception as an important factor in determining crop growth (Heath and Gregory, 1938; Watson, 1947) and with later ones in the context of climate change studies (Jamieson *et al.*, 1998a; Ewert, 2004a).

Using the same parameter values, the summarized *LAI* dynamics approach simulates higher yields than the detailed *LAI* dynamics approach (Fig. 2.3b). We assumed the  $fT_{\text{sum sen}}$  parameter to have the same value in both approaches, as it was difficult to find an unambiguous definition of this parameter (i.e. onset of leaf senescence). In some cases,  $fT_{\text{sum sen}}$  is equivalent with the physiological meaning of leaf senescence, i.e. when leaves actually start to senesce (Havelka *et al.*, 1984), while in some other cases, it is a visual interpretation of the phenomenon (Mi *et al.*, 2000; Araus and Tapia, 1987), when the death rate of leaves overrides their growth rates. We considered the timing of the onset of senescence to be equal in the two approaches, i.e. at anthesis, in line with the detailed approach. However, the original description of the summarized approach defined the timing of the onset of senescence more on a visual observation: “*LAI* will remain constant until leaf-senescence begins to exceed leaf growth” (Neitsch *et al.*, 2005, p. 294). Furthermore, we assumed the timing of the onset of senescence to be identical across locations. However, phenological characteristics (e.g. temperature sum requirements till anthesis) of wheat vary among cultivars (Slafer and Rawson, 1994), suggesting the need to also define location-specific values for  $fT_{\text{sum sen}}$ . Hence, looking at differences in simulated yield due to the different modelling approaches, we attributed the different responses of the models to the use of the same parameter values, although the underlying assumptions, lumped in the  $fT_{\text{sum sen}}$  parameter value, are essentially different for the two approaches.

## 5. Concluding remarks

We focused on potential production as a first step to investigate the effect of modelling detail under a wide range of climatic conditions. From the two key processes determining growth, i.e. light interception and utilization, we found that light interception as determined by *LAI* dynamics is most important in explaining yield sensitivity to climatic variability. We also showed that a different light interception approach results in significant differences in simulated yields, irrespective of the location. We conclude that for large scale applications of crop models particular attention should be given to the simulation of light interception via the *LAI* approach used. Most critical in this respect is the representation of leaf senescence, particularly the onset, which is modelled differently in crop models, but has considerable impact on the model outputs. Accordingly, further research should attempt to improve the representation of leaf senescence in crop models for large scale applications.

We also found that an oversimplification of processes can lead to omission of important relationships, as for the application of the *RUE* concept. We propose that models using the concept of *RUE* should adjust seasonal *RUE* by temperature and radiation effects. However, further research is needed to quantify these relationships.

Our results provide first indications about the needed physiological detail in process-based models to capture the effect of climate variability on potential crop productivity across large areas. We demonstrated that through an integrated analysis of detailed and summarized approaches more insight can be gained about the structure of crop models for large scale applications, in order to support the selections concerning the trade-off between data availability and modelling detail. As our study refers to potential production only, the analysis should be extended in a next step to also look at e.g. the effects of the rainfall distribution within the season on crop growth and yield (Adam *et al.*, 2008).

## Acknowledgements

This work has been carried out as part of the SEAMLESS integrated project, EU 6th Framework Programme for Research, Technological Development and Demonstration, Priority 1.1.6.3. Global Change and Ecosystems (European Commission, DG Research, Contract No. 010036-2). The authors are grateful to C. Müller (Potsdam Institute for Climate Impact Research-PIK) for his help to incorporate the LPJmL model into our framework, in an early stage of the study.





## Chapter 3

# **The effect of temporal aggregation of weather input data on crop growth models' results**

Based on:  
Van Bussel, L.G.J., Müller, C., Van Keulen, H., Ewert, F., Leffelaar, P.A.:  
The effect of temporal aggregation of weather input data on  
crop growth models' results.  
Agricultural and Forest Meteorology, vol. 151 (2011), 607-619



## Abstract

Weather data are essential inputs for crop growth models, which are primarily developed for field level applications using site-specific daily weather data. Daily weather data are often not available, especially when models are applied to large regions and/or for future projections. It is possible to generate daily weather data from aggregated weather data, such as average monthly weather data, e.g. through a linear interpolation method. But, due to the nonlinearity of many weather–crop relationships, results of simulations using linearly interpolated data will deviate from those with actual (daily) data. The objective of this study was to analyse the sensitivity of different modelling approaches to the temporal resolution of weather input data. We used spring wheat as an example and considered three combinations of summarized and detailed approaches to model leaf area index development and associated radiation interception and biomass productivity, reflecting the typical range of detail in the structure of most models. Models were run with actual weather data and with aggregated weather data from which day-to-day variation had been removed by linear interpolation between monthly averages.

Results from different climatic regions in Europe show that simulated biomass differs between model simulations using actual or aggregated temperature and/or radiation data. In addition, we find a relationship between the sensitivity of an approach to interpolation of input data and the degree of detail in that modelling approach: increasing detail results in higher sensitivity. Moreover, the magnitude of the day-to-day variability in weather conditions affects the results: increasing variability results in stronger differences between model results. Our results have implications for the choice of a specific approach to model a certain process depending on the available temporal resolution of input data.

## 1. Introduction

In recent years, crop productivity assessments have extended from the plot and field scale to the regional or even global scale including much longer time horizons (100 years or more), e.g. to study the effects of global climate change on global crop productivity (Ewert, 2004b; Leemans, 1997). The only suitable tools for quantitative assessment of future global crop productivity are crop growth models. Early crop growth models mainly concentrated on plot and field scale (Hansen *et al.*, 2006; Monteith, 2000; Van Ittersum *et al.*, 2003) for assessments covering time-horizons of a season or a year. Due to the change in the scale of crop productivity assessments, crop growth models, with varying degree of detail, are increasingly applied at the continental or global scale, for example: LPJmL (Lund Potsdam Jena managed Land; Bondeau *et al.*, 2007), DAYCENT (Stehfest *et al.*, 2007), GEPIC (Liu *et al.*, 2007), GLAM (Challinor *et al.*, 2004), GAEZ (Tubiello and Fischer, 2007), and WOFOST (Reidsma *et al.*, 2009).

If crop growth models are applied at large scales, problems arise with respect to missing input data (Nonhebel, 1994) and lack of parameter values for different regions with regard to e.g. specific cultivar characteristics. Applying models in regions with missing input data or in regions beyond the domain for which they were developed and validated, may lead to unreliable results (Ewert *et al.*, 2005; Irmak *et al.*, 2005).

Field-scale crop growth models are typically based and validated on site-specific daily weather input data. Historical global daily weather data sets are available, see e.g. Sheffield *et al.* (2006) and Hirabayashi *et al.* (2008), with spatial scales of  $1^\circ \times 1^\circ$  and  $0.5^\circ \times 0.5^\circ$  grid cells, respectively. For climate change scenarios, some global circulation models (GCMs) provide daily weather data (LLNL, 1989), however, GCM performance at this level of temporal detail has hardly been evaluated; posing considerable limitations on the use of daily weather data from GCMs in climate change impact studies. Alternatively, monthly weather data aggregates for climate change scenarios are available from large-scale climate data sets. Missing daily weather data, such as radiation and temperature, can then be generated on the basis of these average monthly weather data (Nonhebel, 1994; Soltani *et al.*, 2004). Conversion from aggregated, monthly data to daily data can be achieved by (a) simple linear interpolation between monthly averages, as e.g. applied in the LPJmL model (Bondeau *et al.*, 2007; Sitch *et al.*, 2003) and the GLAM model (Challinor *et al.*, 2004) or (b) assuming that weather conditions for all days within one month are identical to the monthly averages, as e.g. applied in a global application of DAYCENT (Stehfest *et al.*, 2007). In addition, monthly averages can be disaggregated to

daily values using weather generators, such as stochastic weather generators (e.g. applied by Semenov, 2009), parametric weather generators (e.g. applied by Liu *et al.*, 2009), or semi-parametric weather generators (e.g. applied by Apipattanavis *et al.*, 2010).

Crop growth is the result of nonlinear, dynamic relations between weather, soil water and nutrients, management, and specific crop characteristics (Hammer *et al.*, 2002; Hansen *et al.*, 2006; Semenov and Porter, 1995). Some processes, e.g. photosynthesis, show continuous and mainly nonlinear changes in their rates if temperature changes. Other processes, such as phenological development, show a much more linear change with variation in temperature. Finally, crops also respond to absolute changes in temperature, i.e. if a crop experiences temperatures outside the range of those typically experienced, significant yield losses may be the result (Porter and Semenov, 2005), e.g. a short period of extremely high temperatures near anthesis in wheat can result in a high number of sterile florets (Ferris *et al.*, 1998; Mitchell *et al.*, 1993). These relationships are implemented in crop growth models in various ways, with different levels of abstraction being used.

Generated weather data, based on linear interpolation or on the assumption of identical weather conditions within one month, lack day-to-day variability in weather patterns, e.g. extreme temperatures are eliminated, in contrast to weather data generated by a weather generator. However, weather generators suffer from various shortcomings, such as lack of available observed site-specific daily weather data in order to calibrate the weather generator (stochastic and semi-parametric weather generators) or normal distributed data (parametric weather generators) (Apipattanavis *et al.*, 2010). Moreover, so far, weather generators have only been tested for specific regions or sites, which leaves doubt about their applicability at the global scale.

Although linear interpolation is a pragmatic method to generate daily weather data at the global scale, its applicability needs to be carefully examined, because of the nonlinear relationships implemented in crop growth models, which can bias model results considerably (Hansen *et al.*, 2006; Nonhebel, 1994; Semenov and Porter, 1995). Especially in regions with high day-to-day weather variability, linearly generated weather data will show substantial deviations from actual weather. Consequently, differences in model results are likely to be largest in regions with high day-to-day variability. As extreme weather events have been projected to occur more frequently in the future (Beniston *et al.*, 2007; Easterling *et al.*, 2000; Salinger *et al.*, 2005), the use of interpolated data will exclude this aspect of climate change from impact studies.

Temporal aggregation of temperature and radiation data will have different effects on different processes considered in crop growth models, as these differ in their sensitivity to temperature and radiation. Moreover, the degree of detail taken into account in modelling specific processes may determine their sensitivity to temporally aggregated data. Our hypothesis is that a detailed model is more sensitive to the use of aggregated data than a more summarized model. A detailed model is defined in this study as a more explanatory model, i.e. a model that contains most of the interactions and elements important for the system. In contrast, a summarized model is in general more descriptive, it often contains simplified representations of the complicated interactions and processes in the system. The difference in sensitivity between detailed and summarized models is expected due to differences in their characteristic times (or reaction rates) and in their number of nonlinear relationships considered. Crop growth models applied at the continental or global scale differ in their level of detail to simulate the various processes of crop growth. Consequently, the use of temporally aggregated weather data may have different effects on simulation results among global crop growth models.

Therefore, the objective of this study is to examine the sensitivity of crop models with different modelling detail to the temporal resolution of weather input data. This should provide more insight in the upscaling of important crop growth processes from field to regional level for global applications. We use spring wheat (*Triticum aestivum*) as an example and analyse two important processes, leaf area development, to simulate radiation interception, and biomass productivity. For each process a summarized and a more detailed modelling approach is used. None of the models used here covers damage due to extreme weather events such as heat stress. These impacts on crop yields are of increasing concern due to expected future climate changes (Battisti and Naylor, 2009; Long and Ort, 2010; Soussana *et al.*, 2010) and are likely to be very sensitive to the temporal resolution of input data if included in crop growth models. To examine the possible impacts, we have tested a simple threshold model with daily observed and monthly aggregated data sets, and discuss the implications for modelling. Consequently, the effects of temporal resolution of input data on results of crop growth models have to be studied, as data aggregation leads to information losses.

Results are presented for nine locations across Europe, to analyse the effects under different climatic conditions. For each location, both fully irrigated and rainfed conditions were considered.

## 2. Material and methods

In crop growth models, two processes play an important role in determining biomass dynamics: radiation interception by leaves and utilization of the intercepted radiation to produce biomass via the photosynthesis process (Gabrielle et al., 1998; Monteith, 1977; Van Delden et al., 2001; Yin et al., 2000). In this study we applied three combinations of summarized and detailed approaches to model radiation interception and biomass productivity, reflecting a range of detail in model structure: a summarized biomass productivity approach was combined with a summarized and a detailed leaf area index approach (Fig. 3.1a and b, respectively) and a detailed biomass productivity approach was combined with a summarized leaf area index approach (Fig. 3.1c). For each biomass productivity approach, a specific water balance was used to simulate effects of water stress. Details of the approaches and water balances used are given below and in Appendix A.

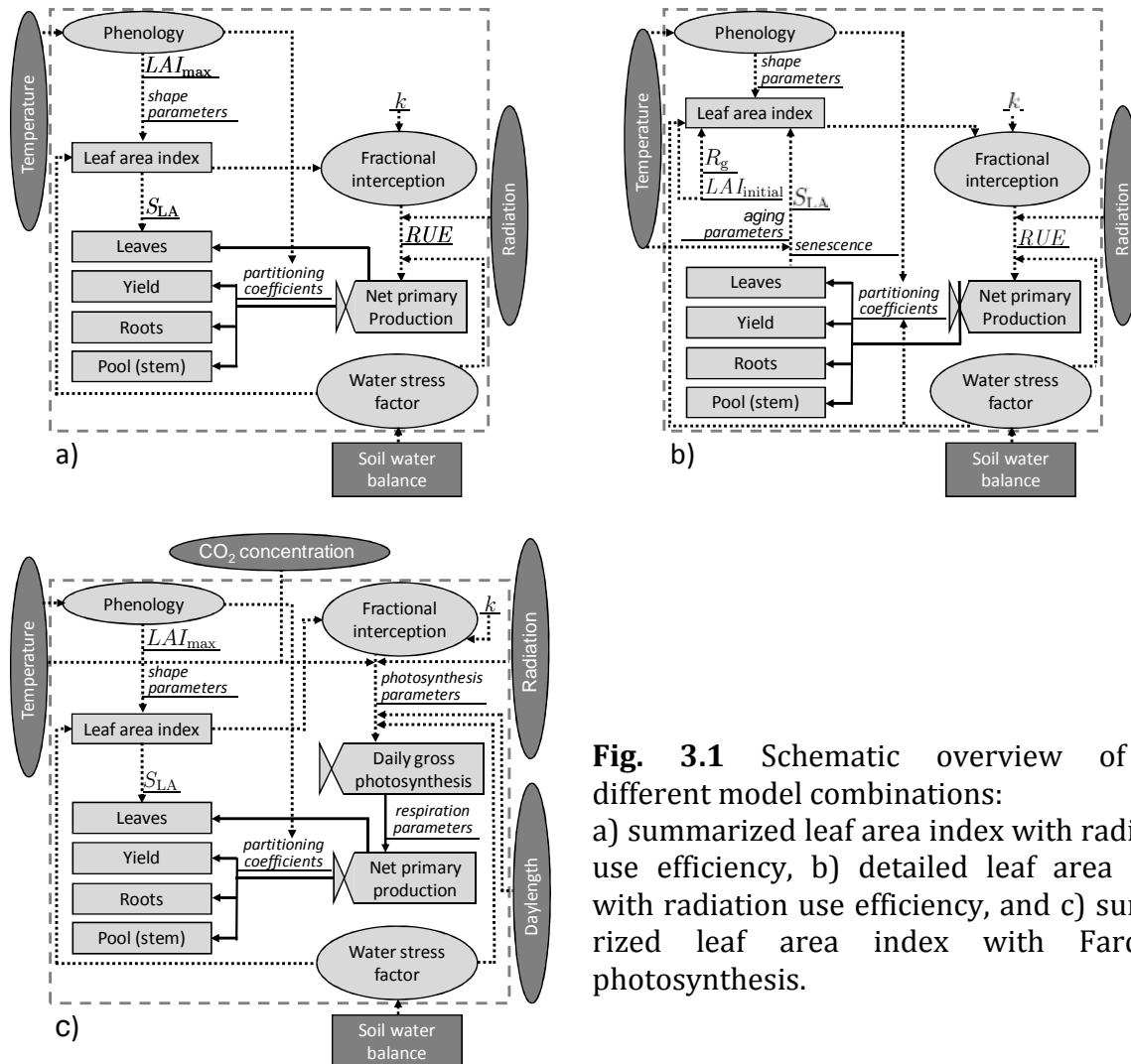


**Fig. 3.1** Schematic overview of the different model combinations: a) summarized leaf area index with radiation use efficiency, b) detailed leaf area index with radiation use efficiency, and c) summarized leaf area index with Farquhar photosynthesis.

Adam *et al.* (2011) evaluated the different model combinations against observed data for a wide range of climatic conditions under potential growing conditions, using observed daily weather data. They concluded that, after calibration, all three model combinations were able to reproduce observed yields within reasonable limits.

The three model combinations to calculate crop productivity were driven by both actual and interpolated weather data. To quantify the sensitivity, the average relative differences ( $B_d$ , %) between total standing biomass at the end of the growing season with interpolated weather data ( $B_i$ , gC m<sup>-2</sup>) and with actual weather data ( $B_a$ , gC m<sup>-2</sup>) over the nine stations were calculated:

$$B_d = \sum_{k=1}^9 \left| 1 - \frac{B_{i_k}}{B_{a_k}} \right| \times \frac{1}{9} \times 100\% \quad (\text{Eq. 3.1})$$

absolute values were used to avoid cancelling out of results.

## 2.1 Radiation interception

### 2.1.1 Detailed leaf area index approach

A relatively detailed approach to model leaf area index ( $LAI$ , m<sup>2</sup> m<sup>-2</sup>) dynamics is described by Spitters and Schapendonk (1990) and was applied in the light interception and utilization model (LINTUL) in several case studies of maize (Farré *et al.*, 2000) and potatoes (Spitters and Schapendonk, 1990). Adapted versions of LINTUL (with the same  $LAI$  approach, but different assimilation approaches) were used for spring wheat (Ewert *et al.*, 1999; Van Oijen and Ewert, 1999).

Growth of  $LAI$  is divided into two phases. During the juvenile stage, or until a certain  $LAI$  threshold is reached ( $LAI_j$ , m<sup>2</sup> m<sup>-2</sup>), expansion of  $LAI$  is exponential. It is governed by temperature through its effect on cell division and extension. If water stress occurs, increase in  $LAI$  is reduced by a water stress factor: the ratio between actual and potential transpiration. Beyond the juvenile stage,  $LAI$  expansion is restricted by the supply of assimilates and is calculated using the simulated rate of increase in leaf weight, which is based on the total biomass increment multiplied with a partitioning coefficient, defining the fraction of biomass allocated to the leaves, and with a constant specific leaf area of new leaves ( $S_{LA}$ , m<sup>2</sup> gC<sup>-1</sup>). To account for the effect of water stress on  $LAI$  beyond the juvenile stage, the increase in leaf weight is reduced through the water stress factor. Leaves die proportionally to their weight with a relative death rate, as a result of self-shading ( $R_{d-sh}$ , d<sup>-1</sup>) and, in the post-anthesis stage, from aging ( $R_{d-ag}$ , d<sup>-1</sup>), which is affected by temperature (Fig. 3.2).

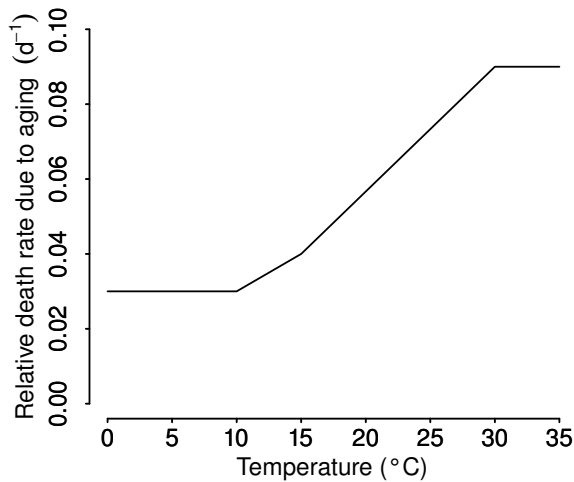


**Fig. 3.2** The relative death rate of leaves ( $\text{d}^{-1}$ ) as a function of temperature ( $^{\circ}\text{C}$ ), as used in the detailed leaf area index approach.

### 2.1.2 Summarized leaf area index approach

A more summarized approach to model  $LAI$  dynamics is based on the concept of the SWAT (Soil and Water Assessment Tool, Neitsch *et al.*, 2005) model and is applied in the LPJmL model.  $LAI$  at any point in time is calculated as a fraction of a predefined maximum leaf area index ( $LAI_{\max}$ ,  $\text{m}^2 \text{m}^{-2}$ ). This fraction is calculated by a forcing function, defined in terms of sigmoidal and quadratic functions. Potential  $LAI$  is reduced if the required biomass to support the calculated  $LAI$  is not available. To account for water stress, in the pre-anthesis phase a water stress factor is included in the rate equation for  $LAI$  growth. The water stress factor is either based on the ratio of actual and potential transpiration (in combination with the radiation use efficiency approach), or based on the maximum transpiration rate that can be sustained under optimum soil moisture conditions, soil moisture content, potential canopy conductance, potential evapotranspiration, and a scaling factor (in combination with the Farquhar photosynthesis approach) as described in Section 2.2.1.

The main difference between the two  $LAI$  approaches is the strong feedback between biomass production and  $LAI$  growth in the detailed  $LAI$  approach, while this feedback is weaker in the summarized  $LAI$  approach. Growth of  $LAI$  in the detailed approach is dependent on so-called allocation factors, i.e. the daily produced biomass is allocated to the different organs in dependence of development stage. Biomass allocated to the leaves is used to calculate  $LAI$  using  $S_{LA}$ . This implies that, in the detailed approach, unfavourable growing conditions in the beginning of the growing period may have strong effects on final yield levels. A negative feedback may occur: unfavourable growing conditions result in low biomass production, therefore little biomass is allocated to the leaves and this results in low radiation interception, which implies again low biomass produc-

tion. The effect of unfavourable growing conditions is less strong in the summarized *LAI* approach, as leaf area is only reduced if water stress occurs or if biomass production is insufficient to sustain the root and leaf biomass (Eq. A.3.12).

## 2.2 Biomass productivity

### 2.2.1 Detailed biomass productivity approach

A detailed approach to model biomass productivity is the biochemical photosynthesis model of Farquhar *et al.* (1980) with simplifications by Collatz *et al.* (1991). In the process of photosynthesis, CO<sub>2</sub> is converted into carbohydrates through activation of plant enzymes by light. Photosynthesis is either limited by intercepted radiation ( $J_e$ , gC m<sup>-2</sup> h<sup>-1</sup>) or by the availability of the enzyme Rubisco ( $J_c$ , gC m<sup>-2</sup> h<sup>-1</sup>). Intercepted radiation is computed from current *LAI* and a constant light extinction coefficient ( $k$ , –), using Beer's law. Daily gross photosynthesis is the gradual transition between the two limiting rates and is influenced by ambient temperature, CO<sub>2</sub> concentration, and radiation intensities. Daily net photosynthesis ( $A_{nd}$ , gC m<sup>-2</sup> d<sup>-1</sup>) is calculated as daily gross photosynthesis minus the “dark” respiration ( $R_d$ , gC m<sup>-2</sup> d<sup>-1</sup>); Fig. 3.3 shows the effect of temperature on daily net photosynthesis for a number of (constant) radiation intensities and a (constant) CO<sub>2</sub> concentration of 350 ppm by volume.

To calculate daily net primary productivity (*NPP*, gC m<sup>-2</sup> d<sup>-1</sup>), maintenance respiration is subtracted from daily net photosynthesis, based on tissue-specific C:N ratios, temperature, and the amount of biomass per organ. The remainder is reduced by 25% to account for growth respiration.

In case of water stress, the model simulates a limited opening of the stomata, causing a change in ratio between intercellular and ambient CO<sub>2</sub> concentrations, which results in a reduced photosynthetic rate (Gerten *et al.*, 2004; Haxeltine and Prentice, 1996b; Sitch *et al.*, 2003). Water available for the crop is calculated through a water balance, in which the soil is represented by a simple bucket, containing two layers, each with a fixed thickness. Water content of both layers is updated daily, taking into account transpiration, evaporation, runoff, and percolation through the layers (for more details, see Gerten *et al.*, 2004 and Appendix A).



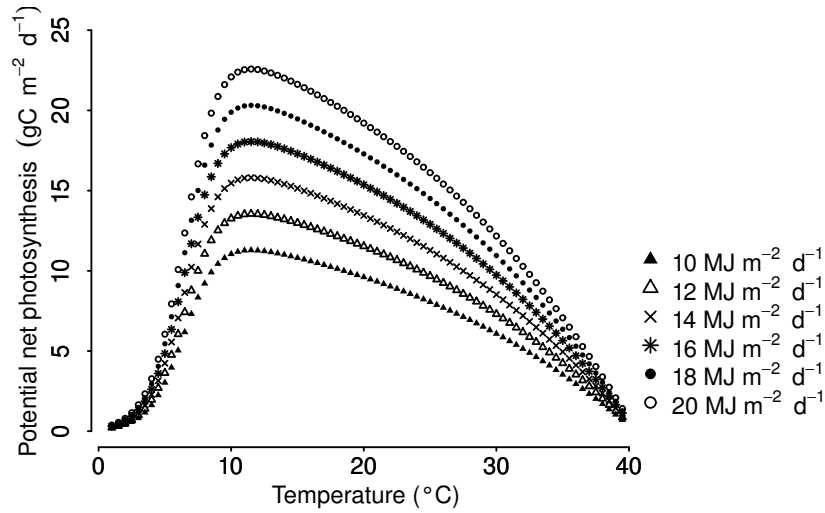


**Fig. 3.3** Temperature response of the daily net rate of photosynthesis, at an ambient  $\text{CO}_2$  concentration of 350 ppm and various radiation intensities, as simulated with Farquhar photosynthesis.

### 2.2.2 Summarized biomass productivity approach

A more summarized approach to model biomass productivity is the radiation use efficiency ( $RUE$ ,  $\text{gC MJ}^{-1}$ ) approach. For crops, a linear relation exists between accumulated intercepted radiation and accumulated biomass, the slope representing the  $RUE$  value (Monteith, 1977), which combines the effects of photosynthesis and respiration (Goudriaan and Monteith, 1990). The daily fraction of intercepted radiation by the crop is computed from current  $LAI$  and a constant light extinction coefficient, using Beer's law. Daily net primary productivity ( $NPP$ ,  $\text{gC m}^{-2} \text{d}^{-1}$ ) is calculated by multiplying the fraction of intercepted radiation with: daily incoming short-wave radiation ( $R_{\text{dr}}$ ,  $\text{MJ m}^{-2} \text{d}^{-1}$ ), 0.5 (to convert short-wave radiation into photosynthetically active radiation), and radiation use efficiency (Eq. A.3.34).

In the absence of water stress, radiation use efficiency is constant; with water stress, it is reduced by the ratio of actual and potential transpiration. Water available for the crop is calculated through a water balance, in which the soil is represented by a simple bucket, consisting of single layer that increases in thickness in downward direction with the growing roots. Water content of the layer is updated daily, taking into account transpiration, evaporation, runoff, and percolation through the layer (for more details, see Farré *et al.* (2000) and Appendix A).

The main difference between the two biomass productivity approaches is the dependence of the detailed approach on incoming radiation,  $\text{CO}_2$  concentration, and temperature, while biomass productivity calculated according to the summarized approach is only dependent on incoming radiation. Furthermore, the

detailed approach includes a coupled photosynthesis-water balance scheme, which allows for accounting for changes in water use efficiency, under changing temperatures or at higher CO<sub>2</sub> concentrations.

Table 3.1 shows the location-specific (phenological) crop parameters; other crop parameters with regard to radiation interception and biomass productivity are kept constant across the locations (Table 3.2).

**Table 3.1**  
Location-specific crop phenological parameters.

Location (country, lat. (°), long. (°))	Day of emergence (day of year)	Temperature sum until anthesis (°Cd)	Temperature sum until maturity (°Cd)
UK (52°21', -0°07')	56	1185	1693
Denmark (57°06', 9°51')	95	1104	1577
The Netherlands (52°06', 5°10')	85	1347	1924
Germany (48°07', 11°42')	91	968	1383
France (centre) (47°58', 1°45')	69	1160	1657
France (south) (43°37', 1°22')	41	1504	2149
Spain (centre) (40°27', -3°33')	36	1470	2022
Spain (south) (37°25', -5°52')	36	1540	2200
Italy (42°25', 14°12')	36	1431	2044

*Source:* Boons-Prins *et al.* (1993), assuming that sowing dates and temperature sums until maturity of spring barley are representative for spring wheat.

**Table 3.2**

Most important parameters for the different model approaches and their values.

Symbol	Parameter	Value and unit	Source
Parameters for the summarized leaf area index approach			
$fLAI_1$ and $fLAI_2$	Fraction of leaf area index at the first and second inflexion points on the leaf area development curve	0.05 and 0.95 (–)	
$fT_{sum1}$ and $fT_{sum2}$	Fraction of temperature sum at the first and second inflexion points on the leaf area development curve	0.05 and 0.45 (–)	
$fT_{sum a}$	Fraction of the total temperature sum when anthesis is reached and senescence starts	0.70 (–)	
$S_{LA}$	Specific leaf area of leaves	$0.053 \text{ m}^2 (\text{g C})^{-1}$	
$LAI_{max}$	Maximum leaf area index	$5.0 \text{ m}^2 \text{ m}^{-2}$	
Parameters for the detailed leaf area index approach			
$R_g$	Maximum relative growth rate of leaf area index	$0.0108 (\text{°Cd})^{-1}$	
$LAI_i$	Initial leaf area index	$0.025 \text{ m}^2 \text{ m}^{-2}$	
$fT_j$	Fraction of temperature sum when juvenile stage ends	0.15 (–)	
$fT_{sum a}$	Fraction of temperature sum when anthesis starts	0.70 (–)	
$LAI_j$	Threshold leaf area index when juvenile stage ends	$0.75 \text{ m}^2 \text{ m}^{-2}$	
$T_{base}$	Base temperature	$0 \text{ °C}$	(a)
$S_{LA}$	Specific leaf area of leaves	$0.053 \text{ m}^2 (\text{g C})^{-1}$	
$R_{d-shmx}$	Maximum death rate due to shading	$0.03 \text{ d}^{-1}$	(b)
$LAI_c$	Critical leaf area index above which self-shading is assumed to start	$4.0 \text{ m}^2 \text{ m}^{-2}$	(b)
Parameters for the radiation use efficiency approach			
$RUE$	Radiation use efficiency based on total daily radiation	$1.38 \text{ gC MJ}^{-1}$	
$k$	Light extinction coefficient	0.5 (–)	(c)
Parameters for Farquhar photosynthesis approach (C3 plants)			
$K_{25}$ and $Q_{10}$	The value of the parameter at 25 °C and the relative change in the parameter for a 10 °C change in temperature, respectively		
$K_C$	Michaelis constant for $\text{CO}_2$	$30 \text{ Pa}$ ( $Q_{10}=2.1$ )	(c)
$K_O$	Michaelis constant for $\text{O}_2$	$30 \times 10^3 \text{ Pa}$ ( $Q_{10}=1.2$ )	(c)
$\tau$	$\text{CO}_2/\text{O}_2$ specific ratio	$2600 \mu\text{mol } \mu\text{mol}^{-1}$ ( $Q_{10}=0.57$ )	(c)
$\alpha_{C3}$	C3 quantum efficiency	$0.08 \mu\text{mol } \mu\text{mol}^{-1}$	(c)
$b_{C3}$	$R_a/V_m$ ratio for C3 plants	$0.015 (\text{gC m}^{-2} \text{ d}^{-1}) / (\text{gC m}^{-2} \text{ d}^{-1})$	(c)
$\lambda_{mC3}$	Optimal $C_i/C_a$ for C3 plants.	$0.8 \text{ Pa Pa}^{-1}$	(d)
$P$	Atmospheric pressure	$100 \times 10^3 \text{ Pa}$	(c)
$O_2$	Partial pressure of $\text{O}_2$	$20.9 \times 10^3 \text{ Pa}$	(c)

Symbol	Parameter	Value and unit	Source
$C_{\text{mass}}$	Molar mass of carbon	12 gC mol <sup>-1</sup>	
$k$	Light extinction coefficient	0.5 (-)	(c)
$C_q$	Conversion factor for solar radiation at 550 nm from MJ m <sup>-2</sup> d <sup>-1</sup> to mol photons m <sup>-2</sup> d <sup>-1</sup>	4.6 × 10 <sup>-3</sup> mol photons MJ <sup>-1</sup>	
$c_a$	Ambient mole fraction CO <sub>2</sub>	μmol mol <sup>-1</sup>	
$\theta$	Co-limitation parameter	0.7 (-)	(c)
$\alpha_{\text{max}}$	Maximum Priestley-Taylor coefficient	1.391 (-)	(e)
$g_m$	Scaling conductance	3.26 mm s <sup>-1</sup>	(e)
$g_{\text{min}}$	Minimum canopy conductance, which accounts for water stress not directly related with photosynthesis	0.5 mm s <sup>-1</sup>	(e)

(a) Kiniry *et al.* (1995).

(b) Van Keulen and Seligman (1987).

(c) Haxeltine and Prentice (1996b).

(d) Sitch *et al.* (2003).

(e) Gerten *et al.* (2004)

## 2.3 Weather data

Weather input data for the model runs were extracted from a database described by Van Kraalingen *et al.* (1991), for various locations in Europe (Fig. 3.4), for the year 1982. It contains daily data for minimum and maximum temperature ( $T_{\text{min}}$ ,  $T_{\text{max}}$ , °C), daily incoming short-wave radiation ( $R_{\text{dr}}$ , MJ m<sup>-2</sup> d<sup>-1</sup>), daily precipitation ( $P$ , mm d<sup>-1</sup>), vapour pressure ( $e$ , kPa), and wind speed ( $u$ , m s<sup>-1</sup>). Daily average temperature ( $T_{\text{average}}$ , °C), used in the radiation interception and biomass production approaches, is calculated from minimum and maximum temperatures. Data were used from various European weather stations (see Table 3.1).



**Fig. 3.4** Locations of the nine weather stations used in this study.

We concentrated in this study on the effects of linear interpolation of temperature and radiation data only, as effects of disaggregation of precipitation data strongly depend on the soil–water model considered. We here focus on crop growth processes only and do not compare different levels of detail in soil–water models, that would allow addressing the effects of disaggregating precipitation data. Besides, monthly precipitation is mostly disaggregated to daily values in crop growth models on the basis of precipitation generators rather than through linear interpolation (e.g. Bondeau *et al.*, 2007; Liu *et al.*, 2007). Therefore, precipitation is given as daily values in all simulations.

### 2.3.1 Linear interpolation of temperature and radiation data

Actual daily temperature and radiation values from the nine weather stations were used to derive interpolated daily values for temperature and radiation. Average monthly values, which were assigned to the middle of each month (e.g.  $MD_{i=1} = 15$  and  $MD_{i=2} = 46$ ), were calculated from the actual weather data. Interpolated daily values for weather variable at day  $k$  ( $X_k$ , °C or MJ m<sup>-2</sup> d<sup>-1</sup>) were calculated as:

$$X_k = X_i + \frac{DOY_k - MD_i}{MD_{i+1} - MD_i} \times (X_{i+1} - X_i) \quad (\text{Eq. 3.2})$$

where  $X_i$  and  $X_{i+1}$  are monthly averages of weather variable  $X$  (°C or MJ m<sup>-2</sup> d<sup>-1</sup>) at the middle day of month  $MD_i$  and  $MD_{i+1}$ , respectively, and  $DOY_k$  is the  $k^{\text{th}}$  day of the year (Sitch *et al.*, 2003; Soltani *et al.*, 2004). The same procedure was applied to derive interpolated daily  $T_{\text{max}}$  values (°C).

As a measure for the day-to-day variability in weather conditions, the average annual difference (for temperature or radiation) ( $W_d$ , °C or MJ m<sup>-2</sup> d<sup>-1</sup>) between linearly interpolated data ( $W_i$ , °C or MJ m<sup>-2</sup> d<sup>-1</sup>) and actual data ( $W_a$ , °C or MJ m<sup>-2</sup> d<sup>-1</sup>) was computed:

$$W_d = \sum_{k=1}^{365} |W_{i_k} - W_{a_k}| \times \frac{1}{365} \quad (\text{Eq. 3.3})$$

A larger difference indicates larger day-to-day variability.

### 2.3.2 Occurrence of high temperatures

Extremely high temperatures may strongly influence yields through their effects on grain set, since harmful effects occur already after exposure to high temperatures for durations as short as one day (Saini and Aspinall, 1982). In line with a study by Semenov (2009), we summed the number of days with a daily maximum temperature exceeding 27 °C and 31 °C during the ten days after anthesis; two threshold temperatures were used, as wheat cultivars differ in their tolerance to extreme temperatures (Mitchell *et al.*, 1993; Porter and Gawith, 1999). Anthesis was defined as a fixed fraction (0.7) of the temperature sum till maturity (Table 3.1). Days were summed for the nine locations, based on the data-sets with (1) actual daily  $T_{\max}$ , (2) interpolated daily  $T_{\max}$ , (3) actual daily  $T_{\text{average}}$ , and (4) interpolated daily  $T_{\text{average}}$ .

## 3. Results

### 3.1 Weather data

Day-to-day variability in weather conditions was calculated in order to examine its correlation with possible differences between model results due to the use of input data with different temporal resolutions. Among the considered study locations, day-to-day variability in weather conditions was highest in Germany and lowest in southern Spain (Fig. 3.5 and Table 3.3). Day-to-day variability in weather conditions in Denmark, The Netherlands, France, and the United Kingdom was comparable to that in Germany, while variability in Italy and in central Spain was comparable to that in southern Spain (Table 3.3).

**Table 3.3**

Day-to-day variability in the weather conditions.

Location	Average annual deviation between actual and average temperature (°C)	Average annual deviation between actual and average radiation(MJ m <sup>-2</sup> )
UK	2.22	3.12
Denmark	2.19	3.15
The Netherlands	2.28	3.13
Germany	2.61	3.42
France (centre)	2.40	3.16
France (south)	2.19	3.22
Spain (centre)	1.80	2.68
Spain (south)	1.66	2.30
Italy	1.80	2.71

During the ten days following anthesis, actual daily  $T_{\max}$  exceeded at least during one day the threshold temperature of 27 °C in all locations, except those in the United Kingdom and in central France. In The Netherlands, southern France, Spain, and Italy, actual daily  $T_{\max}$  also exceeded at least once the threshold temperature of 31 °C in the ten days following anthesis. If interpolated daily  $T_{\max}$  data were used, only in southern France, Spain, and Italy  $T_{\max}$  exceeded 27 °C,  $T_{\max}$  never exceeded 31 °C. However,  $T_{\max}$  exceeded 27 °C on more days if interpolated daily  $T_{\max}$  was used than with actual daily  $T_{\max}$ . Daily  $T_{\text{average}}$  (actual and interpolated) never exceeded 27 °C during the ten days following anthesis (Table 3.4).

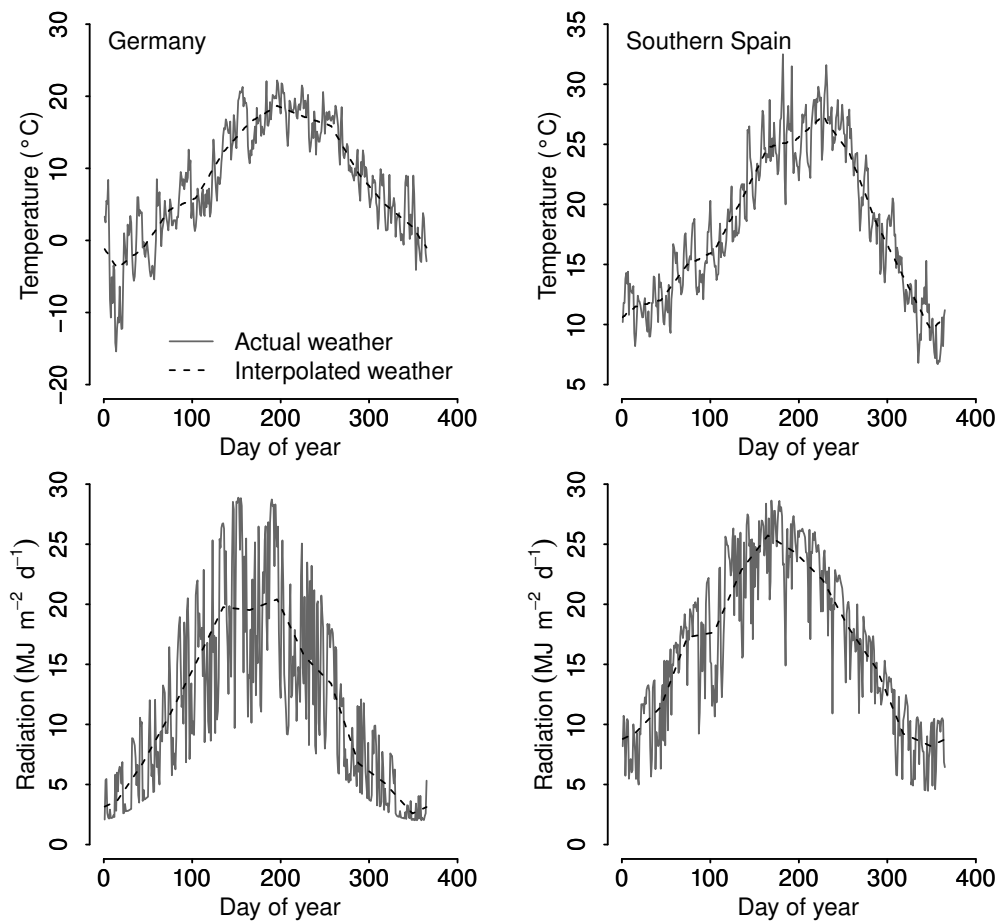


**Fig. 3.5** Actual and interpolated (daily) temperature (°C) and radiation (MJ m<sup>-2</sup> d<sup>-1</sup>) from weather stations in Germany (left panel) and southern Spain (right panel) in 1982.

**Table 3.4**

Number of days when  $T_{\max}$  exceeded a certain threshold temperature for two input data sets;  $T_{\text{average}}$  (actual daily and interpolated daily) never exceeded 27 °C.

Location	Days with actual daily $T_{\max}$ above:		Days with interpolated daily $T_{\max}$ above:	
	27 °C	31 °C	27 °C	31 °C
United Kingdom	0	0	0	0
Denmark	2	0	0	0
The Netherlands	4	1	0	0
Germany	1	0	0	0
France (centre)	0	0	0	0
France (south)	5	1	3	0
Spain (centre)	9	3	10	0
Spain (south)	6	3	10	0
Italy	6	2	10	0

### 3.2 Total biomass for actual and linearly interpolated weather data

Sensitivity of the different model combinations to interpolation of input data was tested for interpolation of temperature and radiation separately and for the combination of both interpolated temperature and radiation. Fig. 3.6 shows the average (relative) differences between simulated total standing biomass with actual weather data and with interpolated weather data based on the nine stations (see Eq. 3.1), for irrigated and rainfed conditions.

The models respond differently to the interpolation of the different types of input data. Differences under rainfed conditions are in general larger than under irrigated conditions, especially for the combination of both interpolated radiation and temperature. Using the Farquhar photosynthesis model with the summarized *LAI* approach, under rainfed conditions, results in an average difference of 15% (averaged over the nine stations, Fig. 3.6) in simulated total biomass between simulations with actual and simulations with the combination of both interpolated temperature and radiation, with a maximum of 38% in Germany (Fig. 3.7). Using the *RUE* approach combined with the detailed *LAI* approach, under rainfed conditions, results in an average difference of 9% between simulations with actual and simulations with interpolated temperature and actual radiation data, with a maximum of 30% in the UK. The most summarized combination (*RUE* and summarized *LAI* approach), under rainfed conditions, results in the lowest average difference (4%) between simulations with actual and those with actual temperature and interpolated radiation, with a maximum of 9% in Denmark.



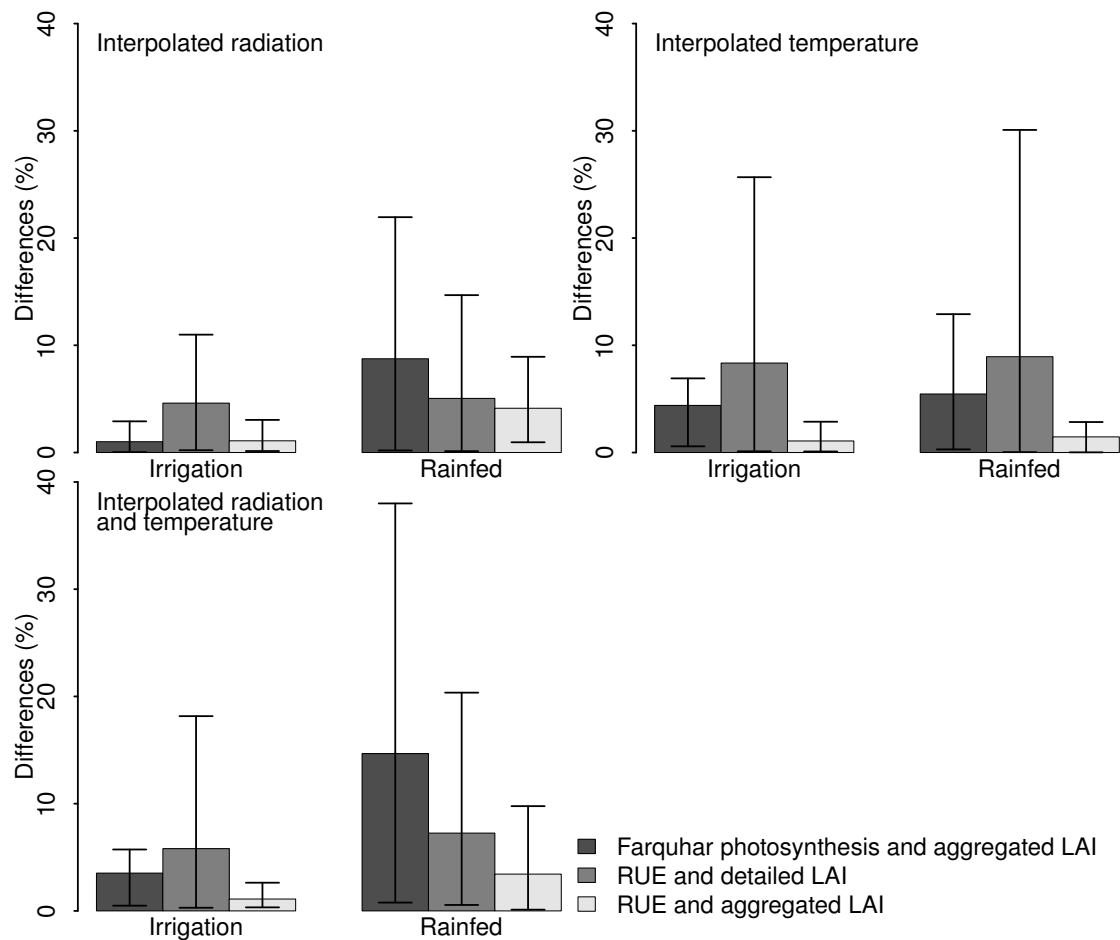


**Fig. 3.6** Average differences (%) based on all nine locations in simulated total biomass at the end of the growing season, using “actual temperature and actual radiation” compared to the use of interpolated data, for irrigated and rainfed conditions. The error bars indicate the maximum and minimum differences.

The effects vary among locations as shown for two contrasting locations: southern Spain and Germany (Fig. 3.7). Locations with a low day-to-day variability in weather conditions, such as southern Spain, show small differences as a result of the use of interpolated temperature and/or radiation data, for both irrigated and rainfed conditions. In contrast, locations with a high day-to-day variability, such as Germany, especially the use of the Farquhar photosynthesis approach results in large differences of up to 37%, if interpolated data for both temperature and radiation are used (Fig. 3.7).

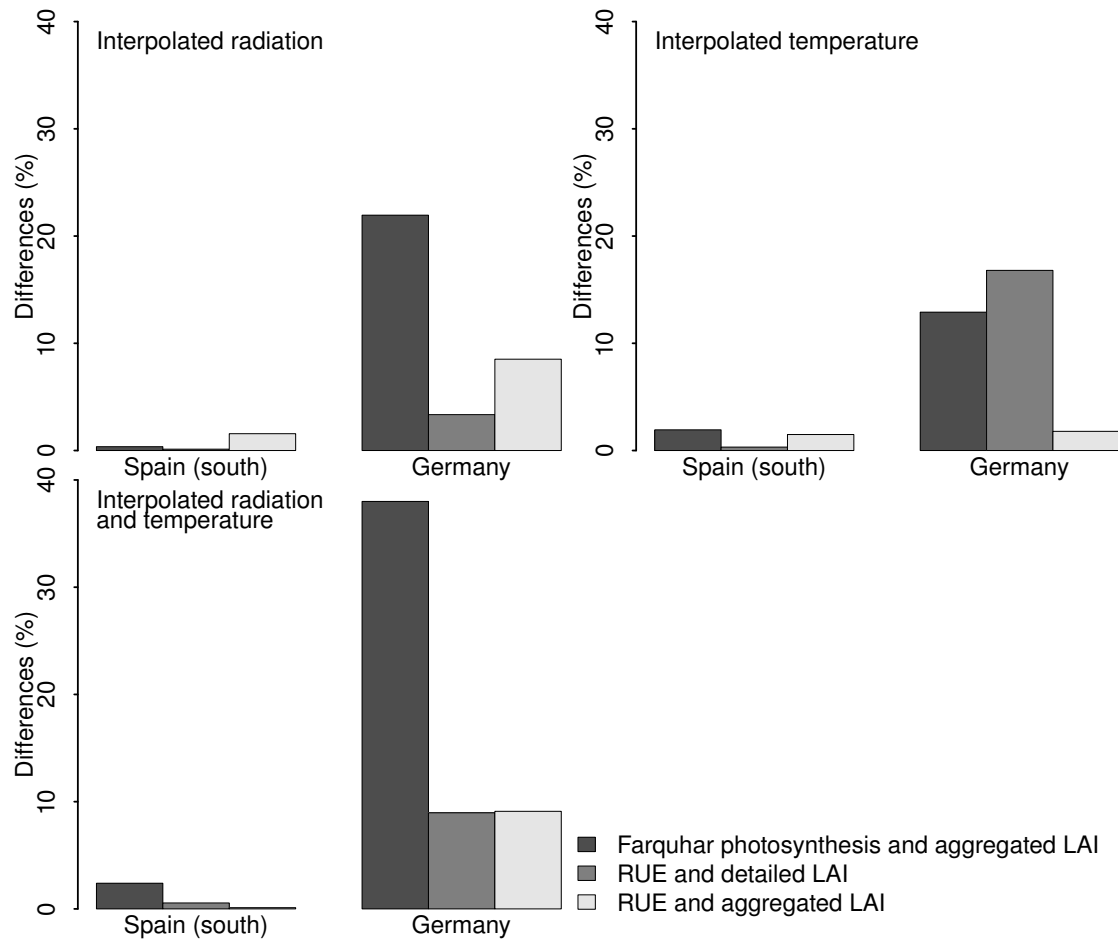


**Fig. 3.7** Differences (%) in simulated total biomass at the end of the growing season using “actual temperature and actual radiation” compared to the use of interpolated data for southern Spain and Germany for rainfed conditions.

In Fig. 3.8 we show the relationship between the day-to-day variability in weather variables (see Eq. 3.3), and the difference between model results with actual and interpolated weather data (see Eq. 3.1), for the model combination with the detailed biomass model (Fig. 3.1c). It is evident that for this model combination a systematic positive linear relationship exists, i.e. a higher day-to-day variability in weather conditions results in a larger difference in biomass production between input data sets. Relationships between day-to-day-variability in weather conditions and differences in simulation results for the other combinations of approaches are less distinct (not shown).

The use of aggregated temperature data results for several stations in a small change in the timing of anthesis and in at most one day change in the simulated length of the growing season. Therefore, differences in simulated biomass are not attributable to simulated differences in length of the growing period, but are almost exclusively due to weather variability during the growing period.

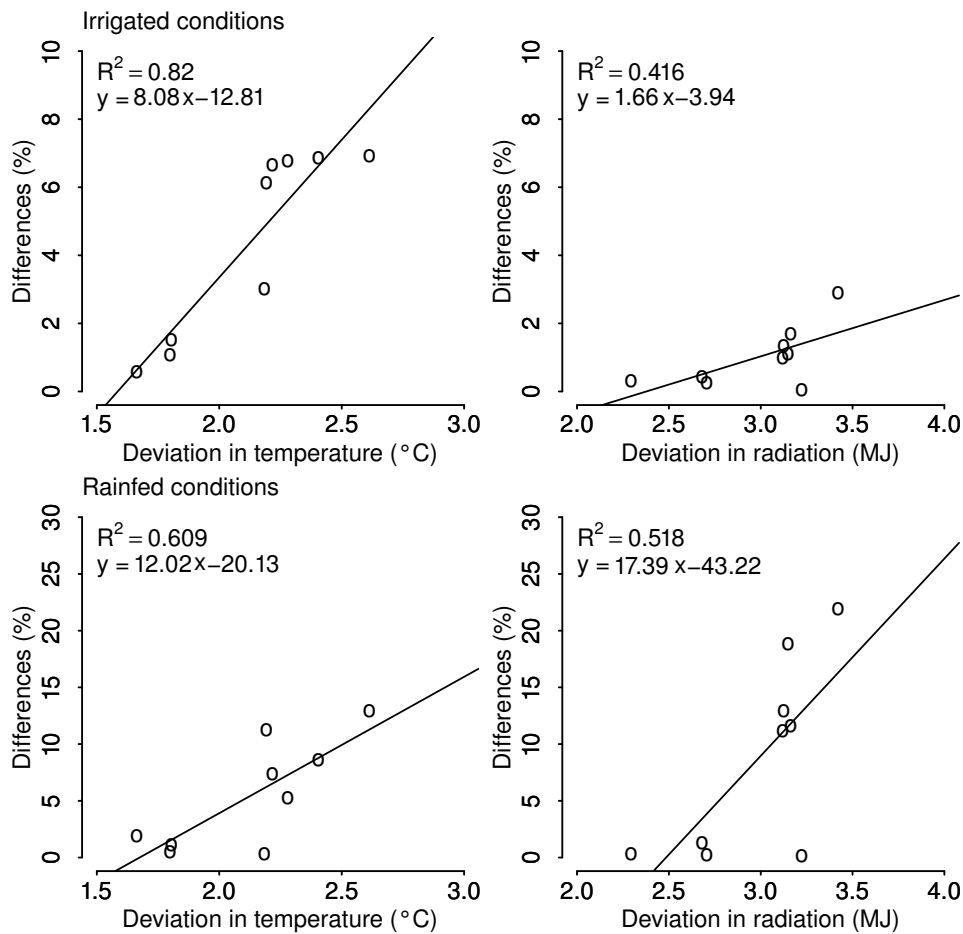


**Fig. 3.8** Relation between the average annual difference between actual and interpolated weather data on the one hand (x-axis, indicating the magnitude of the day-to-day variability of the weather variables, Eq. 3.3), and the difference between model runs driven by actual and interpolated weather data on the other hand (y-axis, Eq. 3.1); for the combination of the Farquhar photosynthesis and the summarized leaf area index approach.

## 4. Discussion and conclusions

The objective of this study was to analyse the sensitivity of crop modelling approaches, representing growth processes, with different detail, in response to changes in the temporal resolution of weather input data. Our results show that the simulated biomass depends on whether actual or interpolated temperature and/or radiation data are used. This is in line with earlier results of Nonhebel (1994) and Soltani *et al.* (2004). Nonhebel (1994) studied locations with high day-to-day variability in weather conditions and found overestimates of 5–15% for simulated potential yields as a result of using average weather data. Soltani *et al.* (2004) found significant over-estimates of yield with linearly interpolated input data at the locations with optimal or supra optimal air temperatures for crop growth and a high day-to-day variability. Importantly, in the present study,

we find in addition, that the sensitivity to the interpolation of input data not only depends on the magnitude of the day-to-day weather variability, but also increases with increasing detail in the process modelling. For the most summarized model combination, the difference at a particular site between simulated biomass with actual and simulated biomass with linearly interpolated input data is at most 10%, while for the most detailed model combination it is 37%.

The large differences (higher simulated biomass with aggregated weather data) in the model with the Farquhar photosynthesis approach can be explained by the nonlinear temperature effect on the assimilation rate incorporated in that approach (Fig. 3.3). Due to the lack of day-to-day variability in linearly interpolated weather data, temperatures are more often at or near optimum values for growth, resulting in higher photosynthetic rates. In contrast, the more linear nature of the other approaches resulted in smaller differences. Furthermore, we found for the Farquhar photosynthesis approach a positive linear relationship between the day-to-day variability in weather conditions and the differences in simulated biomass between simulations driven with actual and with linearly interpolated input data (Fig. 3.8). This indicates that in locations with high day-to-day variability in weather conditions, and therefore large differences between actual and linearly interpolated weather data, differences due to the use of linearly interpolated input data are large.

The required structure, parameter values and input data for a model to assess effects of extreme weather events, e.g. heat waves, on crop growth are not yet fully understood. Existing models that include these effects, often apply threshold approaches, as e.g.  $T_{\max}$  thresholds for heat stress (Challinor *et al.*, 2005; Teixeira *et al.*, 2010). Our results, however, suggest that current threshold models cannot be simply applied with temporally aggregated weather data, if calibrated with more detailed weather data. We cannot conclude that threshold models are generally unsuitable in combination with aggregated data, but at least current threshold values will have to be re-parameterized if weather data with different characteristics (interpolated vs. actual; mean vs. maximum) are being used. Furthermore, whether threshold temperature models for heat damage to crops can be applied with interpolated monthly data also largely depends on the local day-to-day temperature variability and their statistical distribution characteristics. An in-depth analysis of a global set of daily temperature measurements would be required, which is beyond the scope of this study.

In addition to heat stress, effects such as yield reductions due to ozone pollution are also simulated using threshold values (e.g. Ewert and Porter, 2000). This effect has not been considered here, as it is not addressed in any global-scale

crop growth model, however, it is likely that re-parameterization is also advisable if input data with a different temporal resolution are being used, than that applied in the original model.

Based on the results presented here, we stress the importance of the provision of daily weather data. Such data may be generated through weather generators, in combination with or directly by global circulation models. However, site-specific observed daily weather data, which are often required to calibrate weather generators, are currently unavailable for large parts of the Earth (Liu *et al.*, 2009), which hampers the application of weather generators at the global scale. For that reason, we stress that observed daily weather data should be made available for more regions and measurement sites. Results of weather generators should be tested for various climates, especially for climates with extreme temperatures, in order to assess their applicability in climate impact assessments, which may require rather detailed crop growth models, at least for conditions of high day-to-day weather variability.

Our hypothesis that model sensitivity to the use of temporally aggregated data increases with an increasing degree of detail in the modelling approach, is supported by the results of this study. This observation has implications for the choice of a specific approach to model a certain process, which thus depends on the temporal resolution of the available input data. However, whether model uncertainty is unnecessarily increased if detailed approaches are combined with temporarily sparse weather data, needs further evaluation. Nevertheless, we suggest that the available temporal resolution of the input data and the implications for model results and model applicability need to be taken into account in the design of a (global) crop growth model. More detailed models need to be (re-)evaluated or re-parameterised if driven with less detailed input data, while more summarized models may prove to be unsuitable for studies addressing the effects of changes in day-to-day weather patterns, such as studies on weather extremes.

## Acknowledgements

The authors are grateful for the valuable comments of two anonymous reviewers, who proposed useful revisions to a previous version of this paper.



## Chapter 4

### **Effects of data aggregation on simulations of crop phenology**

Based on:  
Van Bussel, L.G.J., Ewert, F., Leffelaar, P.A.:  
Effects of data aggregation on simulations of crop phenology.  
Agriculture, Ecosystems and Environment, vol. 142 (2011), 75-84

## Abstract

Policy decisions are often taken at the regional scale, while crop models, supporting these decisions, have been developed for individual locations, expecting location-specific, spatially homogeneous input data. Crop models are able to account for the variation in climatic conditions and management activities and their effects on crop productivity. However, regional applications require consideration of spatial variability in these factors. Several studies have analysed effects of using spatially aggregated climate data on model outcomes. The effects of spatially aggregated sowing dates on simulations of crop phenological development have not been studied, however. We investigated the impact of spatial aggregation of sowing dates and temperatures on the simulated occurrence of ear emergence and physiological maturity of winter wheat in Germany, using the phenological model of AFRCWHEAT2.

We observed time ranges for crop emergence exceeding 90 d, whereas for harvesting this was more than 75 d. Spatial aggregation to 100 km × 100 km reduced this range to less than 30 and 20 d for emergence and harvest, respectively. Differences among selected regions were relatively small, suggesting that non-climatic factors largely determined the spatial variability in sowing dates and consecutive phenological stages. Application of the AFRCWHEAT2 phenology model using location-specific weather data and emergence dates, and an identical crop parameter set across Germany gave similar deviations in all studied regions, suggesting that varietal differences were less important among regions than within regions. Importantly, bias in model outcomes as a result of using aggregated input data was small. Increase in resolution from 100km to 50km resulted in slight improvements in the simulations. We conclude that using spatially aggregated weather data and emergence dates to simulate the length of the growing season for winter wheat in Germany is justified for grid cells with a maximum area of 100 km × 100 km and for the model considered here. As spatial variability of sowing dates within a region or country can be large, it is important to obtain information about the representative sowing date for the region.

## 1. Introduction

Results of crop models are often used to inform policy makers about the effects of climate change on the productivity of crops (Boote *et al.*, 1996; Hansen and Jones, 2000; Harrison *et al.*, 2000; Leemans, 1997; Tubiello and Ewert, 2002). However, there is often a mismatch between the scale of policy decision support and the scale for which crop models have been developed. Recommendations to mitigate the effects or to adapt to climate change often refer to large scales such as regions or countries (Hansen and Jones, 2000; Harrison *et al.*, 2000). On the other hand, crop growth and development models have been developed for individual locations, expecting location-specific, spatially homogenous input data (De Wit *et al.*, 2005; Hansen and Jones, 2000; Mearns *et al.*, 2001; Monteith, 2000; Tao *et al.*, 2009; Van Ittersum *et al.*, 2003). However, crop models are increasingly applied to larger scales (e.g. Bondeau *et al.*, 2007; Challinor *et al.*, 2009, 2004; Tan and Shibasaki, 2003), but systematic evaluations of the effects of spatially heterogeneous input data on the simulations of growth and development processes are scarce.

Winter wheat (*Triticum aestivum*) yields are determined to a large extent by the length and timing of the various phenological stages (Ewert *et al.*, 1996; Jamieson *et al.*, 1998b). These are governed by the interactions of genetic properties and environmental conditions, such as temperature and day length (Kirby *et al.*, 1987; Porter *et al.*, 1987), modified by crop management, especially sowing date and cultivar selection.

A suitable cultivar and an optimal sowing date should be selected to maximize grain yields, e.g. in northern regions grain filling should be finished before the new winter starts, whereas in southern regions grain filling should be completed before the onset of the dry and hot summer (Dennett, 1999; Gomez-Macpherson and Richards, 1995; Nonhebel, 1996; Worland *et al.*, 1994). However, optimal sowing dates cannot always be realized for a variety of reasons related to e.g. limited water availability in the soil during the sowing period (Gomez-Macpherson and Richards, 1995; Sharma *et al.*, 2008; Stephens and Lyons, 1998), delayed harvest of the preceding crops or limited machinery and labour capacity (Dennett, 1999), resulting in substantial heterogeneity in sowing dates for winter wheat in a region (Harrison *et al.*, 2000). Stephens and Lyons (1998) investigated the spatial and temporal variability in sowing dates of wheat for several Australian States. However, variability at smaller scales was not investigated. Chmielewski *et al.* (2004) reported on temporal variability in sowing dates for crops in Germany, but did not address their spatial variability.



The availability of climate change projections by Regional Climate Models (RCMs) is increasing, however, they are still in an early stage of development with therefore considerable limitations. As a result, climatic input data for crop models used in large-scale climate change impact assessment studies are usually derived from General Circulation Models (GCMs). GCMs use spatial grids with resolutions typically of the order of hundreds of square kilometres (Challinor *et al.*, 2009, 2003; Mearns *et al.*, 2001). In those large-scale grids, however, heterogeneity in growing conditions within a grid cell is neglected. The same applies to other inputs for crop models, such as sowing date (Abildtrup *et al.*, 2006).

To generate reliable model results for regional application and/or estimate associated uncertainties, it is important to understand and consider the effects of such data generalization on simulation results. It is expected that with increasing spatial aggregation, local extremes will be averaged out, with unknown implications for the simulation results.

Several studies have analysed the effects of using spatially aggregated climate data on simulated yields by crop models. It has been shown (Easterling *et al.*, 1998) that agreement between simulated and observed yields for wheat and maize improves considerably when climate data were disaggregated from  $2.8^{\circ} \times 2.8^{\circ}$  to approximately  $1^{\circ} \times 1^{\circ}$  resolution, with disaggregation below  $0.5^{\circ} \times 0.5^{\circ}$  showing no further improvement. Disaggregation of soil data showed little effect on model results (Easterling *et al.*, 1998). Olesen *et al.* (2000) and De Wit *et al.* (2005) reported as well that a grid cell size of  $0.5^{\circ} \times 0.5^{\circ}$  is an appropriate size to simulate yields at regional scale. However, other studies showed (e.g. Baron *et al.*, 2005; Wassenaar *et al.*, 1999) that especially in regions where water-limitations played a role, model results for wheat and millet yields were sensitive to aggregation of precipitation and soil data.

The effects of spatially aggregated sowing dates on simulations of crop development have not systematically been studied. It is unclear to what extent heterogeneity in sowing dates within a region will affect the simulation results, particularly for day length- and vernalization-sensitive winter crops. Unclear is also how the use of aggregated climate data affects simulations of crop development without and in combination with aggregated sowing dates.

Therefore, the present paper investigates the impact of different levels of aggregation of observed sowing dates and temperatures on the simulated timing of the development stages of ear emergence and physiological maturity of winter wheat for different regions across Germany. Long-term temporal changes in stage occurrence as presented by Chmielewski *et al.* (2004) and Estrella *et al.*

(2007) to identify climate change impacts are not subject of this study. However, our analysis covers several years to investigate temporal variability in phenological development and possible interactions with the spatial pattern of stage occurrence. Furthermore, spatial and temporal heterogeneity in selected phenological stages are studied in detail.

## **2. Materials and methods**

### **2.1 Data description**

The weather data and observed dates of phenological events of wheat used in this research were derived from the climate data bank (KLIDABA) of the Deutscher Wetterdienst (German Meteorological Service). Observations on crop phenological stages on production fields were recorded by about 1500 voluntary observers across Germany. As observations have been carried out by volunteers, only selected stages have been recorded, instead of more frequent observations as typical for field experiments (e.g. Porter *et al.*, 1987). It can also not be ensured that all observers identified the precise occurrence of a stage and not only the stage when observing the crop through regular visits. This might have resulted in deviations, but as the dataset is extensive, both in space and over time, spatial and temporal patterns of stage occurrence will still be realistic and an acceptable basis for model evaluation. Only locations were selected with complete time series for the phenological stages considered (emergence, ear emergence and harvest) and weather data for the period 1983 through 1988. The period 1995 through 1998 and specifically the year 1995 were selected, as data were most complete for all regions in Germany. We considered crop emergence as starting point for the model simulations, as data were more reliable than sowing dates: in the database, observed sowing dates sometimes refer to the onset of field preparation, such as tilling and drilling.

### **2.2 Description of the crop model**

The phenological model AFRCWHEAT2 simulates the timing of different developmental stages of wheat, using the common temperature sum approach, modified by the effects of photoperiod and vernalization. The model has been tested under a range of conditions, such as in New Zealand (Jamieson *et al.*, 2007; Porter *et al.*, 1993), northeast Germany (Ewert *et al.*, 1996), the Netherlands, Belgium, Ireland, United Kingdom, Sweden, France, Germany, and Denmark (Ewert *et al.*, 1999) and in a large-scale application across Europe (Harrison *et al.*, 2000).

AFRCWHEAT2 is described in detail in Weir *et al.* (1984) and Ewert *et al.* (1996). Here, we report only the basic aspects of the model. To simulate the timing of developmental stages, temperature is accumulated above a base temperature and corrected for effects of photoperiod and vernalization, in dependence of developmental stage. The photoperiod and vernalization effects are computed on the basis of cultivar-specific parameters. It is assumed that vernalization is optimal at temperatures between 3 and 10 °C; effectiveness is zero if temperature is lower than −4 °C or higher than 17 °C and a linear increase and decrease is considered between −4 and 3 °C and 10 and 17 °C, respectively (Ewert *et al.*, 1996; Weir *et al.*, 1984). Required input data for the model as used in this study are temperature (daily minimum and maximum), latitude, emergence date, and cultivar-specific parameters.

To examine the behaviour of the model, six 100 km × 100 km grid cells across Germany (Fig. 4.1), representing three agro-environmental zones (Atlantic Central, Atlantic North, and Continental; Metzger *et al.*, 2005), were selected. In each grid cell, ten observed ear emergence and harvest dates were compared with their simulated results for the period 1983 through 1988, using information from weather stations and observed emergence dates in the vicinity.

Because of lack of information about the cultivar grown at each location, we assumed the same cultivar, characterized by specific crop parameters, to be grown in all locations across Germany. This yields information on the possibility of using identical parameter values across a large area, such as Germany. The parameter values (Table 4.1) were estimated based on field trials for a medium maturity class variety, typically grown in Germany.

For each region, average goodness-of-fit of the model was expressed in root mean squared errors (RMSE) and averaged over five years:

$$\text{RMSE} = \sqrt{\frac{1}{n} \sum_{i=1}^n (x_{\text{sim}_i} - x_{\text{obs}_i})^2} \quad (\text{Eq. 4.1})$$

where  $i$  is the observation number,  $n$  the total number of observations (which varies among regions),  $x_{\text{sim}_i}$  the simulated dates, and  $x_{\text{obs}_i}$  the observed dates. Two values for RMSE were calculated per region:  $\text{RMSE}_{\text{date}}$ , expressing the deviation in number of days between observed and simulated dates and  $\text{RMSE}_{\text{length}}$ , expressing the deviation between observed and simulated lengths of the phenological phase (in percentages of the observed lengths).

Furthermore, based on the five years, average observed and simulated dates for ear emergence and harvest, average observed and simulated lengths of the development periods from emergence till ear emergence and from emergence till harvest were calculated per region.

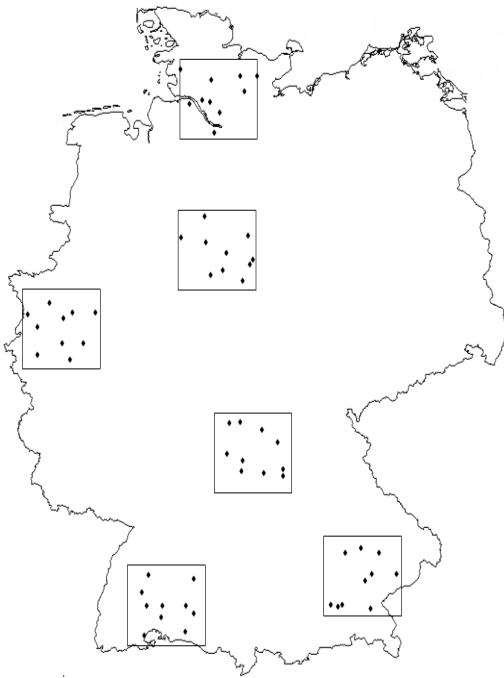


**Fig. 4.1** Locations of the observation stations (weather data and emergence dates) in six regions in Germany selected for this study.

**Table 4.1**  
Cultivar-specific parameter values.

Parameter	Value	Parameter	Value
$T_b$ emergence – anthesis	1.0 °C	$PVTT_{\text{emergence-double ridge}}$	270 °Cd
$T_b$ anthesis – maturity	9.0 °C	$PTT_{\text{double ridge-terminal spikelet}}$	90 °Cd
$P_b$ emergence – double ridge	0 h	$PTT_{\text{terminal spikelet-flag leaf emergence}}$	310 °Cd
$P_b$ double ridge – anthesis	7 h	$PTT_{\text{flag leaf emergence-awn emergence}}$	140 °Cd
$P_{\text{opt}}$	20 h	$PTT_{\text{awn emergence-beginning anthesis}}$	100 °Cd
$V_b$	8 d	$PTT_{\text{beginning anthesis-end of anthesis}}$	40 °Cd
$V_{\text{sat}}$	33 d	$TT_{\text{anthesis-start of grain filling}}$	100 °Cd
$V_{\text{min}}$	-4.0 °C	$TT_{\text{grain filling}}$	320 °Cd
$V_{\text{max}}$	17.0 °C	$TT_{\text{end of grain filling-mature crop}}$	60 °Cd
Optimum temperature range for vernalization	3.0 – 10.0 °C		

$T_b$  base temperature,  $P_b$  base photoperiod,  $P_{\text{opt}}$  optimum photoperiod,  $V_b$  base vernalization,  $V_{\text{sat}}$  saturated vernalization,  $V_{\text{min}}$  base temperature for vernalization,  $V_{\text{max}}$  maximum temperature for vernalization,  $PVTT$  photo-vernal-thermal time,  $PTT$  photo-thermal time,  $TT$  thermal time

## 2.3 Aggregation procedure

### 2.3.1 Effect of grid cell size on spatial heterogeneity of phenological stages

Germany was divided into grid cells with an area of  $10 \text{ km} \times 10 \text{ km}$ . To obtain one (aggregated) date per grid cell, data (of emergence, ear emergence, and harvest dates) of all observation stations falling into a common grid cell were spatially aggregated by calculating their arithmetic mean for the year 1995. Aggregated dates per grid cell for all development stages were also calculated for grid cells with areas of  $20 \text{ km} \times 20 \text{ km}$  through to  $100 \text{ km} \times 100 \text{ km}$  in steps of  $10 \text{ km}$ . The earliest and latest of the aggregated dates were identified for the whole of Germany for each phenological stage and per grid cell size.

### 2.3.2 Spatial and temporal heterogeneity of emergence, ear emergence, and harvest dates

In order to assess possible spatial patterns of phenological events, cumulative relative frequency distributions of observed emergence, ear emergence and harvest dates were created for the whole of Germany for each year of the period from 1995 to 1998. In addition, semi-variograms to determine the degree of spatial dependency of observations were calculated and fitted with the program Vesper; 100 lags and a 50% lag tolerance were used for the calculations, and exponential models were fitted to the variograms.

Spatial and temporal heterogeneity in observed emergence, ear emergence, and harvest dates were studied in more detail in six selected  $100 \text{ km} \times 100 \text{ km}$  grid cells (Fig. 4.1). Spatial heterogeneity among locations for one randomly chosen year (1986) was determined based on the average, earliest, and latest dates for each of the selected phenological events per grid cell, which were calculated based on ten randomly selected observations per event and per grid cell. The temporal heterogeneity for the period 1983 through 1988 was determined based on one randomly selected observation per event and per grid cell.

### 2.3.3 Effects of data aggregation on simulated results

In each of the six  $100 \text{ km} \times 100 \text{ km}$  grid cells, ten combinations of an observed emergence date with a weather station in the vicinity were selected for the period 1983 through 1988. Subsequently, the  $100 \text{ km} \times 100 \text{ km}$  grid cells were divided into four  $50 \text{ km} \times 50 \text{ km}$  grid cells, with the northwest  $50 \text{ km} \times 50 \text{ km}$  grid being used for the analyses, assuming that this was a representative grid. Data of combined observations of emergence dates and weather at specific locations falling into a common grid cell of  $50 \text{ km} \times 50 \text{ km}$  or  $100 \text{ km} \times 100 \text{ km}$

were spatially aggregated by calculating the arithmetic mean from the occurring values.

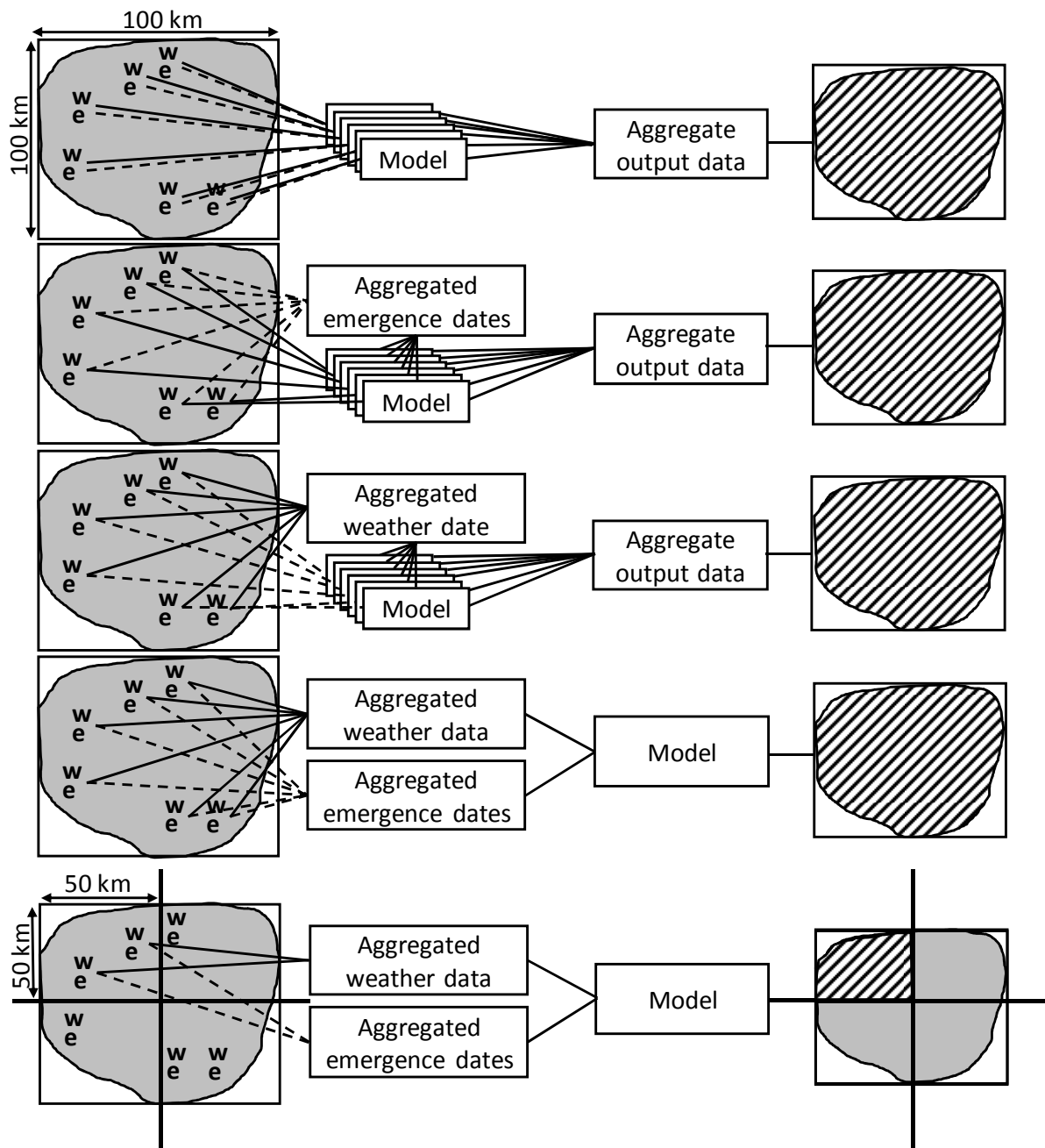


**Fig. 4.2** Overview of the model runs: w = weather data measured (—), e = emergence date observation (---). Data were aggregated based on the two grid cell resolutions (100 km × 100 km and 50 km × 50 km).

To be able to distinguish between the effects of aggregated emergence dates and aggregated weather, the model was run with either aggregated emergence dates or aggregated weather, or with their combination (Fig. 4.2). Simulated dates and lengths of development periods were averaged over the years and compared with averaged observed dates and lengths, goodness-of-fit of the

model being expressed in RMSE (Eq. 4.1). The spatial heterogeneity in weather conditions for each 100 km × 100 km grid cell was expressed in the difference in highest and lowest temperatures on each day among the ten weather stations.

### 3. Results and discussion

#### 3.1 Variability in observed phenological stages across Germany

##### 3.1.1 Spatial variability in stage occurrence

Fig. 4.3 shows the cumulative relative frequency distributions of all observed emergence, ear emergence and harvest dates for the whole of Germany for the period 1995 through 1998.

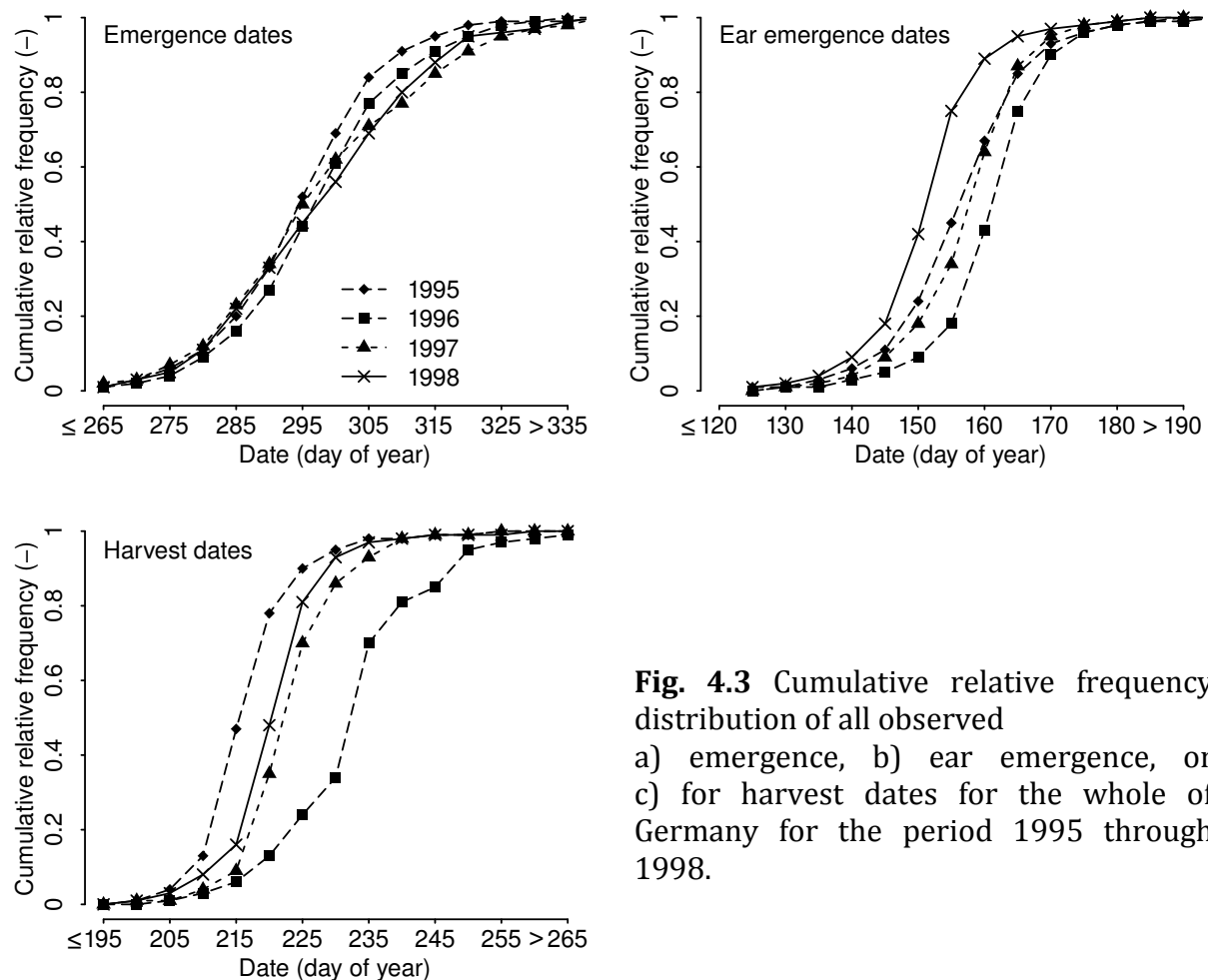


**Fig. 4.3** Cumulative relative frequency distribution of all observed  
a) emergence, b) ear emergence, or  
c) for harvest dates for the whole of  
Germany for the period 1995 through  
1998.

The slopes around the inflexion points of the development stages are different. The less steep slope for emergence indicates that the spread in observed emergence dates is larger than that for both ear emergence and harvest dates. Or in other words, the slopes of the graphs indicate that the variance in dates for the four years is largest for emergence and smaller, but similar, for ear emergence and harvest. The mean observed dates for emergence are approximately the same for all years. The mean observed ear emergence and harvest dates are different for the four years, most likely associated with inter-annual variability in weather conditions.

Semi-variogram parameters based on data from the whole of Germany for the years 1995 through 1998 are given in Table 4.2 and the semi-variograms from the year 1997 are given in Fig. 4.4 as examples. The parameter range represents the lag distance beyond which there is no autocorrelation among variables (Webster and Oliver, 2001) and is therefore a measure of the sampling distance. Ranges are different for emergence on the one hand and ear emergence and harvest on the other hand. The values for ear emergence and harvest indicate that in this case sampling grid cell sizes in the range 50 km × 50 km to 100 km × 100 km are reasonable.

**Table 4.2**

Semi-variogram parameters for different development stages and years of winter wheat grown in Germany.

Year	Sill	Nugget	Range (km)
Emergence			
1995	10126	126.4	103967
1996	10138	138.1	75519
1997	10201	201.4	42047
1998	10203	202.6	92336
Ear emergence			
1995	106	80.1	32
1996	84	64.4	94
1997	76	57.6	42
1998	170	82.1	2579
Harvest			
1995	64	41.5	119
1996	138	57.3	60
1997	69	31.7	27
1998	10061	60.9	277683



The differences in ranges might be explained by the differential influences of management and climate. Sowing, and therefore emergence, is mainly driven by management and only partly by climate; harvest date and especially ear emergence are more strongly influenced by climatic conditions. Climatic conditions are spatially dependent with a variability range of 50 – 100 km in most years according to Table 4.3.

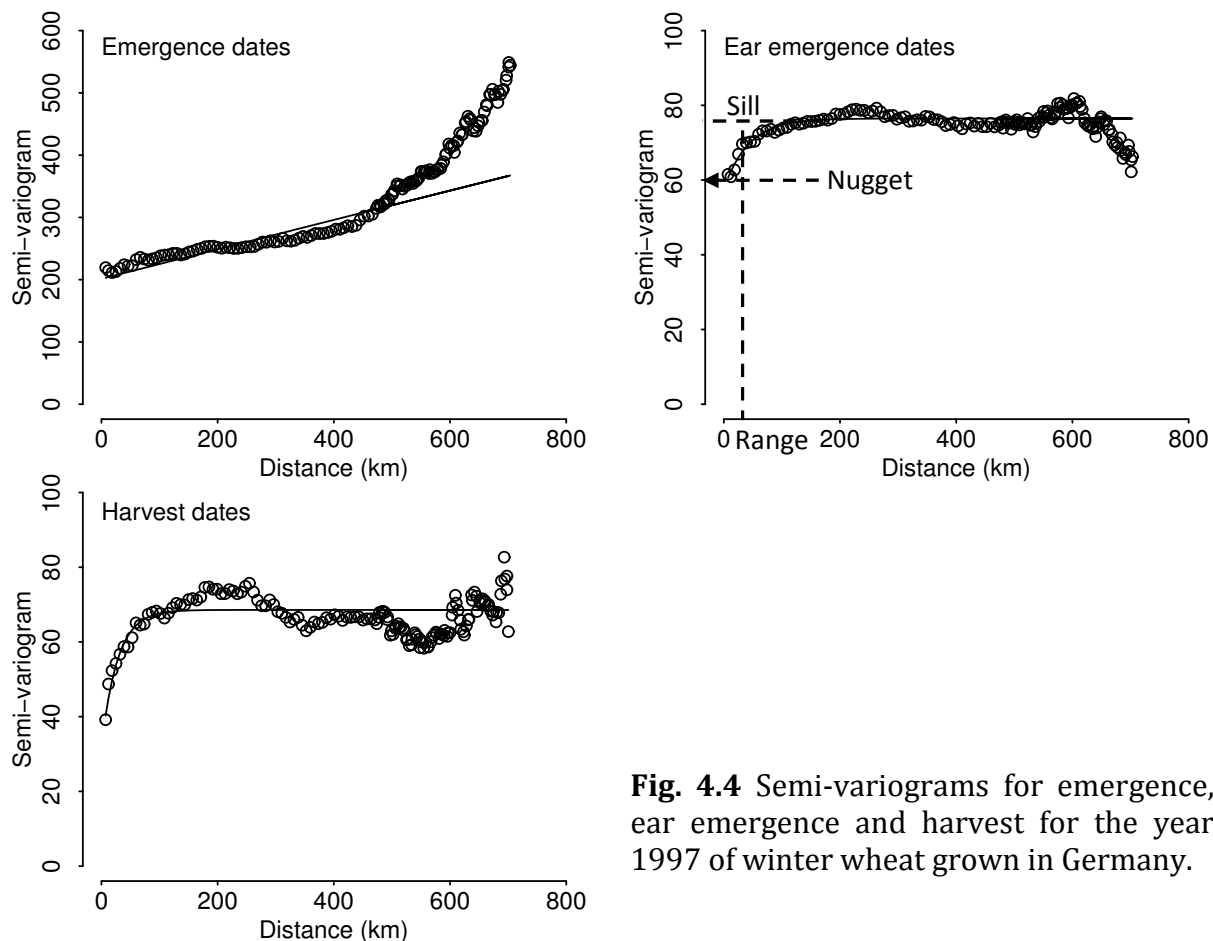


**Fig. 4.4** Semi-variograms for emergence, ear emergence and harvest for the year 1997 of winter wheat grown in Germany.

**Table 4.3**

Mean difference between the highest minimum and maximum temperatures and the lowest minimum and maximum temperatures for the ten weather stations within a 100 km × 100 km grid cell per region, averaged for the year 1984.

Region	Minimum temperature (°C)	Maximum temperature (°C)
Baden-Württemberg	5.7	5.5
Bayern	3.2	3.3
Nordrhein-Westfalen	4.0	2.9
Schleswig-Holstein	2.5	2.0
Hessen	2.6	2.2
Niedersachsen	3.9	4.1

### 3.1.2 Effects of aggregation on spatial heterogeneity of phenological stages

Aggregated emergence dates for the  $10 \times 10$ ,  $50 \times 50$ , and  $100 \text{ km} \times 100 \text{ km}$  grids from the year 1995 are shown in Fig. 4.5. The results of the  $10 \times 10$  resolution show that, in spite of the large number of observers, aggregation of data is necessary to obtain a full cover of emergence dates for the whole of Germany. At  $50 \text{ km} \times 50 \text{ km}$  resolution, only at the northern border of Germany full data cover is not attained; at  $60 \text{ km} \times 60 \text{ km}$  resolution, full data cover is attained by aggregation (not shown).

Aggregation results in reduced heterogeneity: increasing aggregation results in reduced spatial variability for emergence, harvesting, and ear emergence dates (Figs 4.5 and 4.6).

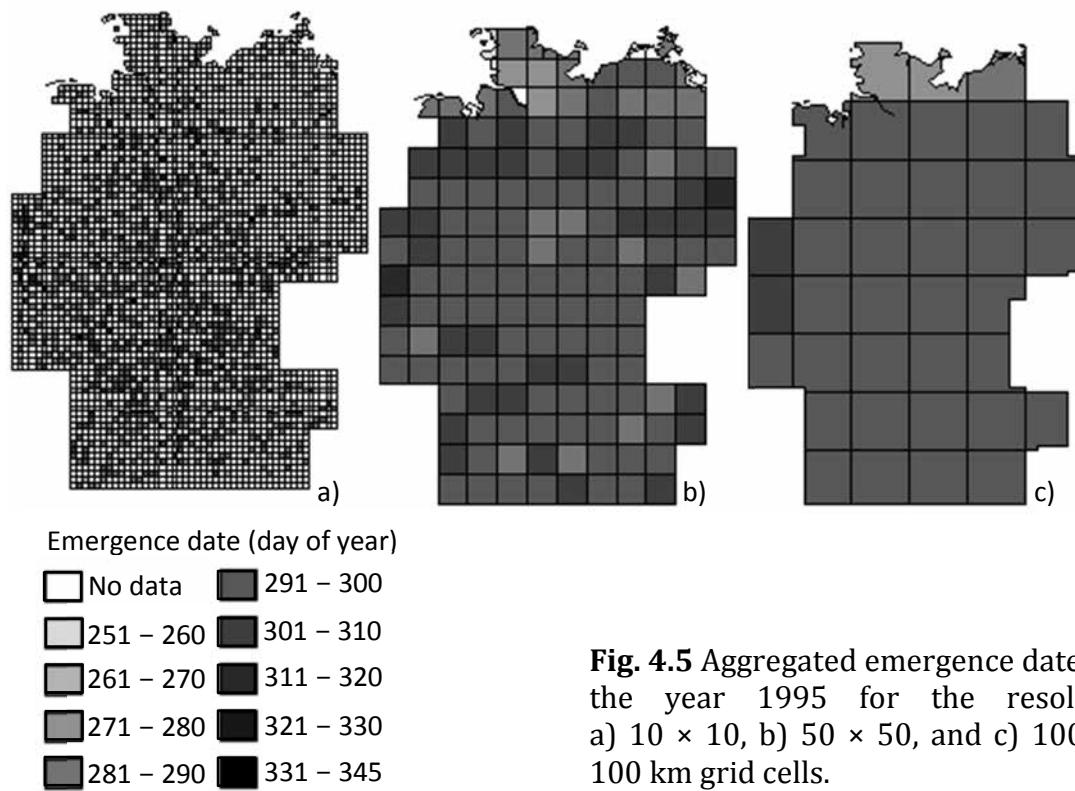


**Fig. 4.5** Aggregated emergence dates from the year 1995 for the resolutions: a)  $10 \times 10$ , b)  $50 \times 50$ , and c)  $100 \text{ km} \times 100 \text{ km}$  grid cells.

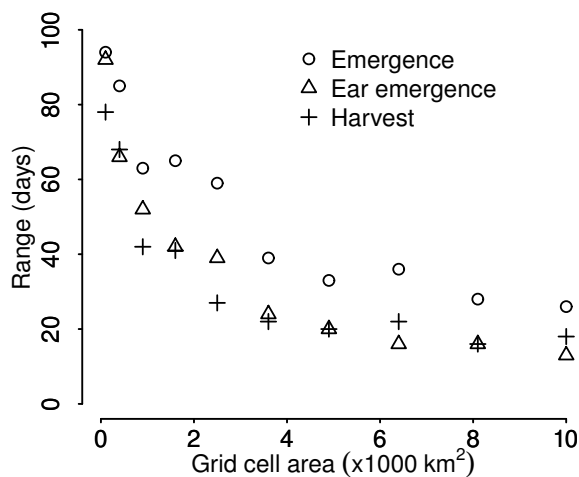


**Fig. 4.6** Range (=latest–earliest dates) in aggregated emergence, ear emergence, and harvest dates for different grid cell areas, based on data from the whole of Germany.

### 3.1.3 Spatial vs. temporal heterogeneity of phenological stages

Spatial and temporal heterogeneity in the timing of emergence, ear emergence and harvest dates across Germany are compared for observations in the six 100 km × 100 km grid cells (Fig. 4.1) for the period 1983 until 1988. Fig. 4.7 shows the average, earliest and latest dates of emergence, ear emergence and harvest within each 100 km × 100 km grid cell. Ranges in stage occurrence differ among regions. The temporal range in emergence dates between 1983 and 1988 for a randomly selected observation was narrowest in Schleswig–Holstein (12 d), widest in Baden–Württemberg (36 d) and for all regions on average 21 d. The spatial range in emergence dates for the year 1986 for different locations was narrowest in Baden–Württemberg (32 d), widest in Hessen (64 d) and for all regions on average 44 d. The temporal heterogeneity is thus smaller than the spatial heterogeneity. A possible explanation might be that individual farmers are inclined to sow at approximately the same date each year, while planning of sowing is different among farmers within a region.

Spatial heterogeneity in sowing dates was also found in Australia, where the average range in sowing (earliest–latest) for a 13-year period was about a month at State level (Stephens and Lyons, 1998), which is, despite the larger area, slightly narrower than the results observed here.

Average temporal heterogeneity is equal for crop emergence and ear emergence dates (21 d), but larger for harvest dates (41 d). The range in ear emergence dates might be explained by inter-annual variability in weather conditions. That variability may also explain the range in harvest dates, but additional heterogeneity might originate from planning of harvest activities based on available machinery and labour, explaining the wider range in harvest dates.

## 3.2 Simulation of phenological stages across Germany

### 3.2.1 Comparison of simulated (AFRCWHEAT2) with observed data

To assess the predictive accuracy of AFRCWHEAT2, the average observed and simulated dates ( $\overline{D_{\text{obs}}}$  and  $\overline{D_{\text{sim}}}$ ) for ear emergence and harvest, the average observed and simulated lengths ( $\overline{L_{\text{obs}}}$  and  $\overline{L_{\text{sim}}}$ ) of the period from emergence till ear emergence and from emergence till harvest, the spatial range in observed and simulated dates ( $\overline{R_{\text{obs}}}$  and  $\overline{R_{\text{sim}}}$ ), as well as the root mean squared errors (RMSE) were calculated per region (Table 4.4).

Simulated ear emergence is in general later than the observations. Average  $\text{RMSE}_{\text{date}} = 13.8$  d, with a maximum deviation for Baden–Württemberg (16.8 d) and a minimum for Nordrhein–Westfalen (9.6 d).

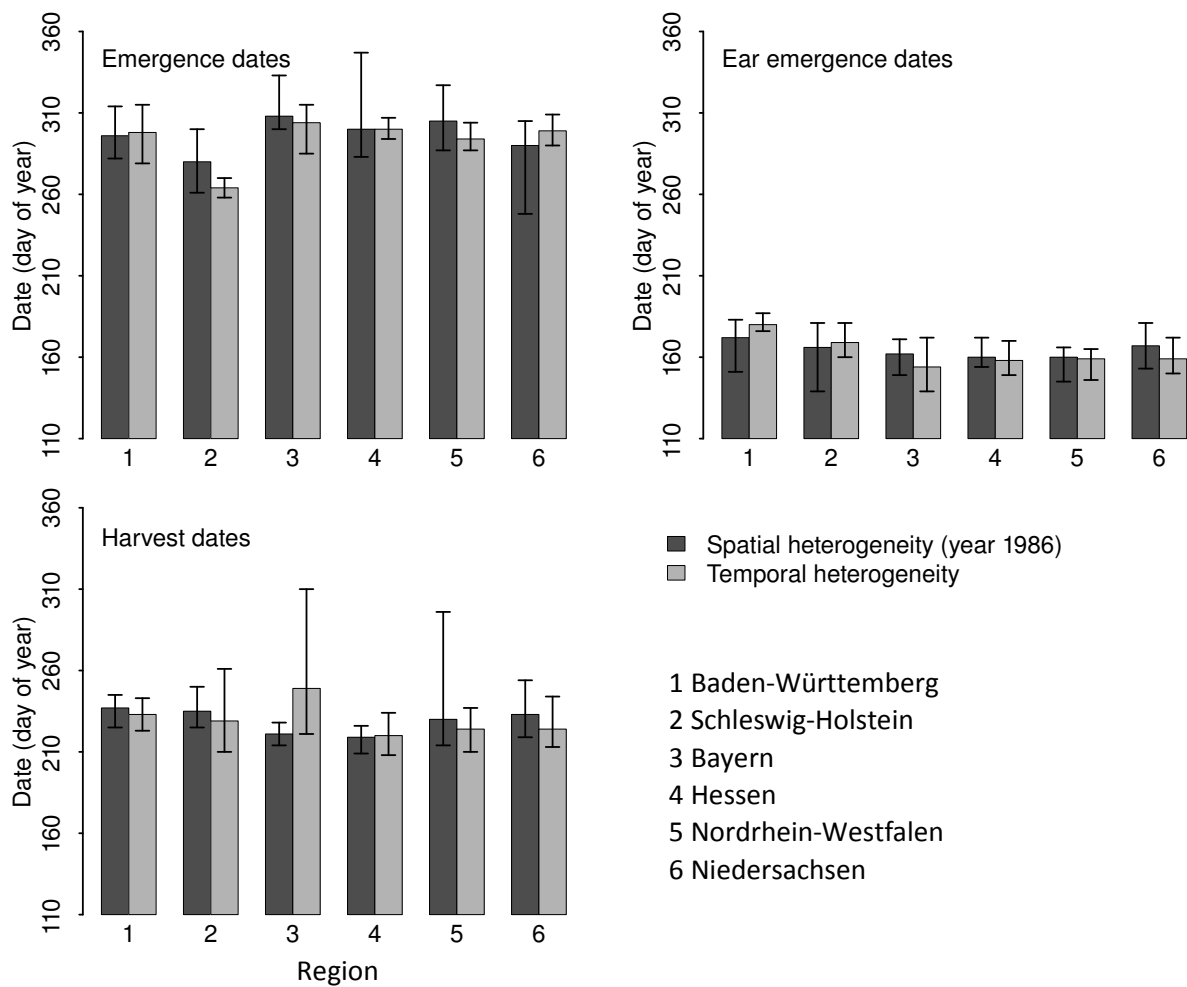


**Fig. 4.7** Average and range (= latest – earliest, indicated by error bar) in emergence, ear emergence, and harvest dates for 100 km × 100 km grid cells for each region.

The period from emergence to harvest is longer than from emergence till ear emergence, this implies that the same calculated average  $RMSE_{date}$  (13.8 d) indicates slightly smaller deviations in simulated harvest dates, with a maximum deviation for Nordrhein–Westfalen (19.0 d) and a minimum for Hessen (6.9 d). The delay in simulated ear emergence dates is less visible for simulated harvest dates. Ranges in observed dates, for both ear emergence and harvest, are in general wider than ranges in simulated dates.

**Table 4.4**

Root mean squared errors (RMSE) for lengths of development periods from emergence till ear emergence and from emergence till harvest ( $RMSE_{length}$ ) and for ear emergence and harvest dates ( $RMSE_{date}$ ), average observed and simulated dates ( $\overline{D_{obs}}$  and  $\overline{D_{sim}}$ ) for ear emergence and harvest, average observed and simulated lengths ( $\overline{L_{obs}}$  and  $\overline{L_{sim}}$ ) of the period from emergence till ear emergence and from emergence till harvest, as well as the range in observed and simulated dates (= latest – earliest date) ( $\overline{R_{obs}}$  and  $\overline{R_{sim}}$ ) per region.

Region	$RMSE_{length}$ (%)	$RMSE_{date}$ (d)	$\overline{D_{obs}}$ (day of year)	$\overline{D_{sim}}$ (day of year)	$\overline{L_{obs}}$	$\overline{L_{sim}}$ (d)	$\overline{R_{obs}}$	$\overline{R_{sim}}$
Emergence – ear emergence								
Baden-Württemberg	7.0 (n = 44)	16.8	171	182	239	250	49	33
Schleswig-Holstein	6.2 (n = 44)	15.1	162	170	243	252	53	29
Bayern	6.7 (n = 45)	14.9	164	176	222	234	35	25
Hessen	6.5 (n = 46)	14.3	159	172	222	233	35	27
Nordrhein-Westfalen	4.5 (n = 38)	9.6	159	164	215	217	45	33
Niedersachsen	5.1 (n = 50)	12.1	168	171	239	242	42	38
Emergence - harvest								
Baden-Württemberg	5.8 (n = 44)	17.7	238	247	306	315	57	67
Schleswig-Holstein	3.5 (n = 49)	11.0	236	233	317	315	41	39
Bayern	4.8 (n = 47)	13.7	229	232	287	290	96	33
Hessen	2.4 (n = 49)	6.9	228	228	290	289	49	34
Nordrhein-Westfalen	6.7 (n = 46)	19.0	231	222	285	275	93	40
Niedersachsen	4.7 (n = 50)	14.3	235	234	306	305	44	65

Important for crop yields are, in addition to the timing of a development stage, the lengths of the various phases and in particular that of the grain filling phase. For the length of the period between emergence and ear emergence  $RMSE_{length}$  is 6.0%, with a maximum for Bayern (7.0%) and a minimum for Nordrhein–Westfalen (4.5%). The length of the period between emergence and harvest is simulated more accurately with an average  $RMSE_{length}$  of 4.7%, with a maximum for Baden–Württemberg (5.8%) and a minimum for Hessen (2.4%). Fig. 4.8 shows the scatter plots for the location with the largest deviations between simulations and observations (Baden–Württemberg) and that with the smallest deviations (Hessen). Results for the other regions are given in Table 4.4.

Differences between simulations and observations may be explained by the effect of management on, e.g. harvest time, which may be based either on development stage of the crop (physiological maturity) as well as on availability of machinery and labour. This could also explain the wider ranges in the observations than in the simulations. Furthermore, observation errors could be a contributing factor.

$RMSE_{date}$  found by Porter *et al.* (1993) and Jamieson *et al.* (2007) for simulations with AFRCWHEAT2 and experimental data from New Zealand, range from 4.5 to 7.3 d for several development stages. These smaller deviations are, however, based on calibrated models, while we used the same parameter values across the whole of Germany. Also, development stages can be recorded more precisely in field experiments by trained technicians than by many different observers in commercial fields across the country.

### 3.2.2 Effects of data aggregation on model outcomes

To quantify the bias in model results due to the use of aggregated input data, the six 100 km × 100 km grid cells in Germany were used, each comprising ten observation points of emergence dates for winter wheat and nearby weather stations. To quantify the bias at an intermediate level of aggregation, the 100 km × 100 km grid cells were divided into four 50 km × 50 km grid cells. AFRCWHEAT2 was run with either non-aggregated or aggregated input data at the two spatial resolutions (Fig. 4.2).

Deviations between observations and simulation for ear emergence and harvest dates and the length of two phases (from emergence till ear emergence and from emergence till harvest) are small for all input data sets (Fig. 4.9; Table 4.5). Deviations are largest for ear emergence, with a maximum of 4.4% for the length of the period from emergence till ear emergence, if aggregated weather data are used.

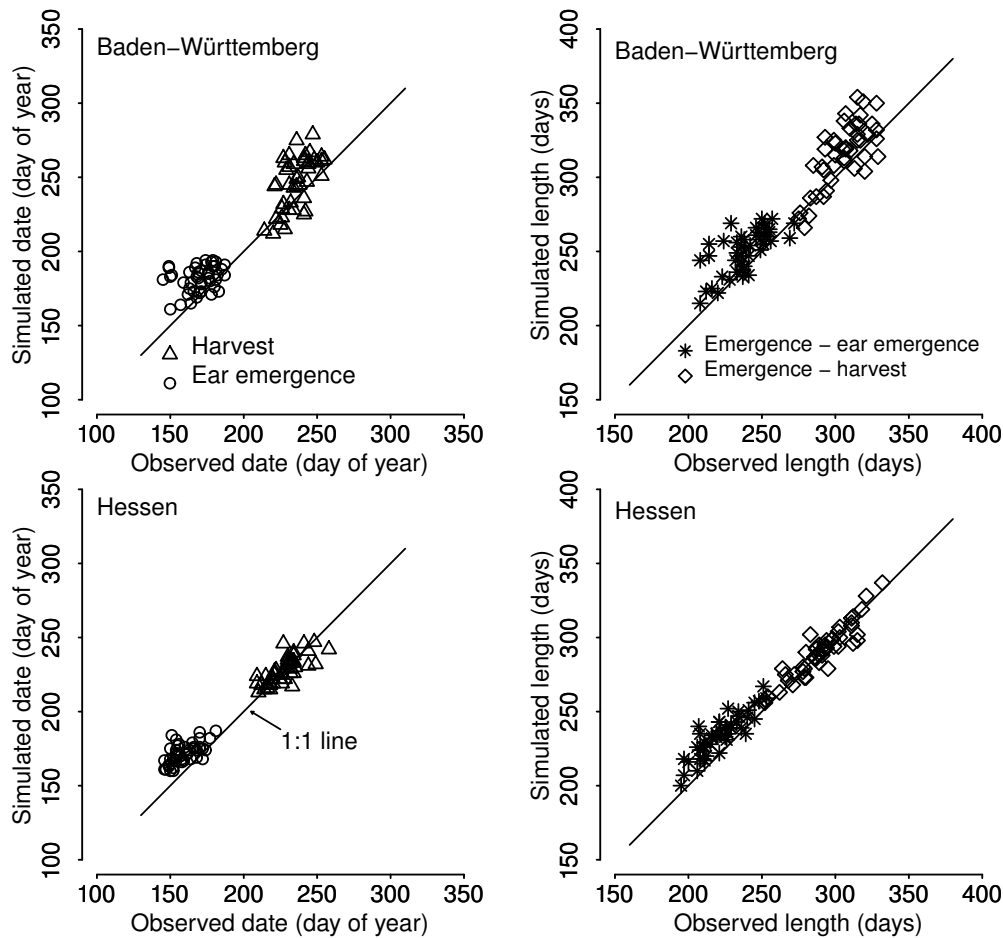


**Fig. 4.8** Scatter plots showing simulated dates (y-axis) (day of year for ear emergence and harvest (left figures); and lengths from emergence till ear emergence and from emergence till harvest (right figures)) plotted versus observed data (x-axis) for Baden-Württemberg (top figures) and Hessen (bottom figures). AFRCWHEAT2 was run with location-specific information.

For the 50 km × 50 km grid cells deviations between simulations and observations are generally smaller, in line with our expectations; however, improvements are only small. Results from Baden-Württemberg again show the largest deviations between observations and simulations (Fig. 4.9).

Our results indicate that the use of the combination of aggregated weather data and aggregated emergence dates in the model results in the largest deviations from observations. Considering aggregated weather data and emergence dates separately indicates that especially aggregation of weather data influences model results. However, deviations are only small and comparable with deviations using location-specific data, which is in line with conclusions from other studies (De Wit *et al.*, 2005; Easterling *et al.*, 1998; Olesen *et al.*, 2000).

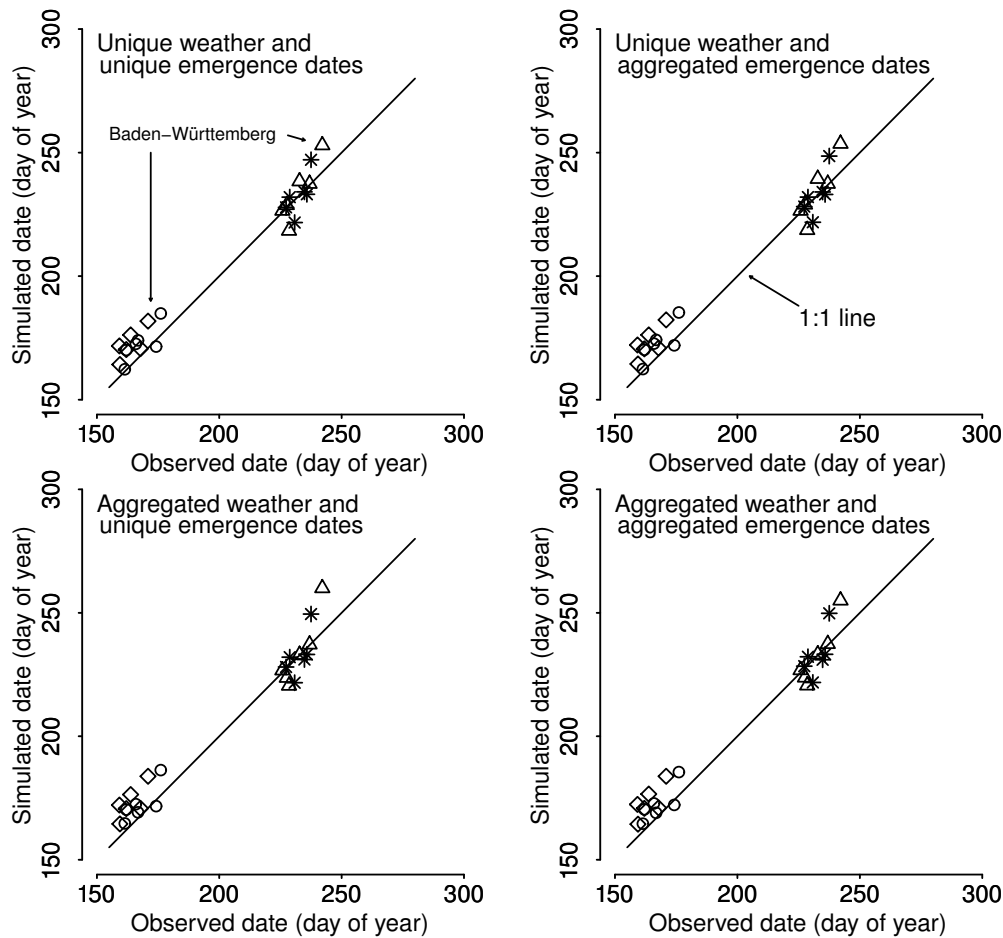


**Fig. 4.9** Effects of aggregation of input data on model results: ear emergence dates (o resolution of 50 km and ◇ resolution of 100 km); and harvest dates (Δ resolution of 50 km and \* resolution of 100 km).

As shown in Section 3.1, observed emergence dates show large spatial heterogeneity. As an example of the spatial heterogeneity in temperatures, the range in temperatures within the 100 km × 100 km grid cell in Baden-Württemberg, showing the largest variability in measured temperatures (Table 4.3), is shown in Fig. 4.10. Spatial aggregation results in disappearance of extreme values of emergence dates and temperatures, which especially influences model results if the model uses non-linear relationships. The small deviations in simulated length of the growing season when using spatially aggregated input data in our simulations can be explained by two aspects. First, AFRCWHEAT2 uses only one non-linear relationship (that between temperature and vernalization effectiveness), in which, moreover, the optimum temperature range is rather wide (3–10 °C). Second, differences in temperature among stations are rather small in all regions (Fig. 4.10; Table 4.3), so aggregation of weather data results in only minimum levelling out of extreme values.



**Table 4.5**

Root mean squared errors ( $RMSE_{length}$ ) for lengths of development periods from emergence till ear emergence and from emergence till harvest and  $RMSE_{date}$  for ear emergence and harvest dates for different levels of aggregation of input data.

Input data	RMSE <sub>length</sub> (%)	RMSE <sub>date</sub> (d)	RMSE <sub>length</sub> (%)	RMSE <sub>date</sub> (d)
	50 km		100 km	
Emergence - ear emergence				
Unique weather date and unique emergence date	2.7	6.4	4.1	9.4
Aggregated weather data and unique emergence date	2.7	6.3	4.4	10.0
Unique weather data and aggregated emergence date	2.7	6.4	4.2	9.6
Aggregated weather data and aggregated emergence date	2.6	6.0	4.4	10.0
Emergence - harvest				
Unique weather data and unique emergence date	2.2	6.5	1.9	5.6
Aggregated weather data and unique emergence date	2.7	8.2	2.2	6.5
Unique weather data and aggregated emergence date	2.3	6.8	2.1	6.1
Aggregated weather date and aggregated emergence date	2.1	6.4	2.2	6.7

## 4. Conclusions

We have shown that the spatial heterogeneity in timing of phenological stages from crop emergence to harvest in a region or country can be large. Our study indicates that it is possible to capture the average response pattern of the development of winter wheat across a larger country such as Germany, with one crop phenological parameter set. The remaining unexplained variation can (at least partially) be attributed to cultivation of a range of varieties, which we did not consider in our study.

We did not specifically address the uncertainties in model outcomes originating from e.g. uncertainties in parameter values or input data. Probabilistic modelling, as in Bayesian approaches, could be a helpful mean in this respect to quantify such uncertainties and should be further explored in future studies.

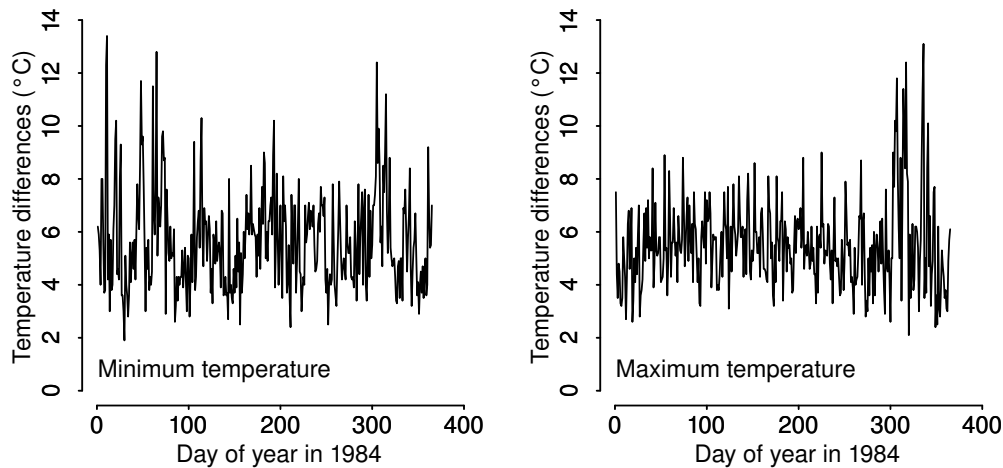


**Fig. 4.10** The largest differences between the highest and lowest temperatures observed (minimum and maximum temperature) within the Baden-Württemberg 100 km × 100 km grid cell for the ten weather stations.

Aggregation of available phenological information improves the spatial data coverage of a region, but reduces spatial heterogeneity. Importantly, the use of aggregated weather data and emergence dates for simulations of crop phenology has little effect on the aggregated predicted phenological events. Our results suggest that for the model used in this study, spatially aggregated weather data and emergence dates to simulate the length of the growing season for winter wheat is justified for grid cells with a maximum area of 100 km × 100 km for a number of regions in Germany.

Our results should also be applicable to other regions in Europe and elsewhere in the world with similar climatic conditions, and for other models that are mainly based on linear relationships for estimating phenological development. Caution is required in regions with high spatial variability in weather conditions or with models comprising more non-linear relationships. In those situations, aggregation errors are likely to be larger and smaller spatial scales should be applied for regional modelling of phenological development.

## Acknowledgements

The authors are grateful for the valuable comments of Herman van Keulen and two anonymous reviewers, who proposed important revisions to a previous version of this paper. Thanks to Madeleine Florin for her help with the semi-variograms.





## Chapter 5

# **Climate-driven simulation of global crop sowing dates**

Based on:  
Waha\*, K., Van Bussel\*, L.G.J., Müller, C., Bondeau, A.:  
Climate-driven simulation of global crop sowing dates.  
Global Ecology and Biogeography, in press  
\*These authors contributed equally

## Abstract

In this study we aimed to simulate the sowing dates of 11 major annual crops at the global scale at high spatial resolution, based on climatic conditions and crop-specific temperature requirements. Sowing dates under rainfed conditions are simulated deterministically based on a set of rules depending on crop- and climate-specific characteristics. We assume that farmers base their timing of sowing on experiences with past precipitation and temperature conditions, with the intra-annual variability being especially important. The start of the growing period is assumed to be dependent either on the onset of the wet season or on the exceeding of a crop-specific temperature threshold for emergence. To validate our methodology, a global data set of observed monthly growing periods (MIRCA2000) is used. We show simulated sowing dates for 11 major field crops world-wide and give rules for determining their sowing dates in a specific climatic region. For all simulated crops, except for rapeseed and cassava, in at least 50% of the grid cells and on at least 60% of the cultivated area, the difference between simulated and observed sowing dates is less than 1 month. Deviations of more than 5 months occur in regions characterized by multiple-cropping systems, in tropical regions which, despite seasonality, have favourable conditions throughout the year, and in countries with large climatic gradients. Sowing dates under rainfed conditions for various annual crops can be satisfactorily estimated from climatic conditions for large parts of the earth. Our methodology is globally applicable, and therefore suitable for simulating sowing dates as input for crop growth models applied at the global scale and taking climate change into account.

## 1. Introduction

In addition to soil characteristics, the suitability of a region for agricultural production is largely determined by climate. Precipitation controls the availability of water in rainfed and to some extent in irrigated production systems, temperature controls the length and timing of the various phenological stages on one hand and the productivity of crops on the other hand (Larcher, 1995; Porter and Semenov, 2005), and available radiation controls, via energy supply, the photosynthetic rate (Larcher, 1995). Furthermore, low temperatures and inadequate soil water availability during germination lead to low emergence rates and poor stand establishment, due to seed and seedling diseases, as shown, for example, in sugar beet (Jaggard and Qi, 2006) and soybean (Tanner and Hume, 1978), leading to low yield levels. To maximize or optimize production, farmers therefore aim to select suitable cropping periods, crops and management strategies.

With climate change, climatic conditions during the growing period will change (Burke *et al.*, 2009). Both mean and extreme temperatures are expected to increase for large parts of the earth with rising CO<sub>2</sub> concentrations (Yonetani and Gordon, 2001). To cope with these changing climatic conditions, adaptation strategies are required, e.g. changing the timing of sowing (Rosenzweig and Parry, 1994; Tubiello *et al.*, 2000).

Crop growth models are suitable tools for the quantitative assessment of future global crop productivity. They are increasingly applied at global scale (e.g. Bondeau *et al.*, 2007; Liu *et al.* 2007; Parry *et al.* 2004; Stehfest *et al.* 2007; Tao *et al.* 2009). Key inputs for crop growth models are weather data and information on management strategies, e.g. the choice of crop types, varieties and sowing dates. Future weather data for global application of crop growth models are usually provided by global circulation models (GCMs). It can be assumed that farmers will adapt sowing dates to changes in climatic conditions and therefore current sowing date patterns (Portmann *et al.*, 2008; Sacks *et al.*, 2010) will change over time. To adequately simulate sowing dates for future climatic conditions, it is necessary to understand the role of climate in the determination of sowing dates.

Different approaches are applied in existing crop models to determine current and future sowing dates. Crop models such as LPJmL (Bondeau *et al.*, 2007) identify sowing dates from climate data and crop water and temperature requirements for sowing. Another approach is to optimize sowing dates using the crop model by selecting the date which leads to the highest crop yield, a method applied, for example, in DayCent (Stehfest *et al.*, 2007), or by selecting the

optimal growing period based on pre-defined crop-specific requirements, as in GAEZ (Fischer *et al.*, 2002). Finally, pre-defined sowing dates based on observations have been used, e.g. in the Global Crop Water Model (GCWM) (Siebert and Döll, 2008) and in GEPIC (Liu *et al.*, 2007).

In contrast to pre-defined sowing dates, determining sowing dates from climate data, as well as the optimization of sowing dates, provides the opportunity to simulate changing sowing dates under future climatic conditions. However, outcomes of the optimization method are largely dependent on the crop model used, adding extra uncertainties to the outcomes. The calculation procedure currently applied in LPJmL (Bondeau *et al.*, 2007) is not applicable for all crops in different climatic regions and has only been evaluated for temperate cereals. Therefore, our aims are to: (1) describe an improved method to identify sowing dates within a suitable cropping window, based on climate data and crop-specific requirements at global scale, and (2) evaluate the agreement with global observations of sowing dates. Non-climatic reasons for the timing of sowing, such as the demand for a particular agricultural product during a certain period or the availability of labour and fertilizer, are not considered in the simulations of sowing dates. The outcomes of our analysis will be: (1) a set of rules to determine the start of the growing period for major crops in different climates; (2) an evaluation of the importance of climate in determining sowing dates; and (3) maps of simulated global patterns of sowing dates. Our outcomes will lead to improved simulation of crop phenology at the global scale, which will make an important contribution to estimates of carbon and water fluxes in dynamic global vegetation models. Furthermore, sowing dates in suitable cropping windows under future climatic conditions can be estimated, and are likely to improve integrated assessments of global crop productivity under climate change.

## 2. Materials and methods

### 2.1 Input climate data

Monthly data of temperature, precipitation and number of wet days on a  $0.5^\circ \times 0.5^\circ$  resolution are based on a data set compiled by the Climatic Research Unit (Mitchell and Jones, 2005). A weather generator distributes monthly precipitation to observed number of wet days, which are distributed over the month taking into account the transition probabilities between wet and dry phases (Geng *et al.*, 1986). Daily mean temperatures are obtained by linear interpolation between monthly mean temperatures.

## 2.2 Deterministic simulation of sowing dates

Sowing dates, averaged over the period from 1998 to 2002, were simulated deterministically, based on a set of rules depending on crop and climate characteristics. Sowing dates were simulated for 11 major field crops (wheat, rice, maize, millet, pulses, sugar beet, cassava, sunflower, soybean, groundnut and rapeseed) under rainfed conditions. We did not consider irrigated systems, because if irrigation is applied, sowing dates are strongly determined by the availability of irrigation water (e.g. melting glaciers upstream) and labour, factors not considered in the methodology.

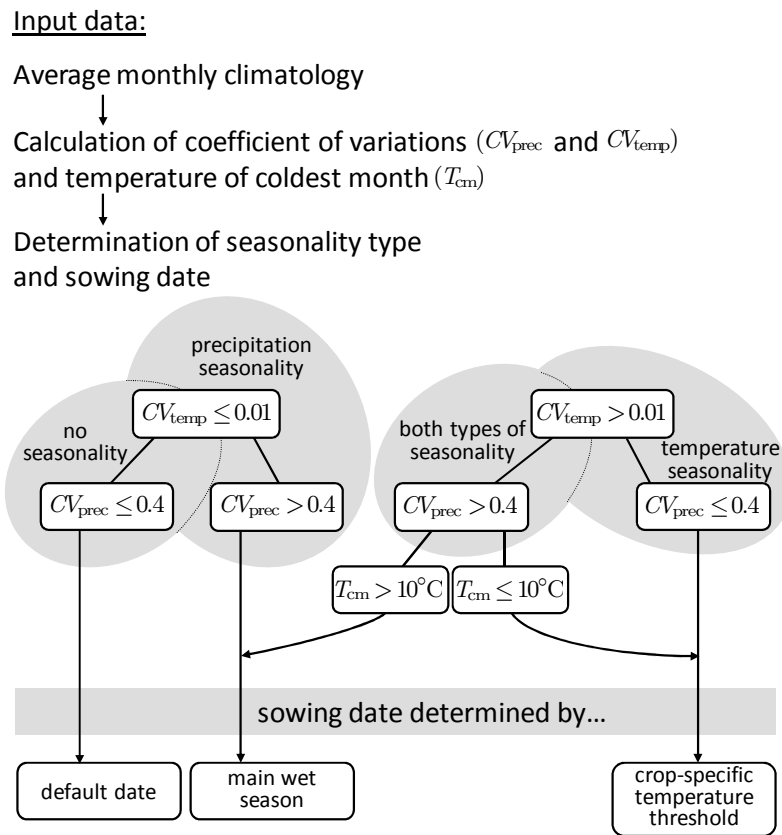


**Fig. 5.1** Procedure to determine seasonality type and sowing date. Annual variation coefficients for precipitation ( $CV_{prec}$ ) and temperature ( $CV_{temp}$ ) are calculated from past monthly climate data.  $T_{cm}$  is temperature of the coldest month.

We assumed that farmers base the timing of their sowing on experiences with past weather conditions: e.g. in southern India, farmers use a planting window for rainfed groundnut based on experiences of about 20 years (Gadgil *et al.*, 2002), in the African Sahel, knowledge for decision making is influenced by previous generations' observations (Nyong *et al.*, 2007), while farmers in the south-eastern USA are expected to adapt their management to changes in climatic conditions within 10 years (Easterling *et al.*, 2003). In order to be able to



use a generic rule across the earth we represented the experiences of farmers with past weather conditions by exponential weighted moving average climatology. This gave a higher importance to the monthly climate data from the most recent years than the monthly climate data from less recent years for the calculation of the average monthly climate data. Consequently, the month of sowing is determined by past climatic conditions, whereas the actual sowing date within that month is simulated based on the daily temperature and precipitation conditions from the specific year. Figure 5.1 shows a schematic overview of the methodology followed.

### 2.2.1 Determination of seasonality types

We assumed that the timing of sowing is dependent on precipitation and temperature conditions, with the intra-annual variability of precipitation and temperature being especially important. Precipitation and temperature seasonality of each location are characterized by the annual variation coefficients for precipitation ( $CV_{\text{prec}}$ ) and temperature ( $CV_{\text{temp}}$ ), calculated from past monthly climate data. To prevent interference from negative temperatures if expressed in °C, temperatures are converted to kelvin. The variation coefficients are calculated as the ratio of the standard deviation to the mean:

$$CV_j = \frac{\sigma_j}{\mu_j} \quad (\text{Eq. 5.1})$$

with

$$\sigma_j = \sqrt{\frac{1}{12-1} \times \sum_{m=1}^{12} (\bar{X}_{m,j} - \mu_j)^2}, \quad (\text{Eq. 5.2})$$

$$\mu_j = \frac{1}{12} \times \sum_{m=1}^{12} \bar{X}_{m,j}, \quad (\text{Eq. 5.3})$$

and

$$\bar{X}_{m,j} = \alpha \times X_{m,j} + (1 - \alpha) \times \bar{X}_{m,j-1} \quad (\text{Eq. 5.4})$$

where  $X_{m,j}$  is the mean temperature (K) or precipitation (mm) of month  $m$  in year  $j$ ,  $\bar{X}_{m,j}$  the exponential weighted moving average temperature or precipitation of month  $m$  in year  $j$ ,  $\mu_j$  the annual mean temperature or precipitation in year  $j$ ,  $\sigma_j$  the standard deviation of temperature or precipitation in year  $j$ , and  $\alpha$  the coefficient representing the degree of weighting decrease (with a value of 0.05). The calculation was initialized by  $\bar{X}_{m,j=1} = X_{m,j=1}$ .

Variation coefficients are commonly used to distinguish different seasonality types (Walsh and Lawler, 1981; Jackson, 1989; Hulme, 1992). Walsh and Lawler (1981) provided a classification scheme for characterizing the precipitation pattern of a certain region based on the value of  $CV_{\text{prec}}$  and suggested describing a region with a  $CV_{\text{prec}}$  exceeding 0.4 as ‘rather seasonal’ or ‘seasonal’. We could not find such a value for  $CV_{\text{temp}}$  in the literature; however, in order to simulate a reasonable global distribution of temperate and tropical regions, we assumed temperature seasonality if  $CV_{\text{temp}}$  exceeds 0.01. Accordingly, four seasonality types can be distinguished: (1) no temperature and no precipitation seasonality, (2) precipitation seasonality, (3) temperature seasonality, and (4) temperature and precipitation seasonality.

In situations with a combined temperature and precipitation seasonality, we additionally considered the mean temperature of the coldest month. If the mean temperature of the coldest month exceeded 10 °C, we assumed absence of a cold season, i.e. the risk of occurrence of frost is negligible, which is in line with the definition of Fischer *et al.* (2002). Consequently, temperatures are high enough to sow year-round, therefore precipitation seasonality is determining the timing of sowing. If the mean temperature of the coldest month is equal to or below 10 °C, we assumed temperature seasonality to be determining the timing of sowing.

### 2.2.2 Determination of the start of the growing period

The growing period is the period between sowing and harvesting of a crop. We applied specific rules per seasonality type to simulate sowing dates (Fig. 5.1). In regions with no seasonality in precipitation and temperature conditions, crops can be sown at any moment and we assigned a default date as sowing date (1 January, for technical reasons).

In regions with precipitation seasonality, we assumed that farmers sow at the onset of the main wet season. The precipitation-to-potential-evapotranspiration ratio is used to characterize the wetness of months, as suggested by Thornthwaite (1948). Potential evapotranspiration is calculated using the Priestley–Taylor equations (Priestley and Taylor, 1972), with a value of 1.391 for the Priestley–Taylor coefficient (Gerten *et al.*, 2004). As a region may experience two or more wet seasons, the main wet season is identified by the largest sum of monthly precipitation-to-potential-evapotranspiration ratios of four consecutive months; the 4 months period was selected because the length of that period captures the length of the growing period of the majority of the simulated crops. Crops are sown at the first wet day in the main wet season of the simulation year,

i.e. with a daily precipitation higher than 0.1 mm, which is in line with the definition of New *et al.* (1999).

In regions with temperature seasonality, the onset of the growing period depends on temperature. Crop emergence is related to temperature; accordingly, sowing starts when daily average temperatures exceed a certain threshold (Larcher, 1995). Crop varieties such as winter wheat and winter rapeseed require vernalizing temperatures and are therefore sown in autumn. Accordingly, for those crops, temperatures should fall below a crop-specific temperature threshold (Table 5.1). To be certain to fulfil vernalization requirements, crop-specific temperature thresholds are set around optimum vernalization temperatures, which resembles the practice applied by farmers in southern Europe for example (Harrison *et al.*, 2000). Earlier research, i.e. the analysis of Sacks *et al.* (2010) on crop planting dates, showed that temperatures at which sowing usually begins vary among crops, but are rather uniform or in the same range for a given crop throughout large regions. For simplicity, we assumed that one crop-specific temperature threshold is applicable globally. The sowing month is the month in which mean monthly temperatures of the past ( $\bar{X}_{m,j}$ ) exceed (or fall below) the temperature threshold. In addition, typical daily temperatures of the preceding month are checked. If the typical daily temperature of the last day of this preceding month already exceeds (or falls below) the temperature threshold, this month is selected as the sowing month. Typical daily temperatures are computed by linearly interpolating the mean monthly temperatures of the past ( $\bar{X}_{m,j}$ ). Next, daily average temperature data of the simulated year determine the specific date of sowing in the sowing month, in order to consider the climatic specificity of the simulated year.

We derived the temperature thresholds, for non-vernalizing crops only, by decreasing and increasing the temperature thresholds given by Bondeau *et al.* (2007) for sowing by  $-4^{\circ}\text{C}$  to  $+8^{\circ}\text{C}$  and selected the temperature thresholds that resulted in an optimal agreement between observed and simulated sowing dates in regions with temperature seasonality. The resulting temperature thresholds for sowing are plausible when compared with base temperatures for emergence found in the literature (Table 5.1). Although our temperature thresholds are slightly higher or at the top end of the range of base temperatures found, temperatures just above these base temperatures for emergence will result in retarded emergence (Jaggard and Qi, 2006).

**Table 5.1**

Crop-specific temperature thresholds for sowing.

Crop	Base temperature for emergence found in literature			Temperature used in this study (°C)
	Reference	Temperature (°C)	Range (°C)	
Cassava	Hillocks and Thresh, 2002	16	12 – 17	22
	Keating and Evenson, 1979	12 – 17		
Groundnut	Angus <i>et al.</i> , 1980	13.3	8 – 13.3	15
	Mohamed <i>et al.</i> , 1988	8 – 11.5		
	Prasad <i>et al.</i> , 2006	11 – 13		
Maize	Birch <i>et al.</i> , 1998	8	8 – 12.8	14
	Coffman, 1923	10		
	Grubben and Partohardjono, 1996	10		
	Kiniry <i>et al.</i> , 1995	12.8		
	Pan <i>et al.</i> , 1999	10		
	Warrington and Kanemasu, 1983	9		
Millet	Garcia-Huidobro <i>et al.</i> , 1982	10 – 12	7.7 – 13.5	12
	Grubben and Partohardjono, 1996	12		
	Kamkar <i>et al.</i> , 2006	7.7 – 9.9		
	Mohamed <i>et al.</i> , 1988	8 – 13.5		
Pulses	Angus <i>et al.</i> , 1980 – field pea	1.4	1.4 – 11	10
	Angus <i>et al.</i> , 1980 – cowpea	11		
	Angus <i>et al.</i> , 1980 – mungbean	10.8		
Rice	Rehm and Espig, 1991	10	10 – 19	18
	Yoshida, 1977	16 – 19		
Soybean	Angus <i>et al.</i> , 1980	9.9	5 – 10	13
	Tanner and Hume, 1978	10		
	Whigham and Minor, 1978	5		
Spring rapeseed	Angus <i>et al.</i> , 1980	2.6	1 – 2.6	5
	Booth and Gunstone, 2004	2		
	Vigil <i>et al.</i> , 1997	1		
Spring wheat	Addae and Pearson, 1992	0.4	0.4 – 2.8	5
	Del Pozo <i>et al.</i> , 1987	2		
	Khah <i>et al.</i> , 1986	1.9		
	Kiniry <i>et al.</i> , 1995	2.8		
Sugar beet	Jaggard and Qi, 2006	3	3 – 4	8
	Rehm and Espig, 1991	4		
Sunflower	Angus <i>et al.</i> , 1980	7.9	3.3 – 7.9	13
	Khalifa <i>et al.</i> , 2000	3.3 – 6.7		
Winter rapeseed*				≤ 17
Winter wheat*				≤ 12

\*Winter wheat and winter rapeseed are sown in autumn, as both crops have to be exposed to vernalizing temperatures. Their base temperatures for emergence have been selected around the optimum vernalization temperatures.

## 2.3 Procedure to validate the methodology

### 2.3.1 Data set of observed growing periods: MIRCA2000

To validate our methodology, the global data set of observed growing areas and growing periods, MIRCA2000 (Portmann *et al.*, 2008) at a spatial resolution of  $0.5^\circ \times 0.5^\circ$  and a temporal resolution of 1 month was used. Monthly data in MIRCA2000 were converted to daily data following the approach of Portmann *et al.* (2010), by assuming that the growing period starts at the first day of the month reported in MIRCA2000. The data set includes 26 annual and perennial crops and covers the time period between 1998 and 2002. For most countries, MIRCA2000 was derived from national statistics. For China, India, the USA, Brazil, Argentina, Indonesia, and Australia, subnational information was used as well, mainly from the Global Information and Early Warning System on food and agriculture (FAO-GIEWS) and from the United States Department of Agriculture (USDA). Based on the extent of cropland, derived from satellite-based remote sensing information and national statistics (Ramankutty *et al.*, 2008), the growing area combined with the growing period of each crop was distributed to grid cells at a spatial resolution of  $5' \times 5'$ , which were finally aggregated to grid cells of  $0.5^\circ \times 0.5^\circ$  (Portmann *et al.*, 2008). Sacks *et al.* (2010) recently compiled a similar data set of crop planting dates, also using cropping calendars from FAO-GIEWS and USDA. MIRCA2000, in contrast, distinguishes between rainfed and irrigated crops, which allows a comparison of sowing dates for rainfed crops only.

MIRCA2000 distinguishes up to five possible growing periods per grid cell, reflecting different varieties of wheat, rice and cassava and/or multiple-cropping systems of maize and rice, but for most crops only one growing period per year is reported. For wheat, spring varieties and winter varieties are distinguished; for rice a number of growing periods are distinguished, i.e. for upland rice, deep-water rice and paddy rice, with up to three growing periods for paddy rice (Portmann *et al.*, 2010). For cassava, an early and a late ripening variety with different sowing dates are distinguished.

In contrast, we assumed only one growing period per year in single-cropping systems. For wheat and rapeseed, we distinguished between spring and winter varieties: in regions with suitable climatic conditions for both varieties, the winter variety has been selected. If daily average temperatures exceed  $12^\circ\text{C}$  ( $17^\circ\text{C}$  for rapeseed) year round or drop below that threshold before 15 September (Northern Hemisphere) or before 31 March (Southern Hemisphere), the spring variety was selected. As MIRCA2000 reports several growing periods for some crops, it was difficult to select the most suitable growing period for

comparison. Consequently, we selected the best corresponding growing period, indicating the reasonableness of the simulated sowing dates but not their representativeness. Portmann *et al.* (2010) reported several uncertainties and limitations of MIRCA2000: data gaps and uncertainties in the underlying national census data, the lack of subnational data for some larger countries and therefore neglect of possible effects on growing periods due to climatic gradients, and the fact that very complex cultivation systems, in which more than one crop is grown on the same field at the same time, could not be represented adequately. These constraints, as well as the temporal resolution of 1 month of MIRCA2000 should be taken into account when assessing the comparison between observed and simulated sowing dates.

### 2.3.2 Methodology for comparing observed and simulated sowing dates

To assess the degree of agreement between simulated and observed sowing dates, two indices of agreement were calculated for each crop: the mean absolute error ( $ME$ ) and the Willmott coefficient of agreement ( $W$ ) (Willmott, 1982):

$$ME = \frac{\sum_{i=1}^N |S_i - O_i| \times A_i}{\sum_{i=1}^N A_i} \quad (\text{Eq. 5.5})$$

$$W = 1 - \frac{\sum_{i=1}^N (S_i - O_i)^2 \times A_i}{\sum_{i=1}^N (|S_i - \bar{O}| + |O_i - \bar{O}|)^2 \times A_i} \quad (\text{Eq. 5.6})$$

where  $S_i$  is the simulated and  $O_i$  the observed sowing date (day of year) in grid cell  $i$ ,  $\bar{O}$  the mean observed sowing date (day of year),  $A_i$  the cultivated area (ha) of the crop in grid cell  $i$ , and  $N$  the number of grid cells.

Indices are area-weighted, so the agreement in the main growing areas of a crop is considered more important than the agreement in areas where the crop is grown on smaller areas.  $W$  is dimensionless, ranging from 0 to 1, with 1 showing perfect agreement.  $ME$  indicates the global average error between simulations and observations,  $W$  additionally considers systematic differences between simulations and observations (Willmott, 1982). In addition to the two indices of agreement, we calculated the cumulative frequency distribution of the mean absolute error in days between the observed and simulated sowing dates, to show the frequency of grid cells and of cultivated area below a certain threshold.

### 3. Results

We show the global distribution of seasonality types (Fig. 5.2) as well as sowing dates simulated with the presented methodology and the comparison with observed sowing dates from MIRCA2000 (Figs B5.1 – AB.11 in Appendix B). To assess these results, we performed a sensitivity analysis of crop yields on sowing dates (see Fig. B5.12). Regions without seasonality are not considered in the evaluation of results, because sowing dates do not substantially affect crop yield there, as indicated by the sensitivity analysis (Fig. B5.12).

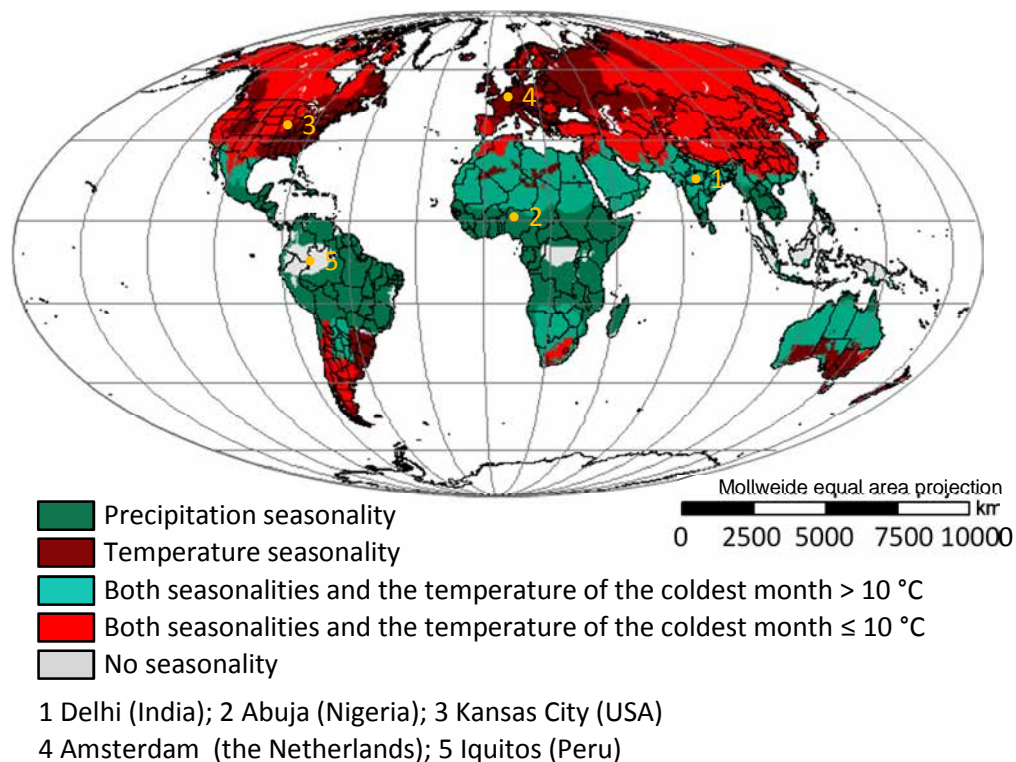


**Fig. 5.2** Global distribution of seasonality types. Seasonality types are based on the annual patterns of precipitation and temperature. For each seasonality type one example region is marked.

#### 3.1 Seasonality types

The spatial pattern of the calculated seasonality types (Fig. 5.2) resembles the distribution of various climates across the earth. Locations around the equator in the humid tropics are characterized by a lack of seasonality in both temperature and precipitation (e.g. Iquitos, Peru). The semi-humid tropics, with dry and wet seasons, are characterized by precipitation seasonality only (e.g. Abuja, Nigeria). The temperate zones in the humid middle latitudes with warm summers and cool winters are characterized by temperature seasonality (e.g. Amsterdam, the Netherlands). In locations with precipitation seasonality and a distinct cold

season (e.g. Kansas City, USA), low temperatures limit the growing period of crops and sowing dates are simulated based on temperature. If a cold season is absent in a location with precipitation seasonality (e.g. Delhi, India), sowing dates are simulated based on precipitation. Figure 5.3 shows annual variations in temperature and precipitation for five locations and Fig. 5.2 indicates their location.

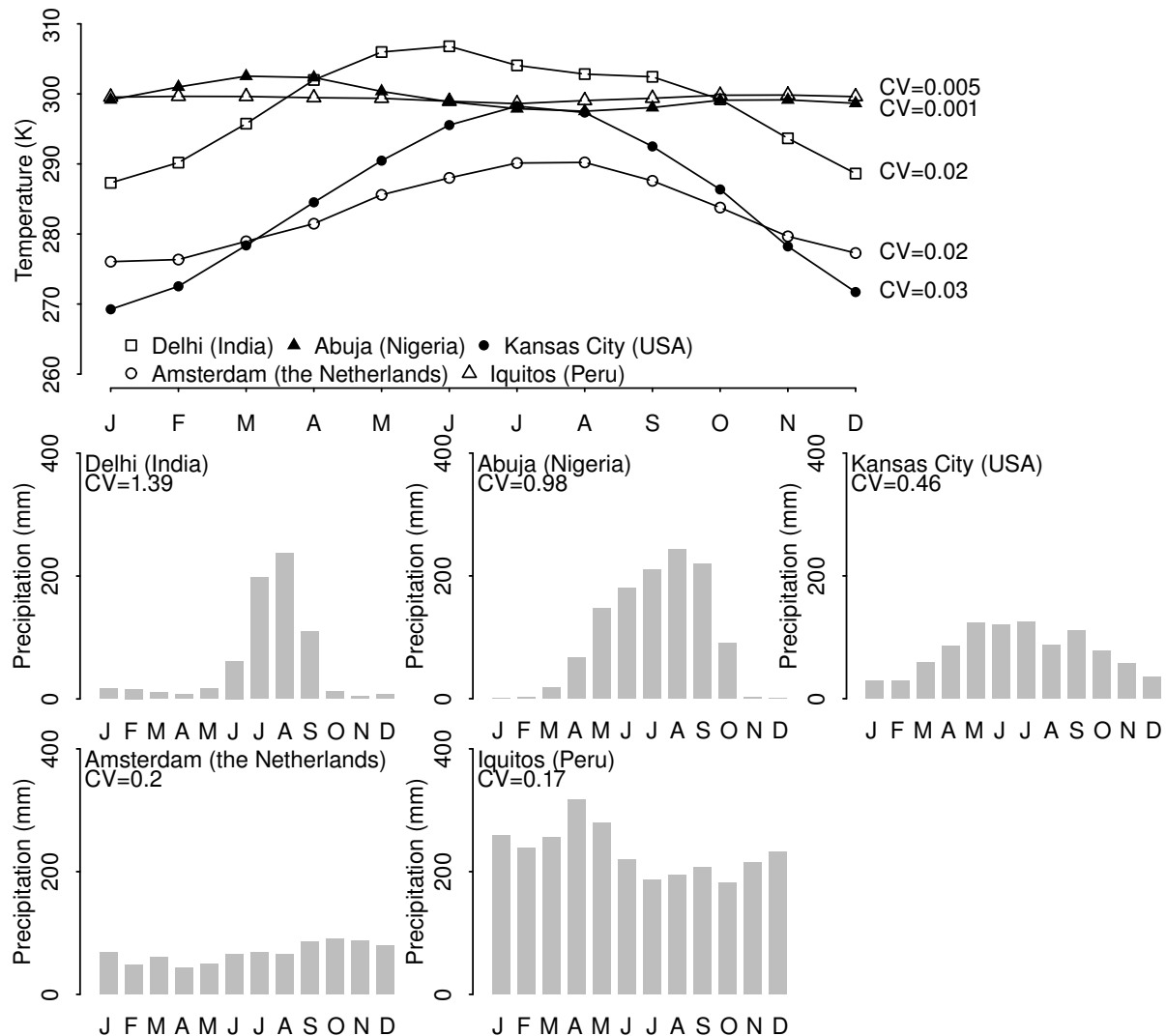


**Fig. 5.3** Annual variations in temperature (above) and precipitation (below) for five locations.

### 3.2 Comparison of observed and simulated sowing dates

Figures B5.1 – B5.11 show simulated and observed sowing dates, as well as the deviations per crop. As a condensed overview, Fig. 5.4 shows the cumulative frequency distribution of the mean absolute error between observations and simulations for all crops, for all grid cells combined, and separately for the two rules.



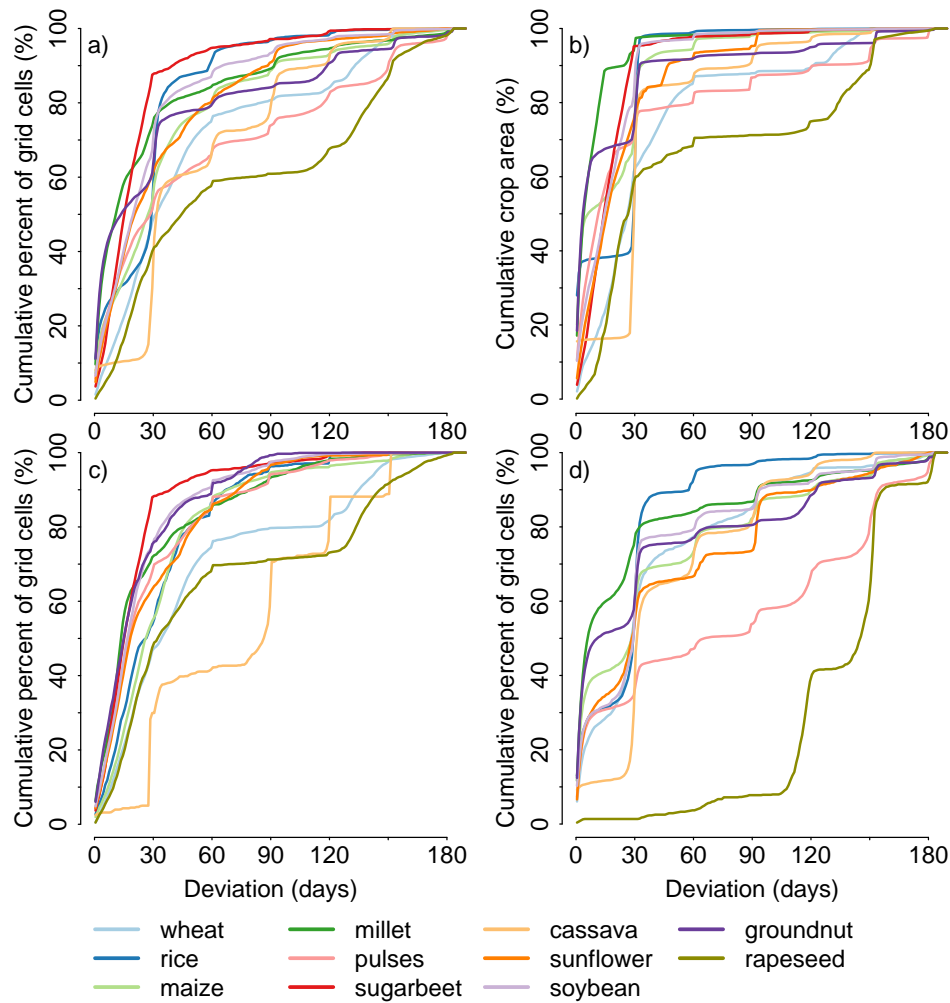


**Fig. 5.4** Cumulative percentage of grid cells (or crop area in a grid cell) with certain differences between observed and simulated sowing date. Deviations are shown for: a) all grid cells, b) crop area of all grid cells, c) grid cells where sowing dates are determined by a temperature threshold, and d) grid cells where sowing dates are determined by the onset of the main wet season. Grid cells with a crop area smaller than 0.001% of the grid cell area are not considered in the calculations. Curves are only shown if the number of grid cells in which a specific rule to determine the sowing date for a specific crop is applied exceeds 1% of all grid cells.

Figure 5.4 and the difference maps (Figs B5.1a – B5.11a) indicate close agreement for rice, millet, sugar beet, sunflower, soybean and groundnut globally, as well as close agreement for pulses in regions where temperature seasonality determines sowing dates. Figure 5.4 shows that for all crops except rapeseed and cassava, in at least 50% of the grid cells and on at least 60% of the cultivated area the error between simulations and observations is less than 1 month. Even in regions where simulated sowing dates deviate from observed sowing dates by 1 month, the results from the sensitivity analysis suggest that this range hardly affects computed crop yields from a global dynamic vegetation

**Table 5.2**

Indices of agreement between simulated sowing dates and observed sowing dates.

	Mean absolute error (days)			Willmott coefficient (-)				
	Sowing date determined by:			Sowing date determined by:			% of all cells	
	Wet season	Temp. threshold	All cells	Wet season	Temp. threshold	All cells	Wet season	Temp. threshold
Wheat	37 (37*)	45 (30*)	44 (30*)	0.9 (0.9*)	0.88 (0.96*)	0.88 (0.96*)	18 (22*)	82 (78*)
Rice	<b>22</b>	23	24	0.92	<b>0.94</b>	0.92	82	18
Maize	38	<b>32</b>	34	<b>0.89</b>	0.87	0.89	48	52
Millet	<b>14</b>	33	15	<b>0.95</b>	0.86	0.91	63	37
Pulses	79	<b>37</b>	69	0.62	<b>0.84</b>	0.63	50	50
Sugar beet		<b>18</b>	18		<b>0.71</b>	0.81	1	99
Cassava	<b>48</b>	51	48	0.93	<b>0.96</b>	0.93	83	17
Sunflower	43	<b>22</b>	25	0.88	<b>0.93</b>	0.93	25	75
Soybean	36	<b>33</b>	34	<b>0.94</b>	0.93	0.95	32	68
Groundnut	33	<b>19</b>	31	0.82	<b>0.97</b>	0.84	81	19
Rapeseed	133	<b>39</b>	54	0.14	<b>0.91</b>	0.85	16	84

Bold values indicate which rule determining sowing date results in a closer agreement. Indices of agreement are only shown if the number of cells in which a specific rule for determining the sowing date is applied is > 1% of all cells. Grid cells with a crop area smaller than 0.001% of the grid area are not considered in the calculations.

\* indices of agreement without Russia

and crop model (Fig. B5.12), if they fall within a suitable growing period (e.g. the main wet season or spring season).

Poor agreement, with differences between simulations and observations of more than 5 months, is found for wheat in Russia, for maize and cassava in Southeast Asia and China (and in East Africa for maize), for pulses in Southeast Asia, India, West and East Africa, the south-east region of Brazil and southern Australia, for groundnut in India and Indonesia, and for rapeseed in northern India, southern Australia and southern Europe. Deviations are also large for crops growing in the southern part of the Democratic Republic of Congo, in Indo-China and in regions around the equator.

Table 5.2 shows both *ME* and *W* for each crop for all cells where the crop is grown and differentiated for the rules to determine sowing date. The *ME* for all cells is less than 2 months, with the exception of pulses. For wheat (without Russia), rice, millet, sugar beet and sunflower, the agreement is even closer, with a difference of at most 1 month between simulations and observations. The *W* values are high, and show close agreement between simulations and observations (*W* > 0.8) with the exception of pulses. Both indices show closer

agreement for pulses, groundnut, sunflower and rapeseed in regions where sowing dates are determined by the temperature threshold than in regions where the onset of the main wet season determines sowing date. In contrast, both indices show closest agreement for millet in regions where sowing dates are determined by the onset of the wet season.

## 4. Discussion

Non-climatic reasons can considerably affect the timing of sowing. They arise from social attitudes and customs, religious traditions and the demand for certain agricultural products (Gill, 1991). In addition, agronomic practices, technological changes and farm size can influence the timing of sowing. Depending on crop rotation, sowing can be affected by the harvest of the preceding crop (Dennett, 1999), and available labour and machinery, depending on farm size, determine whether sowing can be completed in the desired time period (Kucharik, 2006). The timing of sowing may also be influenced by the weather later in the growing season, e.g. in order to avoid possible dry spells during certain stages of crop development that are relatively sensitive to drought stress. Information on these technological and socio-economic conditions and their influence on the timing of sowing is scarce at the global scale and has therefore not been considered in this study. The results of our study (Figs 5.4 & B5.1 – B5.11) show, however, that close agreement between simulated and observed sowing dates for large parts of the earth for wheat, rice, millet, soybean, sugar beet and sunflower, as well as for pulses and maize in temperate regions, can be realized based on climatic conditions only. For most crops, the disagreement between simulated and observed sowing dates is only 1 month or less for the largest part of the global total cropping area (Fig. 5.4b). At least 80% of the global cropping area displays a disagreement of less than 2 months (except for rapeseed, Fig. 5.4b). However, some regions show mediocre or poor agreement between simulated and observed sowing dates. The agreement is especially poor in tropical regions, where, despite a possible seasonality, climatic conditions are favourable throughout the year, and in regions characterized by multiple-cropping systems. Furthermore, agreement is poor in temperate regions, where both spring and winter varieties of wheat and rapeseed are grown, and in regions where observations are lacking or have been replaced or adjusted in MIRCA2000.

In the sections below the most likely reasons for strong disagreements are identified in example regions. Reasons can be limitations and uncertainties in MIRCA2000, e.g. the spatial scale of MIRCA2000 or data gaps, uncertainties in our methodology, the use of one global temperature threshold for sowing

temperatures, which is known to vary between regions (Sacks *et al.*, 2010), or the application of specific crop management techniques, e.g. multiple-cropping systems.

#### 4.1 Pulses and groundnuts in multiple-cropping systems

The poor agreement between simulated and observed sowing dates for pulses in Southeast Asia, India, West and East Africa, and south-east Brazil, and for groundnuts in India (Fig. B5.10a), originates from a mismatch in the production systems assumed. In these regions, it is common practice to grow pulses and groundnuts in multiple-cropping systems. In the south-eastern region of Brazil, with wet seasons long enough for a multiple-cropping system of maize and beans, beans are sown in combination with maize or after maize has been harvested (Woolley *et al.*, 1991). In West and East Africa, cowpea is largely grown as a second crop in multiple-cropping systems with maize or cassava (in humid zones) and millet (in dry zones) (Mortimore *et al.*, 1997). These patterns are reflected in MIRCA2000. In contrast, we have assumed only single-cropping systems, so that sowing of pulses and groundnut starts at the beginning of the wet season, i.e. too early in comparison to the observations. Where cowpea is grown as a single crop, as in coastal regions of East Africa (Mortimore *et al.*, 1997), there is close agreement with the observed sowing dates (Fig. B5.5a).

The deviations in India for pulses (Fig. B5.5a), and for groundnut in western India (Fig. B5.10a), are associated with the occurrence of multiple-cropping systems. Here, cowpea is grown in mixtures with sorghum and millet (Steele and Mehra, 1980) and groundnuts may be grown in the dry season following rice, often under irrigation (Norman *et al.*, 1995).

#### 4.2 Maize in multiple-cropping systems in Southeast Asia

In Southeast Asia, as well as in China, a large number of crops may be grown on the same plot. According to Portmann *et al.* (2010), this indicates high land use intensities with multiple-cropping systems. Intensive rice and wheat production are common practice in Asia (Devendra and Thomas, 2002), and maize has a subsidiary place in some of the Asian cropping systems as a second crop following the wet-season rice crop (Norman *et al.*, 1995). This rice–maize multiple-cropping system is covered by MIRCA2000, e.g. in China and Burma. As a consequence, the simulated growing period of maize starts earlier in the year than the observed growing period (Fig. B5.3a).

### 4.3 Wheat and rapeseed in temperate regions

The poor agreement for wheat and rapeseed in temperate regions of Russia, Australia, and small parts of Europe (Fig. B5.11a) is the result of disagreement between the simulated and observed varieties of wheat and rapeseed. In Russia, MIRCA2000 overestimates the share of winter wheat (Portmann *et al.*, 2010), because the cropping calendar for Russia is partly derived from the cropping calendars from Ukraine, Norway and Romania, where mainly winter wheat is grown (Portmann *et al.*, 2008). In contrast, we exclude winter wheat in Russia because temperatures drop below 12 °C before 15 September, and consequently spring wheat is simulated in Russia. This is in line with the cropping calendar from USDA, which reports, in addition to winter wheat, large areas of spring wheat in Russia (USDA, 1994). In other temperate regions the agreement between simulated and observed sowing dates is good with only 1 month deviation, and simulated sowing dates are similar to those shown in Bondeau *et al.* (2007).

For rapeseed in southern and eastern Australia, our rules simulate sowing dates in May and June (Fig. B5.11b), whereas MIRCA2000 reports a sowing date in December (Fig. B5.11c). However, in line with the simulations, West *et al.* (2001) and Robertson *et al.* (2009) confirm that rapeseed is grown as a winter crop, starting in May and June in Australia. In Europe, winter rapeseed is also the dominant cultivar due to its higher yield levels. Sowing dates of winter rapeseed in southern Europe can be extended from mid-August to early September, as indicated by Booth and Gunstone (2004) and USDA (1994), which is in line with the simulated sowing dates in countries like Spain, France, Hungary, Ukraine and Romania for example (Fig. B5.11b). MIRCA2000, however, identifies spring rapeseed sown in May in those countries.

### 4.4 Cassava in multiple-cropping systems

MIRCA2000 reports that in China, Thailand and Vietnam, cassava is sown in March as an early ripening variety. In China, farmers plant cassava from February to April before the wet season starts in order to use the cover of cassava plants to avoid soil losses due to the impact of heavy rains (Yinong *et al.*, 2001). Planting before the onset of the wet season may also avoid damage from pests (Evangelio, 2001). These practices explain the differences in southern China and Southeast Asia between observed and simulated sowing dates (Fig. B5.7a), because the simulated sowing dates are associated with the main wet season starting in May to July, not with the agronomic practices described in the literature.

## 4.5 Specific climatic conditions in temperate regions

Other examples of differences between observed and simulated sowing dates occur in European countries, partly in countries which are characterized by a Mediterranean climate. For sugar beet, both MIRCA2000 and our simulations indicate mainly spring sowings in the Mediterranean region. However, the mediterranean climate is characterized by mild winters and winter rainfall. In those regions, sugar beet is therefore sown in autumn, avoiding the high temperatures and high evapotranspirational demand of summer (Castillo Garcia and Lopez Bellido, 1986; Rinaldi and Vonella, 2006; Elzebroek and Wind, 2008). The effect of this specific climatic condition on sowing dates is not reflected in MIRCA2000, or in our simulations.

## 4.6 Limitations of MIRCA2000

Large differences between observed and simulated sowing dates occur in countries characterized by strong climatic gradients, associated with the size of countries (e.g. Russia, Democratic Republic of Congo, Mexico), or to large climatic variability, associated with large differences in elevation (e.g. Kenya). These gradients and variability influencing sowing dates are captured in our methodology, but not in MIRCA2000, where sowing dates for one spatial unit (country or subnational unit) are assigned to grid cells of  $0.5^{\circ} \times 0.5^{\circ}$ . An example is the large difference between observations and simulations in the southern part of the Democratic Republic of Congo, where in MIRCA2000 missing observations were replaced by the cropping calendar from the neighbouring country Rwanda (Portmann *et al.*, 2008). While this procedure might be adequate for the northern parts of the Democratic Republic of Congo which are characterized by the same bimodal seasonal rainfall distribution, it is not adequate for the southern parts, where the main wet season does not start until November/December (McGregor and Nieuwolt, 1998).

Deficiencies in simulated sowing dates may strongly influence the results of applications of the sowing date algorithm, depending on the application and model used. A deviation of sowing dates by 2 or 3 months (e.g. sunflower in France, sugar beet in Spain, soybean in the northern USA, or maize in Europe; see Figs B5.1 – B5.11) could already strongly affect the results of crop model applications, e.g. the assessment of crop evapotranspiration and crop virtual water content. The level of agreement per crop and region is therefore depicted in Figs B5.1 – B5.11, which allows for a more detailed evaluation when to use our sowing date algorithm with caution.

## 5. Conclusions

This study presents a novel approach for deterministically simulating sowing dates under rainfed conditions for various annual field crops. We show that sowing dates for large parts of the earth can be satisfactorily estimated from climatic conditions only. Close agreement is achieved between simulated and observed sowing dates, although substantial deviations occur in: (1) tropical regions and (2) regions with high land-use intensity and multiple-cropping systems. Even if those regions show seasonality in temperature or precipitation, climatic conditions can be suitable throughout the year for crop growth. In both types of regions, climatic conditions are of minor importance for the timing of sowing, instead it is determined mainly by other criteria such as the demand for special agricultural products, availability of labour and machines, and religious and/or social traditions (Gill, 1991; Kucharik, 2006). Furthermore, certain cropping practices and crop rotations are applied in order to avoid pests and disease infestations. These agronomic practices cannot be considered in our methodology due to lack of information at the global scale. Differences between simulated and observed sowing dates in regions without precipitation and temperature seasonality have little impact on the computed crop yield in global crop growth models such as LPJmL. Sowing date deviations of 1 month or more, in locations with temperature and precipitation seasonality may lead to substantially different simulated crop yields. In the LPJmL model with the currently implemented cultivars, sowing dates simulated with the presented methodology are within the most productive cropping window for almost all locations displayed in Fig. B5.12. However, the interaction of sowing dates, management options, and cultivar characteristics will have to be evaluated further.

Our methodology is explicitly developed for the global scale. Climate and soil characteristics, as well as agricultural management practices, can vary considerably among regions. If applied at smaller scales, parameter values as proposed here should be adapted, e.g. the temperature threshold for sowing can show spatial variability (Sacks *et al.*, 2010), and important socio-economic and technical drivers should be considered to attain higher accuracy. In addition, if reliable daily minimum and maximum temperature and precipitation data are available, rules should be adapted in order to consider avoidance of damage by frost or extreme high temperatures. At the global scale, our methodology is suitable for simulating sowing dates for global crop growth models. In our methodology, we are able to apply current and future climate input data. We are therefore able

to account for some possible global responses to climate change by farmers changing their sowing dates.

## **Acknowledgements**

We would like to thank Felix Portmann and Stefan Siebert for making available the MIRCA2000 data set, as well as the LPJmL crop modelling team, Herman van Keulen and Peter Leffelaar for valuable discussions on the methodology and results. Furthermore we are grateful for the comments of two anonymous referees on a previous version of the manuscript, and to Benjamin Gaede and Alison Schlums who did the spell and grammar check. K.W. and C.M. gratefully acknowledge financial support from projects with the International Food Policy Research Institute (6012001) and the International Livestock Research Institute (81102850) funded through the German Federal Ministry for Economic Cooperation and Development.

## **Biosketch**

The focus of our research is on the analysis of interactions between atmosphere and biosphere at the global scale under both current and future climates. Agricultural ecosystems are of special interest for us because they provide services for humans, like, e.g. food, bioenergy and carbon sequestration. To simulate and quantify the interactions between biosphere and atmosphere, we apply and further develop the global dynamic vegetation and water balance model LPJmL. For further information see: [www.pps.wur.nl/UK](http://www.pps.wur.nl/UK) and [www.pik-potsdam.de/research/cooperations/lpjweb](http://www.pik-potsdam.de/research/cooperations/lpjweb).

Author contributions: K.W., L.G.J.v.B., A.B. and C.M. conceived the idea of simulating sowing dates from climatic conditions and from the intra-annual variability of temperature and precipitation, K.W. and C.M. wrote code and prepared MIRCA2000 for validation, K.W. did the model runs and derived the temperature thresholds for sowing, L.G.J.v.B. carried out the sensitivity analysis, and L.G.J.v.B. and K.W. did literature research, wrote the manuscript, prepared the figures and prepared the supporting material. All authors were involved in developing the methodology and discussing the model outputs.







## Chapter 6

# **Simulation of phenological development of wheat and maize at the global scale**

To be submitted as:  
Van Bussel, L.G.J., Stehfest, E., Siebert, S., Müller, C., Ewert, F.:  
Simulation of phenological development of wheat and maize at  
the global scale.

## Abstract

Crop yields are determined for a large part by the duration and timing of phenological phases, which are influenced by temperature and daylength. Due to the broad range of cultivars adapted to local conditions in daylength and climate, crops like wheat and maize can be cultivated in a wide range of environments. In many field scale crop growth models the effects of temperature (directly and in case of winter varieties also indirectly via vernalization requirements) and photoperiod are implemented to simulate phenology. In contrast, most large scale studies apply only thermal relationships. To our knowledge we present in this study the first attempt to combine thermal relations with the effects of photoperiod to simulate crop phenology at the global scale. We developed simple algorithms to compute location-specific parameter values, which account for differences between cultivars in vernalization requirements and sensitivity to photoperiod and temperature. In the main cropping regions of wheat we were able to simulate lengths of the cropping period that correspond well with observed lengths. Agreement between observed and simulated lengths of the cropping period was lower for maize than for wheat, with in the main maize cropping regions over- and underestimations of 0.5 to 1.5 month. Moreover, we found that interannual variability in simulated harvest dates, in particular of wheat, decreased due to the inclusion of daylength effects. Despite some scope for further improvement the presented methodology provides a good basis for modelling phenological development of crops at global scale in the absence of location-specific variety characteristics of phenological development.

## 1. Introduction

Phenology, which is defined as: “the study of the timing of recurring biological phases, the biotic and abiotic forces that cause the variation in timing, and the interrelation among phases of the same or different species” (Lieth, 1974), has recently emerged as an important research topic (Zhang *et al.*, 2006). Besides the importance of plant phenology for global carbon modelling (Arora & Boer, 2005), as an indicator for climate change (Menzel *et al.*, 2006), or on human health via the start of the pollen season (Van Vliet *et al.*, 2002) also food security is closely related to phenology (Xiao *et al.*, 2009).

Crop yields are determined for a large part by the duration and timing of phenological phases. There should be an appropriate balance between the durations of the vegetative and reproductive phase and the grain filling phase should be finished before the end of the growing season (Hay & Porter, 2006). Vulnerable stages like anthesis (flowering) should occur with an optimum timing, e.g. avoiding episodes of high temperatures (Craufurd & Wheeler, 2009) or periods with large frost risk (Boer *et al.*, 1993; Slafer & Whitechurch, 2001).

Two major components influence the duration and timing of phenological phases: temperature (directly and in case of winter varieties also indirectly via vernalization requirements) and daylength (also referred to as photoperiod). Development is linearly related to temperature, i.e. higher temperatures accelerate development (Slafer & Rawson, 1994). Vernalization is the influence of cold temperatures on the flowering response (Raven *et al.*, 2005), expressed in this study as a required amount of days with vernalizing temperatures. Development is delayed as long as the plant has not experience sufficient days with vernalizing temperatures (Miralles & Slafer, 1999). Finally, photoperiodism is the response to a change in the proportions of light and darkness in a 24-h cycle. For long-day plants (e.g. wheat) development is accelerated if photoperiod increases, for short-day plants (e.g. maize) development is accelerated if photoperiod decreases (Raven *et al.*, 2005).

Crops like wheat and maize are cultivated in a wide range of environments (Gouesnard *et al.*, 2002; Trethowan *et al.*, 2006). This is possible due to the broad range of cultivars adapted to local conditions in photoperiod and climate, especially temperature. This is shown by sensitivity differences between maize and wheat cultivars to changes in photoperiod. Wheat cultivars are known to differ in their vernalization requirements, ranging from spring-type wheat (i.e. no exposure to vernalizing temperatures is required) to true winter wheat (i.e. a certain duration of exposure to vernalizing temperatures is required). Finally, the development rates of maize and wheat cultivars differ in their sensitivity to

temperature. Due to responses to photoperiod and vernalizing temperatures, wheat and maize development is synchronized between plants, so all plants can be harvested at the same time, and between years despite of interannual variability in weather conditions (Hay & Kirby, 1991; Gouesnard *et al.*, 2002; Craufurd & Wheeler, 2009; Wang *et al.*, 2009).

Impact assessments of climate change on future crop productivity typically make use of crop simulation models. The dominant effect of climate change on crop productivity in many of those assessments is often via simulated effects of global warming on phenological development of crops. Given the widely reported sensitivity of crops to photoperiod, its role as key determination of crop adaptation to climatic conditions, and its synchronizing function, it is important to consider it appropriately in phenological modules of crop simulation models. In addition cultivars differences should be accounted for (Craufurd & Wheeler, 2009).

In many field scale crop growth models the effects of photoperiodism are implemented, e.g. in AFRCWHEAT2 (Porter, 1993; Ewert *et al.*, 1996) and CERES-maize (Jones *et al.*, 1986). In contrast, most large scale studies apply only thermal relationships to simulate phenology while the effects of photoperiodism are not considered (Craufurd & Wheeler, 2009), see e.g. Challinor *et al.* (2004), Fisher *et al.* (2005), Bondeau *et al.* (2007), Stehfest *et al.* (2007) or Deryng *et al.* (2011).

For Europe, Harrison *et al.* (2000) developed a method for scaling-up AFRCWHEAT2, from site to continental scale, accounting for effects of photoperiod and temperature. Cultivar differences in vernalization requirements and sensitivity to photoperiod and temperature were taken into account via model parameters. These were derived from previous studies, in which AFRCWHEAT2 had been calibrated and validated for several cultivars. Due to data scarcity, cultivar specific parameter values could not be established for all European regions. Therefore model outcomes could only be interpreted and validated for specific regions. Effects of climate change on phenological development of winter wheat were studied by comparing the relative performance of all available cultivars across the whole region, thus cultivar choice as an adaptation measure to climate change was ignored.

In addition to parameters used in previous simulation studies, some information with respect to cultivar-specific phenological characteristics can be obtained from studies in which cultivars were grown under different, but constant thermal and photoperiod conditions (see e.g. Davidson *et al.*, 1985; Worland *et al.*, 1994; Ortiz Ferrara *et al.*, 1998). The results of these studies give useful indications about the roles of temperature and photoperiod on development and differences between cultivars. However, temperature and photoperiod

conditions continually change in the field and therefore results from those studies are not suitable as a basis for parameter estimation. Moreover, the number of cultivars used world-wide is countless and, in addition, location-specific information with regard to cultivar use is lacking. Consequently, adequate parameter estimates for the large range in cultivars are missing at the global scale.

The results of the large scale crop phenology simulations by Bondeau *et al.* (2007) and Deryng *et al.* (2011), in which only temperature determined phenological development, were evaluated in their studies for a single year only. However, photoperiod effects on development should have consequences for e.g. the interannual variability in simulated harvest dates, but were not evaluated in their studies or in other global studies. Thus, in this study we examined these consequences. We hypothesized that accounting for the effects of photoperiod and vernalization results in less interannual variability in the lengths of cropping periods than simulation of phenology based on thermal requirements only.

The objectives of this study were therefore: (1) to develop simple algorithms to compute location-specific parameters, which account for differences between cultivars in vernalization requirements and sensitivity to photoperiod and temperature, based on observations and information from literature; (2) to evaluate if and how well simulated harvest dates can represent observed harvest dates, considering: (i) thermal requirements only and (ii) combinations of thermal with photoperiod and/or vernalization requirements; and (3) to investigate the interannual variability in harvest dates based on: (i) thermal requirements only and (ii) combinations of thermal with photoperiod and/or vernalization requirements; and finally (4) to investigate the required level of accuracy for simulated harvest dates for global crop productivity assessments. Wheat and maize are used as example crops accounting for approximately 30% of the total harvested global crop area (FAO, 2011).

## 2. Data and Methods

In this section we first describe the phenological model ARFCWHEAT2 (Weir *et al.*, 1984; Porter, 1993; Ewert *et al.*, 1996) which we used to simulate the length of the cropping period for wheat and maize. We also provide a description of the input data required for running the model and for evaluating the outcomes. We assumed that farmers choose the best adapted wheat and maize cultivars for their local climatic and photoperiod conditions. This assumption was implemented in ARFCWHEAT2 by adapting several parameters to local conditions. The methodology of computing these location-specific parameters is described in

detail. Finally, the procedures of evaluating the outcomes and the sensitivity of crop yields to simulated harvest dates are presented.

We define in this study “growing season” as the time during which climatic conditions are favourable for crop growth, while the “cropping period” refers to the time from sowing to harvesting.

## 2.1 Input data

### 2.1.1 Dataset of observed cropping periods

To compare simulated with observed lengths of cropping periods we used the global dataset MIRCA2000 (Portmann *et al.*, 2010). MIRCA2000 reports monthly growing areas of 24 different irrigated and rainfed crop classes at a spatial resolution of  $5' \times 5'$  for the period around the year 2000. After aggregating the data to a resolution of  $0.5^\circ \times 0.5^\circ$  the monthly growing areas for rainfed maize and rainfed wheat were extracted.

MIRCA2000 is mainly based on the Global Information and Early Warning System on food and agriculture (FAO-GIEWS) and on data from the United States Department of Agriculture (USDA). We assumed that sowing was at the first day of the first reported cropping month while harvest was assumed to occur at the last day of the last reported cropping month. Day of emergence was set equal to the sowing date and physiological maturity was assumed to correspond with the harvest date. Up to five possible cropping periods per grid cell are indicated in MIRCA2000, reflecting different varieties of wheat and multiple-cropping systems with maize. The cropping periods with the maximum reported area were selected for this study.

Several uncertainties and limitations of MIRCA2000 were reported in Portmann *et al.* (2010): data gaps and uncertainties in the underlying national census data, the lack of sub-national data for some larger countries, and as a result, the omission of possible effects on cropping periods due to climatic gradients in those large counties. Furthermore, complex cultivation systems, in which more than one crop is grown on the same field at the same time, could not be represented adequately. A dataset similar to MIRCA2000 was developed by Sacks *et al.* (2010) but they did not distinguish rainfed and irrigated crops. Since cropping periods often differ between irrigated and rainfed crops we prefer to use MIRCA2000.

### 2.1.2 Photoperiod and temperature data

Daily photoperiod ( $P_i$ , h d<sup>-1</sup>) was calculated based on latitude and day of the year, as described in Monteith and Unsworth (1990). Monthly mean temperature data

on a  $0.5^\circ \times 0.5^\circ$  resolution were provided by the Climate Research Unit dataset TS3.0 (Mitchell & Jones, 2005). Exponentially weighted moving average monthly temperatures ( $\bar{T}_{m,j}$ , °C) were calculated to compute the location-specific parameter values to account for cultivar differences:

$$\bar{T}_{m,j} = \alpha \times T_{m,j} + (1 - \alpha) \times \bar{T}_{m,j-1} \quad (\text{Eq. 6.1})$$

where  $T_{m,j}$  (°C) is the mean monthly temperature of month  $m$  in year  $j$  and  $\alpha$  (–) a coefficient representing the degree of weighting decrease (with a value of 0.05). The calculation was initialised by  $\bar{T}_{m,j=1970} = T_{m,j=1970}$ .

Exponentially weighted moving average monthly temperatures of the previous year were used to compute the location-specific parameter values for the coming year (i.e.  $\bar{T}_{m,j=2004}$  for the year 2005). Exponentially weighted moving averages were used so we could account for farmer experiences with previous climatic conditions and to prevent large interannual variability in the location-specific parameter values. Daily mean temperatures ( $T_i$ , °C) were generated by linear interpolation between the monthly means.

The observed cropping periods from MIRCA2000 refer not to a single year but a number of years around 2000. To evaluate our methodology we therefore used exponentially weighted moving average monthly temperatures for the year 2000 ( $\bar{T}_{m,j=2000}$ ) to compute the location-specific parameter values and to generate the daily mean temperatures (see above) to simulate the harvest dates for the year 2000. To evaluate interannual variability in simulated harvest dates we used the mean monthly temperatures of the years 1995 up to 2005 (e.g.  $T_{m,j=2005}$  for the year 2005) to generate daily mean temperatures. For the generation of location-specific parameters we used the exponentially weighted moving average monthly temperatures of the years 1994 up to 2004 (e.g.  $\bar{T}_{m,j=2004}$  for the year 2005).

## 2.2 Phenological model ARFCWHEAT2

To simulate phenological development of wheat and maize we used the well-established concept of heat units. Daily temperature ( $T_i$ ) is accumulated above a base temperature ( $T_b$ , °C) (i.e. the heat unit sum  $HU_{\text{sum}}$ , °Cd) (until the required heat units from emergence to physiological maturity ( $HU_{\text{req}}$ , °Cd) are reached. The increment in heat units is modified by the effects of photoperiod (photoperiod factor,  $P_{fi}$ , –), and in case of winter wheat by the effects of vernalization (vernalization factor,  $V_{fi}$ , –), as applied in the ARFCWHEAT2 model (Porter, 1993;



Ewert *et al.*, 1996) (see Fig. 6.1 for a graphic description of  $P_{fi}$  and  $V_{fi}$  and their mathematical description):

$$HU_{\text{sum}} = \sum_{i=1}^N (T_i - T_b) \times P_{fi} \times V_{fi} \quad \text{if } HU_{\text{sum}} \leq HU_{\text{req}} \quad (\text{Eq. 6.5})$$

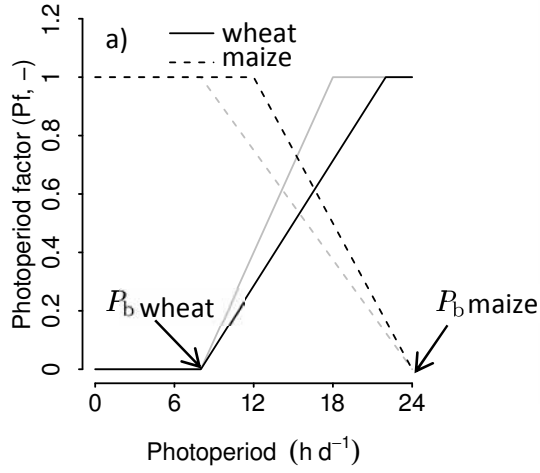
so  $N$  is the simulated length of the cropping period in days. The simulation of maize was stopped when temperatures dropped below the base temperature.

With help of  $HU_{\text{sum}}$  a phenological development scale ( $DVS$ , –) was derived, ranging from 0 (sowing/emergence) to 1 (harvest/physiological maturity) during the cropping period:

$$DVS = \frac{HU_{\text{sum}}}{HU_{\text{req}}} \quad (\text{Eq. 6.6})$$

The development scale was used to determine the timing of the phenological stages flowering ( $DVS_f$ , –) and double ridges (floral initiation) ( $DVS_{dr}$ , –). We assumed that the rate of development of wheat and maize is sensitive to photoperiod from emergence to flowering, as indicated by Craufurd and Wheeler (2009). In addition, the rate of development of winter wheat was modified by the effect of vernalization from emergence to the double ridge stage (Slafer & Rawson, 1994). All wheat cultivars in this study were considered long-day plants; all maize cultivars were considered short-day plants, although there are some wheat cultivars behaving as short-day plants (Evans, 1987).

**Fig. 6.1** a) Effect of photoperiod on phenological development (photoperiod factor,  $P_{fi}$ , –, ranging from 0 to 1):  $P_i$  (h d<sup>-1</sup>) the daily photoperiod,  $P_b$  (h d<sup>-1</sup>) base photoperiod (i.e. the longest (shortest) photoperiod below (above) which no further photoperiod-induced delay in long-day (short-day) plants is observed),  $P_{\text{opt}}$  (h d<sup>-1</sup>) optimum photoperiod (i.e. the shortest (longest) photoperiod above (below) which no photoperiod-induced delay in long-day (short-day) plants is observed); b) daily vernalizing effectiveness ( $V_{\text{eff}}$ , –):  $T_i$  (°C) the daily temperature,  $T_{\text{vn}}$  (–) factors of vernalization effectiveness,  $V_{\text{DD}}$  (d) accumulated vernalized days,  $K$  (–) number of days from sowing to the double ridge stage or till  $V_{\text{DD}} \geq V_{\text{sat}}$ ; c) effect of vernalizing temperatures on phenological development (vernalization factor,  $V_{fi}$ , –, ranging from 0 to 1):  $V_b$  (d) base accumulated vernalized days,  $V_{\text{sat}}$  (d) saturated vernalization requirement (i.e. required duration of exposure to vernalizing temperatures) (adapted from Ewert *et al.*, 1996).



(Eq. 6.2)

wheat

$$P_{fi} = 0 \quad \text{if } P_i < P_b$$

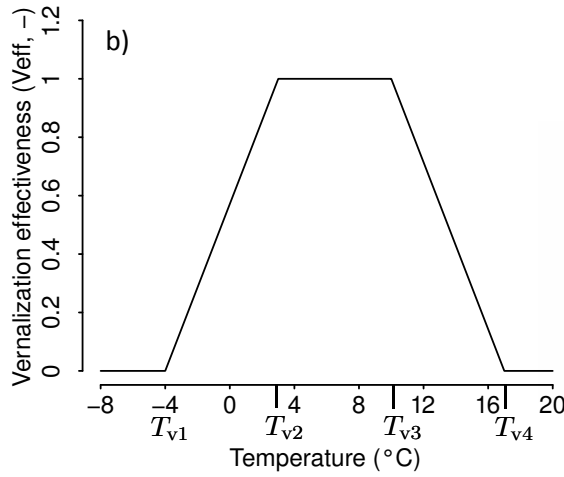
$$P_{fi} = \frac{P_i - P_b}{P_{opt} - P_b} \quad \text{if } P_b \leq P_i \leq P_{opt}$$

$$P_{fi} = 1 \quad \text{if } P_i > P_{opt}$$

maize

$$P_{fi} = \frac{P_i - P_b}{P_{opt} - P_b} \quad \text{if } P_{opt} \leq P_i \leq P_b$$

$$P_{fi} = 1 \quad \text{if } P_i < P_{opt}$$

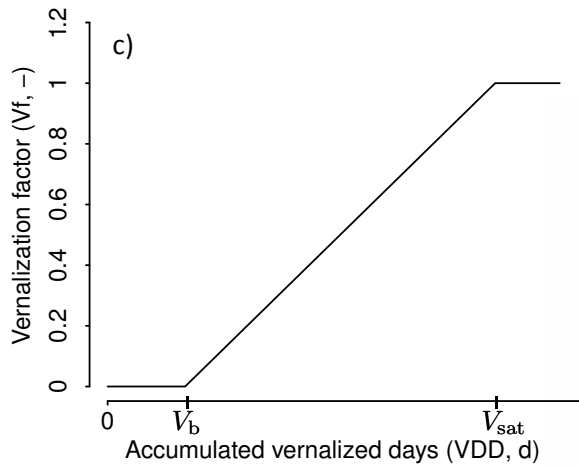


(Eq. 6.3)

$$V_{eff_i} = 1 \quad \text{if } T_{v2} \leq T_i \leq T_{v3}$$

$$V_{eff_i} = \frac{T_i - T_{v1}}{T_{v2} - T_{v1}} \quad \text{if } T_{v1} \leq T_i < T_{v2}$$

$$V_{eff_i} = \frac{T_{v4} - T_i}{T_{v4} - T_{v3}} \quad \text{if } T_{v3} < T_i \leq T_{v4}$$



(Eq. 6.4)

$$V_{DD} = \sum_{i=1}^K V_{eff_i}$$

$$V_{fi} = 0 \quad \text{if } V_{DD} < V_b$$

$$V_{fi} = \frac{V_{DD} - V_b}{V_{sat} - V_b} \quad \text{if } V_b \leq V_{DD} \leq V_{sat}$$

$$V_{fi} = 1 \quad \text{if } V_{DD} > V_{sat} \text{ or } DVS > DVS_{dr}$$

**Table 6.1**  
Crop specific parameter values.

Parameter	Spring wheat	Winter wheat	Maize
Base temperature ( $T_b$ , °C)	0 <sup>a</sup>	0 <sup>a</sup>	8 <sup>a</sup>
Required heat units for maturity ( $HU_{req}$ , °Cd)	Location specific	Location specific	Location specific
Phenological development scale double ridge ( $DVS_{dr}$ , –)	–	0.2 <sup>b</sup>	–
Fraction of $HU_{req}$ when flowering occurs ( $DVS_f$ , –)	0.58 <sup>c</sup>	0.5 <sup>c</sup>	0.7 <sup>c</sup>
Minimum temperature for effective vernalization ( $T_{v1}$ , °C)	–	–4 <sup>d</sup>	–
Minimum temperature for optimal vernalization ( $T_{v2}$ , °C)	–	3 <sup>d</sup>	–
Maximum temperature for optimal vernalization ( $T_{v3}$ , °C)	–	10 <sup>d</sup>	–
Maximum temperature for effective vernalization ( $T_{v4}$ , °C)	–	17 <sup>d</sup>	–
Saturated vernalization requirement (i.e. required duration of exposure to vernalizing temperatures, $V_{sat}$ , d)	–	Location specific, from 0 till 70	–
Maximum saturated vernalization requirement per month possible ( $V_{sat\ max}$ , d)	–	70/5 = 14 (d month <sup>–1</sup> ) <sup>e</sup>	–
Base accumulated vernalized days ( $V_b$ , d)	–	$\frac{1}{5} \times V_{sat}$ <sup>f</sup>	–
Base photoperiod ( $P_b$ , h d <sup>–1</sup> )	8	8 <sup>d</sup>	24
Optimum photoperiod ( $P_{opt}$ , h d <sup>–1</sup> )	Location specific	Location specific	Location specific

<sup>a</sup>Kiniry *et al.* (1995); <sup>b</sup>Van Bussel *et al.* (in press); <sup>c</sup>Kiniry *et al.* (1995); <sup>d</sup>Ewert *et al.* (1996); <sup>e</sup>The value of  $V_{sat\ max}$  was based on a study by Baloch *et al.* (2003), they indicated that winter wheat cultivars with high vernalization requirements need at least 70 days of optimum vernalizing temperatures. We assumed an equal distribution over the five months; <sup>f</sup>Wang and Engel (1998).

Table 6.1 lists the crop-specific parameter values for the simulation of the length of the cropping period. The model was run on a spatial resolution of 0.5° × 0.5°, which is the spatial resolution of the temperature input data.

## 2.3 Simulation of location-specific phenological parameter values

To account for cultivar differences in sensitivity to photoperiod, temperature, and vernalization requirements the following parameters were calibrated for local conditions: optimum photoperiod ( $P_{opt}$ , h d<sup>–1</sup>) and required heat units for maturity ( $HU_{req}$ , d) for spring and winter wheat and maize; and the required duration of exposure to vernalizing temperatures ( $V_{sat}$ , d) and base accumulated vernalized days ( $V_b$ , d) for winter wheat.

### 2.3.1 Vernalization requirements of winter wheat cultivars

Due to the exposure of winter wheat to vernalizing temperatures tolerance to below-freezing temperatures is built up. Once the vernalization requirement is met the tolerance gradually disappears (Mahfoozi *et al.*, 2001). We therefore assumed that the vernalization requirement of cultivars is adapted to winter duration and coldness, i.e. vernalization requirements of cultivars grown on locations with a long and cold winter should be higher than of cultivars grown on locations with milder winters, in line with findings from Iwaki *et al.* (2001).

Ewert *et al.* (1996) indicated that both the effectiveness of temperature on the vernalization process and the vernalization requirements are different among cultivars. Due to data scarcity, however, we assumed equal temperature effectiveness for all cultivars, and only varied the vernalization requirements ( $V_{\text{sat}}$  and  $V_b$ , d) between cultivars.

We used the temperature of the five coldest months of the year as an indicator of the winter duration and coldness, with the assumption that in winter wheat growing regions the frost-period has a maximum length of five months. By considering the five coldest months separately and not their average, influences of possible relatively warm months are minimized. The required amounts of vernalized days in year  $j$  ( $V_{\text{sat},j}$ ) were computed as follows (see also Fig. 6.2):

$$V_{\text{sat},j} = \sum_{m=1}^N V_{\text{sat},m,j} \quad (\text{Eq. 6.7})$$

with:

$$\begin{aligned} V_{\text{sat},m,j} &= V_{\text{sat max}} && \text{if } \bar{T}_{m,j-1} \leq T_{v2} \\ V_{\text{sat},m,j} &= 0 && \text{if } \bar{T}_{m,j-1} \geq T_{v3} \\ V_{\text{sat},m,j} &= \frac{V_{\text{sat max}}}{T_{v3} - T_{v2}} \times \bar{T}_{m,j-1} && \text{if } T_{v2} < \bar{T}_{m,j-1} < T_{v3} \end{aligned}$$

where  $N$  (–) represents the five coldest months,  $V_{\text{sat max}}$  (d month<sup>-1</sup>) the maximum possible required duration of exposure to vernalizing temperatures per month (see Table 6.1),  $\bar{T}_{m,j-1}$  the average monthly temperature of the previous year (Eq. 6.1), and  $T_{v2}$  and  $T_{v3}$  (°C) the minimum and maximum temperatures for optimal vernalization, respectively (Ewert *et al.*, 1996).  $V_b$  was assumed to be one fifth of  $V_{\text{sat}}$ , in line with Wang and Engel (1998). Only optimal temperatures for the vernalizing process were considered in Eq. 6.7, since it is based on monthly temperatures.

Based on Eq. 6.7 we computed vernalization requirements for all locations with autumn sown wheat according to MIRCA2000. We also computed

vernalization requirements for locations with spring sown wheat as indicated by MIRCA2000, but for these locations (i.e. sown during the period from the coldest month up to the warmest month inclusive) we changed the computed vernalization requirements to zero.

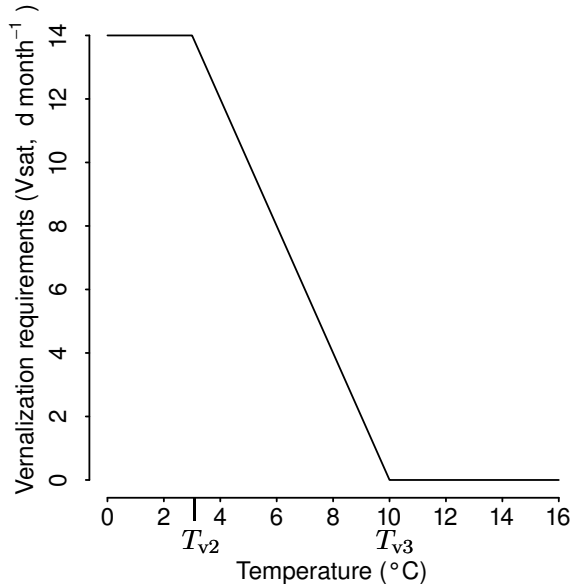


**Fig. 6.2** Required amount of vernalized days per month as a function of temperature.

### 2.3.2 Photoperiodism sensitivity

To simulate differences among cultivars for wheat and maize with respect to photoperiod, we adapted  $P_{opt}$  values to local conditions;  $P_b$  was kept constant among the cultivars, the used  $P_b$  values are based on values reported in literature.

#### Wheat

Wheat cultivars originating from higher latitudes (e.g. UK or Finland) are true photoperiod sensitive cultivars (Worland *et al.*, 1994), while modern cultivars grown in lower latitudes such as the Mediterranean region in west Asia and North Africa are insensitive to photoperiod (Ortiz Ferrara *et al.*, 1998). Miralles and Slafer (1999) indicated that for wheat cultivars with different sensitivities to photoperiod optimum photoperiod differed significantly, ranging from ca. 15 to 21 h d<sup>-1</sup>. Miralles *et al.* (2007) found the optimum photoperiod of Argentinean wheat cultivars to be 13.4 h d<sup>-1</sup>, which approximately coincides with the average maximum photoperiod ( $P_{max}$ , h d<sup>-1</sup>, i.e.  $P$  at June 21<sup>st</sup> in the northern hemisphere and  $P$  at December 21<sup>st</sup> in the southern hemisphere) in the main wheat growing area in Argentina. We therefore characterized sensitivity to photoperiod by setting  $P_{opt}$  equal to the location-specific  $P_{max}$ .

At high latitudes  $P_{\max}$  is higher than at lower latitudes and as a consequence  $P_{\text{opt}}$  is higher for cultivars grown at high latitude. In Fig. 6.1a the solid black line indicates the response to photoperiod of a cultivar from a high-latitude location; the solid grey line indicates the response of a lower-latitude cultivar. The slopes of the lines indicate that with equal photoperiod (e.g. 15 h d<sup>-1</sup>) the photoperiod effect of the high-latitude cultivar is smaller ( $P_f = 0.5$ ) than the lower-latitude cultivar ( $P_f = 0.7$ ). Since the increment in heat units is multiplied with  $P_f$  the delay in development is largest for the high-latitude cultivar, an indication for higher sensitivity to photoperiod.

### Maize

The relative difference in photoperiod between two successive days is smaller at lower latitude locations than at higher latitude locations. It is therefore plausible that the most sensitive responses to photoperiod are found in tropical cultivars of short-day plants (Summerfield *et al.*, 1997). Indeed, maize cultivars adapted to temperate regions (i.e. cool, long-day environments) show lower or no photoperiod sensitivity than tropical cultivars (Bonhomme *et al.*, 1994; Birch *et al.*, 1998). In line with wheat cultivars, maize cultivars also differ in their optimum photoperiod (Birch *et al.*, 1998). Rood and Major (1980) found optimum photoperiods varying from < 14 h d<sup>-1</sup> to 24 h d<sup>-1</sup>. Location-specific  $P_{\text{opt}}$  values for maize were established as follows:

$$P_{\text{opt}} = \max\left(0, P_{\max} \times \left(1 - \frac{1}{P_{\max} - P_{\min}}\right)\right) \quad (\text{Eq. 6.8})$$

where  $P_{\min}$  (h d<sup>-1</sup>) is the minimum photoperiod possible on a certain location (i.e.  $P$  at December 21<sup>st</sup> in the northern hemisphere and at June 21<sup>st</sup> in the southern hemisphere).

$1 - \frac{1}{P_{\max} - P_{\min}}$  was used to account for the annual course of photoperiod. At high latitudes  $P_{\max}$  and the difference between  $P_{\max}$  and  $P_{\min}$  is higher than at lower latitudes, as a consequence  $P_{\text{opt}}$  is also higher and approaching  $P_b$ .

In Fig. 6.1a the dashed black line indicates the response to photoperiod of a cultivar from a high-latitude location; the dashed grey line indicates the response of a lower-latitude cultivar. The slopes of the lines indicate that with equal photoperiod (e.g. 18 h d<sup>-1</sup>) the photoperiod effect of the high-latitude cultivar is smaller ( $V_f = 0.5$ ) than the lower-latitude cultivar ( $V_f = 0.375$ ). Since the increment in heat units is multiplied with  $V_f$  the delay in development is largest for the lower-latitude cultivar, an indication for higher sensitivity to photoperiod.

### 2.3.3 Required heat units from emergence to maturity

To simulate differences among wheat and maize cultivars with respect to temperature we assumed that cultivars adapted to cooler climates require less heat units from emergence to maturity ( $HU_{req}$ , °Cd) than cultivars adapted to warmer climates. A range of  $HU_{req}$  values could not be established from literature. A reasonable range for  $HU_{req}$  was therefore derived based on observed  $HU_{req}$  values, which were calculated with help of the observed cropping periods in MIRCA2000.

The aim of our study was to evaluate if and how well simulated harvest dates represented observed harvest dates, considering: (1) thermal requirements only and (2) the combinations of thermal with photoperiod and/or vernalization requirements. Two models for maize and spring wheat were distinguished: a thermal model, taking into account temperature effects only and a photo-thermal model, taking into account temperature effects combined with photoperiod effects, including the cultivar differences as described above (Section 2.3.2). For winter wheat two additional models were distinguished: temperature effects combined with vernalization effects (vernal-thermal model) and temperature effects combined with vernalization and photoperiod effects (vernal-photo-thermal model), including cultivar differences in vernalization requirements and sensitivity to photoperiod. For each model a specific range for  $HU_{req}$  was required.

For all models we first calculated observed  $HU_{sum}$  values per grid cell, using the observed cropping periods from MIRCA2000. Per model the specific processes implemented in the model were considered in the calculation of observed  $HU_{sum}$  values. Spring and winter wheat were simulated separately. It was assumed that winter wheat was sensitive to vernalization until the required duration of exposure to vernalizing temperatures was met; wheat and maize were sensitive to photoperiod until flowering.

We assumed that location-specific climate conditions could be used to derived  $HU_{req}$  values. Secondly, we therefore examined by means of linear regression analyses which climatic variable explained the patterns in observed  $HU_{sum}$  values best: (1) total annual available heat units ( $HU_{sum\ year}$ , °Cd) (similar to Deryng *et al.*, 2011) or (2) available heat units during an estimated vegetative cropping period ( $HU_{sum\ veg-period}$ , °Cd). Available  $HU_{sum}$  values were calculated based on temperature effects only, with the consideration of crop specific base temperatures. For maize we estimated the vegetative period from May to July in the northern hemisphere and November to January in the southern hemisphere; for wheat from March to June in the northern hemisphere and September to

December in the southern hemisphere.  $HU_{\text{sum veg-period}}$  was chosen as a proxy of the temperature during the whole cropping period, in line with Bignon (1990), who used it for maize in Europe. We assumed this proxy to be valid for maize and wheat for the rest of the world as well.

In addition, we assumed grid cells with  $HU_{\text{sum year}} < 750 \text{ }^{\circ}\text{Cd}$  to be too cold to grow maize. Due to the large spatial resolution of MIRCA2000 some sowing dates are reported in those grid cells, nevertheless we excluded them from the regression analyses. Finally, for maize we divided the observed  $HU_{\text{sum}}$  in two groups, based on  $HU_{\text{sum year}}$ : maize cultivars grown in warm regions ( $HU_{\text{sum year}} \geq 3000 \text{ }^{\circ}\text{Cd}$ ) and maize cultivars grown in cold regions ( $HU_{\text{sum year}} < 3000 \text{ }^{\circ}\text{Cd}$ ).

## 2.4 Procedure of assessing the simulated length of the cropping period

### 2.4.1 Indices of agreement

The simulations were carried out on a  $0.5^{\circ} \times 0.5^{\circ}$  grid, while the observations in MIRCA2000 are reported in administrative units, which are related to administrative boundaries (i.e. countries or states). Therefore, for the comparison between observed and simulated harvest dates, first the lengths of the observed and simulated cropping periods were calculated. Next, simulated cropping periods at the grid cell level were aggregated to one average value per administrative unit, weighted by crop area. To take into account the temporal resolution of one month in MIRCA2000, simulated harvest dates were finally converted into harvest months.

To evaluate if and how well cropping period lengths can be simulated based on location-specific parameters, which were computed with help of simple algorithms, we assessed the degree of agreement between simulated and observed cropping periods. Several indices of agreement were calculated for each crop: the mean absolute error ( $MAE$ , d), the root mean square error ( $RMSE$ , d), and the Willmott coefficient of agreement ( $W$ , dimensionless, ranging from 0 to 1, with 1 showing perfect agreement) (Willmott, 1982).  $MAE$  and  $RMSE$  indicate the global average error between simulations and observations. In addition,  $W$  is a relative measure for the differences (Willmott, 1982). Indices are area-weighted, which implies that deviation in spatial units with a large cropping area is considered more important than deviation in spatial units where the crop is grown less:

$$MAE = \frac{\sum_{i=1}^N |O_i - S_i| \times A_i}{\sum_{i=1}^N A_i} \quad (\text{Eq. 6.9})$$



$$RMSE = \sqrt{\frac{\sum_{i=1}^N (O_i - S_i)^2 \times A_i}{\sum_{i=1}^N A_i}} \quad (\text{Eq. 6.10})$$

$$W = 1 - \frac{\sum_{i=1}^N (O_i - S_i)^2 \times A_i}{\sum_{i=1}^N (|S_i - \bar{O}| + |O_i - \bar{O}|)^2 \times A_i} \quad (\text{Eq. 6.11})$$

where  $S_i$  (months) is the simulated and  $O_i$  (months) the observed length of the cropping period in spatial unit  $i$ ,  $\bar{O}$  (months) the mean observed length of the cropping period based on all spatial units,  $A_i$  (ha) the cultivated area of the crop in spatial unit  $i$ , and  $N$  (–) the number of spatial units.

### 2.4.2 Sensitivity analysis of crop yields for length of cropping period

A possible application of harvest dates simulated with the presented methodology is to provide global crop growth models under future conditions with estimates of suitable cropping windows. To evaluate the required level of accuracy for simulated harvest dates for this application we investigated the sensitivity of simulated crop yields by the LPJmL dynamic global vegetation and crop model (Bondeau *et al.*, 2007) for different cropping period lengths for five contrasting locations (Delhi, India; Abuja, Nigeria; Kansas City, USA; Amsterdam, the Netherlands; Iquitos, Peru).

In LPJmL, crop growth is simulated using a combination of processes (photosynthesis, respiration, evapotranspiration, biomass allocation, and leaf area development) on a daily basis (for more details, see Bondeau *et al.*, 2007). The effects of extreme temperatures on crop growth and development, e.g. frost damage or heat stress is not considered by LPJmL. To simulate phenological development we used the vernal-photo-thermal model for wheat and the photo-thermal for maize. Rainfed yields were simulated for each location for several  $HU_{\text{req}}$  values, and as a consequence, a range of cropping period lengths. Sowing dates (from MIRCA2000) and location-specific parameters were kept constant per location; the monthly climate data of the year 2000 were used.

## 3. Results

### 3.1 Vernalization requirements

Figure 6.3 shows the computed location-specific vernalization requirements for winter wheat. Cultivars grown in large parts of Russia, Western Europe, the northern USA, and north-east Asia have the maximum required duration of exposure to vernalizing temperatures, because winter temperatures are optimal

or winters are long and cold (with too low temperatures for the vernalization process). In southern USA and southern Europe a gradient is visible.

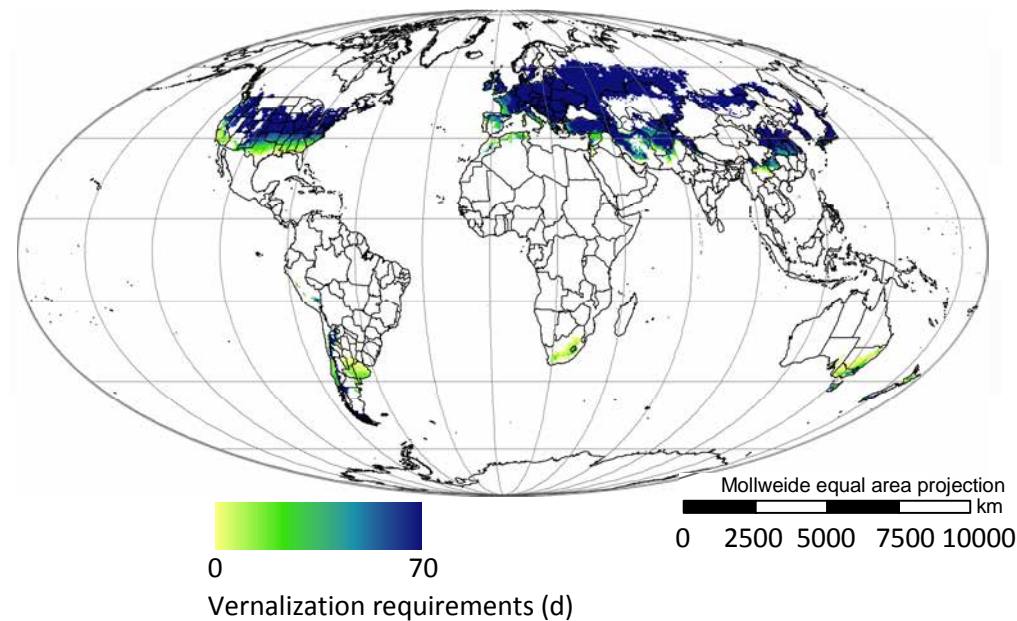


**Fig. 6.3** Computed location-specific vernalization requirements (i.e. required duration of exposure to vernalizing temperatures,  $V_{\text{sat}}$ , d) for winter wheat.

The pattern of the computed vernalization requirements corresponds with information found in literature, e.g. in the south-eastern border of the Australian wheat belt winter wheat is grown, while in rest of the belt spring wheat is grown (Fisher, 1999). Also the low computed vernalization requirements for wheat in west Asia (e.g. Yemen and Saudi Arabia) and north Africa are in line with results of previous studies (see e.g. Ortiz Ferrara *et al.*, 1998). Kato and Yokoyama (1992) determined vernalization requirements of traditional cultivars originating from various countries. They found vernalization requirements of approximately 31 days for landraces originating from western Turkey, Italy, and Greece; 35 days for landraces originating from Afghanistan, Pakistan, Nepal, and Bhutan; 56 days for landraces origination from Georgia, east Turkey, and north and east Iran; 28 days for landraces origination from Armenia; and 7 and 14 days for landraces from Egypt and Ethiopia. This pattern is reflected in our results.

### 3.2 Required heat units for maturity

To explain the patterns in observed  $HU_{\text{sum}}$  values we carried out linear regressions with: (1) total annual available heat units ( $HU_{\text{sum, year}}$ ) and (2) available heat units during an estimated vegetative cropping period ( $HU_{\text{sum veg-period}}$ ). Table 6.2 gives the coefficients of determination ( $R^2$ ) for the two

climatic variables. The  $R^2$  values indicate that for spring and winter wheat available  $HU_{\text{sum year}}$  and available  $HU_{\text{sum veg-period}}$  explained observed  $HU_{\text{sum}}$  values comparably well. For maize however, the observed trends in  $HU_{\text{sum}}$  can best be explained by available  $HU_{\text{sum veg-period}}$ . We therefore used the available  $HU_{\text{sum veg-period}}$  to compute the location-specific  $HU_{\text{req}}$  values. Table 6.2 gives the relationships. The slopes of the relationships are an indicator for the spatial heterogeneity in  $HU_{\text{req}}$  values: a higher value gives higher spatial heterogeneity. Spatial heterogeneity decreases if photoperiod is included in the model (e.g. for spring wheat: 1.06 for the thermal model versus 0.91 for the photo-thermal model).

**Table 6.2**

Coefficients of determination from the linear regression analysis with total annual available heat units ( $HU_{\text{sum year}}$ ) and available heat units during an estimated vegetative cropping period ( $HU_{\text{sum veg-period}}$ ), as well as the accompanying relationships to compute location-specific  $HU_{\text{req}}$  values based on  $HU_{\text{sum veg-period}}$ .

Crop	Relationship	R <sup>2</sup>	
		$HU_{\text{sum veg-period}}$	$HU_{\text{sum year}}$
Thermal model			
Spring wheat	$HU_{\text{req}} = 1.06 \times HU_{\text{sum veg-period}} + 815.08$	0.75	0.77
Winter wheat	$HU_{\text{req}} = 1.18 \times HU_{\text{sum veg-period}} + 941.45$	0.45	0.45
Maize	warm region: $HU_{\text{req}} = 1.4 \times HU_{\text{sum veg-period}} + 399.66$	0.44	0.25
	cold region: $HU_{\text{req}} = 1.82 \times HU_{\text{sum veg-period}} - 150.51$	0.92	0.82
Photo-thermal model			
Spring wheat	$HU_{\text{req}} = 0.91 \times HU_{\text{sum veg-period}} + 775.27$	0.64	0.68
Winter wheat	$HU_{\text{req}} = 0.66 \times HU_{\text{sum veg-period}} + 1126.49$	0.26	0.24
Maize	warm region: $HU_{\text{req}} = 1.06 \times HU_{\text{sum veg-period}} + 145.04$	0.35	0.01
	cold region: $HU_{\text{req}} = 1.52 \times HU_{\text{sum veg-period}} - 72.08$	0.91	0.76
Vernal-thermal model			
Winter wheat	$HU_{\text{req}} = 0.99 \times HU_{\text{sum veg-period}} + 811.52$	0.44	0.46
Vernal-photo-thermal model			
Winter wheat	$HU_{\text{req}} = 0.87 \times HU_{\text{sum veg-period}} + 907.47$	0.36	0.36

### 3.3 Comparison of observed and simulated cropping periods

To evaluate if and how well simulated harvest dates patterns (based on computed location-specific  $HU_{req}$  (see Table 6.2),  $P_{opt}$  and/or  $V_{sat}$  values) represent observed harvest dates, the area weighted indices of agreement between simulated and observed cropping periods for the different models are given in Table 6.3. Scatterplots of observed versus simulated cropping periods based on the vernal-photo-thermal model for wheat and the photo-thermal model for maize are shown in Fig. 6.4. The radius of the circles is a measure for the cultivated crop area in the spatial units of MIRCA2000. Scatterplots for the other models look similar and are therefore not shown.

For wheat, results for the different phenological models are in the same range (Table 6.3), with the vernal-thermal model giving the lowest deviations and the photo-thermal the highest deviations. Average simulated lengths of the cropping period are in the same range as the average observed length; the spatial heterogeneity in the simulated cropping periods is slightly lower than in the observed cropping periods (simulated versus observed coefficient of variation). Agreement between observed and simulated lengths of cropping periods of countries with large wheat cropping areas, such as Russia, Canada, and Turkey, is high (Fig. 6.4a).

**Table 6.3**

Area weighted means, standard deviations, and indices of agreement between simulated and observed cropping periods for wheat and maize.

Crop	Mean (months)*	Coefficient of variation	<i>MAE</i> (months)	<i>RMSE</i> (months)	<i>W</i> (-)
Observations					
Wheat	8.7	3.8	–	–	–
Maize	5.7	2.1	–	–	–
Thermal model					
Wheat	8.6	3.6	0.73	0.92	0.97
Maize	5.5	2.1	0.75	0.92	0.54
Photo-thermal model					
Wheat	8.7	3.6	0.77	0.96	0.97
Maize	5.5	2.1	0.89	1.03	0.42
Vernal-thermal model					
Wheat	8.7	3.7	0.66	0.82	0.98
Vernal-photo-thermal model					
Wheat	9.0	3.6	0.75	0.97	0.97

\*Recalculation of mean, standard deviation, and differences from days to months is done by assuming an equal amount of days per month (i.e.  $365/12 = 30.42$  days per month)

For maize, deviations between observed and simulated cropping periods are slightly lower based on the thermal model than based on the photo-thermal model. The simulated cropping periods underestimate the observed cropping period on average by approximately two weeks; also the spatial heterogeneity in cropping period is underestimated by the simulations (Table 6.3). The scatterplot (Fig. 6.4b) indicates that in countries situated in warmer regions, e.g. Mexico and Nigeria, the model overestimates the length of the cropping period, while in cooler regions, e.g. the USA and Russia, the model underestimates the length of the cropping period.

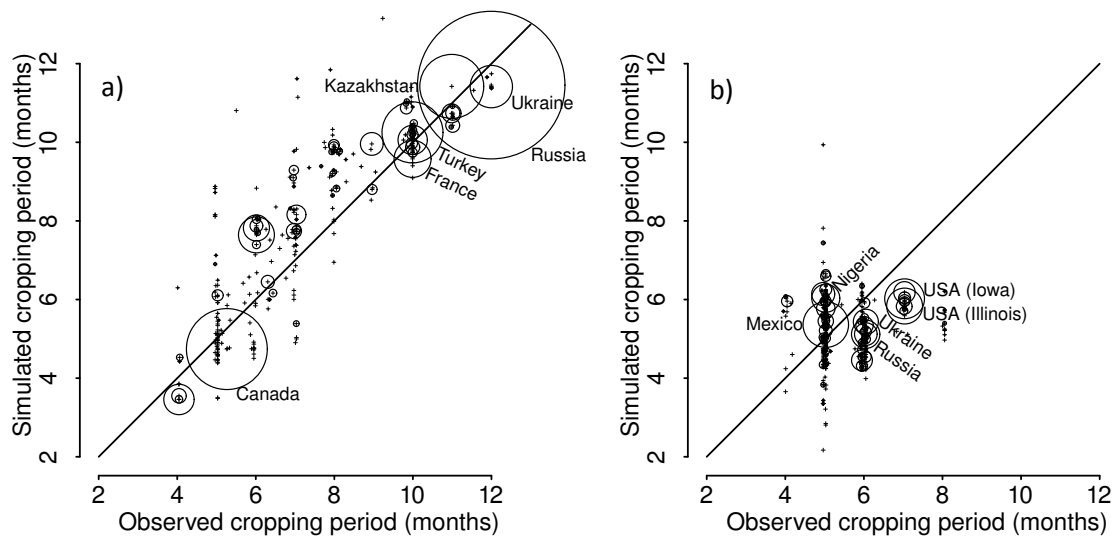


**Fig. 6.4** Scatterplots of observed versus simulated cropping periods per spatial unit of MIRCA2000 for: a) wheat, based on the vernal-photo-thermal model; b) maize, based on the photo-thermal model. The solid line represents the 1:1 line; the extent of the circle represents the cultivated area of the crop per spatial unit.

### 3.4 Interannual variability in harvest dates

To test our hypothesis that accounting for the effects of photoperiod and vernalization results in less interannual variability in the length of cropping periods than simulation of phenology based on thermal requirements only, we used the different models to simulate the lengths of the cropping period for the period 1995 to 2005. As an indicator for interannual variability we calculated the differences between the earliest and latest harvest dates in that period per grid cell and per model. We plotted the relative cumulative frequency distributions of these differences (Fig. 6.5).

Fig. 6.5a indicates that if wheat phenology is simulated based on the thermal model 46% of the grid cells have a difference of more than 20 days between the earliest and latest harvest date, while for the vernal-photo-thermal model this is

only 20%. The initially steeper slopes of the vernal-photo-thermal and photo-thermal model for wheat indicate that accounting for especially photoperiodism results in less variability in harvest dates between years. Accounting for vernalization in the simulation of wheat phenology reduced only slightly the interannual variability in harvest dates. We also mapped the spatial distribution of the differences between the earliest and latest harvest dates (results not shown). The maps indicate that especially in areas with high interannual variability in weather conditions, e.g. north-eastern USA, north and Western Europe, and Russia interannual variability in harvest dates decreases due to inclusion of photoperiod effects in the phenology model.

For maize we did not find the dimming effect of photoperiodism on variability of harvest dates, inclusion of photoperiodism only slightly decreased interannual variability in harvest dates (Fig. 6.5b). This small reduction is a consequence from the low sensitivity to photoperiod in the areas with high interannual variability in weather conditions (e.g. western Europe, north-east USA), while in areas with high sensitivity to photoperiod interannual variability in weather conditions is low (tropics).

### 3.5 Sensitivity analysis of crop yields for length of cropping period

Figure 6 displays the simulated wheat and maize yields per cropping period length for the five locations, compared to the maximum simulated yield per location. For wheat (Fig. 6.6a), an increase in cropping period length gives higher yields in the locations situated in Peru, the Netherlands, and the USA. Yields in the Netherlands and the USA level off if the cropping period length approaches 350 days, this is the result of temperatures becoming unsuitable for the photosynthesis process and autotrophic respiration becomes low as well. The cropping period length for the locations in India and Nigeria shows an optimum range for simulated yields, this results from the occurrence of wet seasons: right timing of water availability during the cropping period gives high yields.

For maize (Fig. 6.6b), cropping periods longer than approximately 150 and 180 days could not be simulated for the locations in the Netherlands and the USA, respectively, because temperatures dropped below the base temperature of maize in autumn. Nevertheless, temperatures below the base temperature are also unfavourable for photosynthesis and therefore simulated yields will not increase, but rather a decrease in yields is possible due to autotrophic respiration in case of longer cropping periods. Similar as with the simulated wheat yields, maize yields in Nigeria and India are optimal within a certain cropping period length.

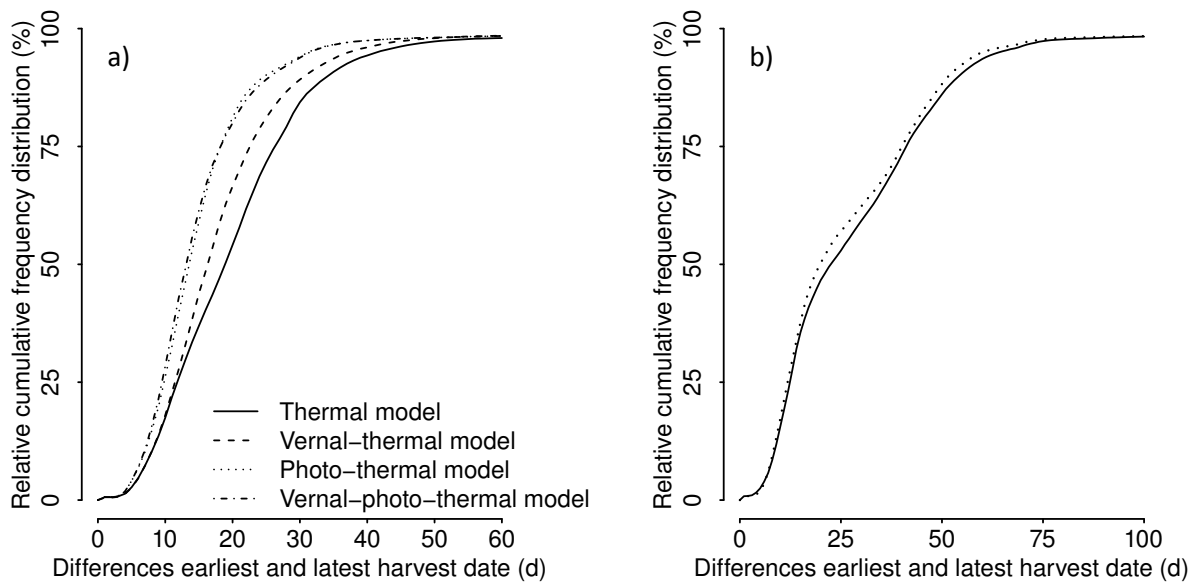


**Fig. 6.5** Relative cumulative frequency distributions of the coefficients of variation of the period 1995 till 2005 for: a) wheat and b) maize. The lines indicate the different models used to simulate the length of the cropping period.

## 4. Discussion and concluding remarks

### 4.1 Simulated cropping period lengths at the global scale

To our knowledge we present in this study the first attempt to include the effects of photoperiod and temperature (directly and indirectly) on crop phenology at the global scale. We developed simple algorithms to compute location-specific parameter values, which account for differences between cultivars in vernalization requirements and sensitivity to photoperiod and temperature. We find that the simulated pattern of required exposure of winter wheat to vernalizing temperatures (i.e. vernalization requirements) matches the observed pattern. Moreover, inclusion of photoperiod and vernalization effects decreases spatial heterogeneity and temporal variability of required heat units from emergence to physiological maturity for wheat. This result is in line with Miralles and Slafer (1999) who reported that differences in development rate among wheat cultivars mainly originate from differences in sensitivity to photoperiod and differences in vernalization requirements.

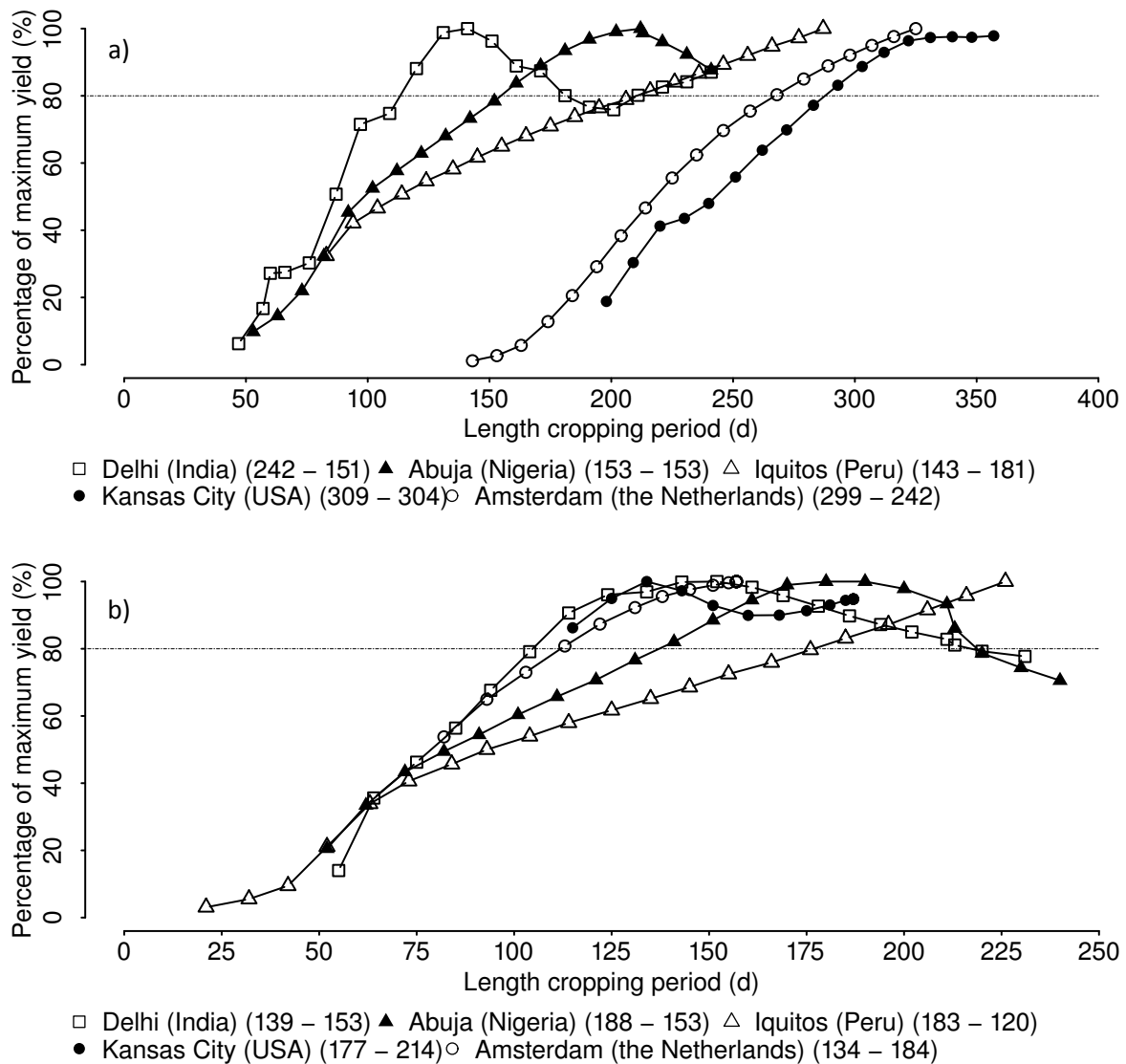


**Fig. 6.6** Sensitivity of a) wheat yields and b) maize yields to cropping period lengths for five locations. Between brackets, the simulated respectively observed cropping period lengths are given. The dashed line indicates 80% of maximum simulated yield.

The indices of agreement between observed and simulated cropping period lengths (Table 6.3) and the scatterplots of observed versus simulated cropping periods (Fig. 6.4) indicate that in general, agreement is lower for maize than for wheat, which is especially visible in the value of the Willmott coefficient. The heat unit requirements could be derived more effectively from general climatic parameters for maize than for wheat (Table 6.2), especially for the cold regions. This can be explained by the different timing of harvest of wheat and maize and their different base temperatures. In cooler regions, such as the USA and Europe, wheat is normally harvested during the warmest period of the year, while maize is harvested in autumn, when temperatures approach the base temperature of



maize. As a consequence, an equal over- or underestimation of the  $HU_{req}$  values gives higher deviations in the simulated harvest dates for maize than for wheat. Finally, deviations between observed and simulated harvest dates might be a consequence of MIRCA2000 reporting harvest dates, while the models simulate physiological maturity; harvesting is derived from maturity, but includes management aspects.

The indices in Table 6.3 indicate that the accuracy of simulated harvest dates for a specific year does not improve if the models are expanded with the effects of photoperiod and/or vernalization. However, the hypothesis that accounting for effects of photoperiod and vernalization decreases interannual variability in lengths of cropping periods is supported by the results of this study (Fig. 6.5). This effect is especially visible for wheat. For maize inclusion of the effect of photoperiod reduced only slightly the interannual variability in lengths of cropping period.

According to good modelling practice models should be as simple as possible given their objectives, but enough detail should be included so effects of major processes are still represented by the model (De Wit, 1968). Including the effects of photoperiodism and vernalization is a clear example of adding extra detail to a model. Here it is shown that the added detail influences the behaviour of the model, i.e. decreased interannual variability. Nevertheless, information with regard to of interannual variability in harvest dates at the global scale is scarce, only information for some crops and a few countries is available, e.g. Germany (Chmielewski *et al.*, 2004; Van Bussel *et al.*, in press) and the USA (Sacks & Kucharik, 2011). Based on this limited amount of data we could not conclude whether interannual variability in simulated crop phenology at the global scale is unrealistic if only thermal relations are applied and needs therefore further evaluation.

## 4.2 Implications for global crop growth modelling

The results of the sensitivity analysis indicate that, deviations between simulated and observed cropping period lengths are acceptable with relatively small impacts on simulated harvest dates (Fig. 6.6). The rather low sensitivity of crop yields for the length of the cropping period is partly the result of the lack of crop damaging factors in LPJmL e.g. heat stress or crop damage by freezing temperatures. In field experiments it is however showed that crop yields are sensitivity to the timing and length of the cropping period (see, e.g. Cirilo & Andrade, 1996; Thomson *et al.*, 1997; Sadras *et al.*, 2009). It is therefore expected that feeding a more detailed crop growth model, which includes e.g. heat and

frost stresses combined with daily weather input data, with the simulated harvest dates will probably give higher sensitivities. Finally, the interaction of simulated sowing dates (see e.g. Waha *et al.*, 2011) with simulated cultivar characteristics will need further evaluation.

Although we have not discussed climate change before, by using the history of climate for parameter generation, our approach explicitly assumes that farmers adapt to climate change via changes in cultivar use. As a consequence, future simulated cropping periods will be similar to those simulated for current climatic conditions as the variety parameters (e.g. sensitivity to vernalization) will change. Therefore, the dominant effect of climate change on crop productivity via simulated effects on phenological development of crops as seen in many climate impact assessments (Craufurd & Wheeler, 2009) will be less visible if our methodology is applied. A change in cultivar use, especially related to the cropping period, is also suggested in other studies to combat the negative effects of climate change (Torriani *et al.*, 2007; Moriondo *et al.*, 2010). Changes in cultivar use have been observed in the past, e.g. improved modern wheat cultivars in the Mediterranean countries are insensitive to vernalization and photoperiod, while old local cultivars show sensitivity to vernalization and photoperiod (Ortiz Ferrara *et al.*, 1998). In the USA, maize cultivar characteristics have changed, with especially an increase in the required heat units for the reproductive phase (Sacks & Kucharik, 2011).

### 4.3 Limitations of our methodology and directions for further research

Only two datasets, with roughly the same data sources, reporting global sowing and harvest dates are available (Portmann *et al.*, 2010; Sacks *et al.*, 2010). No other literature reporting reasonable ranges of observed  $HU_{req}$  across the world is available. Therefore we had to calibrate and evaluate the models with the same dataset. Being aware of this limitation, we still find it valid to test whether observed patterns of harvest dates can be reproduced when cultivar-specific parameters are computed with help of simple algorithms. Clearly, we did not aim at evaluating the concept of heat units but a methodology to model location-specific variety parameters used in the heat unit concept.

We assumed in this study that only photoperiod and temperature conditions determine cultivar characteristics. However, the choice of farmers to grow a certain cultivar with specific characteristics is dependent on numerous other reasons. Socio-economic reasons such as the application of multiple-cropping systems require cultivars with a specific cropping period length, for example in

rice–wheat systems in South and East Asia (Timsina & Connor, 2001) or the demand for specific cultivars with respect to quality, such as bread wheat in western Europe or durum wheat in Italy (Dettori *et al.*, 2011). At large scales information with regard to specific cultivar use or specific agronomic practices is scarce and could therefore not be included in our methodology of generating location-specific cultivar characteristics.

Besides the appropriate length of the cropping period, vulnerable stages like anthesis should occur with an optimum timing (Boer *et al.*, 1993; Slafer & Whitechurch, 2001; Craufurd & Wheeler, 2009). As a consequence, simulation of the right timing of vulnerable stages is essential for accurate simulation of crop productivity (Jamieson *et al.*, 2007). In southern Australia, maximum yields are achieved if anthesis occurs late enough to avoid late spring frosts, but early enough to avoid the grain-filling phase to enter the dry and warm summer (Sharma *et al.*, 2008). Cultivar characteristics can also be adapted to avoid excessive rainfall, such as in Nepal, where early-heading cultivars are used to avoid damage of pre-harvest sprouting by the monsoonal rain in early summer (Kato & Yokoyama, 1992) or to avoid pests and diseases that are only indirectly related to climate (Kouressy *et al.*, 2008). The sensitivity to photoperiod is the major factor determining timing of anthesis (Davidson & Christian, 1984; Slafer & Whitechurch, 2001). These examples show that cultivar characteristics are not only dependent on location-specific photoperiod and temperature conditions, but that more factors play a role. Currently this complex system is not well understood. We therefore stress the importance of collecting anthesis dates, cultivar characteristics, and cultivar use at the global scale to make it possible to understand this complex system and further improve the simulation of crop phenology at the global scale, including accurate simulations of anthesis dates. We also stress the importance of continuously expanding datasets such as MIRCA2000 in space and over time. When data of multiple years are available it is possible to examine interannual variability in phenological events and assess if simulated phenology represent this variability.

#### 4.4 Concluding remarks

We show in this study that for large parts of the globe our methodology to simulate location-specific parameters of heat units including sensitivities to daylength and vernalization is able to estimate reasonably well harvest dates of wheat and maize. Despite some scope for further improvement this methodology provides a good basis for modelling phenological development of crops at global scale in the absence of location-specific variety characteristics of phenological

development. As we explicitly developed this methodology for application at the global scale it may be insufficiently accurate if applied at smaller scales or with a more detailed crop growth model, where a higher accuracy in simulated harvest dates (and intermediate development stages) is required. Further development of the proposed methodology should include the consideration of additional factors such as stress avoidance determining location-specific phenology parameters. Advances in modelling large scale phenology will also depend on available data to test models which are presently only available to a limited extent.





## Chapter 7

### **General discussion**

The general objective of the work described in this thesis was to enhance the understanding of the use of crop growth models for global application. In particular I concentrated on the required level of detail to represent important processes for crop growth in global crop growth models. Moreover, I studied the effects of spatial and temporal aggregation of input data on crop growth model outcomes. Finally, I examined the simulation of crop phenology at the global scale, in particular the simulation of sowing dates of various crops and the generation of phenological parameters to characterize cultivars differences in wheat and maize.

In this final chapter the main findings of the thesis are discussed. I start with the discussion of methodological issues related to large scale crop growth modelling. New insights obtained in this thesis are used to discuss the design of a global crop growth model, followed by directions for additional research for further improvement of global crop growth models.

## **1. Methodological issues of large scale crop growth modelling**

Early crop growth models were mainly developed for the plot and field scale, requiring location-specific, spatially homogenous input data (Hansen and Jones, 2000; Monteith, 2000; Mearns *et al.*, 2001; Van Ittersum *et al.*, 2003; De Wit *et al.*, 2005; Tao *et al.*, 2009). Recently, the scale of crop production assessments has been extended and crop growth models are increasingly applied at the continental or global scale, e.g.: LPJmL (Bondeau *et al.*, 2007), DAYCENT (Stehfest *et al.*, 2007), GEPIC (Liu *et al.*, 2007), GLAM (Challinor *et al.*, 2004), GAEZ (Tubiello and Fischer, 2007), and WOFOST (Reidsma *et al.*, 2009). Data availability normally decreases if the scale of application increases, therefore data availability is one of the problems faced if crop growth models are applied at large scales (Nonhebel, 1994; Therond *et al.*, in press). To overcome the problem of data availability it is either possible to use aggregated data (input or output) or to generate/simulate input data. Both methodologies may have implications for model outcomes. In addition, there may be implications for the model design, since the level of detail to represent a process in a model should be adjusted to the available data (Challinor *et al.*, 2003; Ewert, 2004b).

### **1.1 Model structure related issues**

The appropriate level of detail to represent a process in a model is often seen as a critical, but difficult step in model development (Brooks and Tobias, 1996; Van Delden *et al.*, in press). The level of detail should be a good balance between the objective of the model (Brooks and Tobias, 1996), which includes the scale of

application, and the spatial and temporal resolution of the available data (Challinor *et al.*, 2003; Ewert, 2004b). Table 1.1 (Chapter 1) shows that global crop growth models' objectives and their level of detail to represent processes differ, ranging from less detailed empirical models, e.g. GAEZ aiming at yield simulations, to more detailed mechanistic models, e.g. LPJmL aiming at more comprehensive studies, e.g. the investigation of the impact of agriculture on global carbon and water cycles. Yet, knowledge about the required level of modelling detail to accurately represent crop growth processes in large scale crop growth models is scarce. In addition, Ewert (2004a) indicated that, despite the importance of a good representation of leaf area dynamics for crop production simulations, this process received less research attention compared with photosynthesis.

With a systematic analysis of the importance of model structure for simulating potential yields, considering crop growth models with different levels of detail, we made a start to enhance knowledge related to the required level of detail in large scale crop growth models (Chapter 2). In particular we focussed on the processes of light interception, determined by leaf area dynamics, and light utilization for biomass production, using spring wheat (*Triticum aestivum*) as an example. For each process two approaches with different levels of detail were included in the framework, reflecting the range of detail found in (global) crop growth models. We first tested model performance for several contrasting locations. After calibration, simulated yields reproduced the observed yield with average  $r$ RMSEs ranging between 17% and 32%, depending on the model. Agreement between simulated and observed yields was closest for models which represented leaf area dynamics with the lowest level of detail. The representation of leaf senescence, particularly its onset, was found to be critical for model performance.

In the following part of our study the models were driven with weather data from contrasting locations in Europe to reflect the spatial heterogeneity in weather conditions that is encountered in large scale model applications. We found the choice for the light interception approach significantly influencing model outcomes, with the leaf area dynamics approach with the lowest detail level simulating higher yields than the more detailed approach. This result confirms conclusions from previous studies in which the importance of leaf area index for crop yields was emphasized (Heath and Gregory, 1938; Watson, 1947; Jamieson *et al.*, 1998a; Ewert, 2004a). The two approaches representing light utilization for biomass production gave similar outcomes, but the results suggested that the use of a constant value for the radiation use efficiency (one of the



light utilization approaches) for the whole cropping period may have been an oversimplification of reality.

Recently, Biernath *et al.* (2011) carried out a similar study, in which models with different levels of detail were evaluated for their ability to represent observed growth of spring wheat under elevated atmospheric CO<sub>2</sub> concentrations, including the effects of limited water availability, from so-called open-top chamber (OTC) experiments. Although OTCs are artificial systems they are often used to study the effects of factor combinations which are difficult to investigate under field conditions. Biernath *et al.* (2011) found results which agree well with the results from Chapter 2. Both studies showed that yields simulated by the different models are comparable, despite different approaches to represent the light interception and light utilization processes. In agreement with the conclusions from Chapter 2, Biernath *et al.* (2011) concluded that more mechanistic models do not generally result in better model performance.

In addition to spatial heterogeneity in weather conditions, crop yields also vary between years due to interannual variability in weather conditions (Hansen and Jones, 2000). It is therefore essential to evaluate, besides model outcomes for a specific year, whether observed temporal variability is appropriately reflected in model outcomes. In Chapter 6 we studied if the level of detail considered in a phenological model has implications for the simulated interannual variability in harvest dates. Previous studies indicated that the effect of daylength (also referred to as photoperiod) can synchronize crop development between plants and between years (Hay and Kirby, 1991; Gouesnard *et al.*, 2002; Craufurd and Wheeler, 2009; Wang *et al.*, 2009). In contrast to weather conditions, daylength conditions are equal between years. We therefore expected influences on the simulated interannual variability in harvest dates if effects of daylength were included in the model. Hence, we compared simulated interannual variability in harvest dates by a simple phenological model, which is based on thermal relationships only, an approach often used in global crop growth models (Craufurd and Wheeler, 2009), with model outcomes from a more extended model (i.e. thermal relationships combined with the effects of daylength and/or vernalization), the approach in most field-scale crop growth models (see e.g. Jones *et al.*, 1986; Porter, 1993; Ewert *et al.*, 1996). We found that, after model-specific calibrations, model extension did not improve model performance for a specific year: simulated harvest dates showed mean absolute errors of less than one month at the global scale for the extended and simple models. However, when considering several years, we found that interannual variability in simulated harvest dates changed indeed due to the inclusion of daylength effects. At

locations with a high interannual variability in weather conditions, e.g. Western Europe, simulated interannual variability in wheat harvest dates decreased with approximately 70% (from approximately more than 7 weeks to 2 weeks, the former probably an overestimation according to the results of Chapter 4) due to the consideration of the effects of daylength in the model. To our knowledge, our study was the first to explore required complexity in simulation of crop phenology at the global scale. Previous studies from Porter *et al.* (1993) and Masle *et al.* (1989) indicated that for field-scale conditions considering the effects of daylength and vernalization improved the simulation of phenology. Their conclusions, combined with the effects on interannual variability in harvesting dates, point to the importance of including daylength effects in crop phenology models for global application.

In Chapter 2 & 6 we pointed out to possible risks and consequences of oversimplification of process representations in models. However, including unnecessary detail or adding extra model components might give model users a false sense of accuracy if the required input data is not available or if the process is not fully understood (Van Delden *et al.*, in press) and should therefore be avoided. In this context, information about interannual variability in harvest dates of wheat is very limited at the global scale, with few quantitative indications (see e.g. Chapter 4 for temporal heterogeneity in harvest dates in Germany) and some qualitative indications, e.g. winter wheat in the UK is normally harvested in August (Landau *et al.*, 1998). Although the inclusion of daylength in the simulation of global crop phenology hinted at more realistic interannual variability in harvest dates, observations about interannual variability in harvest dates at the global scale should be collected first before it is justified to extend the model by the daylength effect following the approach proposed in this thesis.

## **1.2 Data related issues**

### **1.2.1 Data aggregation**

In contrast to field scale model applications, large scale applications often rely on data aggregated over space and/or time. With increasing aggregation (i.e. an increase in size of the area or time period from which the synthesis of multiple data points into a single value for the area or time period is composed) variability of data will decrease and local extremes will be levelled out (Easterling *et al.*, 1998; Baron *et al.*, 2005; Hansen and Ines, 2005). To prevent incorrect model outcomes it is important to examine the bias in model outcomes resulting from the removed variability.

The results from Chapter 2 indicated that models with different degrees of detail may simulate similar yields for defined conditions. In Chapter 2 the models were driven by daily weather input data, the temporal resolution required in many field-scale crop growth models (De Wit *et al.*, 2004; Soltani *et al.*, 2004). Availability of daily weather data at high spatial resolutions is limited at the global scale. Instead, monthly weather data aggregates supplied by global circulation models (GCMs) are often used in global crop growth models (Table 1.1, Chapter 1). The day-to-day variability in weather data, which might substantially influence crop yields (Wheeler *et al.*, 2000; Porter and Semenov, 2005) is lacking in those monthly aggregates. Whether daily weather data can be replaced by monthly aggregates in crop growth model applications was therefore studied in Chapter 3. In particular, we studied if the degree of detail in crop growth models determines their sensitivity to temporally aggregated weather input data. We analysed the same models as in Chapter 2, i.e. with different levels of detail in the representation of crop growth processes. The models were run with temperature and radiation data with two temporal resolutions: monthly and daily weather data. The results showed that replacing daily weather data with temporally aggregated weather data resulted in higher simulated amounts of biomass. This difference was as high as 37% at a location characterized by high day-to-day weather variability for rainfed conditions. Similar results were found by Nonhebel (1994) and Soltani *et al.* (2004). Nonhebel (1994) found differences of 5 – 15% for potential yields and up to 50% for rainfed conditions. According to Soltani *et al.* (2004) the use of temporally aggregated weather data resulted in significant differences in simulated biomass, especially due to the lack of extreme temperatures (cold or hot events) in the monthly aggregates. In our study we additionally found that model sensitivity to temporal aggregation of input data increased with increasing detail in the model. The model with the detailed biomass production approach was most sensitive to the aggregation of input data (with a maximum difference of 37%), while the less detailed model showed a maximum difference of 10%. We explained the higher sensitivity of the detailed model by its higher non-linear nature.

Most global crop growth models are run on a grid-based system (see Table 1.1). In grid-based systems spatially aggregated data are used, i.e. it is assumed that data such as weather and crop management are homogeneous within a grid cell of a certain resolution, e.g.  $0.5^{\circ} \times 0.5^{\circ}$  (approximately 50 km  $\times$  50 km around the equator). Several studies investigated the bias in crop growth model outcomes of different levels of spatially aggregated climate data. In general, a grid cell size of  $0.5^{\circ} \times 0.5^{\circ}$  is considered to be appropriate for regional crop

growth simulations (Easterling *et al.*, 2000; Olesen *et al.*, 2000; De Wit *et al.*, 2005), unless water-limitation plays a role, in which case simulations at a finer resolution are required (Wassenaar *et al.*, 1999; Baron *et al.*, 2005). In Chapter 4 we studied the effects of different levels of spatial aggregation of weather data and sowing dates (both input data) on simulation of winter wheat phenology. Analysing observed phenological data in several regions in Germany we found temporal heterogeneity in sowing dates to be smaller than spatial heterogeneity, on average 21 d versus 44 d, an indication that farmers try to sow each year in the same weeks of the year. Based on the results of semi-variograms we showed that to capture observed spatial heterogeneity in ear-emergence and harvest dates, sampling in grid cell sizes ranging from 50 km × 50 km to 100 km × 100 km is reasonable. For sowing dates we could not find such an indication due to its high spatial variability. For winter wheat phenology simulation, which consists of mainly linear relationships to represent the effects of temperature and daylength, we concluded that the use of sowing dates and weather data with a 100 km × 100 km resolution is appropriate for regions with homogenous climatic characteristics such as Germany. In addition, the results indicated that our assumption to use one phenological parameter set to capture the average response pattern of the development of different winter wheat cultivars found in a large country such as Germany, was justified. However, in order to capture the range of wheat development for larger areas, phenological parameter sets reflecting phenological characteristics from more cultivars will be required.

Generalizing the findings from Chapter 3 & 4 it can be concluded that data aggregation might have considerable effects on model outcomes and therefore I stress that the resolution of the available input data in space and over time should be tested for its usefulness in the chosen model. Yet, if the chosen crop growth model contains mainly linear relationships the use of weather input data with a monthly resolution at a 50 km × 50 km grid combined with spatially aggregated sowing dates at a 100 km × 100 km grid seems to be justified for the simulation of wheat growth and development.

### **1.2.2. Data generation**

Generation or simulation of input data for crop growth models is necessary if the spatial resolution of the available data is unsuitable, when data are expected to change under future conditions, or when data are not available. Phenological data, e.g. sowing and harvesting dates, are examples of data that are often simulated within global crop growth models or are required as input data if not simulated. Global crop growth models apply various methodologies to simulate

the cropping period (see Table 1.1). In many quantitative climate change impact assessments crop growth models are used to study the effects of climate change on future crop production. The dominant effect of climate change on crop production in those assessments often goes via simulated effects of global warming on phenological development of crops (Craufurd and Wheeler, 2009). Simulation, including evaluation, of the cropping period deserves therefore considerable research attention. Nevertheless, only recently two comprehensive global data sets of cropping calendars with global coverage, combining several sources of observed cropping calendars, have been developed (Portmann *et al.*, 2010; Sacks *et al.*, 2010). As a consequence until recently simulation of phenology at the global scale, including the simulated start and end of the cropping period, could hardly be evaluated.

In Chapter 5 we aimed at simulating sowing dates (i.e. the start of the cropping period) of several major rainfed crops based on climatic conditions. We assumed farmers to sow either when temperature exceeds a crop-specific threshold or at the onset of the wet season, depending on the interannual variability in climatic conditions. From our results we concluded that our methodology is more accurate in regions in which temperature is the main limiting factor for the length of the growing season in comparison with regions in which precipitation plays a major role. For all considered crops, except for rapeseed and cassava, on at least 60% of the cultivated area the difference between simulated and observed sowing dates, the latter from Portmann *et al.* (2010), is less than one month.

To simulate the end of the cropping period (i.e. harvest dates) we developed simple algorithms to generate unknown crop- and location-specific phenological parameters based on location-specific climatic and daylength characteristics, using wheat and maize as example crops (Chapter 6). In the main cropping regions of wheat (e.g. Russia, Canada, and France) we were able to simulate the lengths of the cropping period that correspond well with observed lengths. Agreement between observed and simulated lengths of the cropping period was lower for maize than for wheat, with in the main maize cropping regions over- and underestimations of 0.5 to 1.5 month.

Recently Deryng *et al.* (2011) presented a similar methodology to simulate the length of the cropping period. Their results for simulated sowing dates are similar, while the presented methodology in this thesis to simulate the length of the cropping period resulted in better simulated harvest dates. For example in the main maize cropping areas of the USA our methodology underestimated the

length of the cropping period by one month, while the methodology of Deryng *et al.* (2011) resulted in an underestimation of two to three months.

The objective of a global crop growth model is generally yield simulation. Therefore, besides the comparison of observed and simulated sowing and harvesting dates, we also evaluated possible consequences for simulated yields related to these deviations (Chapters 5 & 6). We showed that simulated yields are sensitive to the simulated sowing and harvesting dates. Yet, our evaluation of possible consequences for simulated yields related to uncertainties in simulated sowing and harvesting dates showed that simulated yields (for wheat and maize) are rather similar using either simulated sowing and harvesting dates or observed sowing and harvesting dates; the difference not being larger than 20%.

Based on the outcomes of Chapters 5 & 6 I conclude that our methodologies to simulate the length of the cropping period are accurate enough to simulate global crop yields. This conclusion is only valid for the used crop growth model (LPJmL) combined with monthly climate input data. Whether simulated sowing and harvesting dates are accurate enough for more detailed crop growth models in which crop damaging factors such as heat and frost stress are included, combined with more detailed climate input data, needs further evaluation.

### **1.3 Design of global crop growth models: matching data and models**

The first step in developing a model is to define its objective. The main aim of crop growth models embedded in large scale integrated assessment models such as IMAGE 2.4 (MNP, 2006) or SEAMLESS (Van Ittersum *et al.*, 2008) is the simulation of accurate yields for various crops. The main variable of interest in this thesis was therefore yield, or important determining processes of yield such as phenology. Although simulations of water- and nutrient-limited productivity are also important for integrated assessment models, in my opinion for accurate simulation of these production levels, first large scale simulation of potential yields should be carefully examined. Below I propose a structure for a global crop growth model and the suitable temporal and spatial resolutions for input data to simulate potential yields.

In Chapter 4 we concluded that for accurate simulation of crop phenology emergence/sowing dates should be available at a spatial resolution of at least 100 km × 100 km in Germany. For natural vegetation, Rötzer and Chmielewski (2001) found the start of the growing season (as determined by temperature) to move with a speed of 44 km d<sup>-1</sup> from south to north, 200 km d<sup>-1</sup> from west to east, and 32 m d<sup>-1</sup> with increasing altitude across Europe. Their results indicate that temperature gradually changes over space. This knowledge, combined with

the results from Chapter 4, justified our choice in Chapter 5 to generate sowing dates at a resolution of  $0.5^\circ \times 0.5^\circ$ . In Chapter 4 we also concluded that one phenological parameter set is sufficient for accurate simulations of crop phenology for a country as large as Germany; therefore, the spatial scale at which our methodology to generate phenological parameters was applied ( $0.5^\circ \times 0.5^\circ$ ) can be defended (Chapter 6). Moreover, in Chapter 3 we concluded that increasing non-linearity in models gave higher sensitivity to temporal aggregation of climate data. The use of climate data with a monthly resolution in Chapter 6 is justified, as we simulated phenology mainly with help of linear relationships.

Challinor *et al.* (2004) and Bondeau *et al.* (2007) indicated that a mechanistic crop growth model is required to capture the impact of climatic variability on crop yields of large areas. In addition, the level of detail should be adjusted to the resolution of the available data (Challinor *et al.*, 2003; Ewert, 2004b). The level of detail of particularly the representations of light interception and light utilization for biomass production and the resolution of the weather data used differs between large scale crop growth models (Table 1.1). Interestingly, two crop growth models with approximately equal levels of detail to simulate crop growth, GLAM-MOSE2 (Challinor *et al.*, 2004; Osborne *et al.*, 2007) and LPJmL (Bondeau *et al.*, 2007) use climate input data with rather different temporal resolutions, 30 minutes versus monthly, respectively. The results of Chapter 2 indicated that extra detail in the representation of biomass production did not significantly change model results, although the less detailed representation of light utilization for biomass production may have been an oversimplification of reality. In Chapter 3 we found that adding extra detail to a model (i.e. non-linear relationships) resulted in a higher sensitivity of model outcomes to weather data with a low resolution. Whether model uncertainty unnecessarily increases when detailed approaches are combined with climate data with a low resolution needs further examination by using observations of biomass. Nevertheless, combining the conclusions of Chapter 2 & 3 may imply that if the main objective of the model is to simulate yield and if only temporarily sparse weather data are available, the less detailed representations of both light interception and light utilization for biomass production are best suited for a global crop growth model. I therefore plead to let the resolution of the available data influence the final design of a crop growth model as much as the aim of the model.

Based on the conclusions of this thesis and conclusions from previous research, I constructed a schematic overview of a model which I expect to simulate reasonable potential yields at the global scale if only monthly aggregates of climate data at a  $0.5^\circ \times 0.5^\circ$  are available (Fig. 7.1). The proposed model

consists of the light interception representation as applied in the global crop growth model LPJmL, combined with the radiation use efficiency approach (see Chapter see 2 & 3 for detailed descriptions of these approaches) as, among others, applied in the global crop growth models GEPIC, DAYCENT, and PEGASUS, and phenology determining the value of the partitioning coefficients. Simulation of sowing dates and phenological cultivar characteristics should be part of the model (see Chapter 5 & 6), based on location-specific climatic and/or daylength conditions. The question marks in Fig. 7.1 indicate issues which are important for potential yields, but require more research before they can be implemented in the proposed model. These items will be discussed in the next section.

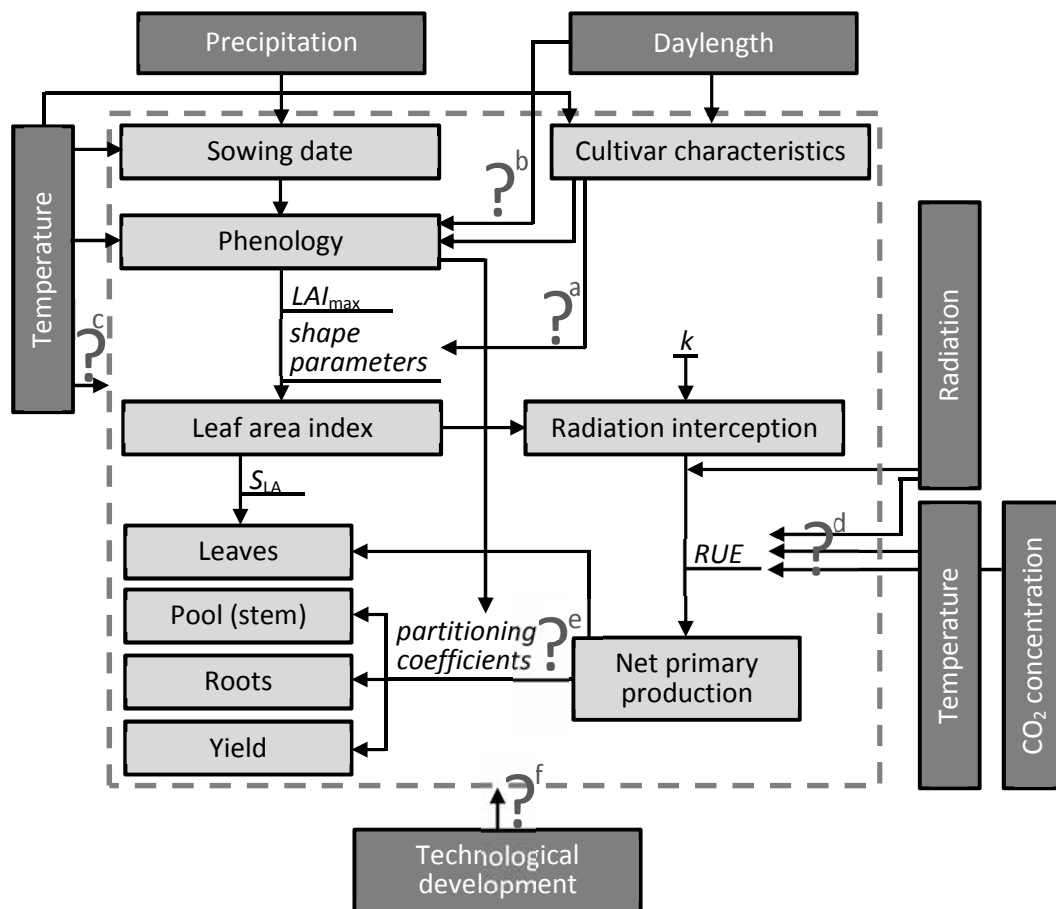


**Fig. 7.1** Schematic overview of the proposed global crop growth model for potential yield simulations at a resolution of  $0.5^\circ \times 0.5^\circ$ ; boxes in light grey indicate processes, state/rate variables, or simulated parameters, boxes in dark grey indicate input data.  $LAI_{max}$  and *shape parameters* define the shape of the leaf area index curve, including the onset of leaf senescence;  $S_{LA}$  influences the biomass allocated to the leaves, the *partitioning coefficients* determine the biomass allocated to the other organs;  $k$  is the light extinction coefficient and  $RUE$  radiation use efficiency. See Chapter 2 & 3 for a description of the leaf area index and biomass production simulation, Chapter 5 & 6 for a description of the simulation of sowing dates and generation of cultivar characteristics. The question marks indicate issues for further research (see Section 1.4).



## 1.4 Directions for future research to improve global potential yield simulations

### 1.4.1 Phenology: simulation of flowering dates at the global scale

In this thesis the importance of the simulation of phenological development of crops for yield simulation has been addressed several times (Chapters 2, 4, 5 & 6). In Chapter 2 we showed the importance of representing the right timing of the onset of leaf senescence for simulated wheat yields; it is expected that also for other crops the timing of leaf senescence is essential for crop growth simulation. Yet, we found that the onset of leaf senescence is not explicitly and unambiguously defined by the crop modelling community, since between modelling approaches the definition of the parameter representing the onset of leaf senescence is different (see e.g. Havelka *et al.* (1984), Mi *et al.* (2000), Araus and Tapia (1987), and Neitsch *et al.* (2005)). Although the exact timing of leaf senescence is not well-defined, it is clear that the onset of leaf senescence is related to the timing of flowering (also referred to as anthesis), as most of the biomass produced after anthesis is used for grain filling (Schnyder, 1993) and hence there is no biomass available to form new leaves after anthesis. In Chapter 6 we indicated that the complex process that determines differences in the timing of flowering between cultivars is not well-understood. To improve the simulation of crop production at the global scale I therefore propose that research that enhances the understanding of the timing of flowering of cultivars used in different regions of the globe should be given priority. The next step should be the development of a methodology that is capable of accurately simulating flowering dates at the global scale, including possible adaptation strategies by farmers to combat negative effects of climate change via changes in cultivar use. Finally simulated flowering dates should be connected to the simulation of leaf area index, so that the onset of leaf senescence is simulated more accurately (via the shape parameters, Fig. 7.1, question mark a). As indicated in Chapter 6, simulated interannual variability of harvesting, and possibly also simulated interannual variability of flowering dates, depends on whether or not daylength is considered in the simulation of crop phenology. However, observations of flowering and harvesting dates for multiple years and multiple regions are required to clarify whether considering the effects of daylength in the simulation of phenology improves the simulation of phenological stages (Fig. 7.1, question mark b).

Due to the expected increase in extreme weather events (Easterling *et al.*, 2000; Salinger *et al.*, 2005; Beniston *et al.*, 2007) possible crop yield losses as a result of extreme temperatures is an emerging research topic. Useful studies

have been carried out at the regional (see Trnka *et al.* (2011) and Challinor *et al.* (2005)) and global scale (see Teixeira *et al.* (under review)). Crops are in particular vulnerable to extreme temperatures during flowering (Mitchell *et al.*, 1993; Ferris *et al.*, 1998; Challinor *et al.*, 2005; Craufurd and Wheeler, 2009). Yet, the above stated studies did not address the simulation of flowering dates (Trnka *et al.*, 2011) or evaluate simulated flowering dates (Challinor *et al.*, 2005; Teixeira *et al.*, under review), which makes the outcomes of these studies questionable. A methodology capable of accurate simulation of the timing of flowering could therefore also improve assessments of possible implications of extreme temperature events on future crop production (Fig. 7.1, question mark c).

#### 1.4.2 Other issues related to potential yield simulation

As indicated in Fig. 1.1 (Chapter 1) atmospheric CO<sub>2</sub> concentration influences potential yields. Both global and field scale crop growth models take this effect into account, e.g. LPJmL and GECROS (Yin and van Laar, 2005), although the best approach of modelling the CO<sub>2</sub> effect on crops is still subject of debate (Long *et al.*, 2006; Ewert *et al.*, 2007; Tubiello *et al.*, 2007). In Chapter 2 we indicated that the use of a constant value for the radiation use efficiency for the whole cropping period may have been an oversimplification of reality. It should therefore be investigated if it is possible to extend the radiation use efficiency approach to account for effects of atmospheric CO<sub>2</sub> concentration and temperature and radiation conditions during the growing season, as proposed by e.g. Reyenga *et al.* (1999) or Stöckle and Kemanian (2009). In particular it should be studied if the approach is suitable for global application, taking into account the spatial and temporal resolution of the available climate data (Fig. 7.1, question mark d).

A challenge for crop growth modellers is to allocate simulated biomass to the different organs of the plant (Kemanian *et al.*, 2007). Existing global crop growth models apply different methodologies, ranging from an empirical approach in which among others leaf area index determines the produced leaf biomass (e.g. in LPJmL), to a more mechanistic approach in which produced leaf biomass determines the leaf area index (e.g. in PEGASUS). To my knowledge a systematic analysis comparing different approaches has not been carried out. Since simulated yield may be sensitive to the allocation approach chosen, enhanced insight in the representation of this process will give scope for further improvement of global crop growth models (Fig. 7.1, question mark e).

As indicated by Ewert *et al.* (2007) technological progress over time, due to improved crop management and cultivars via progress in breeding (e.g. im-

proved harvest index or delay of leaf senescence) is important to account for in global crop growth models, especially if they are applied for future crop production assessments. To be able to account for improved cultivars, a mechanistic approach should be developed which translates improvements in cultivar characteristics into yield increases via parameters that represent cultivar characteristics, e.g. a change in the partitioning coefficients could account for a change in the harvest index. In the absence of such mechanistic approaches for global crop modelling, empirical relationships about yield changes due to technology development as proposed by e.g. Ewert *et al.* (2005) for the European situation, remain most suitable to account for the effects of technology development on crops. It is however important to separate in this approach the effects of yield gap closure (e.g. due to a higher or better balanced application of fertilizers) on the one hand and increases in yield potential (due to progress in breeding) on the other hand. Moreover, it should be studied how to extrapolate these relationships to other regions outside Europe (Fig. 7.1, question mark f).

#### **1.4.3 Evaluation of global crop growth models**

To establish an overall credibility of a model it must be evaluated. In general, the objective of global crop growth models is yield simulation. Observed yield data are therefore required to evaluate global crop growth models. Nevertheless, yield data alone are not sufficient. To assess whether the model is right for the right reasons (i.e. to be able to identify possible compensation errors), evaluation of other simulated variables (e.g. timing and length of cropping period) is also essential. The evaluation of existing global crop growth models has mainly been based on statistics from the Food and Agriculture Organization of the United Nations (FAO) reporting actual yields, often only per country. Recently databases developed with more comprehensive information on harvested area, crop yield (also largely based on FAO statistics (Monfreda *et al.*, 2008)), and cropping periods (Portmann *et al.*, 2010; Sacks *et al.*, 2010) give scope for further evaluation of global crop growth models. The databases were already applied by Deryng *et al.* (2011) for the evaluation of PEGASUS. Importantly, it should be noted that yield data reported by FAO are actual yields, i.e. yields determined by deficiencies in water, nutrients, and other (a)biotic stresses such as heat stress or the effects of pests and diseases, the latter stresses not being captured by global crop growth models (or field-scale crop growth models). Therefore, the usefulness of FAO data for the evaluation of global crop growth models is limited. Obviously, simulated potential yields should at least be higher than yields

reported by FAO. Hence, as a first check of global crop growth models FAO data could be used to examine if simulated potential yields are high enough.

A more promising approach to evaluate simulated potential yields is given by Reidsma *et al.* (2009). In their study, a European database (Farm Accountancy Data Network) was used with among other things regionally averaged observed crop yields and maximum observed crop yields as achieved by the 'best' farmers. They assumed the maximum observed crop yield per region to be indicative for the yield potential for that region. Results from such analyses might be extended to other regions with similar climatic conditions and with knowledge about applied management (e.g. irrigation and fertilisation practices). In addition to this, a global database with experimental yields, including other variables such as leaf area development and timing of senescence, will be a useful instrument for in depth evaluations of global crop growth models. Finally, remote-sensing data may be an addition source of data to evaluate e.g. simulated crop development (Viña *et al.*, 2004).

Besides observations, knowledge from local experts on potential crop yields and possible yield gaps due to water and/or nutrient deficits and/or other (a)biotic stresses may be a valuable addition for the evaluation of global crop growth models. Recently Hengsdijk and Langeveld (2009) made a start with the collection of these data. Finally, as I discussed in Chapter 1, a comparative analysis of yields assessed with different methods, i.e. global crop growth models the frontier function as proposed by Neumann *et al.* (2010) or the statistical approach used by Lobell *et al.* (2011), could help forward the global crop growth modelling community.

## 2. Conclusions

The work described in this thesis enhances understanding related to the upscaling of crop growth models from field to globe. In particular it shows that:

1. for crop growth models applied at large scales, particular attention should be given to the choice of the representation of the leaf area development. A more mechanistic approach does not generally result in better model performance;
2. an increase in the level of detail in models results in higher sensitivity to temporally aggregated input data, hence the temporal resolution of the available input data should define the design of a (global) crop growth model as much as the aim of the model;

3. spatial variability of sowing dates within a region or country can be large, nevertheless, the use of aggregated sowing dates at a 100 km × 100 km resolution in crop growth models results in simulated lengths of cropping periods which deviate less than one week from observed lengths;
4. it is acceptable to simulate missing sowing dates of various crops based on location-specific climatic conditions (i.e. sowing is simulated on the day when temperature exceeds a crop-specific threshold or at the onset of the wet season). The level of accuracy of the simulated sowing dates is high enough for application within a global crop growth model, with differences in simulated yields less than 20%, using either simulated sowing and harvesting dates or observed sowing and harvesting dates;
5. required but unknown parameter values to represent phenological characteristics of wheat and maize cultivars can be generated based on location-specific temperature and daylength conditions. With help of these generated parameters observed lengths of cropping periods can be adequately simulated at the global scale, including a probably realistic interannual variability in cropping period lengths.

# References

- Abildtrup, J., Audsley, E., Fekete-Farkas, M., Giupponi, C., Gylling, M., Rosato, P. & Rounsevell, M. (2006) Socio-economic scenario development for the assessment of climate change impacts on agricultural land use: a pairwise comparison approach. *Environmental Science & Policy*, **9**, 101-115.
- Adam, M., Titttonell, P., Bergez, J.E., Ewert, F. & Leffelaar, P.A. (2008) From detailed to summary models of the Crop-Soilsystem for larger scale applications. *In proceeding of the X ESA Congress, 15-19 September 2008, Bologna, Italy*.
- Adam, M., Van Bussel, L.G.J., Leffelaar, P.A., Van Keulen, H. & Ewert, F. (2011) Effects of modelling detail on simulated crop productivity under a wide range of climatic conditions. *Ecological Modelling*, **222**, 131-143.
- Addae, P.C. & Pearson, C.J. (1992) Thermal requirement for germination and seedling growth of wheat. *Australian Journal of Agricultural Research*, **43**, 585-594.
- Addiscott, T.M. (1998) Modelling concepts and their relation to the scale of the problem. *Nutrient Cycling in Agroecosystems*, **50**, 239-245.
- Alcamo, J., Dronin, N., Endejan, M., Golubev, G. & Kirilenko, A. (2007) A new assessment of climate change impacts on food production shortfalls and water availability in Russia. *Global Environmental Change*, **17**, 429-444.
- Angus, J.F., Cunningham, R.B., Moncur, M.W. & Mackenzie, D.H. (1980) Phasic development in field crops. I. thermal response in the seedling phase. *Field Crops Research*, **3**, 365-378.
- Apipattanavis, S., Bert, F., Podestá, G. & Rajagopalan, B. (2010) Linking weather generators and crop models for assessment of climate forecast outcomes. *Agricultural and Forest Meteorology*, **150**, 166-174.
- Araus, J.L. & Tapia, L. (1987) Photosynthetic gas exchange characteristics of wheat flag leaf blades and sheaths during grain filling: the case of a spring crop grown under Mediterranean climate conditions. *Plant Physiology*, **85**, 667-673.
- Arora, V.K. & Boer, G.J. (2005) A parameterization of leaf phenology for the terrestrial ecosystem component of climate models. *Global Change Biology*, **11**, 39-59.
- Baloch, D.M., Karow, R.S., Marx, E., Kling, J.G. & Witt, M.D. (2003) Vernalization studies with Pacific Northwest wheat. *Agronomy Journal*, **95**, 1201-1208.
- Baron, C., Sultan, B., Balme, M., Sarr, B., Traoré, S., Lebel, T., Janicot, S. & Dingkuhn, M. (2005) From GCM grid cell to agricultural plot: scale issues affecting modelling of climate impact. *Philosophical Transactions of the Royal Society B: Biological Sciences*, **360**, 2095-2108.
- Battisti, D.S. & Naylor, R.L. (2009) Historical warnings of future food insecurity with unprecedented seasonal heat. *Science*, **323**, 240-244.
- Bender, J., Hertstein, U. & Black, C.R. (1999) Growth and yield responses of spring wheat to increasing carbon dioxide, ozone and physiological stresses: a statistical analysis of 'ESPACE-wheat' results. *European Journal of Agronomy*, **10**, 185-195.
- Beniston, M., Stephenson, D.B., Christensen, O.B., Ferro, C.A.T., Frei, C., Goyette, S., Halsnaes, K., Holt, T., Jylhä, K., Koffi, B., Palutikof, J., Schöll, R., Semmler, T. & Woth, K. (2007) Future extreme events in European climate: an exploration of regional climate model projections. *Climatic Change*, **81**, 71-95.
- Beven, K. (1989) Changing ideas in hydrology - The case of physically-based models. *Journal of Hydrology*, **105**, 157-172.
- Biernath, C., Gayler, S., Bittner, S., Klein, C., Högy, P., Fangmeier, A. & Priesack, E. (2011) Evaluating the ability of four crop models to predict different environmental impacts on spring wheat grown in open-top chambers. *European Journal of Agronomy*, **35**, 71-82.
- Bignon, J. (1990) *Agrometeorologie et physiologie du maïs grain dans la commune de Luxembourg*. Commission des Communes Européennes, Luxembourg.

- Birch, C.J., Hammer, G.L. & Rickert, K.G. (1998) Temperature and photoperiod sensitivity of development in five cultivars of maize (*Zea mays* L.) from emergence to tassel initiation. *Field Crops Research*, **55**, 93-107.
- Boer, R., Campbell, L.C. & Fletcher, D.J. (1993) Characteristics of frost in a major wheat-growing region of Australia. *Australian Journal of Agricultural Research*, **44**, 1731-1743.
- Bondeau, A., Smith, P.C., Zaehle, S., Schaphoff, S., Lucht, W., Cramer, W., Gerten, D., Lotze-Campen, H., Müller, C., Reichstein, M. & Smith, B. (2007) Modelling the role of agriculture for the 20th century global terrestrial carbon balance. *Global Change Biology*, **13**, 679-706.
- Bonhomme, R., Derieux, M. & Edmeades, G.O. (1994) Flowering of diverse maize cultivars in relation to temperature and photoperiod in multilocation field trials. *Crop Science*, **34**, 156-164.
- Boons - Prins, E.R., De Koning, G.H.J., Van Diepen, C.A. & Penning de Vries, F.W.T. (1993) *Crop-specific simulation parameters for yield forecasting across the European Community*, pp 43. CABO-DLO, Wageningen.
- Boote, K.J., Jones, J.W. & Pickering, N.B. (1996) Potential uses and limitations of crop models. *Agronomy Journal*, **88**, 704-716.
- Booth, E.J. & Gunstone, F.D. (2004) Rapeseeds and rapeseed oil: agronomy, production and trade. *Rapeseed and canola oil: production, processing, properties and uses* (ed. by Gunstone, F.D.), pp 1-16. Blackwell, Oxford.
- Brooks, R.J. & Tobias, A.M. (1996) Choosing the best model: level of detail, complexity, and model performance. *Mathematical and Computer Modelling*, **24**, 1-14.
- Burke, M.B., Lobell, D.B. & Guarino, L. (2009) Shifts in African crop climates by 2050, and the implications for crop improvement and genetic resources conservation. *Global Environmental Change*, **19**, 317-325.
- Castillo Garcia, J.E. & Lopez Bellido, L. (1986) Growth and yield of autumn-sown sugar beet: effects of sowing time, plant density and cultivar. *Field Crops Research*, **14**, 1-14.
- Challinor, A.J., Slingo, J.M., Wheeler, T.R., Craufurd, P.Q. & Grimes, D.I.F. (2003) Toward a combined seasonal weather and crop productivity forecasting system: determination of the working spatial scale. *Journal of Applied Meteorology*, **42**, 175-192.
- Challinor, A.J., Wheeler, T.R., Craufurd, P.Q., Slingo, J.M. & Grimes, D.I.F. (2004) Design and optimisation of a large-area process-based model for annual crops. *Agricultural and Forest Meteorology*, **124**, 99-120.
- Challinor, A.J., Wheeler, T.R., Craufurd, P.Q. & Slingo, J.M. (2005) Simulation of the impact of high temperature stress on annual crop yields. *Agricultural and Forest Meteorology*, **135**, 180-189.
- Challinor, A.J., Ewert, F., Arnold, S., Simelton, E. & Fraser, E. (2009) Crops and climate change: progress, trends, and challenges in simulating impacts and informing adaptation. *Journal of Experimental Botany*, **60**, 2775-2789.
- Chmielewski, F.-M., Muller, A. & Bruns, E. (2004) Climate changes and trends in phenology of fruit trees and field crops in Germany, 1961-2000. *Agricultural and Forest Meteorology*, **121**, 69-78.
- Choudhury, B.J. (2000) A sensitivity analysis of the radiation use efficiency for gross photosynthesis and net carbon accumulation by wheat. *Agricultural and Forest Meteorology*, **101**, 217-234.
- Choudhury, B.J. (2001) Modeling radiation- and carbon-use efficiencies of maize, sorghum, and rice. *Agricultural and Forest Meteorology*, **106**, 317-330.
- Cirilo, A.G. & Andrade, F.H. (1996) Sowing date and kernel weight in maize. *Crop Science*, **36**, 325-331.
- Coffman, F.A. (1923) The minimum temperature of germination of seeds. *Journal of the American Society of Agronomy*, **15**, 257-270.
- Collatz, G.J., Ball, J.T., Grivet, C. & Berry, J.A. (1991) Physiological and environmental regulation of stomatal conductance, photosynthesis and transpiration: a model that includes a laminar boundary layer. *Agricultural and Forest Meteorology*, **54**, 107-136.

- Collatz, G.J., Ribas-Carbo, M. & Berry, J.A. (1992) Coupled photosynthesis-stomatal conductance model for leaves of C4 plants. *Australian Journal of Plant Physiology*, **19**, 519-538.
- Cramer, W., Bondeau, A., Woodward, F.I., Prentice, I.C., Betts, R.A., Brovkin, V., Cox, P.M., Fisher, V., Foley, J.A., Friend, A.D., Kucharik, C., Lomas, M.R., Ramankutty, N., Sitch, S., Smith, B., White, A. & Young-Molling, C. (2001) Global response of terrestrial ecosystem structure and function to CO<sub>2</sub> and climate change: results from six dynamic global vegetation models. *Global Change Biology*, **7**, 357-373.
- Craufurd, P.Q. & Wheeler, T.R. (2009) Climate change and the flowering time of annual crops. *Journal of Experimental Botany*, **60**, 2529-2539.
- Davidson, J.L. & Christian, K.R. (1984) Flowering in wheat. *Control of crop productivity* (ed. by Pearson, C.J.), pp 111-126. Academic Press, Sydney.
- Davidson, J.L., Christian, K.R., Jones, D.B. & Bremner, P.M. (1985) Responses of wheat to vernalization and photoperiod. *Australian Journal of Agricultural Research*, **36**, 347-359.
- De Vries, W., Kros, J., Van Der Salm, C., Groenenberg, J.E. & Reinds, G.J. (1998) The use of upscaling procedures in the application of soil acidification models at different spatial scales. *Nutrient Cycling in Agroecosystems*, **50**, 223-236.
- De Wit, A.J.W., Boogaard, H.L. & van Diepen, C.A. (2004) Using NOAA-AVHRR estimates of land surface temperature for regional agrometeorological modelling. *International Journal of Applied Earth Observation and Geoinformation*, **5**, 187-204.
- De Wit, A.J.W., Boogaard, H.L. & Van Diepen, C.A. (2005) Spatial resolution of precipitation and radiation: the effect on regional crop yield forecasts. *Agricultural and Forest Meteorology*, **135**, 156-168.
- De Wit, C.T. (1968) *Theorie en model*, pp 11. Veenman, Wageningen.
- Del Pozo, A.H., García-Huidobro, J., Novoa, R. & Villaseca, S. (1987) Relationship of base temperature to development of spring wheat. *Experimental Agriculture*, **23**, 21-30.
- Dennett, M.D. (1999) Effects of sowing date and the determination of optimum sowing date. *Wheat ecology and physiology of yield determination* (ed. by Satorre, E.H. & Slafer, G.A.), pp 123-140. Food Products Press, New York, NY.
- Deryng, D., Sacks, W.J., Barford, C.C. & Ramankutty, N. (2011) Simulating the effects of climate and agricultural management practices on global crop yield. *Global Biogeochemical Cycles*, **25**, GB2006.
- Dettori, M., Cesaraccio, C., Motroni, A., Spano, D. & Duce, P. (2011) Using CERES-Wheat to simulate durum wheat production and phenology in Southern Sardinia, Italy. *Field Crops Research*, **120**, 179-188.
- Devendra, C. & Thomas, D. (2002) Smallholder farming systems in Asia. *Agricultural Systems*, **71**, 17-25.
- Easterling, D.R., Meehl, G.A., Parmesan, C., Changnon, S.A., Karl, T.R. & Mearns, L.O. (2000) Climate extremes: observations, modeling, and impacts. *Science*, **289**, 2068-2074.
- Easterling, W.E., Weiss, A., Hays, C.J. & Mearns, L.O. (1998) Spatial scales of climate information for simulating wheat and maize productivity: the case of the US Great Plains. *Agricultural and Forest Meteorology*, **90**, 51-63.
- Easterling, W.E., Chhetri, N. & Niu, X. (2003) Improving the realism of modeling agronomic adaptation to climate change: Simulating technological substitution. *Climatic Change*, **60**, 149-173.
- Elzebroek, T. & Wind, K. (2008) *Guide to cultivated plants*. CABI, Wallingford.
- Estrella, N., Sparks, T.H. & Menzel, A. (2007) Trends and temperature response in the phenology of crops in Germany. *Global Change Biology*, **13**, 1737-1747.
- Evangelio, F.A. (2001) Cassava agronomy research and adoption of improved practices in the Philippines - major achievements during the past 20 years. *Cassava's potential in Asia in the 21st century: present situation and future research and development needs. Proceedings of the sixth regional workshop, held in Ho Chi Minh city, Vietnam, Feb 21-25, 2000* (ed. by Howeler, R.H. & Tan, S.L.), pp 314-332. CIAT, Cali.



- Evans, L.T. (1987) Short day induction of inflorescence initiation in some winter wheat varieties. *Functional Plant Biology*, **14**, 277-286.
- Ewert, F., Porter, J. & Honermeier, B. (1996) Use of AFRCWHEAT2 to predict the development of main stem and tillers in winter triticale and winter wheat in North East Germany. *European Journal of Agronomy*, **5**, 89-103.
- Ewert, F. & Pleijel, H. (1999) Phenological development, leaf emergence, tillering and leaf area index, and duration of spring wheat across Europe in response to CO<sub>2</sub> and ozone. *European Journal of Agronomy*, **10**, 171-184.
- Ewert, F., Van Oijen, M. & Porter, J.R. (1999) Simulation of growth and development processes of spring wheat in response to CO<sub>2</sub> and ozone for different sites and years in Europe using mechanistic crop simulation models. *European Journal of Agronomy*, **10**, 231-247.
- Ewert, F. & Porter, J.R. (2000) Ozone effects on wheat in relation to CO<sub>2</sub>: modelling short-term and long-term responses of leaf photosynthesis and leaf duration. *Global Change Biology*, **6**, 735-750.
- Ewert, F. (2004a) Modelling plant responses to elevated CO<sub>2</sub>: how important is leaf area index? *Annals of Botany*, **93**, 619-627.
- Ewert, F. (2004b) *Modelling changes in global regionalized food production systems under changing climate and consequences for food security and environment – development of an approach for improved crop modelling within IMAGE*, pp 55. Plant Production Systems Group, Department of Plant Sciences, Wageningen University & Netherlands Environmental Assessment Agency (MNP), National Institute for Public Health and Environment (RIVM).
- Ewert, F., Rounsevell, M.D.A., Reginster, I., Metzger, M.J. & Leemans, R. (2005) Future scenarios of European agricultural land use: I. estimating changes in crop productivity. *Agriculture, Ecosystems & Environment*, **107**, 101-116.
- Ewert, F., Porter, J. R. & Rounsevell, M. D. A. (2007) Crop models, CO<sub>2</sub>, and climate change [2]. *Science*, **315**, 459.
- FAO (2003) World agriculture: towards 2015/2030: an FAO perspective. (ed. by Bruinsma, J.), pp iv, 432. FAO, Earthscan, Rome.
- FAO (2009) *Proceedings of the expert meeting on how to feed the world in 2050: 24-26 June 2009, FAO Headquarters, Rome*, pp 23. FAO, Rome.
- Farquhar, G.G., von Caemmerer, S. & Berry, J.A. (1980) A biochemical model of photosynthetic CO<sub>2</sub> assimilation in leaves of C<sub>3</sub> species. *Planta*, **149**, 78-90.
- Farré, I., Van Oijen, M., Leffelaar, P.A. & Faci, J.M. (2000) Analysis of maize growth for different irrigation strategies in northeastern Spain. *European Journal of Agronomy*, **12**, 225-238.
- Ferris, R., Ellis, R.H., Wheeler, T.R. & Hadley, P. (1998) Effect of high temperature stress at anthesis on grain yield and biomass of field-grown crops of wheat. *Annals of Botany*, **82**, 631-639.
- Fischer, G., Van Velthuisen, H., Shah, M. & Nachtergaele, F.O. (2002) Global agro-ecological assessment for agriculture in the 21st century: methodology and results. *Research Report RR-02-02*, pp xxii, 119 pp and CD-Rom. International Institute for Applied Systems Analysis, Laxenburg, Austria.
- Fischer, G., Shah, M., Tubiello, F.N. & Van Velthuisen, H. (2005) Socio-economic and climate change impacts on agriculture: an integrated assessment, 1990-2080. *Philosophical Transactions of the Royal Society B: Biological Sciences*, **360**, 2067-2083.
- Fisher, R.A. (1999) Wheat cropping in Australia. *Wheat ecology and physiology of yield determination* (ed. by Satorre, E.H. & Slafer, G.A.), pp 277-294. Food Products Press, New York, NY.
- Franck, S., Von Bloh, W., Müller, C., Bondeau, A. & Sakschewski, B. (2011) Harvesting the sun: New estimations of the maximum population of planet Earth. *Ecological Modelling*, **222**, 2019-2026.
- Gabrielle, B., Denoroy, P., Gosse, G., Justes, E. & Andersen, M.N. (1998) A model of leaf area development and senescence for winter oilseed rape. *Field Crops Research*, **57**, 209-222.

- Gadgil, S., Seshagiri Rao, P.R. & Narahari Rao, K. (2002) Use of climate information for farm-level decision making: Rainfed groundnut in southern India. *Agricultural Systems*, **74**, 431-457.
- Garcia-Huidobro, J., Monteith, J.L. & Squire, G.R. (1982) Time, temperature and germination of Pearl Millet (*Pennisetum typhoides* S. & H.): I. constant temperature. *Journal of Experimental Botany*, **33**, 288-296.
- Geng, S., Penning de Vries, F.W.T. & Supit, I. (1986) A simple method for generating daily rainfall data. *Agricultural and Forest Meteorology*, **36**, 363-376.
- Gerten, D., Schaphoff, S., Haberlandt, U., Lucht, W. & Sitch, S. (2004) Terrestrial vegetation and water balance – hydrological evaluation of a dynamic global vegetation model. *Journal of Hydrology*, **286**, 249-270.
- Gerten, D., Heinke, J., Hoff, H., Biemans, H., Fader, M. & Waha, K. (2011) Global water availability and requirements for future food production. *Journal of Hydrometeorology*.
- Gill, G. J. (1991) *Seasonality and agriculture in the developing world: a problem of the poor and powerless*, pp 343. Cambridge University Press, Cambridge.
- Godfray, H.C.J., Crute, I.R., Haddad, L., Lawrence, D., Muir, J.F., Nisbett, N., Pretty, J., Robinson, S., Toulmin, C. & Whiteley, R. (2010) The future of the global food system. *Philosophical Transactions of the Royal Society B: Biological Sciences*, **365**, 2769-2777.
- Gomez-Macpherson, H. & Richards, R.A. (1995) Effect of sowing time on yield and agronomic characteristics of wheat in south-eastern Australia. *Australian Journal of Agricultural Research*, **46**, 1381-1399.
- Goudriaan, J. & Monteith, J.L. (1990) A mathematical function for crop growth based on light interception and leaf area expansion. *Annals of Botany*, **66**, 695-701.
- Goudriaan, J. & Van Laar, H. H. (1994) *Modelling potential crop growth processes: textbook with exercises*. Kluwer, Dordrecht.
- Gouesnard, B., Rebourg, C., Welcker, C. & Charcosset, A. (2002) Analysis of photoperiod sensitivity within a collection of tropical maize populations. *Genetic Resources and Crop Evolution*, **49**, 471-481.
- Government Office for Science. (2011) *The future of food and farming: Challenges and choices for global sustainability report*. Available at: <http://www.bis.gov.uk/assets/bispartners/foresight/docs/food-and-farming/11-546-future-of-food-and-farming-report> (accessed 5 June 2011).
- Grubben, G.J.H. & Partohardjono, S. (1996) *Plant resources of South-East Asia: cereals*. Backhuys, Leiden.
- Hammer, G.L., Kropff, M.J., Sinclair, T.R. & Porter, J.R. (2002) Future contributions of crop modelling – from heuristics and supporting decision making to understanding genetic regulation and aiding crop improvement. *European Journal of Agronomy*, **18**, 15-31.
- Hansen, J.W. & Jones, J.W. (2000) Scaling-up crop models for climate variability applications. *Agricultural Systems*, **65**, 43-72.
- Hansen, J.W. & Ines, A.V.M. (2005) Stochastic disaggregation of monthly rainfall data for crop simulation studies. *Agricultural and Forest Meteorology*, **131**, 233-246.
- Hansen, J.W., Challinor, A., Ines, A., Wheeler, T. & Moron, V. (2006) Translating climate forecasts into agricultural terms: advances and challenges. *Climate Research*, **33**, 27-41.
- Harrison, P.A., Porter, J.R. & Downing, T.E. (2000) Scaling-up the AFRCWHEAT2 model to assess phenological development for wheat in Europe. *Agricultural and Forest Meteorology*, **101**, 167-186.
- Havelka, U.D., Wittenback, V.A. & Boyle, M.G. (1984) CO<sub>2</sub>-Enrichment Effects on Wheat Yield and Physiology. *Crop Science Society of America*, **24**, 1163-1168.
- Haxeltine, A. & Prentice, C.I. (1996a) A general model for the light-use efficiency of primary production. *Functional Ecology*, **10**, 551-561.
- Haxeltine, A. & Prentice, I.C. (1996b) BIOME3: An equilibrium terrestrial biosphere model based on ecophysiological constraints, resource availability, and competition among plant functional types. *Global Biogeochemical Cycles*, **10**, 693-709.

- Hay, R.K.M. & Kirby, E.J.M. (1991) Convergence and synchrony-a review of the coordination of development in wheat. *Australian Journal of Agricultural Research*, **42**, 661-700.
- Hay, R.K.M. & Porter, J.R. (2006) *The physiology of crop yield*, pp XIII, 314 p. Blackwell, Oxford.
- Heath, O.V.S. & Gregory, F.G. (1938) The constancy of the mean net assimilation rate and its ecological importance. *Annals of Botany*, **2**, 811-818.
- Hengsdijk, H. & Langeveld, J.W.A. (2009) *Yield trends and yield gap analysis of major crops in the world*. Wettelijke Onderzoekstaken Natuur & Milieu, Wageningen.
- Hillocks, R.J. & Thresh, J.M. (2002) *Cassava: biology, production and utilization*, pp XI, 332. CABI, Wallingford.
- Hirabayashi, Y., Kanae, S., Motoya, K., Masuda, K. & Döll, P. (2008) A 59-year (1948-2006) global near-surface meteorological data set for land surface models. Part I: development of daily forcing and assessment of precipitation intensity. *Hydrological Research Letters*, **2**, 36-40.
- Hulme, M. (1992) Rainfall changes in Africa: 1931-1960 to 1961-1990. *International Journal of Climatology*, **12**, 685-699.
- Irmak, A., Jones, J.W. & Jagtap, S.S. (2005) Evaluation of the CROPGRO-soybean model for assessing climate impacts on regional soybean yields. *Transactions of the ASAE*, **48**, 2343-2353.
- Iwaki, K., Haruna, S., Niwa, T. & Kato, K. (2001) Adaptation and ecological differentiation in wheat with special reference to geographical variation of growth habit and Vrn genotype. *Plant Breeding*, **120**, 107-114.
- Jackson, I.J. (1989) *Climate, water and agriculture in the tropics*, pp 377. 2nd edn. Longman, Harlow.
- Jacob, D., Bärring, L., Christensen, O., Christensen, J., de Castro, M., Déqué, M., Giorgi, F., Hagemann, S., Hirschi, M., Jones, R., Kjellström, E., Lenderink, G., Rockel, B., Sánchez, E., Schär, C., Seneviratne, S., Somot, S., van Ulden, A. & van den Hurk, B. (2007) An inter-comparison of regional climate models for Europe: model performance in present-day climate. *Climatic Change*, **81**, 31-52.
- Jaggard, K.W. & Qi, A. (2006) *Agronomy. Sugar beet* (ed. by Draycott, A.P.), pp 134-168. Blackwell, Oxford.
- Jagtap, S.S. & Jones, J.W. (2002) Adaptation and evaluation of the CROPGRO-soybean model to predict regional yield and production. *Agriculture, Ecosystems and Environment*, **93**, 73-85.
- Jamieson, P.D., Porter, J.R., Goudriaan, J., Ritchie, J.T., Van Keulen, H. & Stol, W. (1998a) A comparison of the models AFRCWHEAT2, CERES-Wheat, Sirius, SUCROS2 and SWHEAT with measurements from wheat grown under drought. *Field Crops Research*, **55**, 23-44.
- Jamieson, P.D., Brooking, I.R., Semenov, M.A. & Porter, J.R. (1998b) Making sense of wheat development: a critique of methodology. *Field Crops Research*, **55**, 117-127.
- Jamieson, P.D., Brooking, I.R., Semenov, M.A., McMaster, G.S., White, J.W. & Porter, J.R. (2007) Reconciling alternative models of phenological development in winter wheat. *Field Crops Research*, **103**, 36-41.
- Jones, C.A., Kiniry, J.R., Dyke, P.T., Farmer, D.B. & Godwin, D. C. (1986) *CERES-maize: a simulation model of maize growth and development*. Texas A&M University Press, College Station.
- Kamkar, B., Koocheki, A., Nassiri Mahallati, M. & Rezvani Moghaddam, P. (2006) Cardinal temperatures for germination in three millet species (*Panicum miliaceum*, *Pennisetum glaucum* and *Setaria italica*). *Asian Journal of Plant Sciences*, **5**, 316-319.
- Kato, K. & Yokoyama, H. (1992) Geographical variation in heading characters among wheat landraces, *Triticum aestivum* L., and its implication for their adaptability. *Theoretical and Applied Genetics*, **84**, 259-265.
- Keating, B.A. & Evenson, J.P. (1979) Effect of soil temperature on sprouting and sprout elongation of stem cuttings of cassava (*Manihot esculenta* Crantz.). *Field Crops Research*, **2**, 241-251.
- Kemanian, A.R., Stöckle, C.O., Huggins, D.R. & Viegas, L.M. (2007) A simple method to estimate harvest index in grain crops. *Field Crops Research*, **103**, 208-216.

- Keys, E. & McConnell, W.J. (2005) Global change and the intensification of agriculture in the tropics. *Global Environmental Change Part A*, **15**, 320-337.
- Khah, E.M., Ellis, R.H. & Roberts, E.H. (1986) Effects of laboratory germination, soil temperature and moisture content on the emergence of spring wheat. *The Journal of Agricultural Science*, **107**, 431-438.
- Khalifa, F.M., Schneiter, A.A. & Eltayeb, E.I. (2000) Temperature-germination response of sunflower (*Helianthus annuus* L.) genotypes. *Helia*, **23**, 97-104.
- Kimball, B.A., Pinter, J., P.J., Garcia, R.L., LaMorte, R.L., Wall, G.W., Hunsaker, D.J., Wechsung, G., Wechsung, F. & Kartschall, T. (1995) Productivity and water use of wheat under free-air CO<sub>2</sub> enrichment. *Global Change Biology*, **1**, 429-442.
- Kimball, B.A., LaMorte, R.L., Pinter Jr, P.J., Wall, G.W., Hunsaker, D.J., Adamsen, F.J., Leavitt, S.W., Thompson, T.L., Matthias, A.D. & Brooks, T.J. (1999) Free-air CO<sub>2</sub> enrichment and soil nitrogen effects on energy balance and evapotranspiration of wheat. *Water Resources Research*, **35**, 1179-1190.
- Kiniry, J.R., Major, D.J., Izaurralde, R.C., Williams, J.R., Gassman, P.W., Morrison, M., Bergentine, R. & Zentner, R.P. (1995) EPIC model parameters for cereal, oilseed, and forage crops in the northern Great-Plains Region. *Canadian Journal of Plant Science*, **75**, 679-688.
- Kirby, E.J.M., Porter, J.R., Day, W., Adam, J.S., Appleyard, M., Ayling, S., Baker, C.K., Belford, R.K., Biscoe, P.V., Chapman, A., Fuller, M.P., Hampson, J., Hay, R.K.M., Matthews, S., Thompson, W.J., Weir, A.H., Willington, V.B.A. & Wood, D.W. (1987) An analysis of primordium initiation in Avalon winter wheat crops with different sowing dates and at nine sites in England and Scotland. *The Journal of Agricultural Science*, **109**, 123-134.
- Koning, N. & Van Ittersum, M.K. (2009) Will the world have enough to eat? *Current Opinion in Environmental Sustainability*, **1**, 77-82.
- Kouressy, M., Dingkuhn, M., Vaksman, M. & Heinemann, A.B. (2008) Adaptation to diverse semi-arid environments of sorghum genotypes having different plant type and sensitivity to photoperiod. *Agricultural and Forest Meteorology*, **148**, 357-371.
- Kucharik, C.J. (2006) A multidecadal trend of earlier corn planting in the central USA. *Agronomy Journal*, **98**, 1544-1550.
- Landau, S., Mitchell, R.A.C., Barnett, V., Colls, J.J., Craigon, J., Moore, K.L. & Payne, R.W. (1998) Testing winter wheat simulation models' predictions against observed UK grain yields. *Agricultural and Forest Meteorology*, **89**, 85-99.
- Larcher, W. (1995) *Physiological plant ecology*, pp 506. 3rd edn. Springer-Verlag, Berlin, Heidelberg.
- Leemans, R. (1997) Effects of global change on agricultural land use: scaling up from physiological processes to ecosystem dynamics. *Ecology in Agriculture* (ed. by Jackson, L.E.), pp 415-452. Academic Press, San Diego.
- Leffelaar, P.A. (1990) On scale problems in modelling: an example from soil ecology. *Theoretical production ecology: reflections and prospects* (ed. by Rabbinge, R. & Goudriaan, J. & Van Keulen, H. & Penning de Vries, F.W.T. & Van Laar, H.H.), pp 57-73. Pudoc, Wageningen.
- Lieth, H. (1974) *Phenology and seasonality modeling*. Heidelberg.
- Liu, J., Williams, J.R., Zehnder, A.J. B. & Yang, H. (2007) GEPIC – modelling wheat yield and crop water productivity with high resolution on a global scale. *Agricultural Systems*, **94**, 478-493.
- Liu, J., Williams, J.R., Wang, X. & Yang, H. (2009) Using MODAWEC to generate daily weather data for the EPIC model. *Environmental Modelling & Software*, **24**, 655-664.
- LLNL. (1989) Program for climate model diagnosis and intercomparison. <http://www-pcmdi.llnl.gov>
- Lobell, D.B., Schlenker, W. & Costa-Roberts, J. (2011) Climate Trends and Global Crop Production Since 1980. *Science*.
- Long, S.P., Ainsworth, E.A., Leakey, A.D.B., Nosberger, J. & Ort, D.R. (2006) Food for thought: lower-than-expected crop yield stimulation with rising CO<sub>2</sub> concentrations. *Science*, **312**, 1918-1921.

- Long, S.P. & Ort, D.R. (2010) More than taking the heat: crops and global change. *Current Opinion in Plant Biology*, **13**, 240-247.
- Luyten, J.C. (1995) *Sustainable world food production and environment*. AB-DLO, Wageningen.
- Mahfoozi, S., Limin, A.E. & Fowler, D.B. (2001) Influence of Vernalization and Photoperiod Responses on Cold Hardiness in Winter Cereals. *Crop Science*, **41**, 1006-1011.
- Masle, J., Doussinault, G., Farquhar, G.D. & Sun, B. (1989) Foliar stage in wheat correlates better to photothermal time than to thermal time. *Plant, Cell and Environment*, **12**, 235-247.
- Mayer, D.G. & Butler, D.G. (1993) Statistical validation. *Ecological Modelling*, **68**, 21-32.
- McGregor, G.R. & Nieuwolt, S. (1998) *Tropical climatology: an introduction to the climates of the low latitudes*. 2nd edn. Wiley, Chichester.
- McGuire, A.D., Sitch, S., Clein, J.S., Dargaville, R., Esser, G., Foley, J., Heimann, M., Joos, F., Kaplan, J., Kicklighter, D.W., Meier, R.A., Melillo, J.M., Moore, B., III, Prentice, I.C., Ramankutty, N., Reichenau, T., Schloss, A., Tian, H., Williams, L.J. & Wittenberg, U. (2001) Carbon balance of the terrestrial biosphere in the Twentieth Century: Analyses of CO<sub>2</sub>, climate and land use effects with four process-based ecosystem models. *Global Biogeochemical Cycles*, **15**, 183-206.
- Mearns, L.O., Easterling, W.E., Hays, C.J. & Marx, D. (2001) Comparison of agricultural impacts of climate change calculated from high and low resolution climate change scenarios: Part II. Accounting for adaptation and CO<sub>2</sub> direct effects. *Climatic Change*, **51**, 173-197.
- Medlyn, B.E. (1998) Physiological basis of the light use efficiency model. *Tree Physiology*, **18**, 167-176.
- Meinke, H., Hammer, G.L., Van Keulen, H., Rabbinge, R. & Keating, B.A. (1997) Improving wheat simulation capabilities in Australia from a cropping systems perspective: water and nitrogen effects on spring wheat in a semi-arid environment. *European Journal of Agronomy*, **7**, 75-88.
- Menzel, A., Sparks, T.H., Estrella, N., Koch, E., Aaasa, A., Ahas, R., Alm-Kübler, K., Bissolli, P., Braslavská, O., Briede, A., Chmielewski, F.-M., Crepinsek, Z., Curnel, Y., Dahl, Å., Defila, C., Donnelly, A., Filella, Y., Jatczak, K., Måge, F., Mestre, A., Nordli, Ø., Peñuelas, J., Pirinen, P., Remišová, V., Scheifinger, H., Striz, M., Susnik, A., Van Vliet, A.J.H., Wielgolaski, F.E., Zach, S. & Züst, A. (2006) European phenological response to climate change matches the warming pattern. *Global Change Biology*, **12**, 1969-1976.
- Metzger, M.J., Bunce, R.G.H., Jongman, R.H.G., Mächer, C.A. & Watkins, J.W. (2005) A climatic stratification of the environment of Europe. *Global Ecology and Biogeography*, **14**, 549-563.
- Mi, G., Tang, L., Zhang, F. & Zhang, J. (2000) Is nitrogen uptake after anthesis in wheat regulated by sink size? *Field Crops Research*, **68**, 183-190.
- Miralles, D.J. & Slafer, G.A. (1999) Wheat development. *Wheat ecology and physiology of yield determination* (ed. by Satorre, E.H. & Slafer, G.A.), pp 13-43. Food Products Press, New York, NY.
- Miralles, D.J., Spinedi, M.V., Abeledo, L.G. & Abelleira, D. (2007) Variability on photoperiod responses in Argentinean wheat cultivars differing in length of crop cycle. *Wheat production in stressed environments* (ed. by Buck, H.T. & Nisi, J.E. & Salomón, N.), pp 599-609. Springer Netherlands.
- Mitchell, R., Manderscheid, R., Fereres, E., Rodriguez, D., Ewert, F., Semenov, M., Burkart, S., Goudriaan, J., Schütz, M., Fangmeier, A., Jamieson, P., Porter, J., Richter, G., Ruz, C., Gómez, H., Testi, L., Villalobos, F. & Weigel, H. (2000) *IMPETUS Final Report: Improving wheat model accuracy and suitability for regional impact assessment*, pp 150. EC project ENV4-CT97-0496.
- Mitchell, R.A.C., Mitchell, V.J., Driscoll, S.P., Franklin, J. & Lawlor, D.W. (1993) Effects of increased CO<sub>2</sub> concentration and temperature on growth and yield of winter wheat at two levels of nitrogen application. *Plant, Cell and Environment*, **16**, 521-529.
- Mitchell, T.D. & Jones, P.D. (2005) An improved method of constructing a database of monthly climate observations and associated high-resolution grids. *International Journal of Climatology*, **25**, 693-712.
- MNP (2006) *Integrated modelling of global environmental change. An overview of IMAGE 2.4.*, pp 228. Netherlands Environmental Assessment Agency (MNP), Bilthoven, the Netherlands.

- Mohamed, H.A., Clark, J.A. & Ong, C.K. (1988) Genotypic differences in the temperature responses of tropical crops 1. germination characteristics of ground nut (*Arachis Hypogaea* L.) and pearl millet (*Pennisetum Typhoides* S. & H.) *Journal of Experimental Botany*, **39**, 1121-1128.
- Monfreda, C., Ramankutty, N. & Foley, J.A. (2008) Farming the planet: 2. geographic distribution of crop areas, yields, physiological types, and net primary production in the year 2000. *Global Biogeochemical Cycles*, **22**.
- Monteith, J.L. (1977) Climate and efficiency of crop production in Britain. *Philosophical Transactions of the Royal Society B: Biological Sciences*, **281**, 277-294.
- Monteith, J.L. & Unsworth, M.H. (1990) *Principles of environmental physics*, pp XII, 291. Arnold, London.
- Monteith, J.L. (2000) Agricultural meteorology: evolution and application. *Agricultural and Forest Meteorology*, **103**, 5-9.
- Moriondo, M., Bindi, M., Kundzewicz, Z. W., Szwed, M., Chorynski, A., Matczak, P., Radziejewski, M., McEvoy, D. & Wreford, A. (2010) Impact and adaptation opportunities for European agriculture in response to climatic change and variability. *Mitigation and Adaptation Strategies for Global Change*, **15**, 657-679.
- Mortimore, M.J., Singh, B.B., Harris, F. & Blade, S.F. (1997) Cowpea in traditional cropping systems. *Advances in cowpea research* (ed. by Singh, B.B. & Mohan Raj, D.R. & Dashiell, K.E.), pp 99-113. IITA and JIRCAS, Ibadan.
- Neitsch, S.L., Arnold, J.G., Kiniry, J.R., Srinivasan, R. & Williams, J.R. (2002) Soil and water assessment tool user's manual, version 2000. pp 412. USDA-ARS-SR Grassland, Soil and Water Research Laboratory, Agricultural Research Service, Temple, Texas, US.
- Neitsch, S.L., Arnold, J.G., Kiniry, J.R. & Williams, J.R. (2005) Soil and water assessment tool theoretical documentation, version 2005. pp 494. USDA-ARS-SR Grassland, Soil and Water Research Laboratory, Agricultural Research Service, Temple, Texas, US.
- Neumann, K., Verburg, P.H., Stehfest, E. & Müller, C. (2010) The yield gap of global grain production: A spatial analysis. *Agricultural Systems*, **103**, 316-326.
- New, M., Hulme, M. & Jones, P. (1999) Representing twentieth-century space-time climate variability. Part I: development of a 1961-90 mean monthly terrestrial climatology. *Journal of Climate*, **12**, 829-856.
- Nonhebel, S. (1994) The effects of use of average instead of daily weather data in crop growth simulation models. *Agricultural Systems*, **44**, 377-396.
- Nonhebel, S. (1996) Effects of temperature rise and increase in CO<sub>2</sub> concentration on simulated wheat yields in Europe. *Climatic Change*, **34**, 73-90.
- Norman, M.J.T., Pearson, C.J. & Searle, P.G.E. (1995) *The ecology of tropical food crops*. Cambridge University Press, Cambridge.
- Nyong, A., Adesina, F. & Osman Elasha, B. (2007) The value of indigenous knowledge in climate change mitigation and adaptation strategies in the African Sahel. *Mitigation and Adaptation Strategies for Global Change*, **12**, 787-797.
- Olesen, J.E., Bocher, P.K. & Jensen, T. (2000) Comparison of scales of climate and soil data for aggregating simulated yields of winter wheat in Denmark. *Agriculture, Ecosystems & Environment*, **82**, 213-228.
- Ortiz Ferrara, G., Mosaad, M.G., Mahalakshmi, V. & Rajaram, S. (1998) Photoperiod and vernalisation response of Mediterranean wheats, and implications for adaptation. *Euphytica*, **100**, 377-384.
- Osborne, T.M., Lawrence, D.M., Challinor, A.J., Slingo, J.M. & Wheeler, T.R. (2007) Development and assessment of a coupled crop-climate model. *Global Change Biology*, **13**, 169-183.
- Palosuo, T., Kersebaum, K.C., Angulo, C., Hlavinka, P., Moriondo, M., Olesen, J.E., Patil, R.H., Ruget, F., Rumbaur, C., Takáč, J., Trnka, M., Bindi, M., Caldag, B., Ewert, F., Ferrise, R., Mirschel, W., Saylan, L., Šiška, B. & Rötter, R. (in press) Simulation of winter wheat yield and its variability in different climates of Europe. A comparison of eight crop growth models. *European Journal of Agronomy*.

- Pan, B., Bai, Y.M., Leibovitch, S. & Smith, D.L. (1999) Plant-growth-promoting rhizobacteria and kinetin as ways to promote corn growth and yield in a short-growing-season area. *European Journal of Agronomy*, **11**, 179-186.
- Parry, M.L., Rosenzweig, C., Iglesias, A., Livermore, M. & Fischer, G. (2004) Effects of climate change on global food production under SRES emissions and socio-economic scenarios. *Global Environmental Change*, **14**, 53-67.
- Passioura, J.B. (1996) Simulation models: science, snake oil, education, or engineering? *Agronomy Journal*, **88**, 690-694.
- Penman, H.L. (1948) Natural evaporation from open water, bare soil and grass. *Proceedings of the Royal Society of London Series A-Mathematical and Physical Sciences*, **193**, 120-146.
- Penning de Vries, F.W.T. (1982) System analysis and models of crop growth. *Simulation of plant growth and crop production* (ed. by Penning de Vries, F.W.T. & van Laar, H.H.), pp 9-19. Pudoc, Wageningen.
- Penning de Vries, F.W.T., Jansen, D.M. & Ten Berge, H.F.M. (1989) *Simulation of ecophysiological processes of growth in several annual crops*. Pudoc, Wageningen.
- Penning de Vries, F.W.T., Rabbinge, R. & Groot, J.J.R. (1997) Potential and attainable food production and food security in different regions. *Philosophical Transactions of the Royal Society B: Biological Sciences*, **352**, 917-928.
- Porter, J.R., Kirby, E.J.M., Day, W., Adam, J.S., Appleyard, M., Ayling, S., Baker, C. K., Beale, P., Belford, R.K., Biscoe, P.V., Chapman, A., Fuller, M.P., Hampson, J., Hay, R.K.M., Hough, M.N., Matthews, S., Thompson, W.J., Weir, A.H., Willington, V.B.A. & Wood, D.W. (1987) An analysis of morphological development stages in Avalon winter wheat crops with different sowing dates and at ten sites in England and Scotland. *The Journal of Agricultural Science*, **109**, 107-121.
- Porter, J.R. (1993) AFRCWHEAT2: a model of the growth and development of wheat incorporating responses to water and nitrogen. *European Journal of Agronomy*, **2**, 69-82.
- Porter, J.R., Jamieson, P.D. & Wilson, D.R. (1993) Comparison of the wheat simulation models AFRCWHEAT2, Ceres-Wheat and SWheat for non-limiting conditions of crop growth. *Field Crops Research*, **33**, 131-157.
- Porter, J.R. & Gawith, M. (1999) Temperatures and the growth and development of wheat: a review. *European Journal of Agronomy*, **10**, 23-36.
- Porter, J.R. & Semenov, M.A. (2005) Crop responses to climatic variation. *Philosophical Transactions: Biological Sciences*, **360**, 2021-2035.
- Portmann, F., Siebert, S., Bauer, C. & Döll, P. (2008) *Global dataset of monthly growing areas of 26 irrigated crops*. Institute of Physical Geography, University of Frankfurt, Frankfurt am Main.
- Portmann, F.T., Siebert, S. & Doll, P. (2010) MIRCA2000-Global monthly irrigated and rainfed crop areas around the year 2000: a new high-resolution data set for agricultural and hydrological modeling. *Global Biogeochemical Cycles*, **24**, GB1011.
- Prasad, P.V.V., Boote, K.J., Thomas, J.M.G., Allen Jr, L.H. & Gorbett, D.W. (2006) Influence of soil temperature on seedling emergence and early growth of peanut cultivars in field conditions. *Journal of Agronomy and Crop Science*, **192**, 168-177.
- Priestley, C.H.B. & Taylor, R.J. (1972) Assessment of surface heat-flux and evaporation using large-scale parameters. *Monthly Weather Review*, **100**, 81-92.
- Ramankutty, N., Evan, A.T., Monfreda, C. & Foley, J.A. (2008) Farming the planet: 1. geographic distribution of global agricultural lands in the year 2000. *Global Biogeochemical Cycles*, **22**, GB1003.
- Raven, P.H., Evert, R.F. & Eichhorn, S.E. (2005) *Biology of plants*. Freeman, New York, NY.
- Rehm, S. & Espig, G. (1991) *The cultivated plants of the tropics and subtropics: cultivation, economic value, utilization*. CTA, Margraf, Weikersheim
- Reidsma, P., Ewert, F., Boogaard, H. & Van Diepen, K. (2009) Regional crop modelling in Europe: the impact of climatic conditions and farm characteristics on maize yields. *Agricultural Systems*, **100**, 51-60.

- Reidsma, P., Ewert, F., Lansink, A.O. & Leemans, R. (2010) Adaptation to climate change and climate variability in European agriculture: The importance of farm level responses. *European Journal of Agronomy*, **32**, 91-102.
- Reyenga, P.J., Howden, S.M., Meinke, H. & McKeon, G.M. (1999) Modelling global change impacts on wheat cropping in south-east Queensland, Australia. *Environmental Modelling & Software*, **14**, 297-306.
- Rinaldi, M. & Vonella, A.V. (2006) The response of autumn and spring sown sugar beet (*Beta vulgaris* L.) to irrigation in southern Italy: water and radiation use efficiency. *Field Crops Research*, **95**, 103-114.
- Ritchie, J.T. & Otter, S. (1985) Description and performance of CERES-Wheat: a user-oriented wheat yield model. *US Department of Agriculture 38, ARS (1985)* (ed. by Ritchie, J.T. & Otter, S.), pp 159-175.
- Robertson, M.J., Holland, J.F. & Bambach, R. (2009) Canola residues do not reduce establishment, growth, and yield of following summer crops. *Crop and Pasture Science*, **60**, 640-645.
- Rodriguez, D., Ewert, F., Goudriaan, J., Manderscheid, R., Burkart, S. & Weigel, H.J. (2001) Modelling the response of wheat canopy assimilation to atmospheric CO<sub>2</sub> concentrations. *New Phytologist*, **150**, 337-346.
- Rood, S.B. & Major, D.J. (1980) Responses of early corn inbreds to photoperiod. *Crop Science*, **20**, 679-682.
- Rosenzweig, C. & Parry, M.L. (1994) Potential impact of climate change on world food supply. *Nature*, **367**, 133-138.
- Rötzer, T. & Chmielewski, F.-M. (2001) Phenological maps of Europe. *Climate Research*, **18**, 249-257.
- Russell, G. & Wilson, G.W. (1994) *An agro-pedo-climatological knowledge-base of wheat in Europe*, pp 158. Office for Official Publications of the European Communities, Luxembourg.
- Sacks, W.J., Deryng, D., Foley, J.A. & Ramankutty, N. (2010) Crop planting dates: an analysis of global patterns. *Global Ecology and Biogeography*, **19**, 607-620.
- Sacks, W.J. & Kucharik, C.J. (2011) Crop management and phenology trends in the U.S. Corn Belt: Impacts on yields, evapotranspiration and energy balance. *Agricultural and Forest Meteorology*, **151**, 882-894.
- Sadras, V.O., Reynolds, M.P., de la Vega, A.J., Petrie, P.R. & Robinson, R. (2009) Phenotypic plasticity of yield and phenology in wheat, sunflower and grapevine. *Field Crops Research*, **110**, 242-250.
- Saini, H.S. & Aspinall, D. (1982) Abnormal sporogenesis in wheat (*Triticum aestivum* L.) induced by short periods of high temperature. *Annals of Botany*, **49**, 835-846.
- Salinger, M., Sivakumar, M.V.K. & Motha, R. (2005) Reducing vulnerability of agriculture and forestry to climate variability and change: workshop summary and recommendations. *Climatic Change*, **70**, 341-362.
- Schnyder, H. (1993) The Role of Carbohydrate Storage and Redistribution in the Source-Sink Relations of Wheat and Barley During Grain Filling-a Review. *New Phytologist*, **123**, 233-245.
- Scholten, H. (2008) Better modelling practice: an ontological perspective on multidisciplinary, model-based problem solving. pp 314. Wageningen University, Wageningen.
- Semenov, M.A. & Porter, J.R. (1995) Climatic variability and the modelling of crop yields. *Agricultural and Forest Meteorology*, **73**, 265-283.
- Semenov, M.A. (2009) Impacts of climate change on wheat in England and Wales. *Journal of the Royal Society Interface*, **6**, 343-350.
- Sharma, D.L., D'Antuono, M.F., Anderson, W.K., Shackley, B.J., Zaicou-Kunesch, C.M. & Amjad, M. (2008) Variability of optimum sowing time for wheat yield in Western Australia. *Australian Journal of Agricultural Research*, **59**, 958-970.
- Sheffield, J., Goteti, G. & Wood, E.F. (2006) Development of a 50-year high-resolution global dataset of meteorological forcings for land surface modeling. *Journal of Climate*, **19**, 3088-3111.



- Siebert, S. & Döll, P. (2008) *The Global Crop Water Model (GCWM): documentation and first results for irrigated crops*, pp 42. Institute of Physical Geography, University of Frankfurt, Frankfurt am Main.
- Sinclair, T.R. & Muchow, R.C. (1999) Radiation use efficiency. *Advances in Agronomy*, **65**, 215-265.
- Sitch, S., Smith, B., Prentice, I.C., Arneth, A., Bondeau, A., Cramer, W., Kaplan, J. O., Levis, S., Lucht, W., Sykes, M.T., Thonicke, K. & Venevsky, S. (2003) Evaluation of ecosystem dynamics, plant geography and terrestrial carbon cycling in the LPJ dynamic global vegetation model. *Global Change Biology*, **9**, 161-185.
- Slafer, G.A. & Rawson, H.M. (1994) Sensitivity of wheat phasic development to major environmental factors: a re-examination of some assumptions made by physiologists and modellers. *Functional Plant Biology*, **21**, 393-426.
- Slafer, G.A. & Whitechurch, E.M. (2001) Manipulating wheat development to improve adaptation. *Application of physiology in wheat breeding* (ed. by Reynolds, M.P. & Ortiz - Monasterio, J.I. & MacNab, A.), pp 160-170. CIMMYT, Mexico.
- Soltani, A., Meinke, H. & De Voil, P. (2004) Assessing linear interpolation to generate daily radiation and temperature data for use in crop simulations. *European Journal of Agronomy*, **21**, 133-148.
- Soussana, J.-F., Graux, A.-I. & Tubiello, F.N. (2010) Improving the use of modelling for projections of climate change impacts on crops and pastures. *Journal of Experimental Botany*, **61**, 2217-2228.
- Spitters, C.J.T. (1990) Crop growth models: Their usefulness and limitations. *Acta Hort.*, **267**, 349-368.
- Spitters, C.J.T. & Schapendonk, A. (1990) Evaluation of breeding strategies for drought tolerance in potato by means of crop growth simulation. *Plant and Soil*, **123**, 193-203.
- Steele, W.M. & Mehra, K.L. (1980) Structure, evolution and adaptation to farming systems and environments in *Vigna*. *Advances in legume science, Proceedings of the International Legume Conference* (ed. by Summerfield, R.J. & Bunting, A.H.), pp 393-404. Royal Botanic Gardens, Kew.
- Stehfest, E., Heistermann, M., Priess, J.A., Ojima, D.S. & Alcamo, J. (2007) Simulation of global crop production with the ecosystem model DayCent. *Ecological Modelling*, **209**, 203-219.
- Stephens, D.J. & Lyons, T.J. (1998) Variability and trends in sowing dates across the Australian wheat belt. *Australian Journal of Agricultural Research*, **49**, 1111-1118.
- Stöckle, C.O., Donatelli, M. & Nelson, R. (2003) CropSyst, a cropping systems simulation model. *European Journal of Agronomy*, **18**, 289-307.
- Stöckle, C.O. & Kemanian, A.R. (2009) Crop radiation capture and use efficiency: A framework for crop growth analysis, crop physiology. *Crop physiology: applications for genetic improvement and agronomy* (ed. by Sadras, V. & Calderini, D.), pp 145-170. Academic Press, San Diego.
- Summerfield, R.J., Ellis, R.H., Craufurd, P.Q., Aiming, Q., Roberts, E.H. & Wheeler, T.R. (1997) Environmental and genetic regulation of flowering of tropical annual crops. *Euphytica*, **96**, 83-91.
- Tan, G. & Shibasaki, R. (2003) Global estimation of crop productivity and the impacts of global warming by GIS and EPIC integration. *Ecological Modelling*, **168**, 357-370.
- Tanner, J.W. & Hume, D.J. (1978) Management and production. *Soybean physiology, agronomy and utilization* (ed. by Norman, A.G.), pp 157-217. Academic Press, New York, NY.
- Tao, F., Yokozawa, M. & Zhang, Z. (2009) Modelling the impacts of weather and climate variability on crop productivity over a large area: a new process-based model development, optimization, and uncertainties analysis. *Agricultural and Forest Meteorology*, **149**, 831-850.
- Tao, F. & Zhang, Z. (2011) Impacts of climate change as a function of global mean temperature: Maize productivity and water use in China. *Climatic Change*, **105**, 409-432.

- Teixeira, E., Fischer, G., Ewert, F., Van Velthuisen, H., Challinor, A. & Walter, C. (2010) Hot-spots of heat-stress damage for rice and wheat crops due to climate change. *Conference Proceedings, XI ESA Congress*, Montpellier, France.
- Teixeira, E., Fischer, G., Van Velthuisen, H., Walter, C. & Ewert, F. (under review) Global hot-spots of heat stress on agricultural crops due to climate change. ?
- Therond, O., Hengsdijk, H., Casellas, E., Wallach, D., Adam, M., Belhouchette, H., Oomen, R., Russell, G., Ewert, F., Bergez, J.-E., Janssen, S., Wery, J. & Van Ittersum, M.K. (in press) Using a cropping system model at regional scale: Low-data approaches for crop management information and model calibration. *Agriculture, Ecosystems & Environment*.
- Thomson, B.D., Siddique, K.H.M., Barr, M.D. & Wilson, J.M. (1997) Grain legume species in low rainfall mediterranean-type environments I. Phenology and seed yield. *Field Crops Research*, **54**, 173-187.
- Thornley, J.H.M. & France, J. (2007) *Mathematical models in agriculture: quantitative methods for the plant, animal and ecological sciences*, pp xvii, 906. CABI, Wallingford, Oxfordshire.
- Thornthwaite, C.W. (1948) An approach toward a rational classification of climate. *Geographical Review*, **38**, 55-94.
- Timsina, J. & Connor, D. J. (2001) Productivity and management of rice-wheat cropping systems: issues and challenges. *Field Crops Research*, **69**, 93-132.
- Tittonell, P.A. (2008) Msimu wa Kupanda: targeting resources within diverse, heterogenous and dynamic farming systems of East Africa. pp 320. Wageningen University, Wageningen.
- Torriani, D.S., Calanca, P., Schmid, S., Beniston, M. & Fuhrer, J. (2007) Potential effects of changes in mean climate and climate variability on the yield of winter and spring crops in Switzerland. *Climate Research*, **34**, 59-69.
- Trethowan, R., Morgunov, A., He, Z., De Pauw, R., Crossa, J., Warburton, M., Baytasov, A., Zhang, C., Mergoum, M. & Alvarado, G. (2006) The global adaptation of bread wheat at high latitudes. *Euphytica*, **152**, 303-316.
- Trnka, M., Olesen, J. E., Kersebaum, K.C., Skjelvåg, A.O., Eitzinger, J., Seguin, B., Peltonen-Sainio, P., Rötter, R., Iglesias, A.N.A., Orlandini, S., Dubrovský, M., Hlavinka, P., Balek, J., Eckersten, H., Cloppet, E., Calanca, P., Gobin, A., Vučetić, V., Nejedlik, P., Kumar, S., Lalic, B., Mestre, A., Rossi, F., Kozyra, J., Alexandrov, V., Semerádová, D. & Žalud, Z. (2011) Agroclimatic conditions in Europe under climate change. *Global Change Biology*, **17**, 2298-2318.
- Tubiello, F.N., Donatelli, M., Rosenzweig, C. & Stöckle, C.O. (2000) Effects of climate change and elevated CO<sub>2</sub> on cropping systems: model predictions at two Italian locations. *European Journal of Agronomy*, **13**, 179-189.
- Tubiello, F. N. & Ewert, F. (2002) Simulating the effects of elevated CO<sub>2</sub> on crops: approaches and applications for climate change. *European Journal of Agronomy*, **18**, 57-74.
- Tubiello, F. N., Amthor, J. S., Boote, K. J., Donatelli, M., Easterling, W., Fischer, G., Gifford, R. M., Howden, M., Reilly, J. & Rosenzweig, C. (2007) Crop response to elevated CO<sub>2</sub> and world food supply - a comment on "Food for Thought..." by Long et al., Science 312: 1918-1921, 2006. *European Journal of Agronomy*, **26**, 215-223.
- Tubiello, F. N. & Fischer, G. (2007) Reducing climate change impacts on agriculture: global and regional effects of mitigation, 2000-2080. *Technological Forecasting and Social Change*, **74**, 1030-1056.
- USDA (1994) *Major world crop areas and climatic profiles*, pp 293. U.S. Department of Agriculture, Washington.
- Van Bussel, L.G.J., Ewert, F. & Leffelaar, P.A. (in press) Effects of data aggregation on simulations of crop phenology. *Agriculture, Ecosystems & Environment*.
- Van Delden, A., Kropff, M.J. & Haverkort, A.J. (2001) Modeling temperature- and radiation-driven leaf area expansion in the contrasting crops potato and wheat. *Field Crops Research*, **72**, 119-141.
- Van Delden, H., Van Vliet, J., Rutledge, D. T. & Kirkby, M.J. (in press) Comparison of scale and scaling issues in integrated land-use models for policy support. *Agriculture, Ecosystems & Environment*.

- Van Ittersum, M.K. & Rabbinge, R. (1997) Concepts in production ecology for analysis and quantification of agricultural input-output combinations. *Field Crops Research*, **52**, 197-208.
- Van Ittersum, M.K., Leffelaar, P.A., Van Keulen, H., Kropff, M.J., Bastiaans, L. & Goudriaan, J. (2003) On approaches and applications of the Wageningen crop models. *European Journal of Agronomy*, **18**, 201-234.
- Van Ittersum, M.K., Ewert, F., Heckeley, T., Wery, J., Alkan Olsson, J., Andersen, E., Bezlepina, I., Brouwer, F., Donatelli, M., Flichman, G., Olsson, L., Rizzoli, A.E., Van der Wal, T., Wien, J.E. & Wolf, J. (2008) Integrated assessment of agricultural systems – a component-based framework for the European Union (SEAMLESS). *Agricultural Systems*, **96**, 150-165.
- Van Keulen, H. & Seligman, N.G. (1987) *Simulation of water use, nitrogen nutrition and growth of a spring wheat crop*, pp 310. Pudoc, Wageningen.
- Van Kraalingen, D.W.G., Stol, W., Uithol, P.W. J. & Verbeek, M.G.M. (1991) User manual of CABO/TPE Weather System. *CABO/TPE internal communication*. WAU-TPE, Wageningen.
- Van Oijen, M. & Ewert, F. (1999) The effects of climatic variation in Europe on the yield response of spring wheat cv. Minaret to elevated CO<sub>2</sub> and O<sub>3</sub>: an analysis of open-top chamber experiments by means of two crop growth simulation models. *European Journal of Agronomy*, **10**, 249-264.
- Van Oijen, M. (2002) On the use of specific publication criteria for papers on process-based modelling in plant science. *Field Crops Research*, **74**, 197-205.
- Van Vliet, A.J.H., Overeem, A., De Groot, R. ., Jacobs, A.F.G. & Spijksma, F.T.M. (2002) The influence of temperature and climate change on the timing of pollen release in the Netherlands. *International Journal of Climatology*, **22**, 1757-1767.
- Van Waveren, R. H., Groot, S., Scholten, H., Van Geer, F. C., Wösten, J. H. M., Koeze, R. D. & Noort, J. J. (1999) *Good modelling practice handbook*, pp 149. STOWA/RWS-RIZA, Utrecht/Lelystad.
- Vigil, M.F., Anderson, R.L. & Beard, W.E. (1997) Base temperature and growing-degree-hour requirements for the emergence of canola. *Crop Science*, **37**, 844-849.
- Viña, A., Gitelson, A.A., Rundquist, D.C., Keydan, G., Leavitt, B. & Schepers, J. (2004) Monitoring maize (*Zea mays* L.) phenology with remote sensing. *Agronomy Journal*, **96**, 1139-1147.
- Waha, K., van Bussel, L.G.J., Müller, C. & Bondeau, A. (2011) Climate-driven simulation of global crop sowing dates. *Global Ecology and Biogeography*, in press.
- Walsh, R.P.D. & Lawler, D.M. (1981) Rainfall seasonality: description, spatial patterns and change through time. *Weather*, **36**, 201-208.
- Wang, E. & Engel, T. (1998) Simulation of phenological development of wheat crops. *Agricultural Systems*, **58**, 1-24.
- Wang, S., Carver, B. & Yan, L. (2009) Genetic loci in the photoperiod pathway interactively modulate reproductive development of winter wheat. *Theoretical and Applied Genetics*, **118**, 1339-1349.
- Warrington, I. J. & Kanemasu, E. T. (1983) Corn growth response to temperature and photoperiod I. seedling emergence, tassel initiation, and anthesis. *Agronomy Journal*, **75**, 749-754.
- Wassenaar, T., Lagacherie, P., Legros, J.-P. & Rounsevell, M.D.A. (1999) Modelling wheat yield responses to soil and climate variability at the regional scale. *Climate Research*, **11**, 209-220.
- Watson, D.J. (1947) Comparative physiological studies on the growth of field crops: I. variation in net assimilation rate and leaf area between species and varieties, and within and between years. *Annals of Botany*, **11**, 41-76.
- Webster, R. & Oliver, M. (2001) *Geostatistics for environmental scientists*. Wiley, Chichester.
- Weir, A.H., Bragg, P.L., Porter, J.R. & Rayner, J.H. (1984) A winter wheat crop stimulation model without water or nutrient limitations. *Journal of Agricultural Science*, **102**, 371-382.
- West, J.S., Kharbanda, P.D., Barbetti, M.J. & Fitt, B.D.L. (2001) Epidemiology and management of *Leptosphaeria maculans* (phoma stem canker) on oilseed rape in Australia, Canada and Europe. *Plant Pathology*, **50**, 10-27.

- Wheeler, T.R., Craufurd, P.Q., Ellis, R.H., Porter, J.R. & Vara Prasad, P.V. (2000) Temperature variability and the yield of annual crops. *Agriculture, Ecosystems & Environment*, **82**, 159-167.
- Whigham, D.K. & Minor, H.C. (1978) Agronomic characteristics and environmental stress. *Soybean physiology, agronomy, and utilization* (ed. by Norman, A.G.), pp 77-118. Academic Press, New York, NY.
- Whisler, F.D., Acock, B., Baker, D.N., Fye, R.E., Hodges, H.F., Lambert, J.R., Lemmon, H.E., McKinion, J.M., Reddy, V.R. & Brady, N.C. (1986) Crop Simulation Models in Agronomic Systems. *Advances in Agronomy*, pp 141-208. Academic Press.
- Willmott, C.J. (1982) Some comments on the evaluation of model performance. *Bulletin of the American Meteorological Society*, **63**, 1309-1313.
- Wolf, J., Evans, L.G., Semenov, M.A., Eckersten, H. & Iglesias, A. (1996) Comparison of wheat simulation models under climate change. I. Model calibration and sensitivity analyses. *Climate Research*, **07**, 253-270.
- Woolley, J., Ildefonso, R.L., Portes e Castro, T. D. A. & Voss, J. (1991) Bean cropping systems in the tropics and subtropics and their determinants. *Common beans: research for crop improvement* (ed. by van Schoonhoven, A. & Voysest, O.), pp 679-705. CABI, Wallingford.
- Worland, A.J., Appendino, M.L. & Sayers, E.J. (1994) The distribution, in European winter wheats, of genes that influence ecoclimatic adaptability whilst determining photoperiodic insensitivity and plant height. *Euphytica*, **80**, 219-228.
- Xiao, X., Zhang, J., Yan, H., Wu, W. & Biradar, C. (2009) Land surface phenology: Convergence of satellite and CO<sub>2</sub> eddy flux observations. *Phenology of ecosystem processes: Applications in global change research* (ed. by Noormets, A.). Springer-Verlag New York, New York, NY.
- Yin, X., Schapendonk, A.H.C.M., Kropff, M.J., Van Oijen, M. & Bindraban, P.S. (2000) A generic equation for nitrogen-limited leaf area index and its application in crop growth models for predicting leaf senescence. *Annals of Botany*, **85**, 579-585.
- Yin, X. & van Laar, H.H. (2005) *Crop systems dynamics : an ecophysiological simulation model for genotype-by-environment interactions*. Wageningen Academic, Wageningen.
- Yinong, T., Xiong, L. & Shuren, J. (2001) Present situation and future potential of cassava in China. *Cassava's potential in Asia in the 21st century: present situation and future research and development needs. Proceedings of the sixth regional workshop, held in Ho Chi Minh city, Vietnam, Feb 21-25, 2000* (ed. by Howeler, R.H. & Tan, S.L.), pp 71-83. CIAT, Cali.
- Yonetani, T. & Gordon, H.B. (2001) Simulated changes in the frequency of extremes and regional features of seasonal/annual temperature and precipitation when atmospheric CO<sub>2</sub> is doubled. *Journal of Climate*, **14**, 1765-1779.
- Yoshida, S. (1977) Rice. *Ecophysiology of tropical crops* (ed. by Alvim, P.d.T. & Kozlowski, T.T.). Academic Press, New York, NY.
- Zhang, X., Friedl, M.A. & Schaaf, C.B. (2006) Global vegetation phenology from Moderate Resolution Imaging Spectroradiometer (MODIS): Evaluation of global patterns and comparison with in situ measurements. *Journal of Geophysical Research*, **111**, G04017.



# Appendix A

## 1. Radiation interception

### 1.1. Detailed leaf area index approach

During the juvenile stage or until a certain  $LAI$  threshold ( $LAI_j$ ,  $m^2 m^{-2}$ ), the rate of increase of  $LAI$  is exponential and mainly driven by temperature, through its effect on cell division and extension:

$$\frac{dLAI}{dt} = LAI \times R_g \times T_{eff} \times W_f \quad (\text{Eq. A.3.1})$$

$$T_{eff} = \max(0, [T_{average} - T_{base}]) \quad (\text{Eq. A.3.2})$$

where  $R_g$  ( $(^\circ\text{Cd})^{-1}$ ) is the maximum relative growth rate of  $LAI$ ,  $T_{eff}$  ( $^\circ\text{C}$ ) the effective temperature, calculated as the difference between daily average temperature ( $T_{average}$ ,  $^\circ\text{C}$ ) and a base temperature ( $T_{base}$ ,  $^\circ\text{C}$ ), and  $W_f$  (–) a water stress factor, derived from the ratio between actual and potential transpiration.

Beyond the juvenile stage:

$$\frac{dLAI}{dt} = \frac{dW_l}{dt} \times S_{LA} \times W_f \quad (\text{Eq. A.3.3})$$

where  $dW_l/dt$  ( $\text{g C m}^{-2} \text{d}^{-1}$ ) is the simulated rate of increase in leaf weight and  $S_{LA}$  ( $\text{m}^2 (\text{g C})^{-1}$ ) is a constant specific leaf area of new leaves.

The senescence rate is described by:

$$\frac{dLAI}{dt} = -r_d \times LAI \quad (\text{Eq. A.3.4})$$

with:

$$r_d = \max(R_{d-ag}, R_{d-sh}) \text{ and} \quad (\text{Eq. A.3.5})$$

$$R_{d-sh} = \max\left[0, \min\left(R_{d-shmx}, R_{d-shmx} \times \frac{LAI - LAI_c}{LAI_c}\right)\right] \quad (\text{Eq. A.3.6})$$

where  $R_{d-ag}$  is an exogenously defined relation between temperature and the relative death rate due to ageing (Fig. 3.2), which only takes place after anthesis.

$R_{d-sh}$  is the relative death rate due to shading, where  $LAI_c$  ( $m^2 m^{-2}$ ) is the critical value above which shading only takes place and  $R_{d-shmx}$  ( $d^{-1}$ ), the maximum possible relative senescence rate due to shading.

## 1.2. Summarized leaf area index approach

Before senescence starts, the fraction of an exogenously defined maximum leaf area index ( $fLAI_{max}$ , -) is calculated as:

$$fLAI_{max} = \frac{fT_{sum}}{fT_{sum} + \exp(l_1 - l_2 \times fT_{sum})} \quad (\text{Eq. A.3.7})$$

$$l_1 = \ln\left(\frac{fT_{sum1}}{fLAI_1} - fT_{sum1}\right) + l_2 \times fT_{sum1} \quad (\text{Eq. A.3.8})$$

$$l_2 = \frac{\ln\left[\frac{fT_{sum1}}{fLAI_1} - fT_{sum1}\right] - \ln\left[\frac{fT_{sum2}}{fLAI_2} - fT_{sum2}\right]}{fT_{sum2} - fT_{sum1}} \quad (\text{Eq. A.3.9})$$

where  $fT_{sum}$  (-) is the fraction, on a specific day, of the total temperature sum required to reach maturity (based on the effective temperature), and  $l_1$  (-) and  $l_2$  (-) are shape coefficients, calculated from the fractions of leaf area index ( $fLAI_1$ , -;  $fLAI_2$ , -) and the fractions of the temperature sum ( $fT_{sum1}$ , -;  $fT_{sum2}$ , -) at exogenously defined inflexion points on the leaf area development curve. Following the onset of senescence,  $fLAI_{max}$  is calculated as:

$$fLAI_{max} = \frac{(1 - fT_{sum})^2}{(1 - fT_{sum a})^2} \quad (\text{Eq. A.3.10})$$

where  $fT_{sum a}$  (-) is the fraction of the total temperature sum when senescence starts.

Potential leaf area index ( $LAI_p$ ,  $m^2 m^{-2}$ ) is calculated from an exogenously defined crop-specific maximum leaf area index ( $LAI_{max}$ ,  $m^2 m^{-2}$ ) and  $fLAI_{max}$ :

$$LAI_p = fLAI_{max} \times LAI_{max} \quad (\text{Eq. A.3.11})$$

$LAI_p$  is reduced if the biomass required to support the calculated leaf area index is not available:

$$LAI = \min(LAI_p, [B_t - B_r] \times S_{LA}) \quad (\text{Eq. A.3.12})$$

where  $B_t$  and  $B_r$  ( $\text{g C m}^{-2}$ ) are standing total biomass and standing root biomass, respectively (Bondeau *et al.*, 2007; Neitsch *et al.*, 2005).

To account for water stress, in the pre-anthesis phase a water scaler ( $W_s$ , -) is included to reduce  $LAI_p$ . This water stress scaler is either based on the ratio of actual and potential transpiration (in combination with the radiation use efficiency approach), or (in combination with the Farquhar photosynthesis model) as follows:

$$W_s = \frac{S}{(E_q \times \alpha_{\max}) / (1 + \frac{g_m}{g_p})} \quad (\text{Eq. A.3.13})$$

where  $S$  is water supply (see Eq. A.3.30,  $\text{mm d}^{-1}$ ),  $(E_q \times \alpha_{\max})$  potential evapotranspiration ( $\text{mm d}^{-1}$ ),  $g_m$  a scaling factor ( $\text{mm s}^{-1}$ ), and  $g_p$  potential canopy conductance (see Eq. A.3.29,  $\text{mm s}^{-1}$ ) (Gerten *et al.*, 2004).

## 2. Biomass productivity

### 2.1. Detailed biomass productivity approach

Daily net photosynthesis ( $A_{\text{nd}}$ ,  $\text{g C m}^{-2} \text{d}^{-1}$ ) is calculated as the gradual transition between the light-limited ( $J_e$ ,  $\text{g C m}^{-2} \text{h}^{-1}$ ) and Rubisco-limited ( $J_c$ ,  $\text{g C m}^{-2} \text{h}^{-1}$ ) conditions:

$$A_{\text{nd}} = \left( \frac{J_e + J_c - \sqrt{(J_e + J_c)^2 - 4 \times \theta \times J_e \times J_c}}{2 \times \theta} \right) \times d_l - R_d \quad (\text{Eq. A.3.14})$$

where  $\theta$  is a co-limitation parameter (-),  $d_l$  ( $\text{h d}^{-1}$ ) the day length, and  $R_d$  ( $\text{g C m}^{-2} \text{d}^{-1}$ ) the “dark respiration”, with:

$$J_e = \frac{C_1 \times APAR \times C_q}{d_l} \quad (\text{Eq. A.3.15})$$

$$J_c = \frac{C_2 \times V_m}{24} \quad (\text{Eq. A.3.16})$$

where  $APAR$  ( $\text{MJ m}^{-2} \text{d}^{-1}$ ) is daily absorbed photosynthetically active radiation and  $C_q$  ( $\text{mol photons MJ}^{-1}$ ) a conversion factor for solar radiation, with:

$$C_1 = \phi_{\text{TC3}} \times C_{\text{mass}} \times \alpha_{\text{C3}} \times \frac{p_i - \Gamma_*}{p_i + 2 \times \Gamma_*}, \quad (\text{Eq. A.3.17})$$

$$C_2 = \frac{p_i - \Gamma_*}{p_i + K_C \times (1 + \frac{[O_2]}{K_O})}, \quad (\text{Eq. A.3.18})$$



$p_i$  (Pa), the partial pressure of CO<sub>2</sub> in the intercellular air spaces of the leaf:

$$p_i = \lambda \times c_a \times P \text{ and} \quad (\text{Eq. A.3.19})$$

$p_a$  (Pa), the partial pressure of ambient CO<sub>2</sub>:

$$p_a = c_a \times P \quad (\text{Eq. A.3.20})$$

$\Gamma^*$  (Pa), the CO<sub>2</sub> compensation point:

$$\Gamma^* = \frac{[O_2]}{2 \times \tau}, \text{ and} \quad (\text{Eq. A.3.21})$$

the temperature dependent parameters  $K_C$ ,  $K_O$ , and  $\tau$ :

$$K_i = K_{25} \times Q_{10}^{(T-25)/10} \quad (\text{Eq. A.3.22})$$

where the number 24 (h d<sup>-1</sup>) is the number of hours per day,  $\phi_{TC3}$  (–) a temperature stress factor,  $C_{\text{mass}}$  (g mol<sup>-1</sup>) the atomic mass of carbon,  $\alpha_{C3}$  the C3 quantum efficiency (μmol μmol<sup>-1</sup>),  $[O_2]$  (Pa) the partial pressure of oxygen,  $\lambda$  (Pa Pa<sup>-1</sup>) the ratio of  $p_i$  to  $p_a$  ( $\lambda = \lambda_{\text{max}}$  under optimal water conditions),  $c_a$  (μmol mol<sup>-1</sup>) the ambient mole fraction of CO<sub>2</sub>,  $P$  atmospheric pressure (Pa),  $K_C$  (Pa) the Michaelis-Menten constant for CO<sub>2</sub>,  $K_O$  (Pa) the Michaelis-Menten constant for O<sub>2</sub>,  $\tau$  (μmol μmol<sup>-1</sup>) the CO<sub>2</sub>/O<sub>2</sub> specificity ratio, with  $K_i$  either  $K_C$ ,  $K_O$  or  $\tau$ , and  $Q_{10}$  the accompanying  $Q_{10}$  values, and  $V_m$  (g C m<sup>-2</sup> d<sup>-1</sup>) the maximum daily rate of photosynthesis:

$$V_m = \left(\frac{1}{b}\right) \times \left(\frac{C_1}{C_2}\right) \times [(2 \times \theta - 1) \times s - (2 \times \theta \times s - C_2) \times \sigma] \times APAR \times C_q \quad (\text{Eq. A.3.23})$$

with:

$$\sigma = \left[1 - \frac{C_2 - s}{C_2 - \theta \times s}\right]^{1/2}, \quad (\text{Eq. A.3.24})$$

$$s = \frac{24}{d_l} \times b, \text{ and} \quad (\text{Eq. A.3.25})$$

the “dark” respiration ( $R_d$ ):

$$R_d = b \times V_m \quad (\text{Eq. A.3.26})$$

where  $b$  is a constant  $R_d/V_m$  ratio (-).

In case of water stress, the photosynthesis rate is related to canopy conductance through the diffusion gradient in  $\text{CO}_2$  concentration as a result of the difference in  $p_i$  and  $p_a$ . This can be expressed in terms of total daytime net photosynthesis. Total daytime net photosynthesis ( $A_{dt}$ ,  $\text{g C m}^{-2} \text{ d}^{-1}$ ) is calculated as:

$$A_{dt} = A_{nd} + \left(1 - \frac{d_l}{24}\right) \times R_d \quad (\text{Eq. A.3.27})$$

or, expressed in terms of canopy conductance:

$$A_{dt} = \frac{d_l \times (g_c - g_{\min})}{1.6} \times [c_a \times (1 - \lambda)] \quad (\text{Eq. A.3.28})$$

where  $g_c$  ( $\text{mm s}^{-1}$ ) is average daytime canopy conductance,  $g_{\min}$  ( $\text{mm s}^{-1}$ ) the minimum canopy conductance, which accounts for water loss not directly related with photosynthesis, the factor 1.6 accounts for the difference in the diffusion coefficients of  $\text{CO}_2$  and water vapour; in Eq. A.3.28  $A_{dt}$  is expressed in  $\text{mm d}^{-1}$  (the conversion from  $\text{g C m}^{-2} \text{ d}^{-1}$  to  $\text{mm d}^{-1}$  is based on an the ideal gas) and  $d_l$  is expressed in s.  $g_c$  is calculated by rearranging Eq. A.3.28:

$$g_c = g_{\min} + \frac{1.6 \times A_{dt}}{[c_a \times (1 - \lambda)] \times d_l} \quad (\text{Eq. A.3.29})$$

Maximum (non-water limited) daily net potential photosynthesis rate is calculated with help Eq. A.3.28 with  $\lambda = \lambda_{\max}$ , and accordingly, applying Eq. A.3.29 and Eq. A.3.14 with  $\lambda = \lambda_{\max}$  and  $APAR = PAR$ , i.e. all available photosynthetically active radiation, gives the maximum average daytime canopy conductance, i.e. maximum potential canopy conductance ( $g_p$ ,  $\text{mm s}^{-1}$ ).

Water stress occurs when water supply ( $S$ ,  $\text{mm d}^{-1}$ ) is lower than water demand ( $D$ ,  $\text{mm d}^{-1}$ ). Supply is given by the maximum daily transpiration rate possible under well-watered conditions ( $E_{\max}$ ,  $\text{mm d}^{-1}$ ) and the relative soil moisture in the rooting zone ( $W_r$ ,  $\text{m}^3 \text{ m}^{-3}$ ):

$$S = E_{\max} \times W_r \quad (\text{Eq. A.3.30})$$

The soil is represented by a simple bucket containing two layers, each with a fixed thickness and a fixed fraction of the roots present. The soil water content of each layer is updated daily, taking into account transpiration, evaporation, runoff, and percolation through the layers.  $W_r$  is calculated by summing the soil water content of the two soil layers, which are multiplied by the fraction of roots in the specific layer and divided by its thickness. Finally,  $W_r$  is expressed as a fraction of  $W_{\max}$ , which is a soil-specific parameter, indicating the difference between field capacity and wilting point. Initialisation of the water balance is obtained by a spin-up run (for more details, see Gerten *et al.*, 2004). Demand is dependent on the fraction of the daytime the canopy is wet ( $w$ , -), potential evapotranspiration  $((E_q \times \alpha_{\max})$ , mm d<sup>-1</sup>), based on the Priestley-Taylor equations,  $g_p$ , and an empirical parameter  $g_m$  (mm s<sup>-1</sup>):

$$D = (1 - w) \times \frac{(E_q \times \alpha_{\max})}{(1 + \frac{g_m}{g_{\text{pot}}})} \quad (\text{Eq. A.3.31})$$

Water stress results in a lower canopy conductance, therefore, Eqs A.3.20 and A.3.33 are solved simultaneously, using a bisection method, to obtain values of  $A_{\text{nd}}$  and  $\lambda$  under water-limited conditions.

Finally, net primary production ( $NPP$ , g C d<sup>-1</sup> m<sup>-2</sup>) is calculated as:

$$NPP = A_{\text{nd}} - R_r - R_{\text{so}} - R_p - R_g \quad (\text{Eq. A.3.32})$$

where  $R$  (g C m<sup>-2</sup> d<sup>-1</sup>) is the maintenance respiration of roots, storage organs and a reserve pool, respectively, based on tissue-specific C:N ratios, temperature, the amount of biomass, and a respiration rate, and  $R_g$  the growth respiration:

$$R_g = \max(0, 0.25 \times A_{\text{nd}} - R_r - R_{\text{so}} - R_p) \quad (\text{Eq. A.3.33})$$

A more detailed description of the functions used is provided by Haxeltine and Prentice (1996) and Sitch *et al.* (2003).

## 2.2. Summarized biomass productivity approach

Net productivity ( $NPP$ , g C m<sup>-2</sup> d<sup>-1</sup>) is calculated as:

$$NPP = RUE \times R_{dr} \times 0.5 \times (1 - e^{-k \times LAI}) \times W_f \quad (\text{Eq. A.3.34})$$

where  $RUE$  (g C MJ<sup>-1</sup>) is the radiation use efficiency,  $R_{dr}$  (MJ m<sup>-2</sup> d<sup>-1</sup>) daily incoming short-wave radiation, and  $k$  (–) the light extinction coefficient, the number 0.5 (MJ PAR (MJ short-wave radiation)<sup>-1</sup>) is used, because half of the daily incoming short-wave radiation is photosynthetically active radiation, and  $W_f$  (–) a water stress factor, i.e. the ratio of actual and potential transpiration. Potential transpiration is calculated based on the Penman equation (Penman, 1948), actual transpiration is calculated based on its potential value, but also on soil water content ( $W_o$ , m<sup>3</sup> m<sup>-3</sup>) and soil characteristics. Water available for the crop is calculated on the basis of a soil water balance, calculated for one layer. The thickness of the layer increases with increasing root extension. Newly explored soil is assumed to be at field capacity. Water content of the soil is updated daily, taking into account precipitation, transpiration, evaporation, runoff and percolation. Initial water content, fed into the model, is used for initialisation of the water balance (for more details, see Farré *et al.*, 2000).



## **Appendix B**

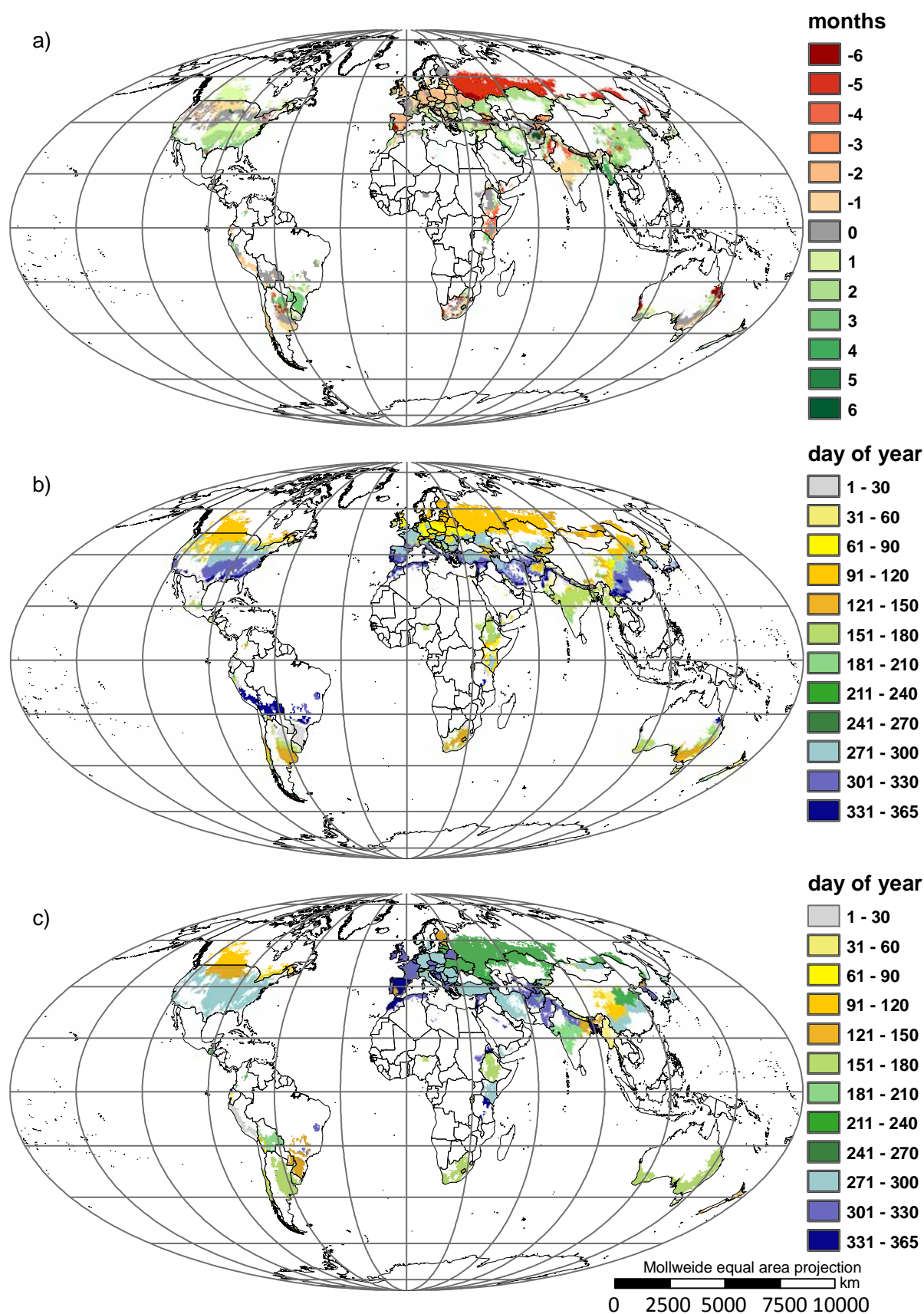


**Fig. B.5.1** Analysis of sowing date patterns of wheat: a) difference between simulated sowing dates and observed sowing dates, b) simulated sowing date, c) observed sowing dates according to MIRCA2000. White colours indicate crop area smaller than 0.001% of grid cell area. Sowing dates in regions without seasonality are not shown.

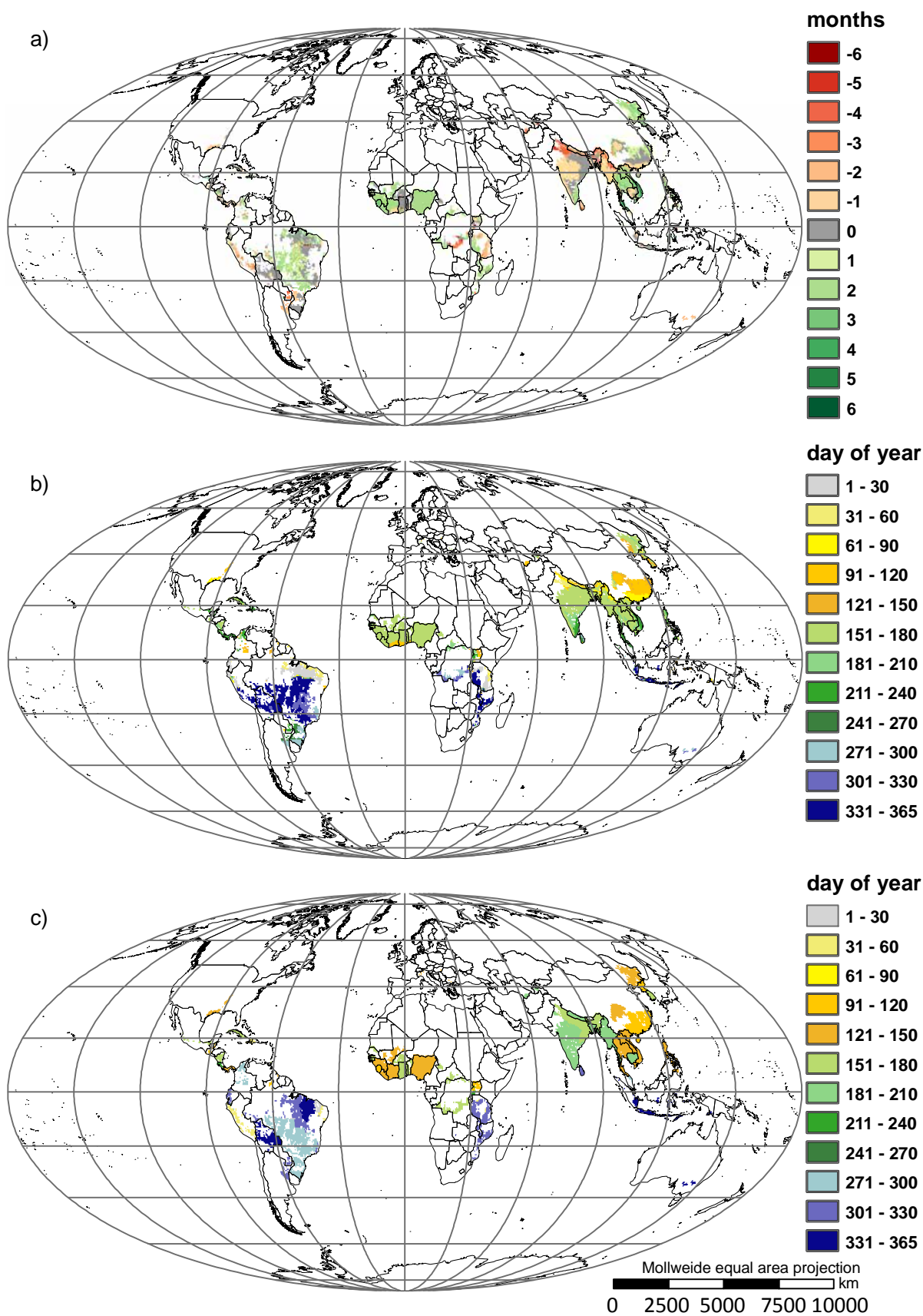


**Fig. B.5.2** Analysis of sowing date patterns of rice: a) difference between simulated sowing dates and observed sowing dates, b) simulated sowing date, c) observed sowing dates according to MIRCA2000. White colours indicate crop area smaller than 0.001% of grid cell area. Sowing dates in regions without seasonality are not shown.



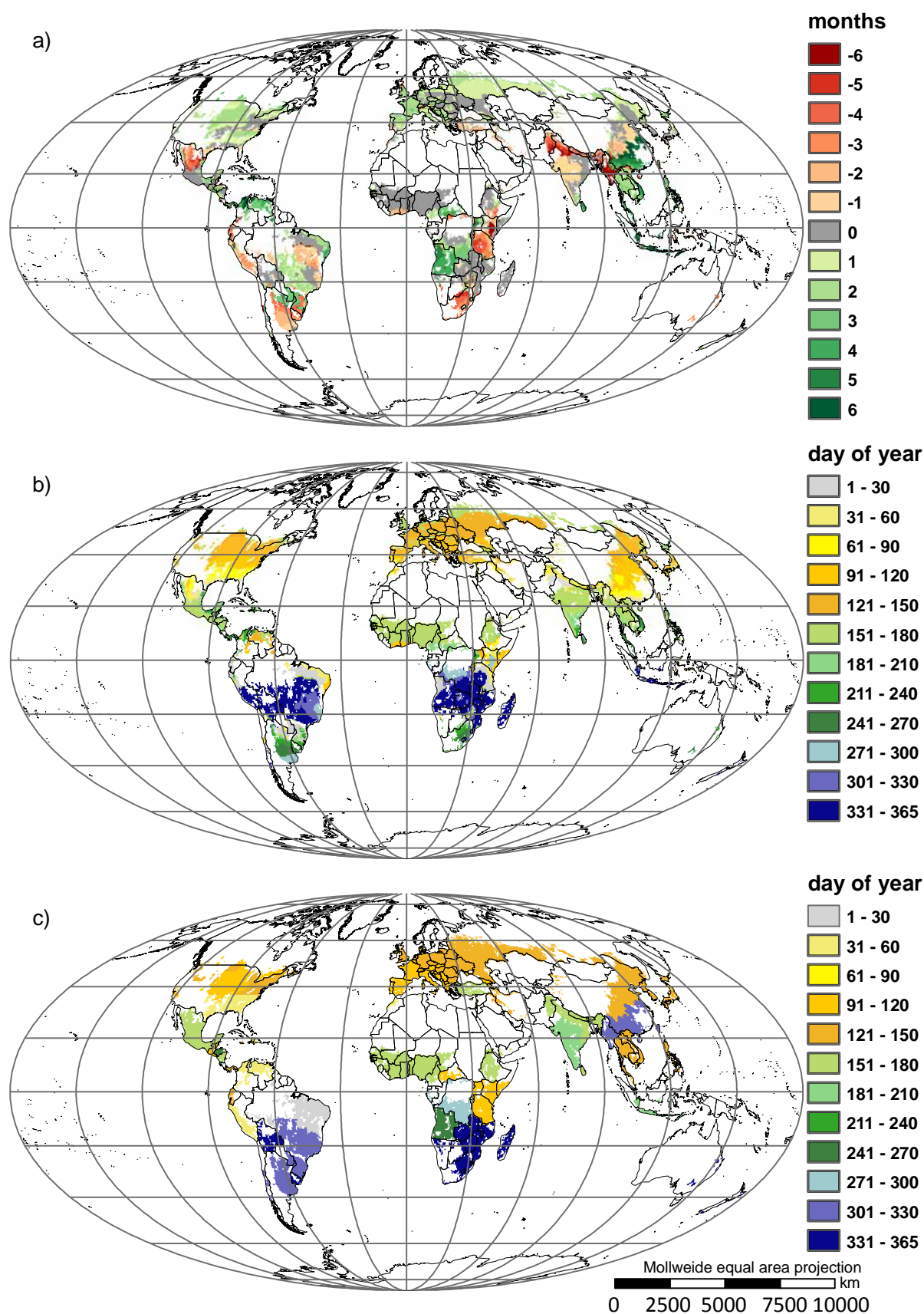


**Fig. B.5.3** Analysis of sowing date patterns of maize: a) difference between simulated sowing dates and observed sowing dates, b) simulated sowing date, c) observed sowing dates according to MIRCA2000. White colours indicate crop area smaller than 0.001% of grid cell area. Sowing dates in regions without seasonality are not shown.

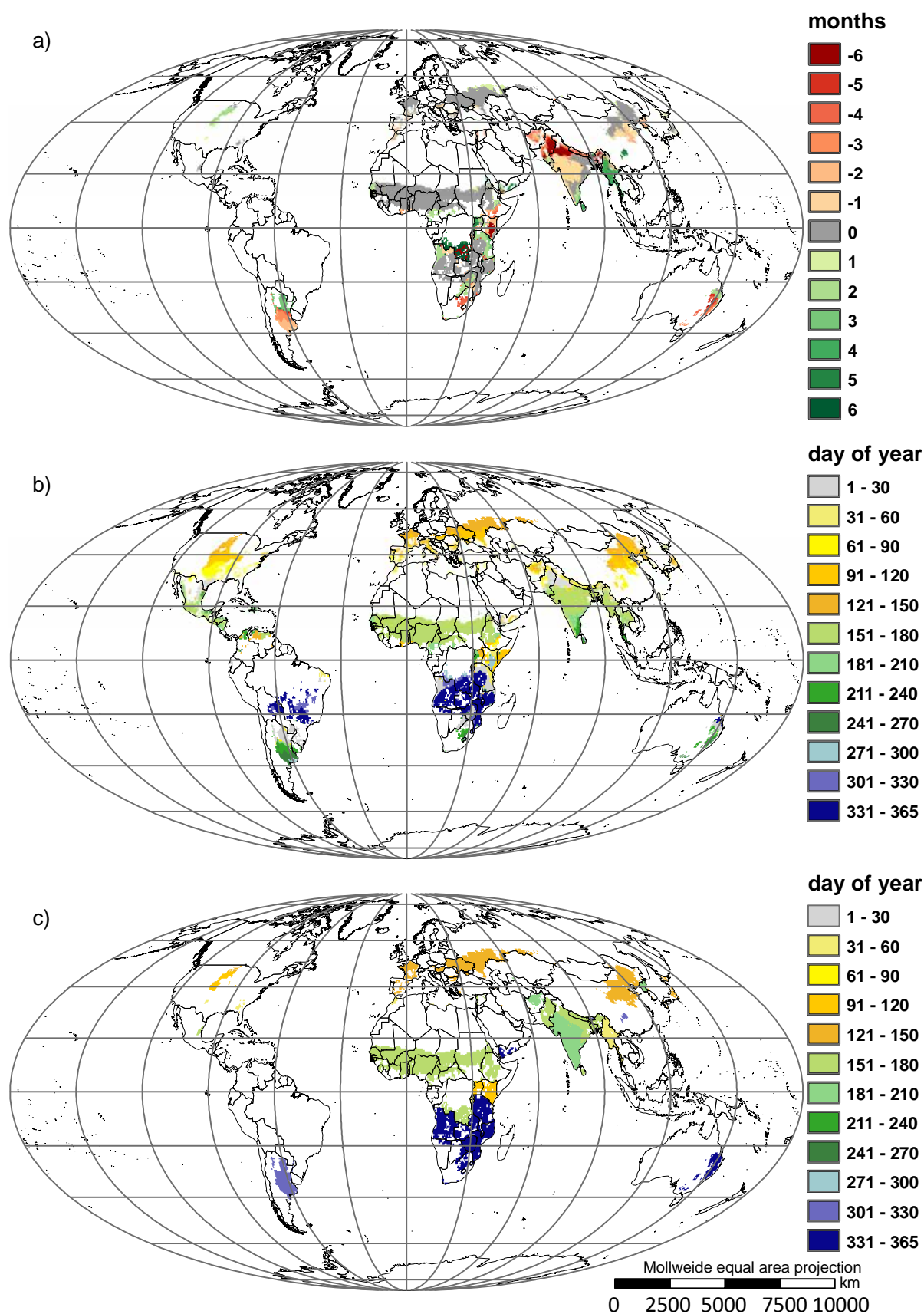


**Fig. B.5.4** Analysis of sowing date patterns of millet: a) difference between simulated sowing dates and observed sowing dates, b) simulated sowing date, c) observed sowing dates according to MIRCA2000. White colours indicate crop area smaller than 0.001% of grid cell area. Sowing dates in regions without seasonality are not shown.

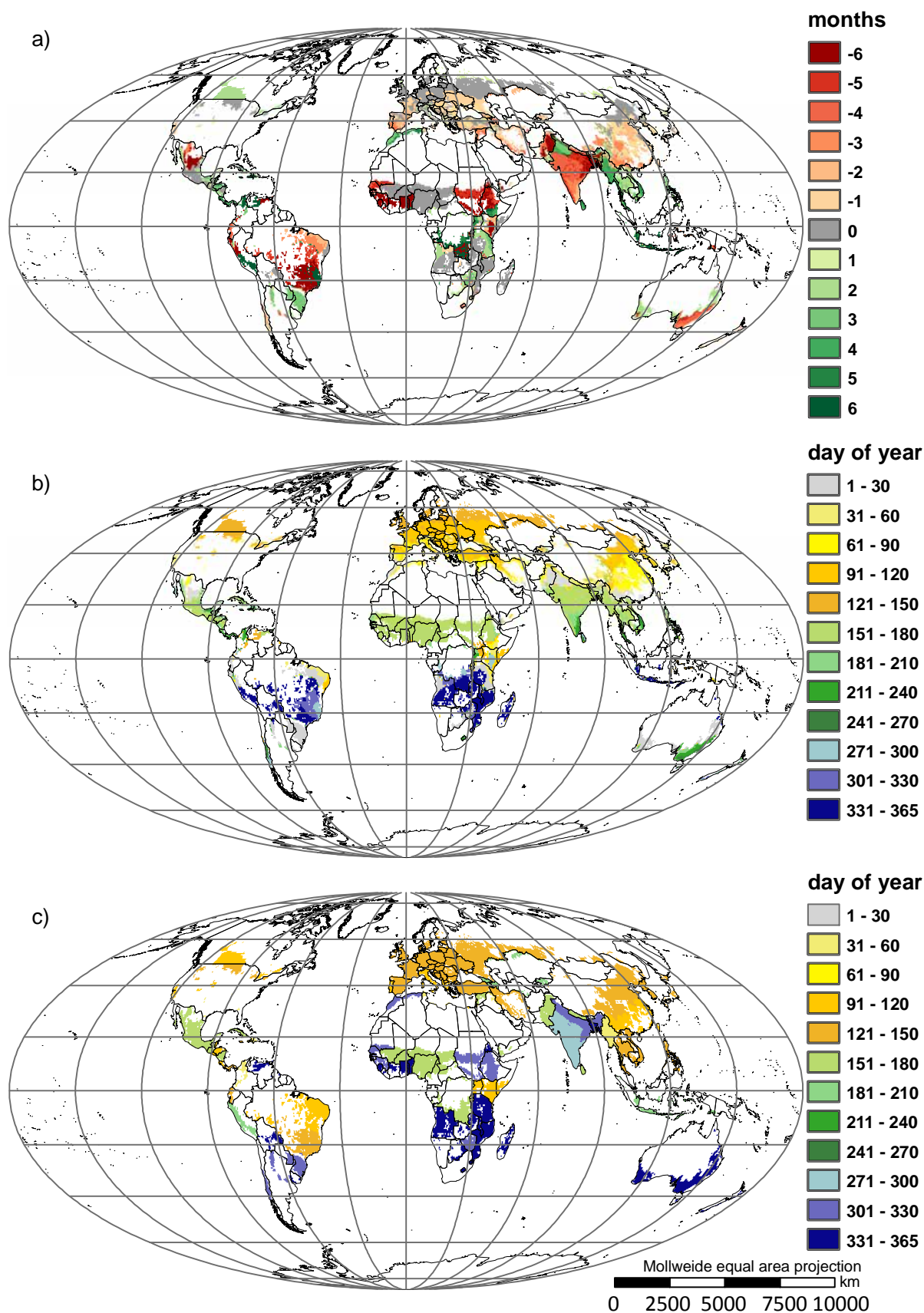


**Fig. B.5.5** Analysis of sowing date patterns of pulses: a) difference between simulated sowing dates and observed sowing dates, b) simulated sowing date, c) observed sowing dates according to MIRCA2000. White colours indicate crop area smaller than 0.001% of grid cell area. Sowing dates in regions without seasonality are not shown.

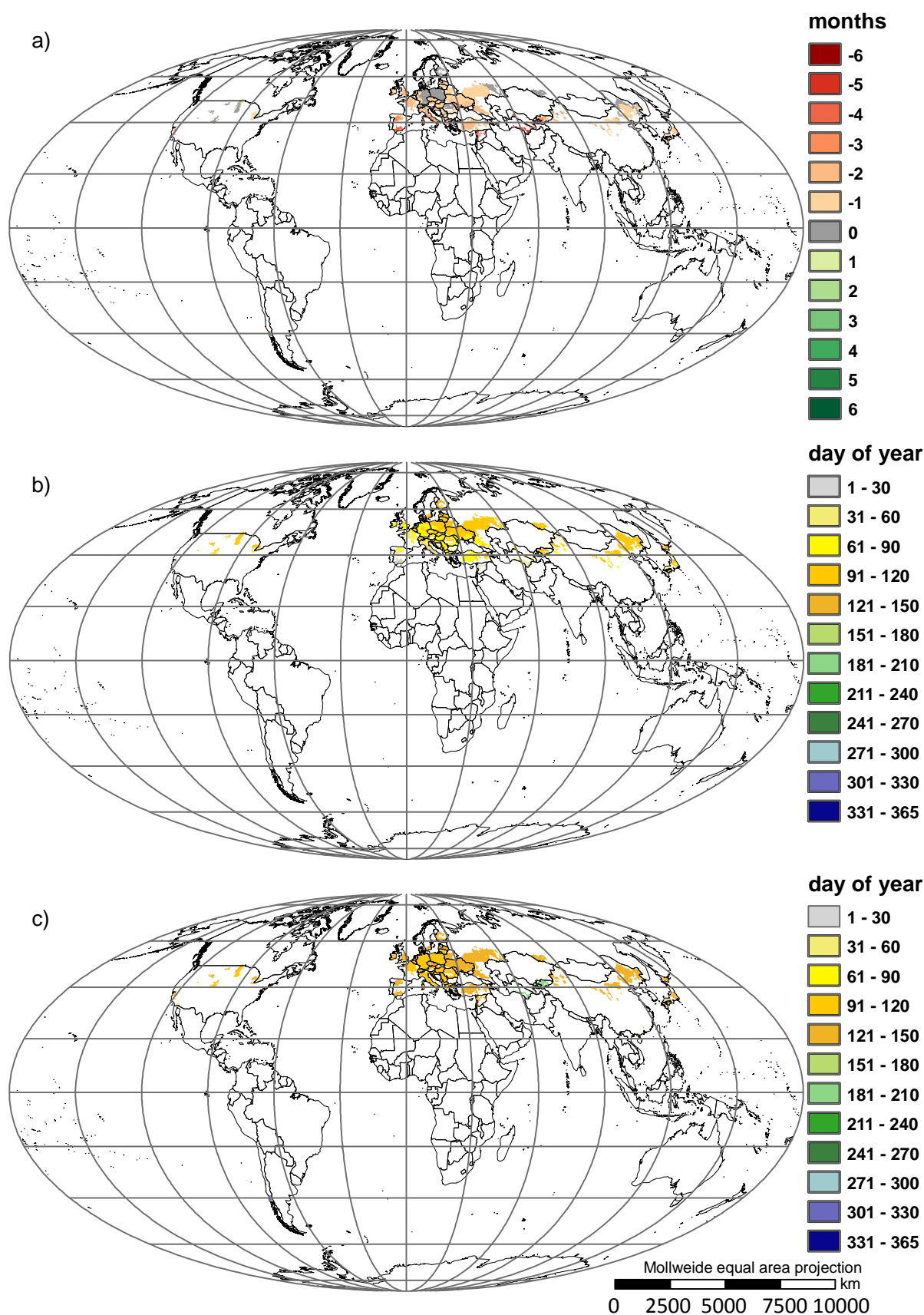


**Fig. B.5.6** Analysis of sowing date patterns of sugar beet: a) difference between simulated sowing dates and observed sowing dates, b) simulated sowing date, c) observed sowing dates according to MIRCA2000. White colours indicate crop area smaller than 0.001% of grid cell area. Sowing dates in regions without seasonality are not shown.



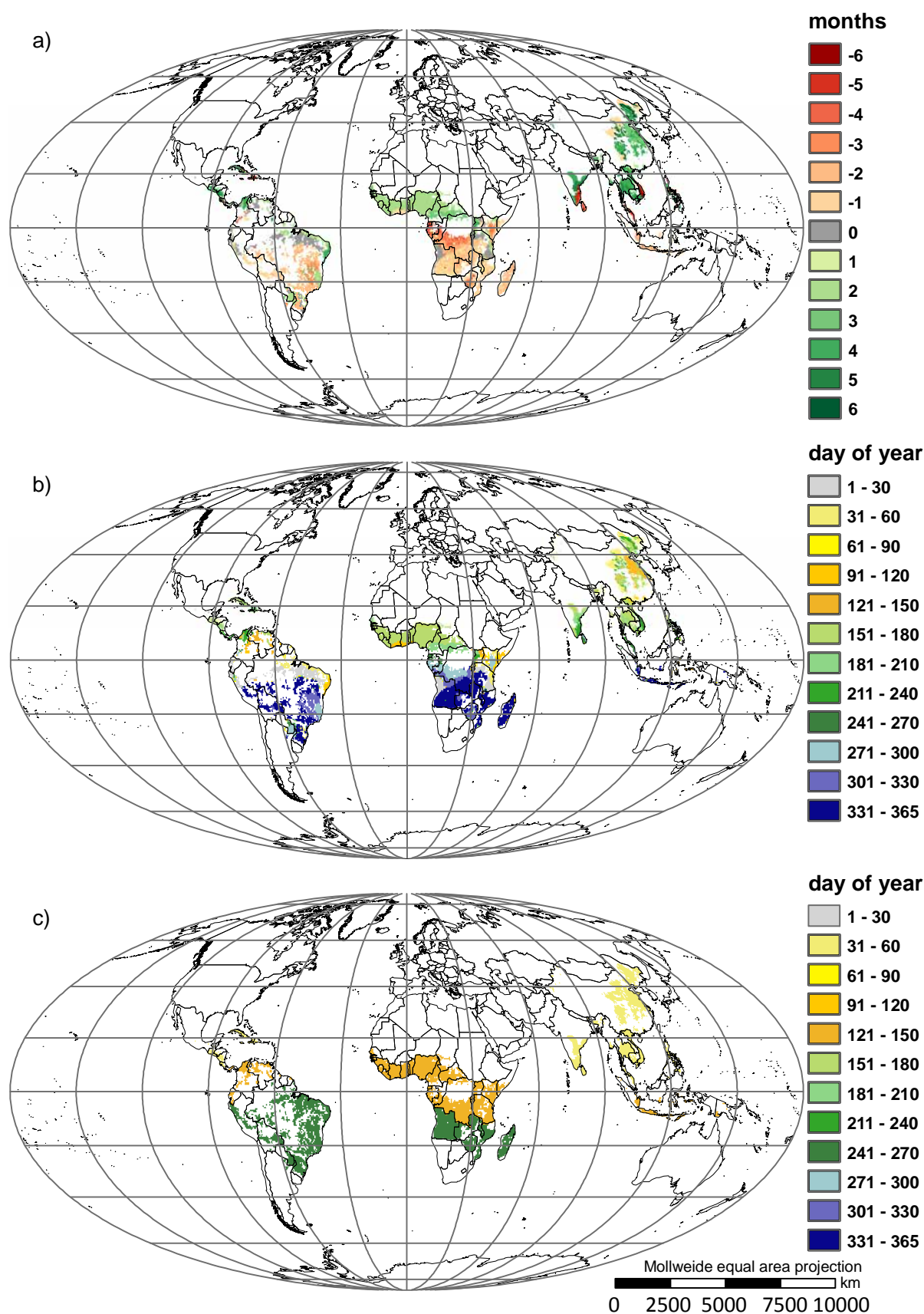


**Fig. B.5.7** Analysis of sowing date patterns of cassava: a) difference between simulated sowing dates and observed sowing dates, b) simulated sowing date, c) observed sowing dates according to MIRCA2000. White colours indicate crop area smaller than 0.001% of grid cell area. Sowing dates in regions without seasonality are not shown.

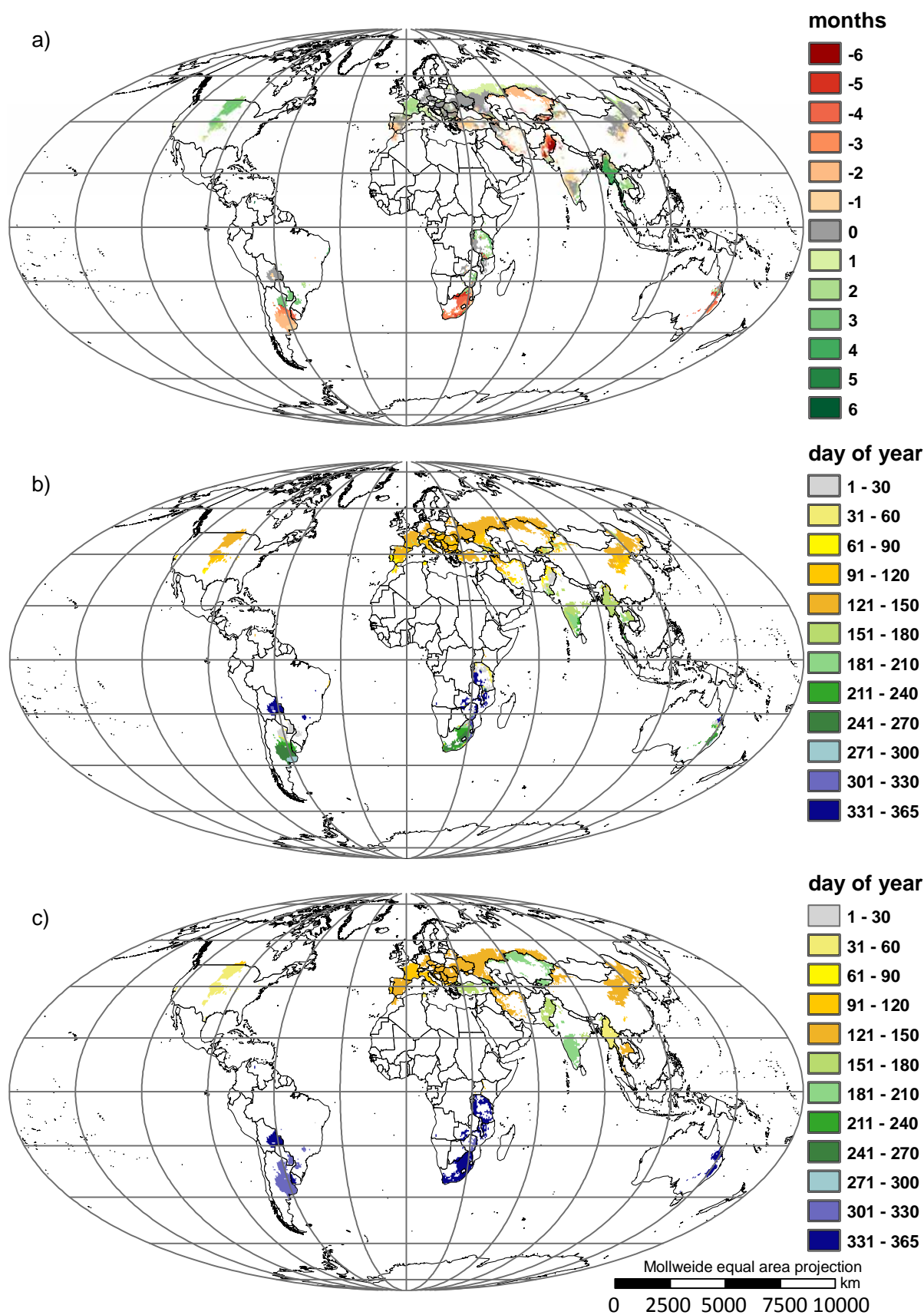


**Fig. B.5.8** Analysis of sowing date patterns of sunflower: a) difference between simulated sowing dates and observed sowing dates, b) simulated sowing date, c) observed sowing dates according to MIRCA2000. White colours indicate crop area smaller than 0.001% of grid cell area. Sowing dates in regions without seasonality are not shown.

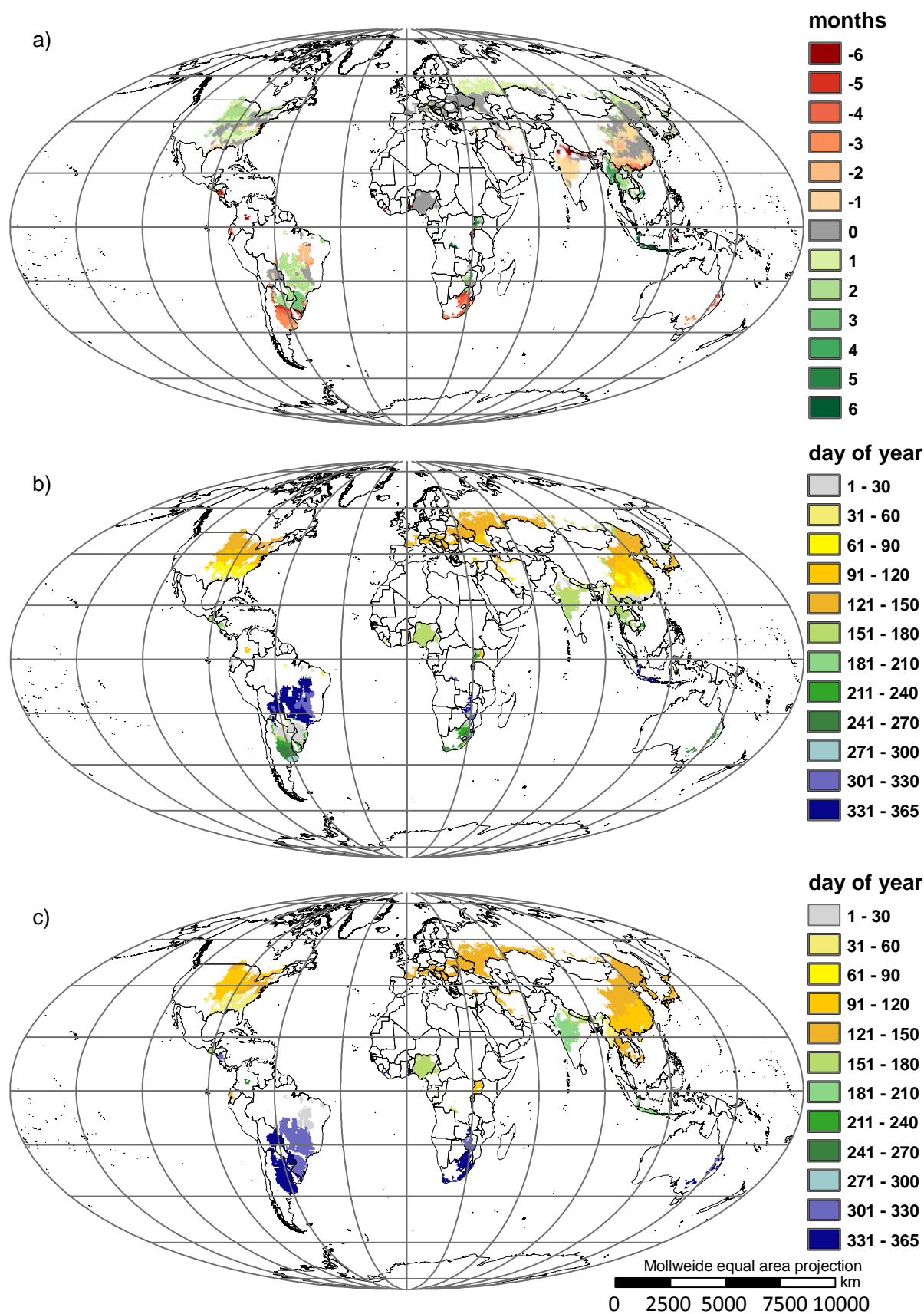


**Fig. B.5.9** Analysis of sowing date patterns of soybean: a) difference between simulated sowing dates and observed sowing dates, b) simulated sowing date, c) observed sowing dates according to MIRCA2000. White colours indicate crop area smaller than 0.001% of grid cell area. Sowing dates in regions without seasonality are not shown.

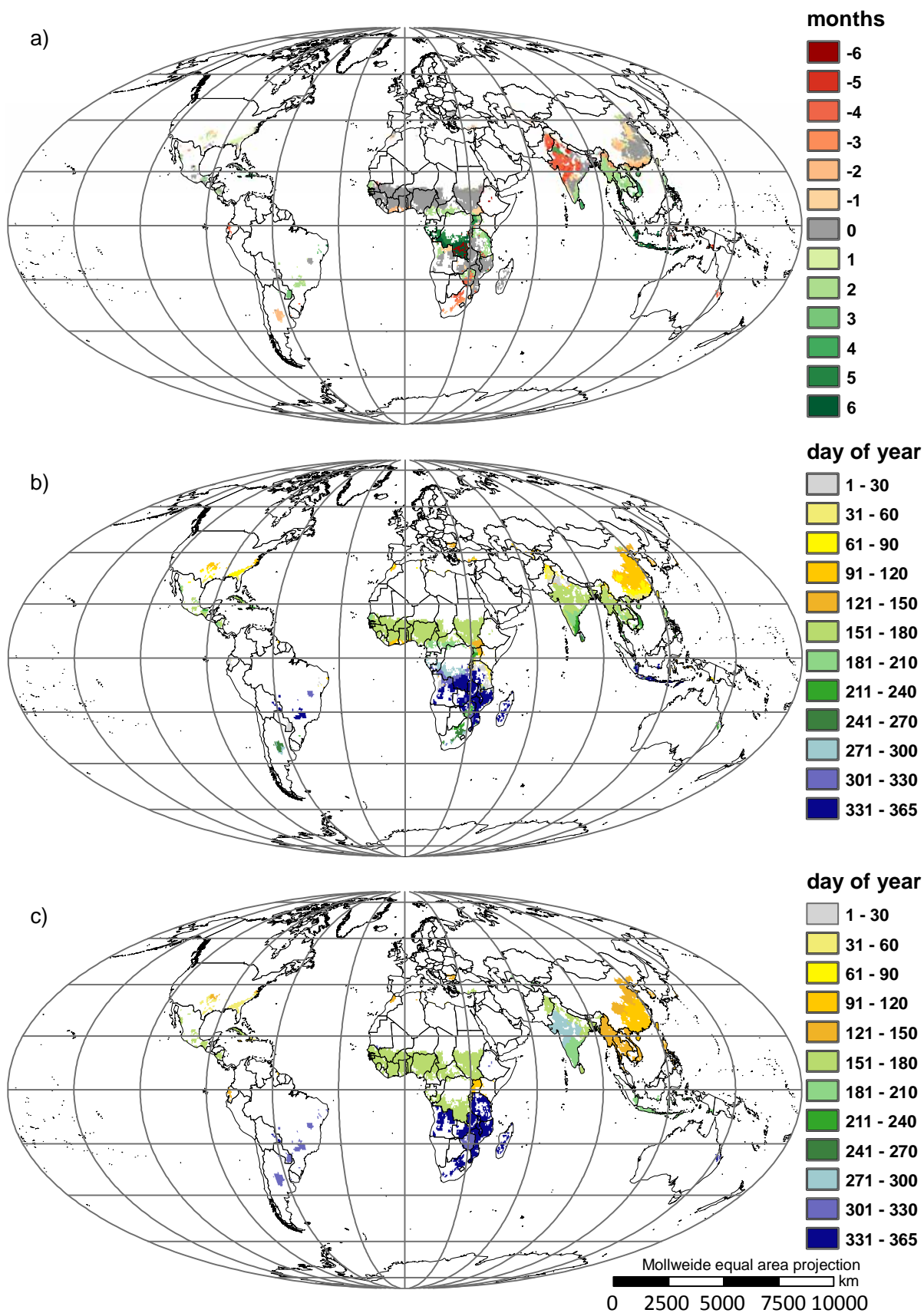


**Fig. B.5.10** Analysis of sowing date patterns of groundnut: a) difference between simulated sowing dates and observed sowing dates, b) simulated sowing date, c) observed sowing dates according to MIRCA2000. White colours indicate crop area smaller than 0.001% of grid cell area. Sowing dates in regions without seasonality are not shown.



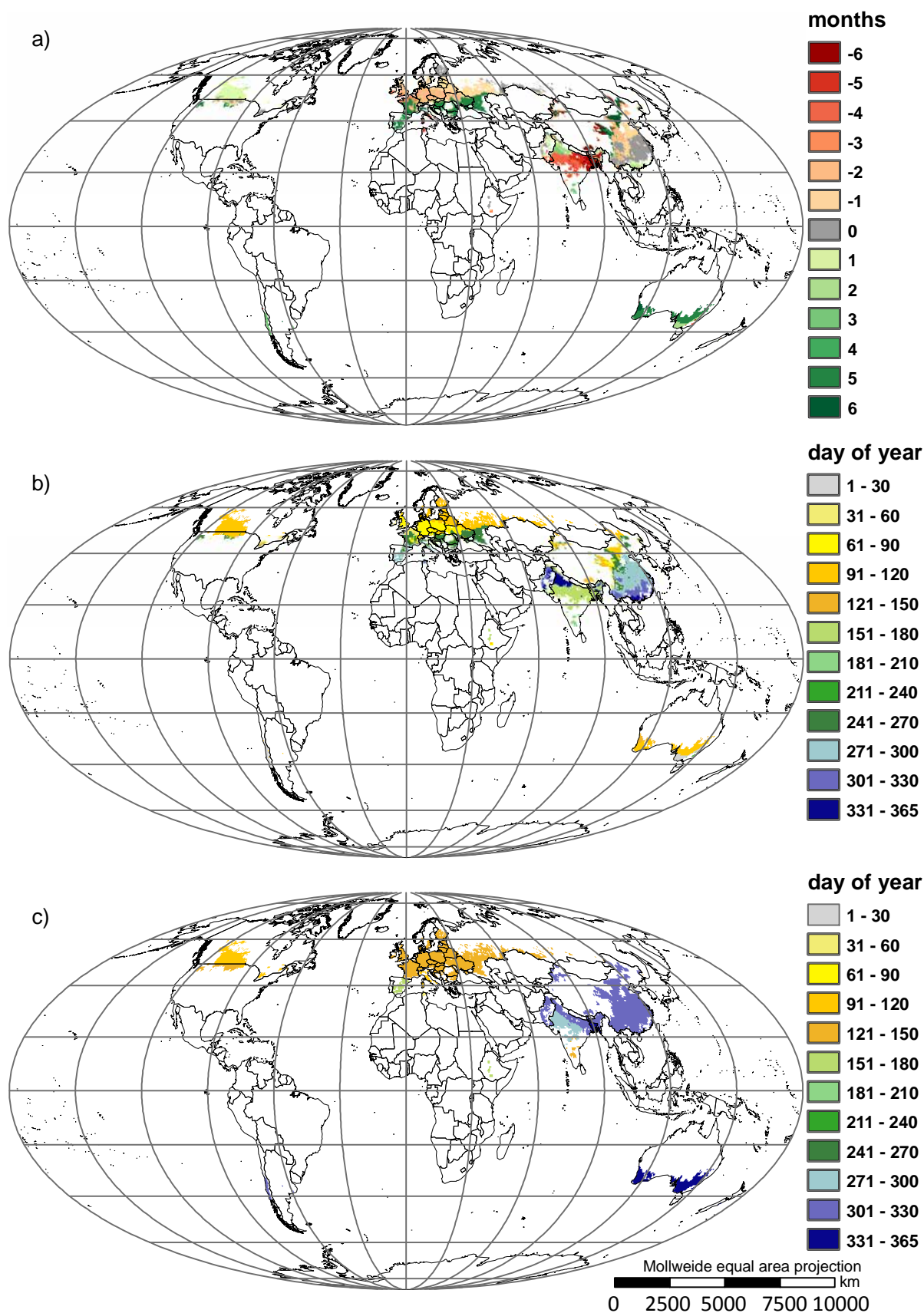


**Fig. B.5.11** Analysis of sowing date patterns of rapeseed: a) difference between simulated sowing dates and observed sowing dates, b) simulated sowing date, c) observed sowing dates according to MIRCA2000. White colours indicate crop area smaller than 0.001% of grid cell area. Sowing dates in regions without seasonality are not shown.

# Sensitivity analysis of crop yields to sowing dates

## Methodology

A possible application of sowing dates simulated with the presented methodology is to provide global crop growth models under future conditions with suitable cropping windows. We tested the sensitivity of the LPJmL dynamic global vegetation and crop model for different sowing dates on simulated crop yields for five locations with different seasonality types, using maize as an example crop. In LPJmL, crop growth is simulated using a combination of processes (photosynthesis, respiration, evapotranspiration, and leaf area development) on a daily basis (for more details, see Bondeau et al., 2007). LPJmL does not consider the effects of extreme temperatures on crop growth and development, e.g. frost damage. Phenological development of maize is simulated by accumulating temperature above the maize specific base temperature (8°C) until maturity is reached, taking into account the effect of photoperiod, as applied in the AFRCWHEAT2 model (Ewert *et al.*, 1996), until anthesis. It was assumed for the five locations that farmers grow cultivars which are adapted to their environment. Required temperature sums till maturity per location-specific cultivar were calculated based on observed sowing and harvest dates, monthly temperature data from the year 1998, and photoperiods. Equal sensitivity to photoperiod between the cultivars was assumed (the optimum photoperiod was assumed to be 12.5h and the base photoperiod 24h). Yield was simulated for each location for a range of sowing dates (52, starting at the first of January, with steps of 7 days) for rainfed conditions, using the monthly climate data of the year 1998, and assuming that farmers grow the same cultivar throughout the whole year. The crop was allowed to grow for a period of maximum 250 days.

## Results and Discussion

In Fig. B.5.12, we display simulated maize yields per sowing date for the five locations, compared to the maximum simulated maize yield per location. The sensitivity of simulated maize yield to the sowing date at a location with no seasonality (Iquitos, Peru) is relatively small: simulated yield is, irrespective of sowing date, always at least 80% of the maximum simulated yield. Larger sensitivity is shown for locations with temperature seasonality (Amsterdam, the Netherlands and Kansas City, USA). In the Netherlands, yields of at least 80% of

the maximum yield are simulated, with sowing dates ranging from day of year 14 to day of year 140. In the USA, yields of at least 80% of the maximum yield are simulated, with sowing dates ranging from day of year 21 to day of year 147. In a location with precipitation seasonality and a long wet season (Abuja, Nigeria), the range of sowing dates which results in simulated yields of at least 80% of the maximum is wider in comparison to a location with a shorter wet season (Delhi, India).

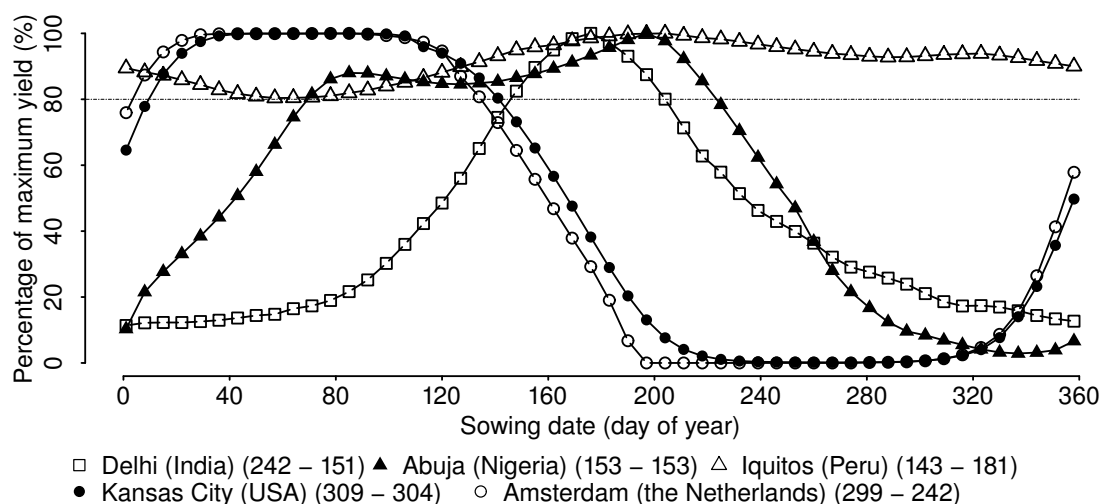


**Fig. B.5.12.** Sensitivity of maize yield to sowing dates for five locations. Between brackets, the simulated respectively observed sowing dates are given. The dashed line indicates 80% of maximum simulated yield.

## Summary

In recent years, the scale of interest for application of crop growth models has extended from the plot and field to the region or even globe. In addition, the time frame of the assessments has increased from a season or a year to much longer time frames, e.g. 50-100 years as considered in climate change impact studies. The application of a crop growth model originally developed for the plot or field scale at larger scales without any adaptation might lead to inaccuracies in model outcomes. Moreover, if crop growth models are applied at large scales, problems arise with respect to missing input data and lack of parameter values for different regions.

The appropriate level of detail to represent a process in a model is often seen as a critical and difficult step in model development. The level of detail should be a good balance between the objective of the model, which includes the scale of application, and the spatial and temporal resolution of the available data. Knowledge about the required level of modelling detail to accurately represent crop growth processes in crop growth models to be applied at large scales is scarce. In this thesis we analysed simulated potential yields, which resulted from models which apply different levels of detail to represent important crop growth processes, for a wide range of climatic conditions. In particular, we focussed on the processes of light interception, determined by leaf area dynamics, and light utilization for biomass production, two key processes for crop growth. Our results indicated that, after location-specific calibration, models with different levels of detail may perform similarly, but model performance was in general best for models which represented leaf area dynamics with the lowest level of detail (i.e. leaf area dynamics are simulated with help of a forcing function, defined in terms of sigmoidal and quadratic functions). Especially the representation of leaf senescence, and in particular its onset, was found to be critical for model performance. Additional tests of the behaviour of the models indicated that the light interception approach significantly influences model outcomes and that the light utilization process with the lowest level of detail (radiation use efficiency approach) may be an oversimplification of reality, since this approach does not consider the effects of high temperatures and high radiation intensities on the light utilization process.

In contrast to field scale model applications, large scale applications often rely on data aggregated over space and/or time, e.g. the use of monthly weather data while crop growth models were originally developed and evaluated for daily weather data. We examined if daily weather data can be replaced by monthly

weather data in crop growth models. In particular, we studied whether the degree of detail in crop growth models determines their sensitivity to temporally aggregated weather input data. Results from different climatic regions in Europe showed that replacing daily weather data with temporally aggregated weather data resulted in higher simulated amounts of biomass. The magnitude of the day-to-day variability in weather conditions affects the results: increasing variability results in stronger differences between model results due to aggregation. In addition, we found increasing detail in a modelling approach to give higher sensitivity to aggregation of input data.

Most global crop growth models are run on a grid-based system. In grid-based systems spatially aggregated data are used, i.e. it is assumed that data such as weather and crop management (e.g. sowing dates or cultivar use) are homogeneous within a grid cell. We investigated the impact of the use of spatially aggregated sowing dates and temperatures on the simulated phenology of winter wheat in Germany. We found model outcomes as a result of using aggregated data to be similar in comparison with the use of non-aggregated data (i.e. location-specific data). We concluded that for simulation of winter wheat phenology, which consists of mainly linear relationships, the use of sowing dates and weather data with a 100 km × 100 km resolution is appropriate for regions with homogenous climatic characteristics, such as Germany. In addition, the results indicated that our assumption to use one phenological parameter set to capture the average response pattern of the development of different winter wheat cultivars found in a large country such as Germany, was justified.

Generation or simulation of input data for crop growth models is necessary if the spatial resolution of the available data is unsuitable, when data are expected to change under future conditions, or when data are not available. Phenological data, e.g. sowing and harvesting dates, are examples of data that are often simulated within global crop growth models. Only recently two comprehensive global data sets of cropping calendars with global coverage, combining several sources of observed cropping calendars, have been developed. As a consequence, until recently simulation of phenology at the global scale, including sowing and harvesting dates, could hardly be evaluated. We aimed at simulating sowing dates of several major rainfed crops based on climatic conditions. We assumed farmers to sow either when temperature exceeds a crop-specific threshold or at the onset of the wet season, depending on the intra-annual variability in climatic conditions. From our results we concluded that our methodology is more accurate in regions where temperature is the main limiting factor for the length of the growing season than in regions where precipitation plays a major role.

Nevertheless for a large part of the globe our methodology is capable of simulating reasonable sowing dates, i.e. for the simulated crops (among others important crops such as maize, wheat, and rice) on at least 60% of the cultivated area the difference between simulated and observed sowing dates is less than one month, except for rapeseed and cassava.

To simulate the end of the cropping period (i.e. harvesting dates) we developed simple algorithms to generate unknown crop- and location-specific phenological parameters based on location-specific climatic and daylength conditions, using wheat and maize as example crops. In the main cropping regions of wheat we were able to simulate lengths of the cropping periods that correspond well with observed lengths, i.e. on average there is a difference of approximately 2 weeks. Our methodology worked less well for maize, i.e. in the main maize cropping regions we over- and underestimated the cropping period length with 0.5 to 1.5 month, which can partly be explained by the high base temperature of maize and the low temperatures during the period in which maize is normally harvested at the northern hemisphere. Importantly, our evaluation of possible consequences for simulated yields related to uncertainties in simulated sowing and harvesting dates showed that simulated yields (for wheat and maize) are rather similar using either simulated sowing and harvesting dates or observed sowing and harvesting dates; the difference not being larger than 20%. The consideration of daylength reduces the simulated interannual variability of phenological stages to values that are probably more realistic compared to simulations of phenology based on temperature alone.

The work described in this thesis enhances understanding related to the upscaling of crop growth models from field to globe. It became clear that for crop growth models designed for large scales particular attention should be given to the choice of the representation of the leaf area development. Moreover, the resolution of the available input data should define the design of a (global) crop growth model as much as the aim of the model. Additionally we found that it is possible to generate missing input data such as sowing and harvesting dates. The thesis concludes with a discussion on a proposed structure of a global crop growth model, in which this enhanced understanding is applied. The model is expected to simulate reasonable potential yields at the global scale if monthly aggregates of climate data at a  $0.5^\circ \times 0.5^\circ$  grid are available. The proposed model consists of a forcing function, defined in terms of sigmoidal and quadratic functions to represent light interception, combined with the radiation use efficiency approach, and phenology determining the allocation of biomass to the organs of the crop. To obtain sowing dates and phenological cultivar characteris-

tics at an appropriate spatial resolution and to be able to take into account possible adaptation of farmers to changes in climatic conditions, these data are simulated within the model, based on location-specific climatic and daylength conditions. Based on the proposed model the thesis finally derives directions for future research to further enhance global crop growth modelling. It is indicated that further improvement of global crop growth models will be possible with increased understanding of the differences in timing of the flowering process between cultivars. In addition, research is required to improve the evaluation process of global crop growth models.

## Samenvatting

Het schaalniveau van de toepassing van gewasgroeimodellen is recentelijk uitgebreid van het perceel en veld naar de regio en zelfs de wereld. Bovendien is de tijdshorizon van de toepassingen toegenomen van een seizoen of een jaar tot veel langere periodes, bijvoorbeeld, zoals gebruikelijk in klimaatimpactstudies, 50-100 jaar. Echter, het toepassen van modellen die oorspronkelijk ontwikkeld zijn voor de perceel- of veldschaal op grotere schaalniveaus zonder enige aanpassing, kan leiden tot fouten en onnauwkeurigheden in de modeluitkomsten. Bovendien ontstaan er meestal problemen met betrekking tot ontbrekende invoergegevens en parameterwaarden voor verschillende regio's als gewasgroeimodellen worden toegepast op grote schaalniveaus.

Het bepalen van de geschikte mate van detail om een proces weer te geven is een cruciale en moeilijke stap in het modelontwikkelingsproces. De mate van detail moet een balans zijn tussen het doel van het model, dat ook het schaalniveau betreft, en de ruimtelijke en temporele resolutie van de beschikbare invoergegevens. Kennis over de benodigde mate van detail om accuraat gewasgroeiprocessen weer te geven in gewasgroeimodellen voor toepassing op grote schaalniveaus is schaars. In dit proefschrift hebben we daarom potentiële opbrengsten geanalyseerd, gesimuleerd door gewasgroeimodellen die verschillende maten van detail toepassen om belangrijke processen voor gewasgroei weer te geven. We hebben hierbij gebruik gemaakt van weersgegevens van locaties met zeer verschillende klimaten. In het bijzonder hebben we de sleutelprocessen voor gewasgroei, namelijk lichtinterceptie, wat bepaald wordt door de groei van het bladoppervlak, en lichtbenutting voor biomassaproductie bestudeerd. Onze analyse liet zien dat, na locatiespecifieke kalibratie, modellen met verschillende maten van detail vergelijkbaar kunnen presteren, maar dat de modelprestatie in het algemeen het best was indien de groei van het bladoppervlak met het minste detail werd weergegeven (d.w.z. de groei van het bladoppervlak wordt gesimuleerd met behulp van sigmoïde en kwadratische functies). Het meest cruciaal voor de modelprestatie bleek de weergave van de bladveroudering, in het bijzonder het tijdstip van begin van de bladveroudering. Aanvullende testen met betrekking tot het gedrag van de modellen gaven aan dat de manier van weergave van de lichtinterceptie een significante invloed heeft op de modeluitkomsten. Verder gaven de uitkomsten aan dat de keuze voor de weergave van de biomassaproductie met het minste detail (stalingsbenuttingsefficiëntie) een te eenvoudige beschrijving van de werkelijkheid kan



zijn, omdat deze de effecten van hoge temperaturen en hoge stralingsintensiteiten niet meeneemt.

Gewasgroeimodellen zijn oorspronkelijk ontwikkeld en geëvalueerd voor het gebruik van dagelijkse weergegevens. Echter, voor toepassingen van modellen op grote schaalniveaus wordt vaak gebruik gemaakt van invoergegevens die zijn samengevoegd in de ruimte en/of over de tijd (aggregatie), bijvoorbeeld weergegevens met een maandelijkse resolutie. We hebben onderzocht of in gewasgroeimodellen dagelijkse weergegevens vervangen kunnen worden door maandelijkse weergegevens. In het bijzonder hebben we bestudeerd of de mate van detail van processen in gewasgroeimodellen de gevoeligheid van de modellen voor het samenvoegen van weergegevens over de tijd beïnvloedt. Resultaten van verschillende klimatologische regio's in Europa wezen uit dat het vervangen van dagelijks weer door maandelijks weer leidt tot grotere hoeveelheden gesimuleerde biomassa. De modeluitkomsten liet zien dat de omvang van de dag-tot-dag variabiliteit in weercondities de modeluitkomsten beïnvloedt: een toenemende variabiliteit resulteert in een groter verschil tussen modeluitkomsten met aan de ene kant dagelijks weer en aan de andere kant maandelijks weer. Bovendien vonden we dat een toenemende mate van detail in een model resulteert in een toenemende gevoeligheid voor de samenvoeging van invoergegevens.

De meeste mondiale gewasgroeimodellen worden toegepast op een grid-gebaseerd systeem. Daarbij wordt aangenomen dat de gegevens, bijvoorbeeld weer en gewasmanagement (zaaidata of het gebruik van bepaalde variëteiten, etc.) homogeen zijn binnen een gridcel. We onderzochten de effecten van het gebruik van ruimtelijk samengevoegde zaaidata en temperatuurgegevens op de simulatie van wintertarwe in Duitsland. We vonden dat het gebruik van samengevoegde gegevens overeenkomende modeluitkomsten geeft met het gebruik van niet-samengevoegde gegevens (d.w.z. locatiespecifieke gegevens). We concludeerden dat voor de simulatie van fenologie van wintertarwe, een proces dat voornamelijk wordt weergegeven met behulp van lineaire relaties, zaaidata en weergegevens op een grid met een resolutie van 100 km × 100 km geschikt zijn voor regio's met homogene klimaatkarakteristieken, zoals Duitsland. Bovendien gaven de resultaten aan dat onze aanname, om één fenologische parameterset te gebruiken om het gemiddelde responspatroon van de ontwikkeling van verschillende wintertarwevariëteiten die in een groot land zoals Duitsland gevonden worden, redelijk was.

Het kan nodig zijn om invoergegevens voor gewasgroeimodellen te genereren of simuleren indien de ruimtelijke resolutie van de beschikbare gegevens

ongeschikt is, indien het te verwachten is dat de gegevens veranderen onder invloed van toekomstige omstandigheden, of indien de gegevens niet beschikbaar zijn. Fenologische gegevens, bijvoorbeeld zaai- en oogstdata, zijn voorbeelden van gegevens die vaak worden gesimuleerd binnen mondiale gewasgroeimodellen. Pas recentelijk zijn twee veelomvattende gegevenssets met geobserveerde gewaskalenders met mondiale dekking ontwikkeld. Daardoor kon de simulatie van fenologie op de mondiale schaal, inclusief zaai- en oogstdata, tot voor kort maar nauwelijks geëvalueerd worden. We hadden daarom tot doel zaaidata van verschillende belangrijke gewassen in de niet geïrrigeerde landbouw te simuleren, gebaseerd op klimatologische condities, en daarna te evalueren. We namen aan dat boeren zaaien, ofwel wanneer de temperatuur een gewasspecifieke drempel overschrijdt, ofwel wanneer het regenseizoen begint; de keuze voor temperatuur of regenseizoen gebaseerde zaaidata is afhankelijk van de variabiliteit in de klimatologische omstandigheden binnen jaren in een gebied. Gebaseerd op onze resultaten konden we concluderen dat onze methode nauwkeuriger is in regio's waar voornamelijk de temperatuur de limiterende factor voor de lengte van het groeiseizoen is, dan in regio's waar hoofdzakelijk neerslag de lengte van het groeiseizoen bepaalt. Desalniettemin zijn we met onze methode in staat om voor een groot deel van de aarde redelijke zaaidata te simuleren. Dat wil zeggen, voor de gesimuleerde gewassen, o.a. de belangrijke gewassen maïs, tarwe en rijst, is het verschil tussen de gesimuleerde en geobserveerde zaaidata minder dan één maand op minimaal 60% van de gecultiveerde oppervlakte; dit gold niet voor koolzaad en cassave.

Om het einde van de groeiperiode (d.w.z. de oogstdatum) te bepalen hebben we eenvoudige algoritmen ontwikkeld, die ontbrekende gewas- en locatiespecifieke fenologische parameters genereren. De algoritmen gebruiken locatiespecifieke klimatologische en daglengte omstandigheden; als voorbeeldgewassen zijn tarwe en mais gebruikt. In de belangrijkste groeigebieden van tarwe kwamen onze gesimuleerde lengtes van de groeiperiode goed overeen met de geobserveerde lengtes, d.w.z. de gemiddelde afwijking tussen de simulaties en observaties was ongeveer twee weken. Onze methode werkte voor mais minder goed; in de belangrijkste groeigebieden werd de groeiperiode over- en onderschat met 0,5 tot 1,5 maand. Deze over- en onderschattingen kunnen gedeeltelijk verklaard worden door de hoge basistemperatuur van mais en de relatief lage temperaturen tijdens de periode wanneer mais normaal gesproken geoogst wordt op het noordelijk halfrond. Desondanks liet onze evaluatie met betrekking tot mogelijke consequenties voor de gesimuleerde opbrengsten als gevolg van onzekerheden in de gesimuleerde zaai- en oogstdata zien dat de gesimuleerde

opbrengsten (voor tarwe en mais) vrijwel gelijk zijn indien ofwel gesimuleerde ofwel geobserveerde zaai- en oogstdata worden gebruikt: het verschil was niet groter dan 20%. Tenslotte werd gevonden dat het mede beschouwen van de effecten van daglengte in de simulatie van wintertarwefenologie de gesimuleerde variabiliteit van fenologische fases tussen jaren reduceert. In vergelijking met simulaties gebaseerd op alleen temperatuur, komt deze gereduceerde variabiliteit hoogstwaarschijnlijk beter overeen met de werkelijke variabiliteit.

De studies beschreven in dit proefschrift hebben het inzicht met betrekking tot het opschalen van gewasgroeimodellen van de veldschaal naar de wereldschaal vergroot. Het is duidelijk geworden dat voor gewasgroeimodellen die ontwikkeld worden voor toepassing op grote schaal, vooral aandacht geschonken dient te worden aan de keuze hoe de groei van het bladoppervlak weer te geven. Bovendien moet de resolutie van de beschikbare invoergegevens het ontwerp van het (mondiale) gewasgroeimodel evenveel beïnvloeden als het doel van het model. Daarnaast werd duidelijk dat het mogelijk is om missende invoergegevens zoals zaai- en oogstdata te simuleren. Het proefschrift sluit af met een voorstel met betrekking tot de structuur van een mondiaal gewasgroeimodel, waarin de verkregen inzichten verwerkt zijn. De verwachting is dat dit mondiale model redelijke potentiële opbrengsten kan simuleren, indien maandelijkse weergegevens op een grid met een resolutie van een  $0,5^\circ \times 0,5^\circ$  beschikbaar zijn. Het voorgestelde model bestaat uit sigmoïde en kwadratische functies om het proces van lichtinterceptie weer te geven, gecombineerd met de stalingsbenuttingsefficiëntieaanpak om de biomassaproductie te berekenen. Tenslotte wordt de toewijzing van de biomassa naar de verschillende organen van het gewas bepaald door de fenologie. Om zaaidata en fenologische variëteitskarakteristieken met een geschikte ruimtelijke resolutie te verkrijgen, en om rekening te kunnen houden met mogelijke aanpassingen van boeren aan veranderende klimatologische omstandigheden, worden deze gegevens gesimuleerd, gebaseerd op locatiespecifieke klimatologische en daglengte omstandigheden. Gebaseerd op het voorgestelde model geeft het proefschrift tenslotte richting aan toekomstig onderzoek voor verdere verbetering van mondiale gewasgroeimodellen. In het bijzonder moet prioriteit worden gegeven aan onderzoek dat verschillen in timing in het bloeiproces tussen variëteiten bestudeert. Bovendien is onderzoek nodig om het evaluatieproces van mondiale gewasgroeimodellen te verbeteren.

## Dankwoord & Acknowledgements

Aangekomen bij deze pagina's van mijn proefschrift bekruipt mij toch wel een gevoel van opluchting, bijna klaar! In dit slotdeel van mijn proefschrift (wat hoogstwaarschijnlijk het meest gelezen zal worden, hoewel ik de voorgaande hoofdstukken ook van harte zou willen aanbevelen) wil ik graag een aantal mensen bedanken, want een proefschrift schrijf je niet alleen, integendeel.

Allereerst wil ik mijn begeleidingsteam bedanken. Ik heb genoten van alle discussies waarin we elke keer weer een stapje verder kwamen. Peter als dagelijkse begeleider ben jij intensief betrokken geweest bij het tot stand komen van dit proefschrift. Ondanks je drukke agenda kon ik altijd bij je naar binnenlopen voor advies, om nieuwe ideeën te bediscussiëren of voor een bemoedigend woord. Frank, your remarks and comments on my manuscripts improved them a lot and I am grateful that you helped me putting my research in a broader context. Herman, ook jou wil ik graag bedanken voor je kritische blik, het onvermoeibaar corrigeren van mijn manuscripten en je enthousiasme. Ik heb veel van je geleerd! En tenslotte Martin, bedankt dat je mijn begeleidingsteam wilde versterken. Jouw inbreng is van groot belang geweest voor de afronding van dit proefschrift.

Andy Challinor, Wolfgang Cramer, Carolien Kroeze and Jochem Evers, I am thankful that you are willing to be a member of the thesis committee.

Elke and Christoph, although you were not official supervisors, I have learnt a lot from you. Thanks for your critical comments on my manuscripts and for the fruitful and interesting discussions during the IMAGE and crop modelling workshops. Christoph, thanks that you were always willing to help me with programming problems. I enjoyed working together with you very much. During the IMAGE and crop modelling workshops much more people participated. In particular I would like to thank Katharina, Hester, Kathleen, Alberte, Tom, Lex, and Bart. Thanks for sharing your knowledge with me and for the nice dinners (met een afzakkertje) after a long day of presentations. Katharina a special thanks to you for our nice teamwork. Stefan thank you for your contribution to Chapter 6. Kathleen en Hester: het was leuk met z'n drieën ons AIO-avontuur te beleven. Kathleen, jij gaf mij het goede voorbeeld en Hester, jij zult spoedig volgen. Eelco, jouw kennis over alle technische aspecten die bij het modelleren en programmeren blijken te horen was van groot belang om de vele technische problemen op te lossen, bedankt! Joost en Pytrik, bedankt voor onze discussies over gewasgroeimodellering en alle informatie en artikelen die jullie mij hebben

gestuurd. Antonio, grazie for your help with the design of the cover of my thesis. It looks wonderful!

For good results a good working atmosphere is indispensable. I therefore would like to thank my colleagues of PPS and CSA for the nice chats during the coffee breaks, lunch breaks, and PV-uitjes. In particular: Sander J., Sander v.D., Ria, Argyris, Bert R., Sander d.V., Charlotte, Maryia, Chrispen, Glaciela, Marcel, Sheida, Bert J., Nico, Gerrie, Maja, Madeleine, Murilo, Mink, Peter E., Roelof, Senthilkumar, Mariana, Rik, Ken, Mark, Michiel, Dirk, Merel, Marieke, Naomi, Aisha, André, Alex-Jan, Ans, Jan, Xinyou, Jochem, Aad, Khan, Peter v.P., Pepijn, Sjanie en Huub.

Gelukkig is er meer in het leven dan promoveren. ZotZ, oftewel Renske, Geke, Hilda, Chantal en Jolanda, bedankt voor alle gezellig uitstapjes, interessante discussies, het lekkere eten en de steun in de afgelopen 11 jaar. Laten we zo doorgaan zodat we in het bejaardenhuis nog steeds bij elkaar op de thee kunnen gaan. Jolanda, bedankt dat ik zoveel van het AIO-leven met jou mocht delen. Fijn dat jij nu mijn paranimf wilt zijn. Brechtje: van AID-zusje tot paranimf, dat zegt wel genoeg, bedankt voor alles! Tienke, bedankt voor alle gezellige lunches en telefoongesprekken. Jouw nuchtere blik is verhelderend. Jacomijn, jammer dat je zo ver weg woont, gelukkig houden we contact! Nynke, bedankt voor de gezellige lunchwandelingen over de campus en onze discussies over de wetenschap en modellen in het algemeen. Cathy, Stefan, Thijs en Ard erg leuk dat we nog steeds herinneringen aan 7C kunnen ophalen. Lydia, bedankt voor de leuke uitstapjes, laten we dit blijven doen. Laura en Maayke, fijn dat we al zo lang vriendinnen zijn! Flavia en Roel, we komen nog een keertje op bezoek in Zwitserland! De Ontzetting, in het bijzonder de klarinetsectie en Jean Pierre, bedankt voor alle mooie muziek: op donderdagavond was er gelukkig geen ruimte meer in mijn hoofd om nog over modellen o.i.d. na te denken.

Tijdens mijn promotietijd verscheen er ook een schoonfamilie in mijn leven: Ton, Trudy, Wendy en Niels, ik voelde me meteen thuis bij jullie, bedankt hiervoor. Graag wil ik ook mijn familie bedanken: Frank, Nellie, Marloes, Anke, Inge, Sander en Antonio, bedankt voor de interesse die jullie in mijn werk hebben getoond. Ik ben blij dat jullie er altijd voor mij zijn.

Tenslotte John, aan jou ben ik de meeste dank verschuldigd. Ongeveer drie jaar geleden verscheen je met een brede glimlach op mijn computerscherm. Nu sta je, nog steeds met een brede glimlach, naast mij in het leven, iets beters kan ik mij niet wensen. Bedankt voor alles, voor je interesse in mijn onderzoek maar bovenal je steun en liefde!

Lenny

## List of co-authors affiliations

### **Dr. Myriam Adam**

Plant Production Systems Group, Wageningen University, P.O. Box 430,  
NL-6700 AK Wageningen, The Netherlands  
Current address: Global Future Project, ICRAF World Agroforestry Centre,  
P.O. Box 30677-00100, Nairobi, Kenya

### **Dr. Alberte Bondeau**

Climate Impacts and Vulnerabilities, Potsdam Institute for Climate Impact  
Research (PIK), P.O. Box 60 12 03, D-14412, Potsdam, Germany

### **Prof. Dr. Frank Ewert**

Plant Production Systems Group, Wageningen University, P.O. Box 430,  
NL-6700 AK Wageningen, The Netherlands  
Current address: Crop Science Group, Institute of Crop Science and Resource  
Conservation (INRES), University of Bonn Katzenburgweg 5, D-53115 Bonn,  
Germany

### **Dr. ir. Peter A. Leffelaar**

Plant Production Systems Group, Wageningen University, P.O. Box 430,  
NL-6700 AK Wageningen, The Netherlands

### **Dr. Christoph Müller**

Current address: Earth System Analysis, Potsdam Institute for Climate Impact  
Research (PIK), P.O. Box 60 12 03, D-14412, Potsdam, Germany  
Netherlands Environmental Assessment Agency (PBL), Global Sustainability and  
Climate, P.O. Box 303, NL-3720 AH Bilthoven, The Netherlands

### **Dr. Stefan Siebert**

Crop Science Group, Institute of Crop Science and Resource Conservation  
(INRES), University of Bonn Katzenburgweg 5, D-53115 Bonn, Germany

### **Dr. Elke Stehfest**

Netherlands Environmental Assessment Agency (PBL), Global Sustainability and  
Climate, P.O. Box 303, NL-3720 AH Bilthoven, The Netherlands

**Prof. Dr. ir. Herman van Keulen**

Plant Production Systems Group, Wageningen University, P.O. Box 430,  
NL-6700 AK Wageningen, The Netherlands

Plant Research International, Wageningen University and Research Centre,  
P.O. Box 616, NL-6700 AP Wageningen, The Netherlands

**Katharina Waha, MSc**

Earth System Analysis, Potsdam Institute for Climate Impact Research (PIK),  
P.O. Box 60 12 03, D-14412, Potsdam, Germany

## Curriculum Vitae

Lenny van Bussel was born on the 9<sup>th</sup> of January, 1982 in Helmond, the Netherlands. After finishing pre-university education in 2000, Lenny started to study Forest and Nature Conservation (specialization: Ecology and Management) at Wageningen University. After her BSc she continued at Wageningen University with the MSc studies Earth System Science and Forest and Nature Conservation (specialization: Ecology and Management). During these studies she did an internship at the former Department of Short Rotation Forestry at the Swedish University of Agricultural Sciences, Uppsala. The aim of this internship was to study the carbon sequestration under *Salix* and *Populus* bioenergy plantations in Sweden. During her MSc Lenny evaluated the impacts of climate change on forests and their goods and services. This was one of the first times she got in touch with vegetation modelling. She concluded her MSc studies with another MSc thesis on the investigation of the potential contribution of a Dutch short-rotation willow plantation to mitigate climate change, which included measurements of willow plants in Flevoland, the Netherlands.

After receiving her two MSc degrees in August 2006, Lenny started her PhD study at the Plant Production Systems Group in October 2006. During her PhD study she worked in close cooperation with the Netherlands Environmental Assessment Agency (PBL) and the Potsdam Institute for Climate Impact Research (PIK). This cooperation resulted in several papers which have been presented at international conferences and published in high impact peer-reviewed journals.

Currently Lenny works as a researcher at RIKILT, Institute of Food Safety.







## List of peer-reviewed publications

- Waha\*, K., Van Bussel\*, L.G.J., Müller, C., Bondeau, A., in press. Climate-driven simulation of global crop sowing dates. *Global Ecology and Biogeography*.  
\*Equal contribution
- Van Bussel, L.G.J., Ewert, F., Leffelaar, P.A., 2011. Effects of data aggregation on simulations of crop phenology. *Agriculture, Ecosystems & Environment*, **142**, 75-84.
- Van Bussel, L.G.J., Müller, C., Van Keulen, H., Ewert, F., Leffelaar, P.A., 2011. The effect of temporal aggregation of weather input data on crop growth models' results. *Agricultural and Forest Meteorology*, **151**, 607-619.
- Adam, M., Van Bussel, L.G.J., Leffelaar, P.A., Van Keulen, H., Ewert, F., 2011. Effects of modelling detail on simulated crop productivity under a wide range of climatic conditions. *Ecological Modelling*, **222**, 131-143.



# PE&RC PhD Education Certificate

With the educational activities listed below the PhD candidate has complied with the educational requirements set by the C.T. de Wit Graduate School for Production Ecology and Resource Conservation (PE&RC) which comprises of a minimum total of 32 ECTS (= 22 weeks of activities)



## **Review of literature (4.2 ECTS)**

- Regional crop modelling (2007)

## **Writing of project proposal (5.6 ECTS)**

- Regional crop modelling (2007)

## **Post-graduate courses (7 ECTS)**

- Summer School on understanding global and environmental change; SENSE (2007)
- Integrated assessment of agriculture and sustainable development; PE&RC (2008)
- i-GIS Course; PE&RC (2009)

## **Laboratory training and working visits (2.8 ECTS)**

- Sowing date simulation; Potsdam Institute for Climate Impact Research, Germany (2009)
- Harvesting date simulation; Crop Science Group, Bonn University, Germany (2009)

## **Invited review of (unpublished) journal manuscript (1 ECTS)**

- Agricultural and Forest Meteorology: Spatio-temporal changes of wheat phenology in China and the roles of temperature and cultivar thermal characteristic (2010)

**Competence strengthening / skills courses (3.5 ECTS)**

- PhD Competence assessment; WGS (2006)
- Personal efficacy; WGS (2007)
- Techniques for writing and presenting a scientific paper; WGS (2009)
- Career orientation; WGS (2010)

**PE&RC Annual meetings, seminars and the PE&RC weekend (2.1 ECTS)**

- PE&RC Weekend (2007)
- PE&RC Day: Is our civilization able to stand the test of time (2007)
- PE&RC Day: Expect the unexpected (2008)
- PE&RC Day: On the origin of communication (2009)
- PE&RC Day: Why and how scientists sell science (2010)

**Discussion groups / local seminars / other scientific meetings (6 ECTS)**

- Statistics, maps and modelling (2006-2010)
- Spatial modelling (2006-2010)

**International symposia, workshops and conferences (10.9 ECTS)**

- Several IMAGE and crop modelling workshops; Bilthoven, the Netherlands; Potsdam, Germany; Wageningen, the Netherlands; Bonn, Germany (2006-2011)
- X Congress of the European Society for Agronomy; Bologna, Italy (2008)
- AgSAP Conference; Noordwijk aan Zee, the Netherlands (2009)
- XI Congress of the European Society of Agronomy; Montpellier, France (2010)

**Lecturing / supervision of practical's / tutorials; 6 days (1 ECTS)**

- Models for forest and nature conservation (2007)

## **Funding**

The research presented in this thesis was financed by the Dutch National Research Programme Climate Changes Spatial Planning (CcSP) within the project IC2 “Integrated analysis of emission reduction over regions, sectors, sources and greenhouse gases”.

<b>Cover design</b>	Antonio Pinna (e-mail address: <a href="mailto:hantropy@hotmail.it">hantropy@hotmail.it</a> )
<b>Cover photo</b>	John Stevens (Wheat field near Kleve, Germany)
<b>Reproduction</b>	Ponsen & Looijen B.V., Ede

# Propositions

1. Availability and aggregation of input data limits the use of detailed crop growth models in climate change impact assessments. (*this thesis*)
2. Development of crop growth models for global application would have been more advanced, if previous research money allocation had been better balanced between studies focussing on light interception and light utilization. (*this thesis*)
3. The mere fact that the emergency timetable of the Dutch railroad company requires testing, makes models of more complex systems, such as the global climate system, questionable.
4. The fact that human suffering may increase by preventive medical examination receives insufficient attention.
5. The supply of additional feeding to animals in Dutch nature reveals short-term thinking.
6. If the trend to make use of open-plan offices has arisen to stimulate social interaction between people, it has failed.
7. A compulsory supply of source code to reviewers of scientific papers which describe newly developed models, will enhance the integrity of science.
8. To fight food waste, urban vegetable gardens should be promoted.

Propositions accompanying the PhD thesis, entitled:  
"From field to globe: Upscaling of crop growth modelling"

Lenny G.J. van Bussel  
Wageningen, 19 October 2011